Ultra Scale-Down Process Synthesis of Microalgae Primary Recovery Operations

A thesis submitted to

University College London

For the degree of

Doctor of Philosophy

By

Hadiza Abubakar Auta

Department of Biochemical Engineering

University College London

ACBE

London WC1A 0AH

Declaration

‘I, Hadiza A. Auta, confirm that the work in this thesis is mine and where information has been derived from other sources, I confirm that this has been duly referenced in this thesis.’

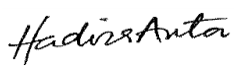

Abstract

The majority of products made by microalgae and requiring extraction before use are restricted, commercially, by the high cost of the harvesting methods employed. Although considerable progress has been made in biofuel development there are still relatively few studies on the initial downstream processing stages. Ultra-scale down (USD) approaches have previously been established to study the impact of the engineering environment on biopharmaceuticals; they are valuable because they enable study of a wide range of operating parameters using minimal quantities of material and resources. The aim of this project is therefore to establish a USD platform for the rapid evaluation of pre-treatment and recovery operations for microalgae downstream processes.

The first objective was to explore flocculation as a pre-treatment step. Flocculation is a difficult process to operate reproducibly, hence standardisation of flocculation conditions becomes vital in order to characterize and quantify process performance. A series of scale-down flocculation reactors were designed, characterised and scaled-up using Chitosan to flocculate heterotrophically grown *Chlorella sorokiniana*. These enabled flocs with defined particle size distributions to be consistently and reproducibly produced. An optimal Chitosan concentration of 9.9 ± 0.4 mg.g^{-1} of algal dry cell weight was determined. Scale-up of the flocculation process from the scale-down reactor (120 mL) to a 7.5L STR stirred tank reactor was achieved at a fixed impeller tip speed during flocculant addition and ageing (0.29 and 0.07 ms^{-1} respectively).

Due to the complex nature of unit operations, it is generally difficult to obtain data at laboratory scale that closely reflects the performance of operations at pilot scale or beyond. For the second objective of this work, a USD model of a cross-flow filtration process for microalgal biomass recovery was established. This could accurately reproduce the flux-TMP (transmembrane pressure) profiles of lab-scale hollow fibre cartridges when operated at a defined shear rate. The benefits of flocculation on filtration performance include a

reduction in membrane cleaning cycles and a 20% reduction in filtration time. Filtration results were also in good agreement between the two scales for both unflocculated and flocculated feeds. The USD method enabled a 14-fold decrease in the volume of material required. It also demonstrated the benefits of flocculation. And lastly, USD was achieved using a 14.5–fold reduction in membrane area at matched volume: surface area ratio.

The third objective was to establish a USD centrifugation method using a rotating disk shear device to expose particles to hydrodynamic shear before centrifugal separation. Evaluation of the influence of flocculation on centrifugation efficiency showed the benefits of increased particle size on clarification. Clarification efficiencies exceeding 99% was obtained even at low centrifugal forces using an optimal Chitosan dosage. The USD findings were validated at pilot scale using a CARR Powerfuge™ centrifuge. Similar clarification performance was predicted using 2000-fold less broth volume than was required for the pilot scale study.

Sonication and homogenization as small scale cell disruption options for lipid release of heterotrophically grown *C.sorokiniana* were explored. Comparison of the optimal conditions of the two methods showed cell disruption and lipid release were similar in both cases on a $g.g^{-1}$ basis. Finally comparison of the transesterified material produced using either USD microfiltration or USD centrifugation steps for harvesting showed major differences in terms of yield of fatty acid methyl esters (FAME). USD methods for evaluation of primary recovery operations and their interactions appear particularly useful in microalgae bioprocess synthesis.

This work is the first to evaluate the use of USD technologies with microalgal cells. It illustrates the power of small-scale mimics to enable rapid selection and optimisation of different process options and thereby rational selection of the overall bioprocess sequence.

Acknowledgement

I would like to express my sincere gratitude to Prof Gary J Lye, for his tremendous support and guidance in relation to my PhD work and to my stay here in the UK as a foreign student. He is an epitome of a true leader and I will forever remain indebted; for making me achieve this milestone and also to see life in a simple perspective. Most of all, he gave me independence, and yet has not hesitated in mentoring, encouraging and providing me a sense of direction when needed. I am also grateful to my advisor Prof Mike Hoare. It was a real pleasure to be under the guidance of these great men. Through them, I have drawn inspiration to aspire to do things well and also share the same with others.

Although this thesis was an independent effort, in life, we come across people who will mean a lot and be of assistance in one way or another. This goes out to my UCL buddies: Ebenezer Ojo, Aminat Omotosho (my very own Aminatu) and Nurashikin Suhaili (for always making me laugh & forget my bad results). Also to my friends Asari Anwanane, Lola Baker, Leonardo Rios (for always coming up with something lively), Olotu Ogonah (for being my expert bioprocess adviser), Rukayya Muazu (my sister, my friend!), Jana Small (my confidant!) Patrick Muguisha and lastly to the numerous friends I made during the course of this project.

The love, support and encouragement given to me by my family throughout the period of this PhD was immeasurable and I can only pray Almighty Allah keeps us together in good health. Special thanks to my mum for always being there to relieve me with some of the household work thereby giving me more time for this work and to my dad for the constant prayers. To my siblings, your constant encouragement and prayers was also a motivation.

My attendance here at UCL Biochemical Engineering would not have been possible if not for the financial support of Petroleum Technology Development Fund (PTDF), Nigeria. I am truly thankful for this support.

Most of all, immense gratitude goes to my husband, Muftau, for always being there for me and our children, Fareeda and Rayyan. His contribution for the overall achievement of this research work is immeasurable. His unwavering love and support has been my strength and comfort. Thank you to Fareeda too for always making trouble in the house and saying No! You have been my source of happiness and a good sister to Rayyan.

Finally, for all those who have contributed in one way or the other, too numerous to mention, thank you.

In Memory of Sa'adiya Pindar

(Aunty S)

This crisis is coming soon, it will bite, not when the last drop of oil is extracted, but when oil extraction can't meet demand – perhaps as soon as 2015 or 2025…

David Goodstein's (2004)

Table of contents

List of Figures

List of Tables

Nomenclature

μ	liquid viscosity
μ_{max}	maximum specific growth rate
A	Area
B_h	baffle height
B_w	baffle width
C_f	final biomass concentration in flocculation reactor
C_i	initial biomass concentration in flocculation reactor
d	particle diameter
D_b	baffle diameter
D_i	impeller diameter
D_T	vessel diameter
ε	local turbulent energy dissipation
ε_{avr}	average turbulent energy dissipation
F_{lab}	calibration factor to allow for non-ideal flow in the lab centrifuge
g	acceleration due to gravity
H_L	height of liquid
H_T	height of tank
k'	velocity coefficient
L	Length
N	bowl speed
OD_f	optical density of feed
OD_s	optical density of supernatant
OD_{ws}	optical density feed after prolonged centrifugation
P_f	kinematic viscosity
P_p	permeate pressure
P_r	feed pressure
Q	flow rate
r	radius

t_{add}	flocculant addition time
T_{cf}	temperature correction factor
t_d	doubling time
t_m	mixing time
V	volume
V_{lab}	volume of feed in the centrifuge tube
V_s	settling velocity
V_{tip}	impeller tip speed
X_s	segregation index
γ	shear rate
γ_m	membrane shear rate
ν	kinematic viscosity
ρ	density
ρ_c	suspended particles
ρ_L	density of the liquid phase
ρ_s	density of spin fluid
Σ	sigma factor
ω	angular velocity

Abbreviations

AOM	Algogenic organic matter
ATP	Adenosine triphosphate
CFD	Computational fluid dynamics
CFF	Cross flow filtration
CFPP	Cold filter plugging point
CN	Cetane number
DAF	Dissolved air flotation
DCW	Dry cell weight
DSP	Downstream processing
EOM	Extracellular organic matter
EPS	Extracellular polymeric substances
FA	Fatty acid
FAME	Fatty acid methyl ester
FGB	First generation biofuels
FhGB	Fourth generation biofuels
GHG	Greenhouse gas
NADP	Nicotinamide adenine dinucleotide phosphate
NADPH	Nicotinamide adenine dinucleotide phosphate hydrogenase
NFF	Normal flow filtration
NWF	Normalised water flux
NWP	Normalised water permeability
PE	Photosynthetic Efficiency
PES	Polyethersulfone
PS	Polysulfone
RDF	Rotating disc filter
SGB	Second generation biofuels
STR	Stirred tank reactor
TGB	Third generation biofuels
TMP	Transmembrane pressure
USD	Ultra-scale down

1. Introduction and Literature Review

1.1 Background and project motivation

Energy is a factor essential in maintaining economic growth and living standards. The global energy market can be divided into the electricity and fuel sector (Schenk *et al.*, 2008). Its sources can be further split into three main categories *viz*: fossil fuels, renewables and nuclear. Fossil fuel consists of petroleum, coal and natural gas. Renewable sources are biofuels, solar, hydroelectric, wind, and geothermal power while nuclear energy sources are radioactive fission and fusion (Demirbaş, 2001). In general, there is a large dependence on fossil fuels in order to meet rising energy demands (Arbex & Perobelli, 2010); an estimated 40% increase by 2030 is projected by the International Energy Agency (IEA) (Chaudhary, 2013). Problems associated with the use of fossil fuels (**Figure 1.1**) and its non-renewable nature has led to research into renewable and sustainable alternatives. Biofuels are the only renewable resources with the potential of favourably competing with fossil fuels. This is because other technologies concentrate on the production of electricity and are not suited to replace fossil fuels especially in the transportation and petro-chemical sectors. For example, planes cannot be battery powered as weight would be excessive (Posten, 2012).

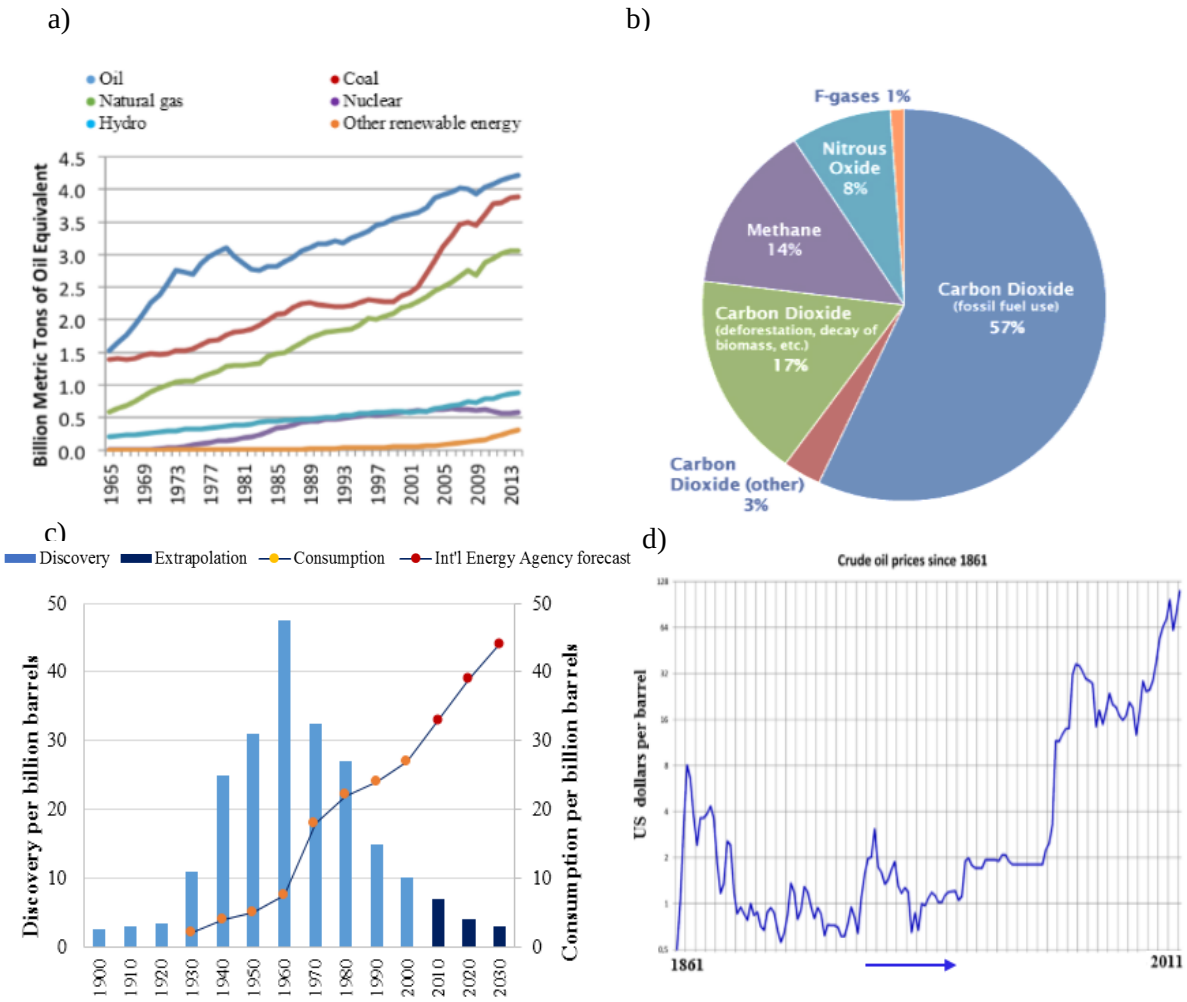

Figure 1-1: Some of the problems associated with fossil fuel usage that led to the need for renewable and sustainable energy sources. (a) World energy consumption relies greatly on oil coal and gas (BP, 2015). (b) Global warming due to the increased release of greenhouse gases with over half attributed to CO_2 released via fossil fuel combustion (IPCC, 2007). (c) Energy security: sources are depleting and consumption is three times the amount being discovered (ASPO, Berlin 2004). (d) Oil price has been increasing over the years (BP, 2011).

1.1.1 Global energy situation

Currently, the use of fossil fuel is indispensable, nonetheless it cannot meet the future demand for energy due to the rapid growth of emerging economies around the world (Chaudhary, 2013). Sources are depleting and global warming is also on the rise (**Figure 1.1**). Biofuels have received considerable attention in recent years due to the fact that they are produced from renewable, biodegradable and non-toxic sources and hence are environmentally sustainable. Also, they already contribute 10% of the global energy supply (Chaudhary, 2013).

Larson in 2008 predicted, that commercial scale biofuel production using biochemical processes will only begin in 10-20 years (Larson, 2008). The Food and Agricultural Organization (FAO) also reported in 2008 that of all the biofuel sources, only bioethanol produced from sugar cane in Brazil could compete economically with fossil fuel, as other sources of biofuel depend largely on subsidies for its production. The report equally stated that by 2017, biodiesel is expected to have a higher global production level (24 million litres) when compared to bioethanol.

In 2009, it was assumed that the global market for biodiesel production will grow exponentially in the following decade with an expected rise from 11.1 – 121 million metric tons occurring between 2008 and 2016 (Deng *et al.*, 2009). In the same year, about a 400% increase in bioethanol production in comparison to that in 2000 was achieved. An increase of 72.2 billion litres of global ethanol production was recorded (Tabatabaei *et al.*, 2011). The European union (EU) has set a compulsory 10% target in the use of biofuel for 2020 with the aim of reducing CO_2 emission by 20% and decreasing the usage of non-renewable sources (Andrew, 2007). In 2012, a continued fall in the price of renewable energy technologies was seen, making renewables increasingly competitive with conventional energy sources (REN21, 2013).

1.2 Overview of biofuels production

Four generations of biofuels can be defined based on advances in production technologies (**Table 1.1**). First generation biofuels (FGB), derived largely from edible sugars and starches (Brennan & Owende, 2010), are faced with the constraint of competing with food and fibre production for arable land thus have an adverse impact on the world food supply (Moore, 2008). Second generation biofuels (SGB), have attracted more interest because they are based on non-edible agricultural residues. However, commercial exploitation has been hindered due to failure in the scaling-up of conversion technologies (FAO, 2008). Moreover, the economics of production still remains a challenge. Third generation biofuels (TGB), involve the production of biodiesel and bioethanol from microalgae and seaweed (Dragone *et al.*, 2010). Fourth generation biofuels (FhGB), are based on further development of microalgae biofuel production, essentially the metabolic engineering of the algae for producing biofuels from oxygenic photosynthetic organisms. This production is still in its early stages and the economic feasibility of FhGB appears superior in the longer term.

Table 1-1: Biofuels classification based on their production technologies. Adapted and modified from Demirbas (2009).

Generation	Feedstock	Examples
FGB	Sugar, starch, vegetable oils, or animal fats	Bioalcohols, vegetable oil, biodiesel, biosyngas, biogas
SGB	Non-food crops, wheat straw, corn, wood, solid waste, energy crop	Bioalcohols, bio-oil, bio-DMF, biohydrogen, bio-Fischer–Tropsch diesel, wood diesel
TGB	Algae	Vegetable oil, biodiesel
FhGB	Vegetable oil, biodiesel	Biogasoline

1.3 Algae

Algae include macroalgae (seaweeds) and microalgae; they consist of several eukaryotic organisms and sometimes prokaryotes (blue-green algae) (Packer, 2009). Algae can exist as either freshwater or marine species; some grow optimally in hypersaline conditions whereas others thrive at intermediate saline levels. Seaweeds are macroscopic multicellular algae while microalgae are microscopic in nature. The former has defined tissues containing specialized cells while the latter are typically autotrophic organisms from a large and diverse group ranging from simple unicellular to multicellular forms. Microalgae make up the majority of the ten million algal species estimated on earth (Barsanti & Gualtieri, 2005). This thesis will consequently focus on microalgae.

1.3.1 Algal physiology

They include Chlorophyceae (green algae), Bacillario-phyceae (diatom), dinoflagellates and Chryosophyceae (golden algae). They can grow in a variety of conditions especially damp areas and water bodies. About 8000 species of green algae containing complex long-chain sugars (polysaccharides) in their cell wall are known (Packer, 2009). The large proportion of carbon possessed by algae is attributed to this property. Proteins, carbohydrates and lipids (oils) are the main biomass components of microalgae; though the composition of each of these components in the biomass varies between strains. Microalgae can be motile or non-motile depending on possession of antenna (flagella).

Algal strains have been widely studied on their biochemical composition due to the various applications of their biomass and metabolites (Guedes *et al.*, 2011). They are able to efficiently produce cellulose, starch and oils in large amounts (Benemann & Oswald, 1996). However, cyanobacteria and some microalgae produce glycogen instead of starch and can produce biohydrogen under anaerobic conditions (Hankamer *et al.*, 2007).

Furthermore, some species contain high proportions of various lipids by dry weight (Metting, 1996; Spolaore *et al.*, 2006). Total lipid and fat content of algae is within 1-70%

of its ash-free dry weight, although reports have shown that species with > 40% are rarely observed (Borowitzka, 1988).

The structures of microalgae cell walls are typically tri-layered which include; polysaccharides such as cellulose, glycoproteins, mannose, protein, uronic acid, xylan or trilaminar layers of algaenan and minerals such as silicates or calcium (Allard *et al.*, 2002; Sugiyama *et al.*, 1991). Microalgae are known to undergo photosynthesis which could be either in the light or dark steps (Calvin cycle). During photosynthesis, adenosine triphosphate (ATP) and nicotinamide adenine dinucleotide phosphate (NADPH) are first produced in the cytoplasm of algae. The NADPH produced is as a result of a reaction between protons and electrons which combines with ferredoxin-$NADP^+$ oxidoreductase; this in turn combines with ATP in some biochemical pathways and Calvincycle to produce biomass (oils, starch, sugars and other bio-molecules).

The growth nutrient requirements of algae include water, CO_2 and sunlight just like higher plants.

1.3.2 Microalgae as a biofuel feedstock

The potential use of microbial, particularly microalgal photosynthesis to produce biofuels is widely recognized (Chisti, 2007; Hu *et al.*, 2008; Huntley & Redalje, 2007). Microalgal use for biofuel production has several advantages over higher plants (Dragone *et al.*, 2010): (1) they have a rapid growth rate, with short growth cycle of 1-10 days when compared to an average food crop which has a harvesting cycle of once or twice a year; (2) they can grow on non-agricultural land (Hu *et al.*, 2008; Wahlen *et al.*, 2011), utilize brackish water (Deng *et al.*, 2009) or wastewater streams (Schenk *et al.*, 2008) for growth; (3) they are grown sustainably in that no pesticides or herbicides are required for cultivation and, depending on species, microalgae can serve as a good source of other products with valuable applications including a wide range of fine chemicals and bulk products such as natural dyes, proteins, pigments, polysaccharides, polyunsaturated fatty acids etc.; (4) they also have the capacity to produce 15–300 times as much biodiesel as first and second

generation sources (Dragone *et al.,* 2010). **Table 1.2** shows that the average biodiesel production yield from microalgae is higher than that obtained from their food crop counterparts.

Table 1-2: Comparison of some sources of biodiesel (where superscripts a and b are 70 and 30% oil by weight in biomass respectively). Adapted from Chisti (2007).

Crop	**Oil Yield ($L.ha^{-1}$)**
Corn	172
Soyabean	446
Canola	1,190
Jathropa	1,892
Coconut	2,689
Palm	5,950
Microalgae[a]	136,900
Microalgae[b]	58,700

Though the potential of microalgae as a biofuel source are clear, a number of limitations for the development of algal biofuel technology to commercial viability exist. These include: (1) a balance between species selection and extraction of valuable co-products for biofuel production; (2) continued development of production systems for example, improved photosynthetic efficiency (Pulz & Scheibenbogen, 1998); (3) accumulating flue gases which are unsuitable in high concentration due to the presence of poisonous compounds such as NO_x and SO_x (Brown, 1996); (4) potential for a negative energy balance after accounting for requirements in pumping, CO_2 transfer, harvesting and extraction (Brennan & Owende, 2010). Microalgae can be used to produce several biofuel products together with electricity depending on the conversion technology used (**Figure 1.2**). Biofuels are not yet economical but improving these technologies can improve process economics so that it is possible to substitute some fossil diesel and contribute to global energy supply whilst providing a positive environmental impact (Wang *et al.*, 2008)

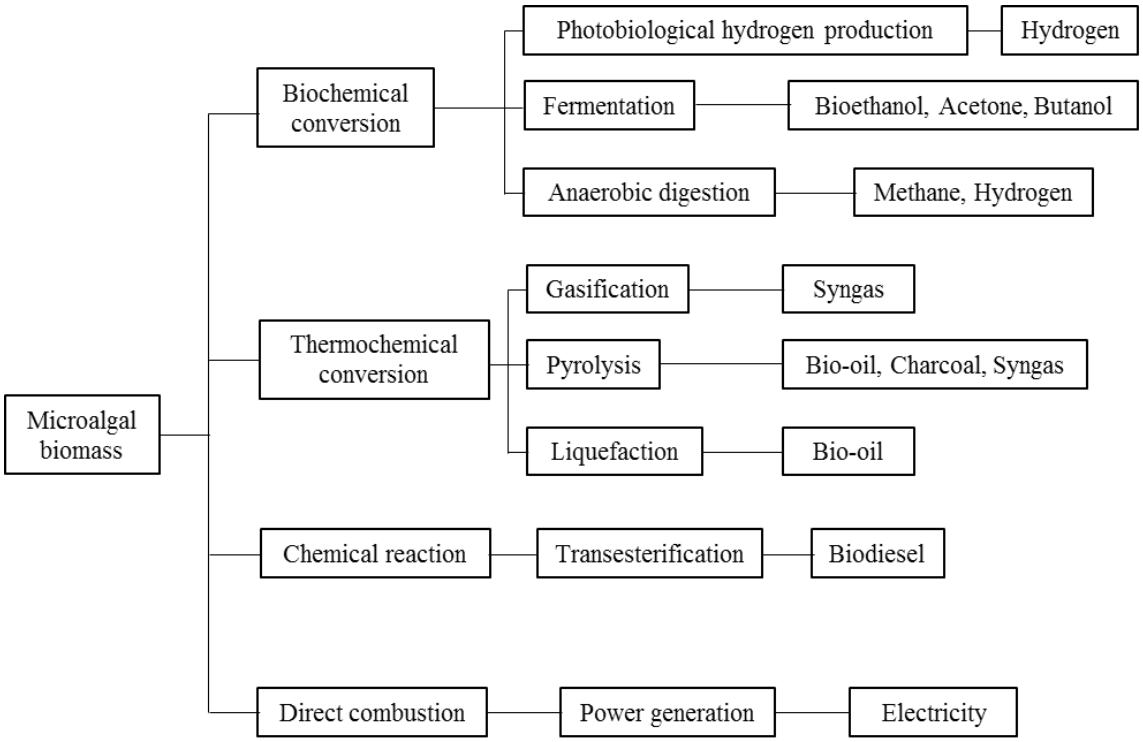

.

Figure 1-2: Biofuel conversion processes from microalgal biomass. Adapted from Wang *et al*. (2008).

1.3.2.1 Impact of strain selection on biofuel production

Several studies have been carried out on the isolation and characterization of numerous microalgae species with research focusing on these as a strategy to improve biofuel production (Sheehan, 1998). Strains contain varied oil content and this impacts on their suitability for biodiesel production. Many microalgae have an oil content in the range of 20-50% dry weight of biomass with doubling times as short as 3.5 hr (Metting, 1996). The doubling time of different species can influence biomass productivities hence impacting on process economics. **Table 1.3** is an example of different microalgal species and strains with different lipid content (% dry weight).

Table 1-3: Lipid content of some microalgae species. Adapted from Spolaore *et al.*(2006).

Specie	Lipid Content (% dry weight)
Scenedesmus obliquus	11 – 55
Scenedesmus dimorphus	6 – 40
Chlorella vulgaris	14 – 56
Chlorella emersonii	63
Chlorella protothecoides	23/55
Chlorella sorokiniana	22
Chlorella minutissima	57
Dunaliella bioculata	8
Dunaliella salina	14 – 20
Neochloris oleoabundans	35 – 65
Spirulina maxima	4 – 9

1.3.2.2 Impact of Photosynthetic Efficiency (PE)

PE is an important characteristic of microalgae as any increase will improve biomass production. It can be defined as the percentage of incident radiation that is converted into biomass (Packer, 2009). In biofuel production system, improving the efficiency of light capture will directly impact on biomass production. However, the photosynthetic machinery can be damaged by excessive light leading to photo-protective mechanisms in algae and higher plants known as photo inhibition (Huntley & Redalje, 2007; Pascal *et al.*, 2005). A study by Mussgnug *et al.*, (2007) showed how modifying the antenna length of *C.reinhardtii* allowed optimal light exposure to all cells in the bioreactor. In addition, as a result of improved PE and appropriate energy supply to all photosynthesizing cells, an increased efficiency in biomass productivity was seen.

1.3.2.3 Impact of lipid productivity

In biodiesel production, one major factor to be considered when choosing algae species is its lipid productivity which is defined as the rate of lipid production per gram of biomass. Microalgae possess a significant variety of valuable lipids and fatty acids (FA) for industrial applications (Behrens & Kyle, 1996). Depending on the species, microalgae

produce different types of lipids, other complex oils and hydrocarbons (Guschina & Harwood, 2006; Metzger & Largeau, 2005). It is the lipid in the form of triglycerols (TG) that is transesterified to form biodiesel (Section 1.5). Lipid accumulation is dependent on many factors ranging from microalgal species to growth conditions. Some algal species produce large quantities of lipid primarily in the form of heavy droplets of TG in the cytoplasm (Boswell *et al.*, 1992). Lastly, biodiesel quality and quantity will greatly depend on the lipid productivity.

1.3.3 Microalgae culture

The use of sunlight as a free natural source of energy is an advantage in commercial algae culture. However, this has its own limitation considering the daily and seasonal variation in sun intensity which could limit the viability of its production to areas with a considerable supply of solar energy. A good example is the outdoor production of phototropic algae which requires sunlight as its energy source; this makes light a key limiting factor (Pulz & Scheibenbogen, 1998).

Microalgae can grow as either autotrophic, heterotrophic or as mixotrophic organisms. When they grow as autotrophs, they require only a light source and inorganic compounds like salt and CO_2 for growth; whereas heterotrophic growth makes use of organic compounds sourced externally as an energy source. Some algae can also grow mixotrophically, in the sense that they require exogenous organic nutrient as well as light for photosynthesis (Lee, 1980).

Due to the limitations of sunlight energy, synthetic methods of production have been developed. Currently, fluorescent lamps are used to simulate phototrophic conditions (Muller-Feuga *et al.*, 1998). Although a higher overall energy input is required, fluorescent lamps permit continuous light production. In choosing this artificial lighting system, understanding the algal morphology, especially absorption of light by photosynthetic pigments is important.

In a natural setting, CO_2 is usually available for algae to fix from three different forms, namely: the atmosphere; in discharge gases from heavy industries; or as soluble carbonates (Wang *et al.,* 2008). Whereas in an artificial setting, atmospheric CO_2 levels of up to 150,000 ppm (Bilanovic *et al.,* 2009) can be mimicked by feeding soluble carbonates such as Na_2CO_3 and $NaHCO_3$ (Colman & Rotatore, 1995; Huertas *et al.*, 2000) or from other outside sources i.e. power plants (Brown, 1996; Doucha *et al.*, 2005; Kadam, 2002).

In terms of elemental requirements, nitrogen, phosphorus and silicon are some of the inorganic nutrients which algae require for growth. Ammonium is the most preferred nitrogen source for algae (Grobbelaar, 2007; Kaplan *et al.*, 2008; Wilhelm *et al.*, 2006), while some have the ability to fix nitrogen directly from the atmosphere in the form of NO_X (Moreno et al., 2003; Welsh *et al.*, 2000). Phosphorus is only required in small quantity (Çelekli *et al.,* 2009) but it needs to be supplied in excess since it can complex with metal ions, hence not all the phosphorus added is available for algal growth (Chisti, 2007).

Microalgae can also grow in aqueous media and can utilize wastewater for growth, thereby reducing the competition on fresh water sources and needing less water than terrestrial crops (Dismukes *et al.*, 2008). Wastewater is rich in valuable nutrients such as nitrogen and phosphorus (Aslan & Kapdan, 2006; Shi *et al.*, 2007), but the presence of excessive trace elements, heavy metals and other contaminants in solution causes problems in biofuel production. Reports have shown that heavy metals such as cadmium regulate important cellular processes like lipid biosynthesis (Gillet *et al.*, 2006; Yang *et al.*, 2000). Other minerals that algae require in sufficient amounts can be lethal or inhibitory at excessive levels (Tripathi & Gaur, 2004) e.g. copper.

Different cultivation methods that could be used in microalgae production are open system and closed photobioreactors. Each has its advantages and limitations as summarised in **Table 1.4**.

1.3.3.1 Open pond production systems

This type of algae production system can be categorized into natural waters and artificial ponds or containers. The dimensions are between 0.2-0.5 m deep with circulation and mixing required to support algal growth. The microalgae CO_2 requirement is usually satisfied from the surface air, but submerged aerators may be installed to enhance CO_2 absorption (Terry & Raymond, 1985). The open pond method is considered a more economically viable manner for large scale production of microalgae when compared to closed photobiorector system.

Open ponds have a number of limitation when it comes to location selection due to the possible threat of pollution and contamination from other organisms such as other protozoa and other algal species (Pulz & Scheibenbogen, 1998). Single-culture cultivation is achievable by maintaining an extreme culture environment (e.g. low pH), though few strains are suitable for this production type and prolonged production periods can lead to bacterial and other biological contaminants (Lee, 2001). Light limitation is evident in this production system as a result of the thickness of the top layer and this will result in low productivities (Ugwu *et al.*, 2008).

1.3.3.2 Closed photobioreactor system

In the past years, algal technologies have attracted considerable interest (Posten, 2009), with the majority of studies focusing on photobioreactor designs. Closed photobioreactors technologies are aimed at overcoming pollution and contamination risks whilst improving algal biomass productivity. This type of production system includes flat bed, tubular or column photobioreactors. Photobiorectors consist of an arrangement of straight plastic or glass tubes. The tubular arrangement captures sunlight and can be aligned horizontally (Molina *et al.*, 2001), vertically (Miron *et al.,* 1999), inclined (Ugwu *et al.*, 2008) or as a helix (Watanabe & Saiki, 1997), and the tubes are usually 0.1 m or less in diameter.

The cost of a closed bioreactor system is higher than open ponds but they are more ideal for growing sensitive strains due to their ability to prevent contamination. They have the

Table 1-4: Advantages and limitations of various algae culture systems. Adapted and modified from Dragone *et al.* (2010).

Production System	Advantages	Limitations
Raceway pond	Relatively cheap	Poor biomass productivity
	Easy to clean	Large area of land required
	Utilises non-agricultural land	Limited to few strains of algae
	Low energy inputs	Poor mixing, light and CO_2 utilisation
	Easy maintenance	Cultures are easily contaminated
Tubular photobioreactor	Large illumination surface area	Some degree of wall growth
	Suitable for outdoor cultures	Fouling
	Relatively cheap	Requires large footprint
	Good biomass productivities	Gradients of pH, dissolved oxygen and CO_2 along the tubes
Flatplate photobioreactor	High biomass productivities	Difficult scale-up
	Easy to sterilise	Difficult temperature control
	Low oxygen build-up	Small degree of hydrodynamic stress
	Readily tempered	Some degree of wall growth
	Good light path	
	Large illumination surface area	
	Suitable for outdoor cultures	
Column photobioreactor	Compact	Expensive compared to open ponds
	Low energy consumption	Small illumination area
	High mass transfer	Sophisticated construction
	Good mixing with low shear stress	Shear stress
	Easy to sterilise	
	Reduced photoinhibition and photo-oxidation	

advantage of better controlled growth condition, a higher volumetric mass transfer rate as well as more efficient mixing (Eriksen, 2008).

1.4 Harvesting techniques in algal bioprocessing

Algae cultures are known to have a high water content which has to be removed during harvesting and processing. One of the major areas of focus in algal production is the high operational cost of the harvesting and dewatering operations used (Greenwell *et al*., 2010; Uduman *et al.,* 2010). Pressures to achieve efficient dewatering processes are on the rise (Titchener-Hooker *et al.,* 2008) as the primary recovery stages account for about 20 – 30% of the cost of production (Gudin C, 1986). Research to date has explored a range of microalgal harvesting technologies from dissolved air floatation, flocculation using different techniques, drying, microfiltration and centrifugation. Studies have shown that no combination or single harvesting method best suits all microalgal species or class of product (Mata *et al.*, 2010; Schenk *et al.*, 2008).

Biomass recovery becomes particularly difficult when there is a low cell density in the range of 0.3 – 5 $g.L^{-1}$ and a small algal size between 2 – 40 µm (Li *et al.*, 2008). Economic production of microalgae involves selecting an appropriate harvesting technique which will be dependent on factors such as density and size of the species as well as the value of the target product (Olaizola, 2003). Microalgae harvesting is normally a two stage process involving bulk harvesting and thickening.

Bulk harvesting: The cell mass in the bulk suspension is separated in this stage, with concentration factors generally in the range of 100-800 times in order to attain 2-7% w/w total solid matter. This values are however dependent on the technologies used e.g. flocculation, gravity sedimentation or flotation and most importantly, the initial biomass concentration.

Thickening: This stage further concentrates the slurry obtained from the bulk harvest stage and is achieved using techniques such as filtration, ultrasonic aggregation and centrifugation. This stage is recognized for its high energy intensity.

1.4.1 Bulk harvesting methods

1.4.1.1 Flocculation

Flocculation is a bulk harvesting process that is commonly used to concentrate algae (Grima *et al.*, 2003) prior to further recovery stages such as filtration or gravity sedimentation (Rao *et al.*, 2007). This method involves the sedimentation or floatation and aggregation of algal biomass so as to increase the effective particle size. There are two stages involved in flocculation process: The first is perikinetic flocculation which is a random process and arises from thermal agitation (Brownian movement). Flocculation in this stage commences immediately after destabilization and is complete within seconds though there is a limiting floc size beyond which Brownian motion has little or no effect. The rate of flocculation of a suspension due to perikinetic flocculation may be described by a second order rate law. The second is orthokinetic flocculation which is a process that develops from induced velocity gradients in the liquid. Such velocity gradients may be induced by setting the liquid in motion by:

- mechanical agitation or passage of sample around baffles within a flocculation reactor;
- the tortuous path through interstices of a granular filter bed and
- flocs that are sufficiently formed by sedimentation within a settling basin.

The effect of velocity gradients within a liquid body is to set up relative velocities between particles thereby providing opportunity for contact. Hence for a given flocculation system, the applied velocity gradient is the principal parameter governing the orthokinetic flocculation rate while the extent of flocculation is governed by both the time taken for the flocculation to occur and the velocity applied. The degree of particle aggregation and rate of the aggregates breakup are influenced by the afore mentioned parameters (Bratby, 2006).

Microalgae cells are known to possess a negative charge on their outermost cell wall that prevents them from aggregating naturally in a suspension (Brennan & Owende, 2010). Addition of multivalent cations and cationic polymers which act as flocculants neutralises

or decreases the negative charge. Aggregation is usually enhanced through a process known as bridging which involves the physical linkage of one or more particles together (Grima *et al.,* 2003). A number of approaches to flocculation methods exist, and this includes:

- Direct addition of flocculating agents;
- Bioflocculation, which involves the addition of polyelectrolytes or flocculating microarganisms to aid flocculation
- Natural flocculation or autoflocculation: some algae flocculate naturally while others aggregate in response to a stimuli such as pH, nitrogen stress or dissolved oxygen levels (Benemann & Oswald, 1996; Uduman *et al.*, 2010). However, autoflocculation is considered slow, unreliable and species specific (Schenk *et al.*, 2008) and therefore can only be applied in particular cases.

Numerous flocculation methods have been tried and two of the above flocculation method can be utilized in a single step. For example, Knuckey *et al*., (2006) developed a process which entailed adjusting the pH of the algae culture to 10 or 10.6, before Magnafloc LT-25 (a non-ionic polymer) is added. Additionally, Chitosan was successfully used as a bioflocculant with pre-pH adjustment by Divakaran & Pillai, (2002) and the residual media could be used for producing fresh algae culture.

In mixing or raceway ponds, flocculation processes are carried out using adjacent settling ponds. Effective flocculants like inorganic chemicals (e.g. ferric chloride, alum and lime) are not economical for large cell productions and usually renders the eventual algal-chemical sludge inappropriate for other downstream uses for example anaerobic digestion and or animal feed supply. In contrast, organic cationic polyelectrolytes, for example Chitosan, are needed in small quantities and allows the use of the eventual residues for downstream purposes (Grima *et al*., 2003). Lavoie *et al*. (1984) showed the feasibility of using Chitosan in an economical way to flocculate freshwater grown algae and subsequent use as animal feed. The pH of the algae culture, the concentration of cells and flocculating agent greatly influence the effectiveness of flocculation (Clasen *et al*., 2000).

1.4.1.2 Flotation

Flotation, otherwise known as 'inverted' sedimentation does not require the addition of chemicals like flocculation though sometimes chemical coagulation is employed to aid the process. This method is focused on the trapping of algae cells using dispersed micro-air bubbles (Wang *et al.*, 2008). Nevertheless, for flotation to be successful, it is vital for the particles to be hydrophobic (Gochin & Solari, 1983).

Some algae strains float naturally on water surfaces as their lipid content increases and usually, oxygen generation under light by algae produces gas bubbles which assist in flotation (Bruton *et al.*, 2009). Microbubbles can be generated through several techniques and this including: turbulent microflotation (Miettinen *et al.*, 2010), induced air flotation (IAF) (Hanotu *et al.*, 2012), dissolved air flotation (DAF) (Edzwald, 2010), and electro-flotation (Hosny, 1996). The generated microbubbles tend to attach to hydrophobic particles resulting in buoyant aggregates which then rise to the surface of the flotation cell where the particles are recovered following bubble rupture (Dai *et al.*, 1998). From the several techniques highlighted, DAF and dispersed air flotation are the most widely developed.

1.4.1.3 Gravity sedimentation

Gravity sedimentation is based upon Stokes law (Schenk *et al.*, 2008) as described in Section 1.4.2.1. It is a method commonly used in waste water treatment to produce algal biomass, and has the ability to treat a large volume of waste water while generating little biomass (Nurdogan & Oswald, 1996). This method is most effectively used for large microalgae such as Spirulina (Muñoz & Guieysse, 2006). Settling or pure sedimentation is used in some algal farms; this is space and time consuming and not an ideal choice for algal biodiesel production.

1.4.2 Thickening (dewatering) techniques

Dewatering is a method for solid-liquid separation. It is aimed at reducing the moisture content of sediments. The major techniques used are centrifugation and microfiltration.

1.4.2.1 Centrifugation

Centrifuges are extensively used in the process industries for solid-liquid separation (Leung, 1998). Centrifugal sedimentation is based on a density difference between two liquid phases or solid and liquid phases; the density gradient is amplified by applying a centrifugal force to the suspension due to rotation at high speeds.

In a dynamic equilibrium as found in a centrifuge, sedimentation involves a balance between two forces: gravitational and hydrodynamic drag forces. While the former is the effective force acting on a particle under gravity, the latter is the force opposing settling. Stokes law is based on an equilibrium between these two forces and states that the sedimentation velocity is proportional to the difference in density between the cells and suspending liquid multiplied by the square of the diameter of the particle and is inversely proportional to viscosity of the liquid (Equation 1.1).

$$v_s = \frac{d^2 g(\rho_L - \rho)}{18\mu} \tag{1-1}$$

where ρ is the density of the liquid phase, ρ_L is the density of particles, d is the particle diameter, g is the gravitational acceleration, μ is the liquid viscosity and V_s is the settling velocity. Stokes law assumes the particles settle without interference and are spherical.

The energy input of centrifugation alone has been valued at 3,000 $kWhton^{-1}$ (Benemann & Oswald, 1996) and hence the choice of centrifugation as a primary recovery method for microalgae harvesting is considered to be energy and cost intensive. Centrifugation is nevertheless a vital secondary harvesting technique to concentrate algal paste (100–200 $g.L^{-1}$) from an initial concentration of 10–20 $g.L^{-1}$. This process is usually used before with oil extraction.

1.4.2.2 Microfiltration

The process of separating solids from liquids with a permeable medium which holds back or retains particles when a suspension passes through it is known as filtration. This is illustrated by the schematic diagram in **Figure 1.3**. In microfiltration, the separation of

solids is usually expressed as mass recovery or total efficiency (retention), while the separation of liquid is usually characterized by the moisture content of the cake or the concentration of solids in the filtrate.

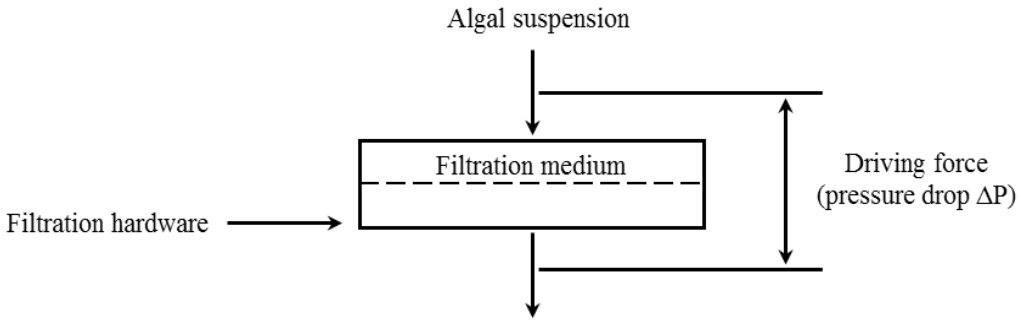

Figure 1-3: Schematic diagram of a filter system adapted from Svarovsky (2001).

Darcys basic filtration equation relating the flow rate Q of a filtrate of viscosity μ (Pa.s) through a bed of thickness L (m) and surface area A (m^2) to the driving pressure ΔP is:

$$Q = K\frac{A\Delta \mathrm{P}}{\mu L} \tag{1-2}$$

Where K is a constant referred to as the permeability of the bed and the equation can be re-written as:

$$Q = \frac{A\Delta P}{\mu R} \tag{1-3}$$

where R is the medium resistance and is equal to L/K which is the ratio of the medium thickness to the permeability of the bed.

Microfiltration is a conventional harvesting process that fits relatively large algae such as *Caelastrum* and Spirulina. Algae species such as *Scenedesmus, Chlorella* and *Dunaleilla* are usually not harvested with filtration as their sizes approach bacterial dimensions (Mohn, 1980). For recovery of cells in this range, membrane microfiltration and ultra-filtration are technically viable alternatives (Petrusevski *et al.*, 1995) because they require

low transmembrane pressure (TMP) and cross-flow velocity conditions (Borowitzka, 1997). In order to promote the efficiency of filtration and because conventional filtration operates under suction and pressure, filtration aids such as cellulose and diatomaceous earth are used (Grima *et al.*, 2003). Mohn in 1980 demonstrated how *Coelastrum proboscideum* produced sludge with 27% w/w solids; showing that filtration processes can achieve a concentration factor of 245 times their starting concentration.

In comparison to centrifugation, membrane filtration can be more cost effective for processing of broth volumes less than 2 m^3day^{-1}. However, due to membrane replacement and the cost of pumping in larger scales of production, it is not considered economical to process volumes greater than 20 m^3day^{-1} (Mackay D, 1988). Similarly, formation of compressible filter cakes, membrane-clogging and in particular high maintenance costs are challenges in large-scale applications of microfiltration. Example of this is the limitation of cost effective cyanobacterium *Spirulina* due to their long spiral shape.

1.5 Cell disruption, lipid extraction and transesterification

Recovery of intracellular products from microalgae requires a cell disruption step. Successfully applied methods include: the use of autoclaving, high pressure homogenisers, acid/base lysis and sonication (Mendes-Pinto *et al.*, 2001). These release the intracellular lipids into the lysis buffer or the suspension medium for extraction to be carried out. Sonication is extensively used at laboratory scale and is effective, however, the lack of information for its feasibility and cost at commercial scale suggests more research into the area is required (Harun *et al.*, 2010).

Numerous methods for extraction of microalgal lipid and related by-products exist but the most common methods include use of chemical solvents, superficial fluid extraction and ultrasound techniques (Harun *et al.*, 2010). The properties of a cell membrane can influence an extraction process. For instance, during solvent extraction, cells are usually exposed to solvents causing an uptake of their molecules which consequently alters cell membrane

thereby enhancing the movement of lipid globules towards the outer cell (Hejazi & Wijffels, 2004). The presence of the cell walls may prevent direct contact of the solvent (Sikkema *et al.*, 1995) and cell membrane and thus impede the extraction process. Hejazi et al (2004) reported that solvent extraction process can be applied to living algae *in situ* in a concept they termed as 'algae-milking'. Also, combine use of organic solvents with methanol and a catalyst is utilized during transesterification to produce biodiesel (Fukuda *et al.*, 2001).

Biodiesel is produced from oils extracted from biological sources through transesterification. Transesterification is a chemical reaction between extracted oil (usually in the form of TG's) and an alcohol in the presence of a catalyst to produce mono-esters (Sharma & Singh, 2009). The reaction (**Figure 1.4**) can be enhanced by a combination of immobilized lipases with methyl esterification (Li *et al.*, 2007).

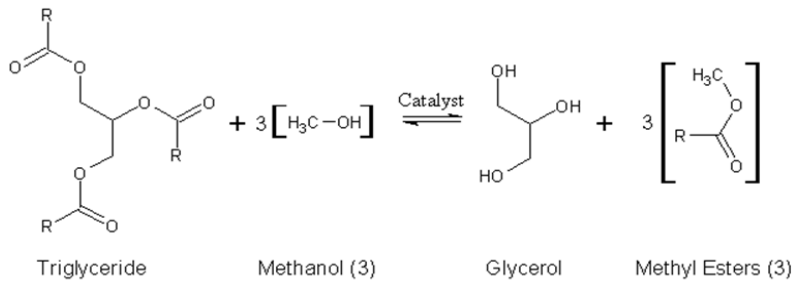

Figure 1-4: Transesterification reaction.

The reaction stoichiometry shows one molecule of parent oil reacting with three molecules of alcohol (methanol) to produce a molecule of glycerol and three molecules of fatty acid methyl esters (FAME) (biodiesel). Glycerol is thus a major by-product of the transesterification reaction.

1.6 Biodiesel production

Biodiesel is produced after extraction and transesterification of microalgal lipids (Section 1.5). **Figure 1.5** is a simple block diagram of biofuel production from microalgae. The

biodiesel produced can be used directly in any kind of diesel engine (Brennan & Owende, 2010) either for transportation or for industrial power generation.

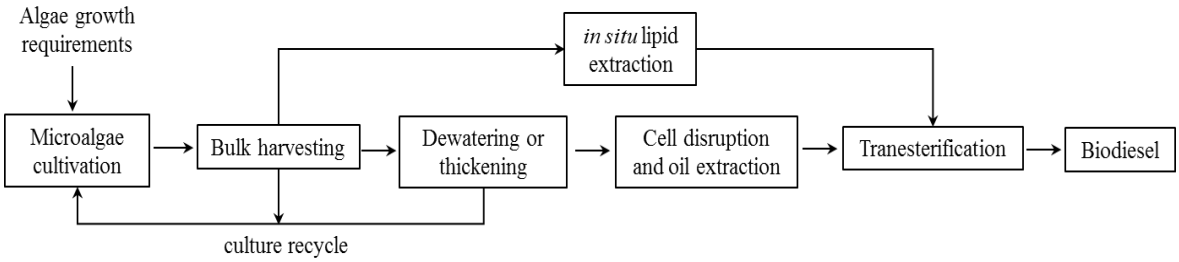

Figure 1-5: An integrated process for biodiesel production from microalgae.

Numerous advantages exist for algal biodiesel. These include being: (1) renewable as they are derived from biomass; (2) quasi-carbon neutral under sustainable production condition; (3) biodegradable and non-toxic i.e. contains reduced levels of soot, particulates, carbon monoxide, SO_x and hydrocarbons. In comparison to petrodiesel, biodiesel has a $33MJL^{-1}$ volumetric energy density, which is about 92% of petrodiesel. Also, biodiesel produces complete combustion when compared to fossil sources due to the presence of longer chains of hydrocarbon. This gives biodiesel an overall efficiency of about 97% of petro diesel (Knothe & Krahl, 2005). Furthermore, a comparison of algal-diesel to first generation biodiesel shows that algal biodiesel is more favourable in the aviation industry where high energy densities and low freezing points are key criteria (NREL, 2006). Additionally, microalgal biodiesel contains reduced CO_2 emissions of up to 78% compared to emissions from petro-diesel (Sheehan, 1998).

Microalgal lipids are easily oxygenated due to their polyunsaturated nature and this increases proportionally to the extent of unsaturation. This was shown by Gunstone & Hilditch (1945) where relative oxidation rates of 25, 12 and 1 were reported for methyl esters of linolenic (18:3), linoleic (18:2) and oleic (18:1) acids respectively. Partial catalytic hydrogenation of these oils can correct the limitation (Dijkstra, 2006). In contrast, the temperature at which the fuel starts to solidify or crystalize and blocks the fuel filters of an engine (cold filter plugging point; CFPP) is lowered by a high degree of polyunsaturation.

With these considerations, colder climates needs higher unsaturated lipid levels of 14:0, 18:1 and 16:1 in the ratio of 1:4:5 as an ideal mix (Schenk *et al.*, 2008). Such biodiesel will possess low oxidative potential while maintaining a good cetane number (CN) and CFPP rating.

For algal biodiesel to be acceptable as an alternative to fossil fuel, its properties must match the International Biodiesel Standard for Vehicles (EN14214). The quality of the alkyl ester plays an important role, as it determines the performance and stability of the fuel (Griffiths & Harrison, 2009). Nonetheless, algal-diesel possesses similar chemical and physical properties to petro-diesel and also compares favourably with those of the international standard (**Table 1.5**).

Table 1-5: Selected properties of first generation biodiesel (FGB), algal biodiesel and typical diesel (Fukuda *et al.*, 2001; Xu *et al.*, 2006).

Fuel Property	**FGB**	**Algal Biodiesel**	**Diesel**	**EN14214 Biodiesel Standard**
HHV (MJ kg^{-1})	31.8–42.3	41	45.9	–
Kinematic viscosity ($mm^2.s^{-1}$)	3.6–9.48	5.2	1.2–3.5	3.5–5.2
Density ($kg.L^{-1}$)	0.86–0.895	0.864	0.83–0.84	0.86–0.90
Carbon (wt%)	77	–	87	–
Hydrogen (wt%)	12	–	13	–
Oxygen (wt%)	11	–	0	–
Sulphur (wt%)	0–0.0015	–	0.05 max	<10
Boiling point (°C)	315–350	–	180–340	–
Flash point (°C)	100–170	115	60–80	>101
Cloud point (°C)	-3 to 12	–	-15 to 5	–
Pour point (°C)	-15 to10	-12	-35 to -15	–
Cetane number	45–65	_	51	>51

1.7 Prospects and challenges for the commercialization of algal biofuels

The combined use of microalgae for renewable energy production, environmental application (CO_2 sequestration or greenhouse gas (GHG) emission mitigation) and wastewater treatment is one of the major features that support its potential for large scale production. More so, Section 1.1 highlights the potentials of biofuel due to the current state of fossil fuel use (**Figure 1.1**). Although considerable progress in biofuels development has been made, scope for improvement in its industrial production is still being researched. Several studies have been carried out on the isolation and characterization of numerous microalgae species (Zimmerman *et al.*, 2011) for biodiesel production; with more focus on high oil content species as explained in Section 1.3.2.

Development of technology for algal products can be quite challenging. In putting conceptual designs and scaling up laboratory trials into industrial scale, a number of considerations have to be met. This could either be susceptible to external influences or cost intensive (Chen *et al.*, 2009). The whole process of algal bioprocessing is faced by the aforementioned problems (from culturing, oil extraction down to deposition of residues), therefore, fundamental developments are needed to optimize every part of the process.

Issues with the culturing of algae lie in the fact that numerous species are being studied with development of techniques for single species cultivation (Ugwu *et al.*, 2008). Also, in order for a strain to make a considerable contribution to the biofuels market at a competitive price, it must possess at least 40% w/w lipids (Ratledge & Cohen, 2008). Another challenge with algal cultivation is scale-up due to the limitation of light penetration usually required for phototrophic or mixotrophic growth. This can be addressed by improving the mixing in bioreactors and open cultivation ponds.

The challenges of downstream processing (DSP) and oil extraction are that the biomass harvesting cost can be significant (Uduman *et al.*, 2010) and a study by Chisti (2007) showed how the recovery process contributed 50% of the final cost of the recovered oil. In another study by Norsker *et al.* (2010), centrifugation was recognized as the critical cost

contributor of the production cost in raceway ponds. Moreover, Grima *et al*. (2003), mentioned centrifugation as an efficient but energy intensive method; whose efficiency depends on the cell settling characteristics and conditions utilized for separation. With reference to extraction of microalgae intracellular lipids, existing methods are complex, costly or underdeveloped. For the methods being explored (Section 1.5), some are characterized with low extraction efficiency as a result of insufficient dewatering or cell disruption (Chen *et al.*, 2009).

Considering the advances in omics and genetic engineering, photobioreactor engineering and bulk harvesting methods, some techno-economic challenges preventing the commercial viability of microalgal products would soon be overcome. For microalgal oils to serve as hydrocarbon feedstocks replacing petroleum, they will need to be sourced at prices closely related to that of crude oil (Chisti, 2007). Equation 1.4 shows this relationship, which assumes algal oil contains 80% of the energy content of crude petroleum.

$$C_{\text{algal oil}} = 6.9 \times 10^{-3}\, C_{\text{petroleum}} \qquad (1\text{-}4)$$

where $C_{\text{algal oil}}$ is the price of microalga oil ($ per litre) and $C_{\text{petroleum}}$ is the price of crude oil ($ per barrel).

1.8 Scale down and USD approaches to dewatering methods

Process development using pilot scale equipment requires large volumes of feed and is expensive and labour-intensive. In bioprocess development, scale-down approaches have been developed so that reduced feedstocks will be utilized and therefore, serves as a tool valuable for time and cost reduction. Scale-down methods involve linearly scaling down all unit operation dimensions or mimicking the procedure using designs that maintain the principles surrounding the process. An example of scale reduction in centrifugation using a disc stack centrifuge was shown by Kempken *et al.*, (1995). This was achieved by using

a geometrically similar machine and reducing the number of active discs available for separation (Mannweiler & Hoare, 1992). Geometric similarity was also used for scroll decanter scale-down (Lydersen *et al.,* 1994). These approaches however, still utilize litres of material and have limitations due to complexity of the design of industrial-scale equipment.

Further work to enhance the predictability of large scale process performance using small-scale models led to development of USD methods. These techniques were significantly different from typical scale-down approaches as they mimic critical parameters which affect large scale equipment performance without maintaining geometric similarity (Titchener-Hooker *et al.,* 2008). For example, simply employing the concept of equivalent settling velocity in traditional laboratory centrifugation using centrifuge tubes was seen not capable of mimicking continuous flow centrifuge performance (Boychyn *et al.*, 2004). More so, Berrill *et al.,* (2008) showed how USD approach was used to optimize flocculation of *E.coli* lysate followed by centrifugal clarification and scale-up verification using disc stack centrifuge.

A range of scale-down techniques for filtration processes and their application has been reviewed by Jaffrin, (2008). In scaling down a filtration process, two variables are considered key. First the feed volume has to be reduced accordingly in order to keep filtration processing times similar at both scales of operation. Therefore, the ratio of feed volume to membrane area is a crucial measure in scale down study and needs to be kept constant. Second, variations in operating conditions of small scale studies can lead to large scale prediction problems and therefore fluctuations in major parameters governing filtration such as pressure and flux control should be avoided (Ma *et al.,* 2010).

1.8.1 USD centrifugation

USD to investigate industrial centrifuges has been extensively researched. Ambler in 1952, showed how sigma theories can be used to compare the performance of geometrically dissimilar centrifuges and also centrifuges of different sizes and design. This approach

maintains the ratio of flow rate to equivalent settling area constant which results in the same centrifugal clarification. The Sigma correlation captures all operating and equipment variables. Therefore, different centrifuge designs result in different expressions for the settling area. A general form of expressing the Sigma Factor (Σ) is given in Equation 1.5. The Sigma Factor for continuous flow tubular-type centrifuge and for a batch laboratory centrifuge is given by Equation 1.6 and 1.7 respectively.

$$\Sigma = (\text{Area}) \times (\text{settling due to gravity}) \equiv (\mathrm{L} \times \mathrm{r})\frac{\mathrm{N}^2\mathrm{r}}{\mathrm{g}} \times \text{geometric factors} \tag{1-5}$$

where N is bowl speed (rev.s^{-1}), L is bowl height (m); r is the characteristic radius (m) and g acceleration due to gravity (ms^{-2}).

$$\Sigma_{tb} = \frac{\pi\omega^2\mathrm{L}}{\mathrm{g}} \times \left[\frac{{\mathrm{r}_0}^2 - {\mathrm{r}_1}^2}{\log_{\mathrm{e}}\left(\frac{2{\mathrm{r}_0}^2}{{\mathrm{r}_0}^2 + {\mathrm{r}_1}^2}\right)}\right] \tag{1-6}$$

where ω is angular velocity (equal to 2πN) (rev.s^{-1}), r_1 and r_0 are the inner and outer radii position of a settling particle and L is the length of the settling tank.

$$\Sigma_{\mathrm{lab}} = \frac{\mathrm{F_{lab}V_{lab}}\omega^2}{2\mathrm{g} \times \mathrm{Ln}\left(\frac{2\mathrm{r}_2}{\mathrm{r}_2 + \mathrm{r}_1}\right)} \tag{1-7}$$

where ω is angular velocity (equal to 2πN)(rev.s^{-1}), r_1 and r_2 are the inner and outer radii i.e. the respective distances between the centre of rotation and the top of the liquid and the bottom of the tube, F_{lab} is the calibration factor to allow for non-ideal flow and V_{lab} is the volume of feed in the centrifuge tube.

In order to achieve a given separation in a continuous gravity settler, it must accommodate the characteristic particle settling velocity via a combination of flow rate and settler cross sectional area (Equation 1.9). Using this analogy in centrifuges (Lander *et al.*, 2005), area

(m^2) is substituted by Σ (m^2) in Equation (1.9) and this provides a velocity expression (Equation 1.10) corresponding to the removal of particles that settle at a given velocity or greater in a normal gravitational field.

$$V = \frac{Q}{A} \tag{1-8}$$

where Q is flow rate ($m^3.s^{-1}$) and A is the cross sectional area (m^2).

$$V = \frac{Q}{\Sigma} \tag{1-9}$$

Boychyn *et al.,* (2000) and (2004) developed a USD method that involved using a bench top centrifuge to mimic the clarification of large scale centrifuges. This method involved a two-step approach to achieve clarification; first by pre-shearing the cell suspension in a small rotating disc device (Section 2.3.3.2) followed by bench top centrifugation (using Sigma theory). Levy *et al.*, (1999) has previously described the construction of the rotating disc device; however the design has been modified (Hutchinson *et al.*, 2006). A study by Mannweiler & Hoare, (1992) showed how the majority of material breakage occurs in the feed zone of a disc-stack centrifuge while Boychyn *et al.*, (2000) affirmed it for a multi-chamber bowl centrifuge. The pre-shearing concept of the USD methodology reproduces the shear forces experienced in the feed zone of large scale centrifuges prior to solid liquid separation. The consequence of this breakage is reduced clarification performance due to increased production of fine particles. **Table 1.6** shows a summary of some USD centrifugation methods to predict large scale centrifuge performance.

1.8.2 USD rotating disc filter (microfiltration)

Shear enhanced filtration otherwise known as dynamic filtration consists of creating a membrane shear rate necessary to maintain filtration using a rotating disc (Jaffrin, 2008). This has been recognized as an efficient factor for increasing permeat flux as well as reducing cake build up in microfiltration. USD filter or RDF, as it is termed (Murkes, 1988)

has been applied using very high levels of flux and transmission (Brou *et al.*, 2003) to separate complex suspensions.

Feed flow rate does not influence the wall shear rate of the RDF (Ma, 2009). In traditional cross flow filtration (CFF), reducing the tube diameter or channel thickness and increasing the axial velocity along the membrane will lead to high shear rates at the membrane surface (Jaffrin, 2008).

Equation 1.10 shows the local shear rate is a function of disc radius for slow rotating speeds using laminar flow (Bouzerar *et al.*, 2000).

$$\gamma = 0.77\rho(k'\omega)^{1.5} r v^{-0.5} \tag{1-10}$$

where ρ is the fluid density, k*'* the velocity coefficient, ω is the rotating speed of the disc, r the radius of the rotating disc and ν the fluid kinematic viscosity. Although Brou *et al.*, (2003) reported that the coefficient could change if a smooth disc was equipped with vanes.

Under turbulent flow condition, local shear rate across the membrane was generated using the Blasius friction coefficient for a flat plate (Equation 1.11) while mean membrane shear rate (γ_m) along the radius of the shear cell is given by Equation 1.12.

$$\gamma = 0.0296(k'\omega)^{1.8} r^{1.6} v^{-0.8} \tag{1-11}$$

$$\gamma_m = 0.0164(k'\omega)^{1.8} r^{1.6} v^{-0.8} = 0.55\gamma_{max} \tag{1-12}$$

Shear rate estimation of the RDF (Section 2.4.2.2) was carried out using computational fluid dynamics (CFD) simulation (Ma *et al.*, 2010) since CFD is widely used in modelling of filtration units (Taha & Cui, 2002) and the hydrodynamics in RDF (Francis *et al.*, 2006). At a certain membrane loading level, Lee *et al.* (1995) observed that there was a critical speed below which the RDF behaved similar to a flat sheet system using an equivalent level of shear. This was confirmed by Ma *et al.*, (2010) using conventional CFF systems. This also served as a motivaton for trying this system to mimic hollow fibres in this thesis.

Table 1-6: Summary of USD methods methods used to predict large scale centrifuge clarification or dewatering performance.

Process Feed	**USD Methodology**	**Scale (mL)**	**Centrifuge type**	**Reference**
Baker's yeast homogenate	Sigma concept	30	Multichamber	Boychyn *et al.* (2000)
Baker's yeast homogenate and protein precipitate	Conventional USD as described by Boychyn, (2000). Further showed how feed breakage occurred during entry to centrifuge feed zone by matching the energy dissipation rate profile of the large scale centrifuge to the high-speed rotating-disc device	15	Multichamber	Boychyn *et al.* (2001)
P.pastoris broth	Mimics high solids density feeds (>10% ww/v) by pre-dilution to (approx. 2% ww/v) followed by USD according to Boychyn, (2000)	15	Disc-stack Carr powerfuge™ Multichamber	Salte *et al.* (2006)
E. coli broth and Baker's yeast suspensions	Same as Salte et al, (2006)	15	Disc-stack Carr powerfuge™	Tustian *et al.* (2007)
Baker's yeast homogenate and polyvinyl acetate particles	Sigma concept - accounting for acceleration and deceleration stages studies of shear insensitive and shear-sensitive materials	10	Disc-stack	Maybury *et al.* (2000)
Mammalian cell culture broths	Sigma concept	10	Disc-stack	Hutchinson *et al.* (2006)
Waste sludge	Mimic residence times (based on scroll speed) and centrifugal forces	10-15	Scroll decanter	Vesilind (1970)
Homogenised Baker's yeast	Mimic residence times (based on scroll speed) and centrifugal forces	15-20	Scroll decanter	Rumpus (1998)
Fungal antibody fragment	USD device and computational fluid dynamics (CFD) simulations	35	Basket Filter	Boulding *et al.* (2002)
P. pastoris	Dewatering at USD level to achieve equivalent height of wet solids at pilot scale	2 - 15	Nozzle centrifuge Disc-stack	Lopes *et al.* (2012)

1.9 Aim and objectives

As described in Section 1.1 the need for a sustainable and economic alternative to fossil fuels is widely recognised. While a number of options are currently being explored (Section 1.2), microalgae represent one of the most promising feedstocks due to the advantages highlighted in Section 1.3.2. These include: production throughout the year (with yields exceeding the best oilseed crops), simple growth requirements and lack of competition with food production or use of arable land. At the same time, the bio-process technology surrounding the economic production of microalgal products at manufacturing scale is still poorly defined. The vast majority of work has focussed on algal strain selection (Section 1.7) and bioreactor technologies for optimum cell growth (Section 1.3.3.2) with relatively few studies on downstream processing operations (Section 1.4).

In terms of research on the harvesting of microalgae cells, studies to date have addressed dissolved air floatation, flocculation using different techniques, drying and microfiltration (Section 1.4). There have been no published studies on centrifugation. The results of the published works tend to indicate that no single harvesting method or combination best suits all microalgal species (Mata *et al.*, 2010) or class of product. Furthermore, the choices being explored have placed a large carbon footprint on microalgal bioprocessing because of the low biomass or product concentrations achieved and hence the scales of operation involved. Dewatering during initial solid-liquid separation operations is important because of the high moisture content of algal biomass on subsequent processing steps and cost (Grima *et al.*, 2003). Primary recovery stages are therefore critical and optimum choices of operations, together with sequence of operations, needs to be explored on a case-by-case basis.

The availability of small scale predictive tools of key product recovery operations will greatly facilitate downstream process synthesis for microalgae. USD technologies represent a promising approach due to the small volumes of material required (2-20 mL)

and their ability to quantitatively predict larger scale process performance (Section 1.8). While USD technologies have been developed to study centrifugation (Boychyn *et al.*, 2004; Tait *et al.*, 2009) and filtration (Jackson *et al.*, 2006; Kong *et al.*, 2010; Ma *et al.*, 2010) of microbial and mammalian cells, no studies have so far been reported on the use of USD technologies with microalgal cells.

The overall **aim** of this project is therefore to establish an ultra scale-down platform for the rapid evaluation of pre-treatment and recovery operations for microalgae downstream process synthesis. **Figure 1.6** shows the emphasis on flocculation as a pre-treatment method (Section 1.4.1.1) and either centrifugation or microfiltration (Section 1.4.2) as the options for solid-liquid separation. In terms of the downstream unit operations these were selected based on their industrial relevance. For example, a hollow fibre membrane configuration was selected for microfiltration studies because feedback from various equipment vendors suggested that a number of companies are currently investigating this technology for microalgae recovery. Similarly the CARR Powerfuge™ was chosen for the study of centrifugation due to its superior dewatering ability over other centrifuges which could benefit subsequent downstream processing steps such as lipid extraction. Specific **objectives** to achieve the overall project aim are as follows:

- To carry out preliminary studies on the growth kinetics of microalgal cultures. This will involve growing several strains in different media in order to ascertain fast growing and high yielding species. This will be necessary in order to reliably produce sufficient material of consistent quality for DSP studies. This work is described in Chapter 3.
- To design and fabricate scale-down flocculation reactors that can mimic the performance of a conventional lab scale stirred flocculation reactor and provide representative quantities of suitable material for subsequent USD studies. The flocculation reactors will be characterised based on mixing time and key flocculation variables in order to ensure reproducible floc size-profile and stability.

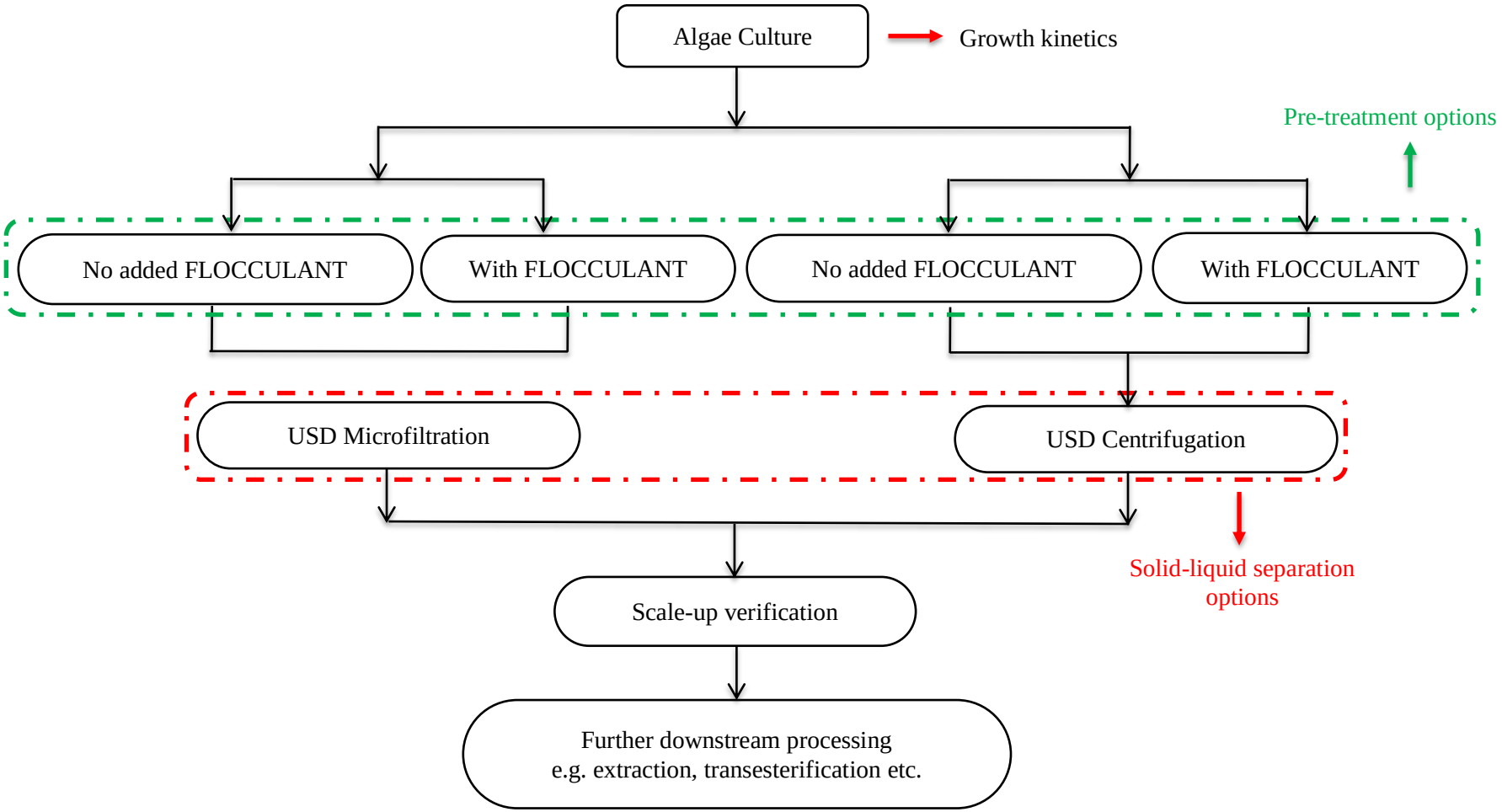

Figure 1-6: Overview of the USD platform to be established in this work. Figure indicates the primary unit operation to be addressed and the various process sequences that need to be evaluated.

The results of this work are also described in Chapter 3.

- To establish a USD method for the study of microalgae microfiltration processes and the impact of flocculation as a pre-treatment step. Once optimized, the effect of growth conditions on membrane fouling will be investigated and filtration performance of flocculated and unflocculated algae broth compared. The results of this work are presented in Chapter 4.
- To establish a USD method for the study of centrifugation for microalgae recovery and the impact of flocculation as a pre-treatment step. This work will also demonstrate how pre-treatment prior to centrifugation influences not just efficiency but also the overall product (lipid) recovery. The results of this work are presented in Chapter 5.
- To establish and compare the use of sonication and homogenization as small scale cell disruption operations for lipid release from harvested cells. The whole USD platform will then be used to study the various downstream process sequences shown in **Figure 1.6** and their impact on overall lipid extraction and transesterification. The results of this work are described in Chapter 6.

In addition to the above, Chapter 2 outlines the experimental methods and equipment used while Chapter 7 provides an analysis of the overall findings and options for further work. In particular, Chapter 7 will consider the benefits of the USD platform and its wider applicability for microalgal downstream process synthesis.

2. Materials and Methods

In this chapter, the general experimental methodologies and analytical techniques used in this thesis will be described. In some cases further specific detail on particular experiments will be provided in the appropriate results chapters.

2.1 Materials

Analytical reagents were of the highest purity available and were purchased from either Sigma-Aldrich (Dorset, UK) or obtained through VWR International (Leicestershire, UK). Filtration materials; 25 mm diameter disc sheets and hollow fibre membranes were purchased from Sterlitech (Kent, US) and GE Healthcare (Amersham, UK) respectively. Normalize Water Permeability (NWP) tests and dilutions requiring deionized (DI) water were performed using water from a Milli-Q® Water Ultra Purification System (Merck Millipore, Hertfordshire, UK). All media and reagents were made up in the same water.

2.2 Algae strain and culture conditions

The microalgae *C.sorokiniana* (UTEX 1230) was obtained from the culture collection of algae at the University of Texas at Austen while *C.vulgaris* (CCAP 13/C), *C.reinhardtii* (CCAP 11/32A) and *S.obliquus* (CCAP 276/3A) were purchased from the Culture Collection of Algae and Protozoa (Argyll, Scotland, UK). The strains were kept on agar plates and slants of modified Tris-Base-Phosphate (TBP) medium. These were maintained

phototrophically at room temperature under continuous illumination of 22 $\mu mols^{-1}m^{-2}$ until a considerable amount of green colonies formed. They were then stored at 4°C. Microalgae broths was produced either phototrophically (with continuous illumination of 54 $\mu mols^{-1}m^{-2}$) or heterotrophically in various growth media such as TBP, Bold Basal Media (BBM) or Euglena Gracilis

medium (EG); the compositions of these media are shown in **Table 2.1**. The initial pH of TBP and BBM medium were adjusted with concentrated HCl to be between 7.0-7.1 while the pH of EG was between 7.1 – 7.2 after medium formulation. Prior to use, each medium was sterilized in a Getinge autoclave (Nottinghamshire, UK) at 120°C for 20 min. When grown heterotrophically, the same media were used supplemented with 10 $g.L^{-1}$ glucose as carbon source, which was pre-sterilised by filtration using Millipore® Stericup™ filtration system (Sigma-Aldrich, Dorset, UK) and added prior to inoculation.

Table 2-1: Composition of TBP (tris acetate phosphate), EG and BBM media used in this work.

TBP (per L)	**EG (per L)**	**BBM (per 400 mL)**
0.4g NH_4Cl	2g Tryptone	10g $NaNO_3$
0.05g $CaCl_2.2H_2O$	2g Yeast extract	1g $CaCl_2.2H_2O$
0.06g $MgSO_4.2H_2O$	1g Lab-Lemco Powder	3g $MgSO_4.7H_2O$
0.12g K_2HPO_4 anhydrous	1g $CH_3COONa{\cdot}3H_2O$	3g K_2HPO_4 anhydrous
0.06g KH_2PO_4 anhydrous	10 mL ~ 0.1g $CaCl_2$	7g KH_2PO_4 anhydrous
100 mL~ 2 mM Tris base		1g NaCl
1 mL trace element**		1 mL Trace element**
		+ 31g KOH

Note** trace elements consists of: 11.14g H_3BO_3, 22g $ZnSO_4{\cdot}7H_2O$, 5.1g $MnCl_2{\cdot}4H_2O$, 5.0g $FeSO_4{\cdot}7H_2O$, 1.60g $CoCl_2{\cdot}6H_2O$, 1.6g $CuSO_4{\cdot}4H_2O$, 1.1g $(NH_4)_6Mo_7O_{24}{\cdot}4H_2O$ and 50g $EDTA{\cdot}Na_2$ in 1L of water.

Seed cultures were grown in 250 mL Erlenmeyer flasks with cells taken directly from a plate and then placed in a Kuhner incubator shaker ISF1-X (Basel, Switzerland) fitted with fluorescent tubes (cool white). The cells were grown for 4 days at 27°C with orbital shaking at 180 rpm and 25 mm throw. Transfer cultures were prepared with this exponentially growing inoculum to a starting optical density (OD) between 0.15 - 0.20 into Erlenmeyer flasks or bioreactors (as described in Section 2.2.1 and 2.2.2).

2.2.1 Shake flask (SF) cultivation

250 mL Erlenmeyer flasks were used for laboratory scale algal cultivation. A total medium volume of 100 mL was used for each batch experiment. Prior to use, flasks were sealed with cotton wool and autoclaved. When utilized for heterotrophic growth, each flask was further covered with aluminium foil whilst in the shaker during growth.

2.2.2 Stirred tank reactor (STR)

Scale-up studies of heterotrophically grown *C.sorokiniana* were carried out in a 7.5 L New Brunswick stirred tank bioreactor using a working volume of 4 L. TBP media was prepared as described in **Table 2.1**. Calibration of pH and dissolved oxygen tension (DOT) probes was performed as per Standard Operating Procedures (SOPs) and the vessel then autoclaved in a Getinge autoclave (Nottinghamshire, UK) at 121ºC for 15 min after which the DOT probe was allowed to polarise for 7 hrs. Bioreactor details and operation are as described by Ojo (2015). Scale-up between the shake flask (250 mL) and STR experiments was on the basis of matched oxygen mass transfer coefficient, k_La (Ojo, 2015).

2.3 Equipment design and operation

2.3.1 Flocculation reactors

2.3.1.1 Laboratory scale flocculation reactor

The laboratory scale STR used in Section 2.2.2 was also used for flocculation scale-up studies. The geometry of this reactor is shown in **Figure 2.1**.

2.3.1.2 Scale-down flocculation reactors

Three different scale-down flocculation reactors (120, 250 and 500 mL total volume) with geometries similar to that of the laboratory scale bioreactor were designed and fabricated in the UCL Department of Biochemical Engineering workshop. These reactors were used for small scale flocculation studies depending on the volume of feed required for subsequent downstream process experiments. Geometric ratios and dimensions of these reactors are shown in **Figure 2.1.** Photographs of the scale-down reactors are shown later in Chapter 3.

Using experimental procedures as described by Rodriguez *et al,* (2013), the reactors were initially characterized based on fluid mixing time. First, a solution containing type 2 pure lab water (ASTMD1193) and pH indicators which has previously been acidified with 0.5M HCl (red colour) was stirred at the desired rotational speed. This gradually turns yellowish-green upon addition of base (NaOH). The time taken for the colour change is the time for homogeneity to be achieved. From this study, an impeller rotational speed of 350 rpm shows the rapid attainment of homogeneity (< 8 s) in all three scale-down reactors. This rotational speed was thus employed during flocculant addition while an impeller rotational speed of 80 rpm was used for floc ageing post formation.

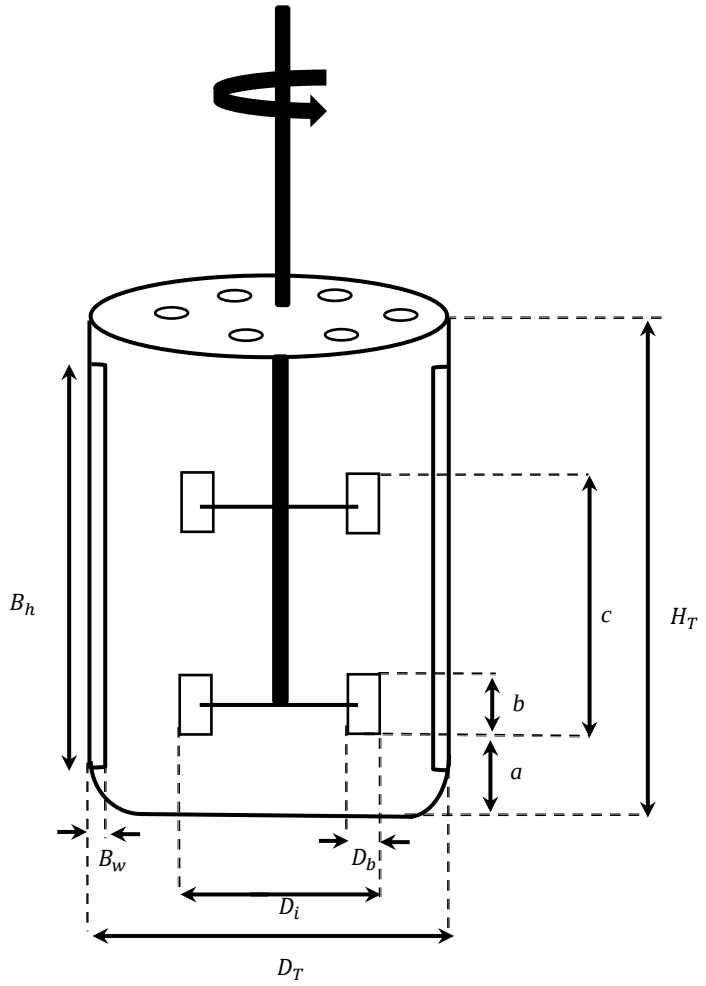

Figure 2-1: Schematic diagram of flocculation reactor (not to scale). Aspect ratio for 7.5 L reactor, D_T:H_T = 1:1.8 and scale-down flocculation reactors, D_T:H_T = 1:1.5. All other dimensions and geometric ratios are as follows: H_T = 18.0 cm, 11.3 cm, 8.9 cm and 7.0 cm for 7.5 L reactor, 500 mL, 250 mL and 120 mL respectively; D_i:D_T = 1:3; D_b:D_i = 1:5; B_w:D_T = 1:10; B_h:H_T = 1:1.05; a:D_T = 1:3; b:D_i = 1:4; c:H_L = 2:3.

2.3.2 Microfiltration equipment

2.3.2.1 AKTA CrossFlow

The AKTA CrossFlow (GE Healthcare, UK) is a fully automated system designed to facilitate process development and optimization of filtration operations. The main components of this instrument are shown in **Figure 2.2a** and these include: transfer valve block (T_1 & T_2), retentate valve block (B), permeate valve block (C), CFF cartridge holder (D), reservoir tank (E), corresponding pumps for each component (transfer lines - T_p, permeate - C_p and feed - F_p) and also their corresponding pressure sensors (transfer lines - P_T, permeate - P_p, retentate - P_R and feed – P_f). An illustration of the fluid flow path is shown in **Figure 2.2b**. This equipment was used in this project to achieve microfiltration at laboratory scale using hollow fibre membranes (as described in Section 2.4.2.1) and for scale down studies using a USD rotating disc filter (Section 2.4.2.2).

2.3.2.2 USD rotating disc filter (RDF)

The RDF is a custom-built USD filtration device that consists of a filtration chamber made of Perspex. It is fitted with a 15 mm diameter stainless steel rotating disc having a 4º conical cross section (driven by high efficiency Out Runner Motor 920 kV Park 400) at the top. The device has an internal diameter of 21 mm and a total volume of 1.7 mL. A flat disc membrane with an effective area of 3.46 cm^2 is placed under the rotating disc in position (6) (**Figure 2.3**) above the permeate port allowing a 1mm gap between the disc and membrane surface. It also consists of an O-ring seal (7) which sits on the filter to ensure chamber is leak-proof. Points a, c and d are connected to the respective pumps via Luer lock feed fittings (1).

a)

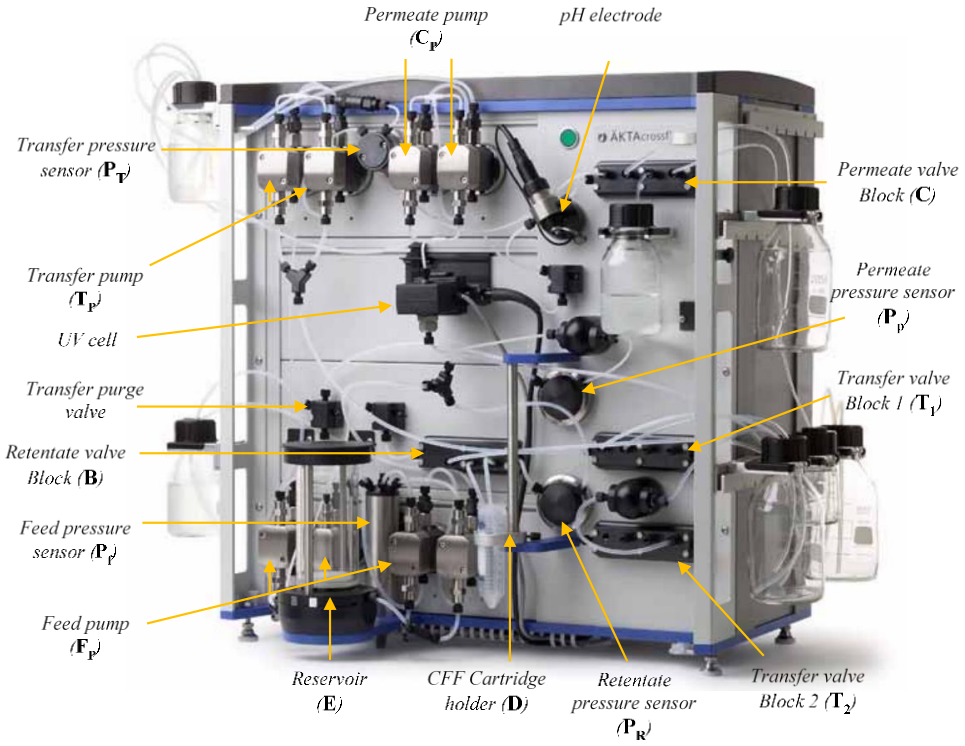

b)

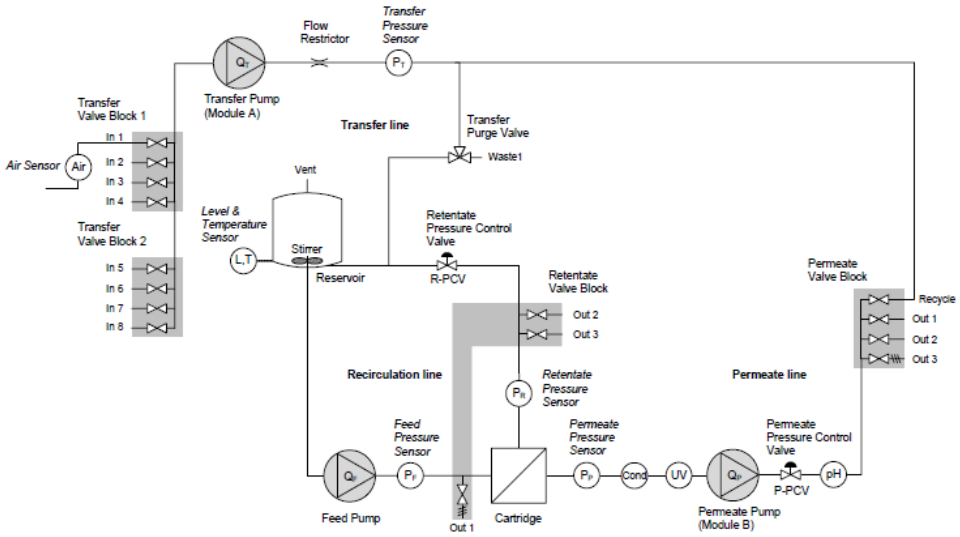

Figure 2-2: AKTA cross flow filtration (CFF) unit used to achieve filtration (a) showing the major components and (b) PID diagram of fluid flow path.

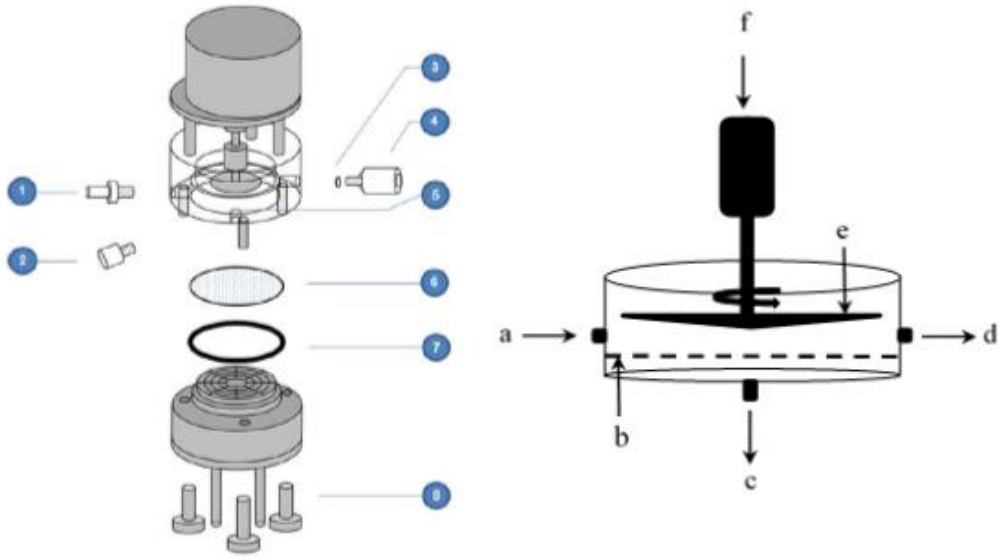

Figure 2-3: Schematic diagram of the USD, RDF filter device showing the different components: a) feed inlet b) membrane disc c) permeate port d) retentate port e) rotating shear disc and f) motor.

2.3.3 Centrifugation

2.3.3.1 CARR Powerfuge™

The CARR powerfuge™ PneumaticScaleAngelus (Cuyahoga Falls, OH, USA) is a tubular bowl centrifuge that can operate between 5000 – 15000 rpm and with an operating feed flow range of 0.1 – 1 L.min^{-1}. **Figure 2.4** shows a cross section of a CARR powerfuge and a picture of the actual equipment used in this thesis. Feed was pumped into the equipment via the top and solids were retained within the bowl. Glycol was circulated through the cooling jacket of the settling bowl to maintain the temperature at 16°C and upon completion of the solid-liquid separation, a scrapper mechanism within the bowl allows the solids to discharge from the bottom of the machine.

2.3.3.2 USD shear device

The USD shear device has a stainless steel chamber that houses a 40 mm diameter-rotating disk (**Figure 2.5a**). The chamber is 50 mm in diameter and has a 10 mm height with total working volume of approximately 20 mL. The device has previously been characterized by Boychyn *et al.* (2004). The disk rotates at an adjustable speed of 1000 - 35000 rpm that generates a maximum elongation strain rate of 1.7×10^4 s^{-1}. For the purpose of this work, rotating disk speeds of 5000, 9209 and 15565 rpm corresponding to a range of energy dissipation rates of 2.86×10^4, 2×10^5 and 1.4×10^6 Wkg^{-1} respectively were employed for a period of 20s at room temperature.

Prior to each experiment, the device was initially washed with DI water. Both flocculated and non-flocculated algae cells were subjected to hydrodynamic forces in this device. For each experiment, the compartment was completely filled with either broth or floc suspensions so as to reduce the possibility of air-liquid interface generation. This device was used for both USD centrifugation and shear studies. All of these experiments were performed in triplicate.

a)

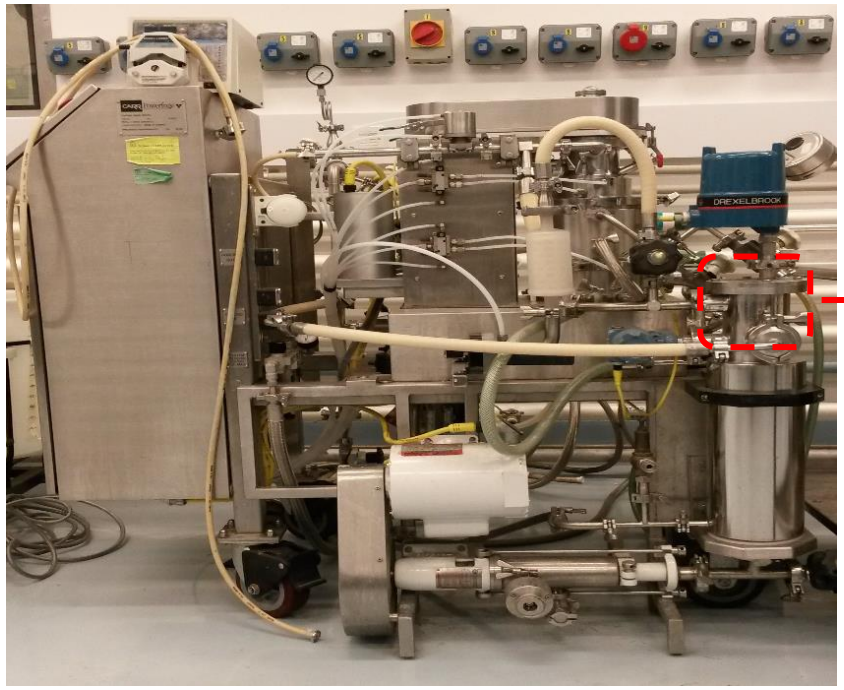

b)

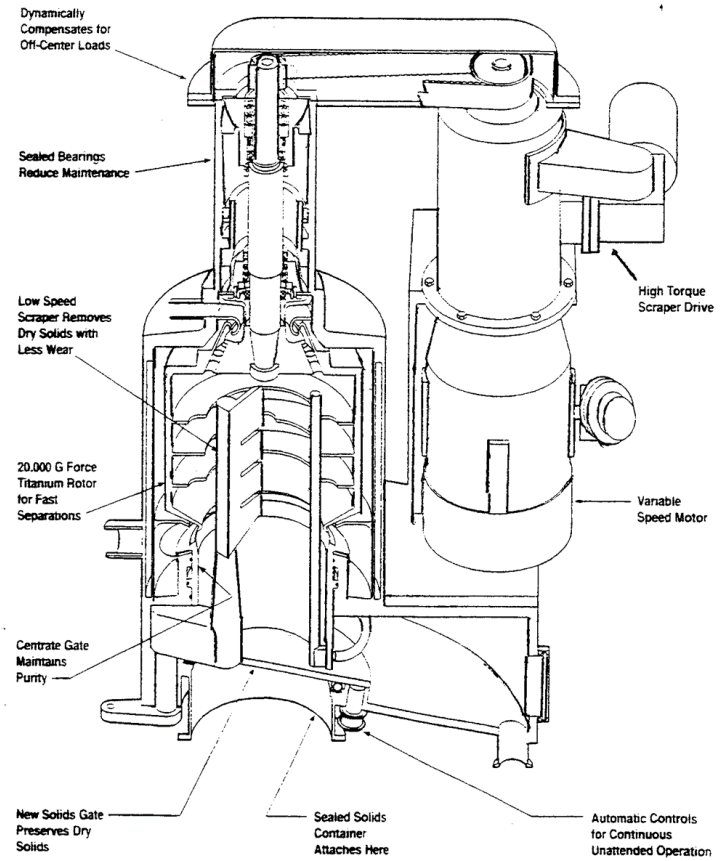

Figure 2-4: (a) Photograph of the pilot scale centrifuge used in this thesis (CARR powerfuge™) with dotted lines indicating the position of the settling bowl and (b) an illustration of the cross section of the feed bowl.

a)

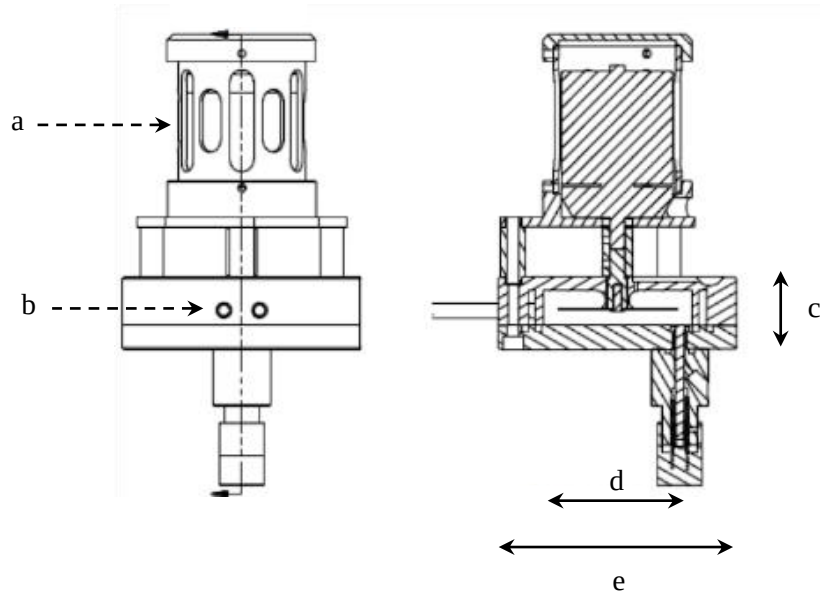

b)

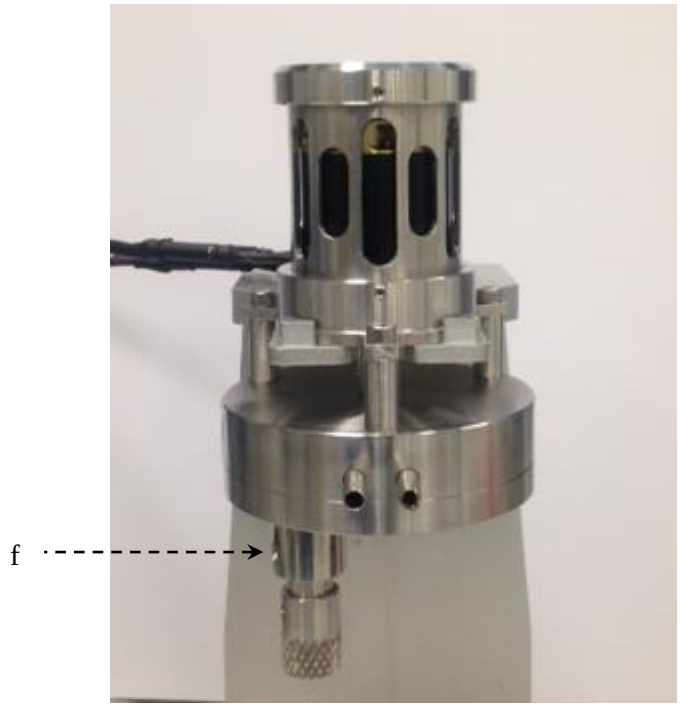

Figure 2-5: a) Schematic diagram of the shear device used for USD centrifugation and shear evaluation of microalgal cells and flocs: a = motor, b = cooling port (water inlet and outlet), c = 1 mm, d = 40 mm, e = 50 mm and b) photograph of the device; f = feed inlet/outlet.

2.4 Experimental procedures

2.4.1 Flocculation

2.4.1.1 Flocculant preparation

Commercially prepared Chitosan powder (VWR international, Leicestershire, UK) was used for all flocculation studies. This was prepared according to Divakaran and Pillai (2002) with minor modifications. Varying amount of Chitosan powder (50 – 500 mg) was weighed and dissolved in an appropriate volume of 0.1M HCl (5 – 50 mL). This was then allowed to mix for one hour and the mixture was made up to 100 mL with DI water to make a final solution containing 0.5 – 5 mg Chitosan per mL.

2.4.1.2 Flocculation procedure

The pH of the algae culture was adjusted to be between 6.0 and 6.1 using concentrated HCl prior to flocculation. The required amount of Chitosan was added at a particular flow rate (or for time of addition studies; t_{add}) over a range of concentrations (0.5-5 mg) or at the optimal concentration. After floc ageing, the broth was remixed (to ensure homogeneity) and sampled into aliquots either for microscopic imaging (Section 2.10.8), shear stability evaluation (Section 2.3.3.2) or solid-liquid separation studies (Section 2.4.2 and 2.4.3). The recovery efficiency of biomass was calculated using Equation 2.1:

$$R = C_i \times \frac{C_f}{C_i} \times 100 \tag{2-1}$$

where C_i and C_f denote the initial and final biomass concentrations at a fixed point in the flocculation reactor.

The flocculation reactors described in Section 2.3.1.2 were used for scale-down flocculation studies. For pilot scale flocculation process, at point of harvest, cells were flocculated *in situ* in the 7.5L STR using the optimal Chitosan dosage. For flocculation studies scale-up was performed on the basis of constant tip speed (Equation 2.2).

$$V_{tip} = \pi N D_i \quad (2\text{-}2)$$

where V_{tip} is the impeller tip speed (s^{-1}), N the rotational speed (rps) and D_i the diameter of the impeller (m).

2.4.2 Microfiltration experiments

2.4.2.1 Laboratory filtration

A hollow fibre membrane modules (UFP-500-E-2U) consisting of a membrane pore size of 500 kD and 1 mm lumen diameter was used for laboratory scale microfiltration (Process optimization) studies. 70 mL of heterotrophically grown algal broth containing 5 $g.L^{-1}$ cells (prepared as described in Section 2.2) was pumped into the reservoir tank of the AKTA crossflow system (**Figure 2.2**). This was operated in total recycle mode where permeate and retentate lines were recycled back to the feed reservoir. Three different flow rates 75, 150 and 300 $mL.min^{-1}$ corresponding to shear rates 2000, 4000 and 8000 s^{-1} respectively were employed and for each experiment, the TMP was increased in a step-wise manner. The shear rate and TMP were calculated using Equation 2.3 and 2.4 respectively:

$$\gamma = \frac{4 \times Q}{F \times \pi r^3} \quad (2\text{-}3)$$

where r is the radius of the lumen (cm) and F is the number of fibres in each cartridge and

$$TMP = \frac{P_f - P_r}{2} - P_p \quad (2\text{-}4)$$

where *P* stands for pressure and subscripts f, r and p stands for feed, retentate and permeate respectively.

Usually, the permeate pressure is atmospheric (therefore, it is neglected) while the feed and retentate pressures were measured and adjusted automatically by the software (unicorn) using the AKTA™ PID control system (**Figure 2.2b**).

In terms of concentration experiments, 10x concentrations were performed using a shear rate of 8000 s^{-1} at a constant TMP of 0.5 bar.

2.4.2.2 Ultra scale-down filtration

Small scale filtration studies (process optimization and concentration experiments) were performed using the RDF (Section 2.3.2.2) which has previously been used to investigate diafiltration and CFF (Ma *et al.*, 2010). All USD filtration experiments were conducted with similar conditions to lab-scale for example at a constant ratio of feed volume to membrane area and shear rates. A correlation between viscosity, surface average shear rate and speed of rotating disc was previously developed by Ma (2010) using CFD simulations and this is given by:

$$\gamma = a\mu^{b}\omega^{1.5} \tag{2-5}$$

where ɣ is the wall shear rate (s^{-1}), a and b the correlation constants ($a = 2.12 \times 10^{-6}$ and $b = -1.375$), μ the viscosity (Pa.s) and ω is the angular velocity $2\pi N$ ($rev.s^{-1}$).

Figure 2.6 shows how USD filtration using rotating disc filter (RDF) was placed in the cartridge holder position of this machine.

Further details of the application of USD filtration method are described in Chapter 4.

2.4.2.3 Normalised water flux (NWF)

NWF was used to ascertain the membrane permeability, cleanliness and monitor the integrity or quality status of the filter membrane. This was achieved using DI water. All filter membranes were characterized based on this parameter when initially purchased.

For hollow fibres, a pre-cleaning step with warm 0.5 M NaOH (for 30 min) in constant recycle mode was carried out prior to this test. The retention of at least 60% of the first NWF is used as a bench mark for membrane cleanliness and reuse. NWF is calculated using the following formula:

a)

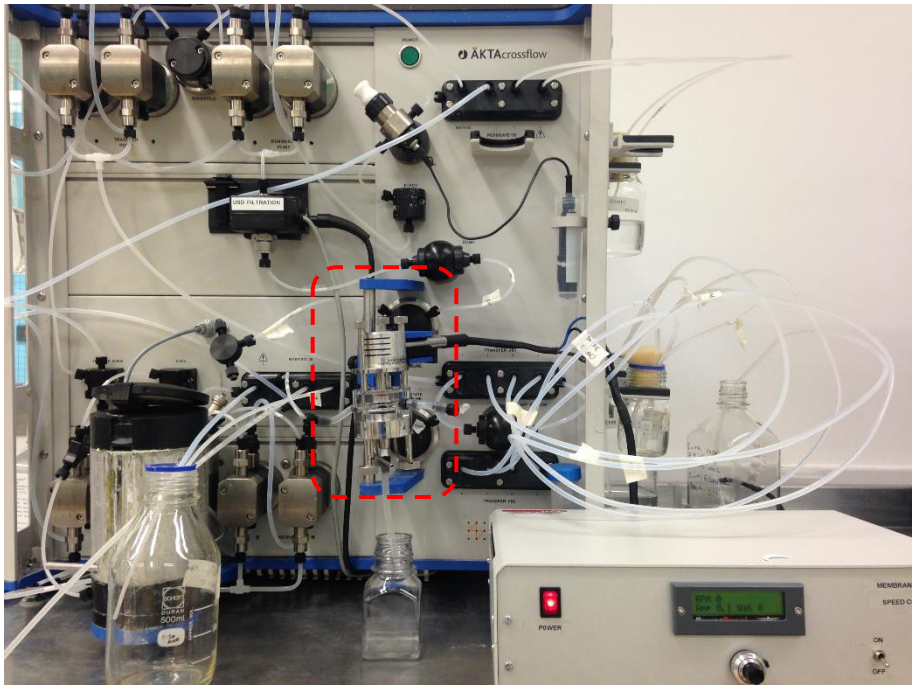

b)

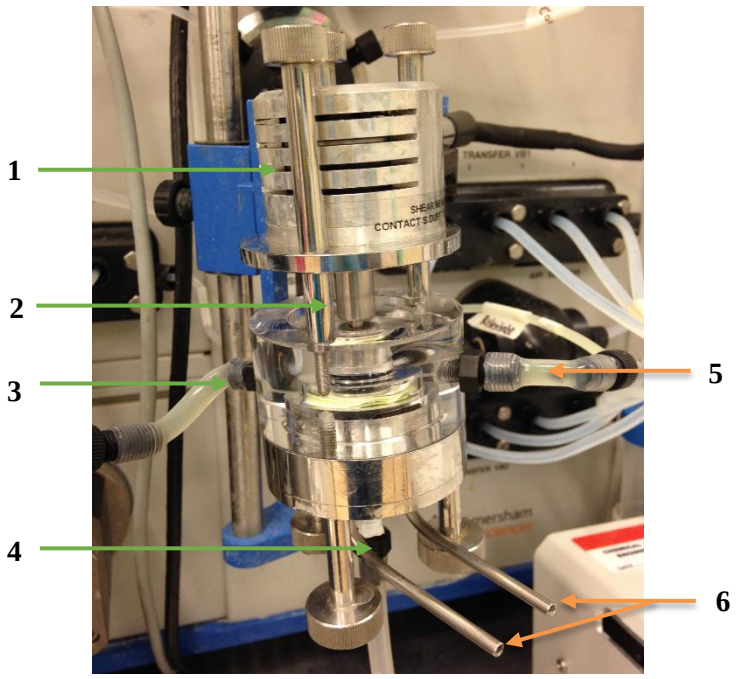

Figure 2-6: AKTA CFF unit showing a) the set up for USD filtration and its speed control unit with red dotted lines highlighting the USD device b) closer view of the USD filtration device with ancillaries (1) motor housing (2) motor coupler (3) feed port (4) permeate port (5) retentate port (6) cooling in and out.

$$NWF = \frac{Flux \times T_{cf}}{TMP} \quad (2\text{-}6)$$

where T_{cf} is the temperature correction factor.

2.4.3 Centrifugation

2.4.3.1 Pilot scale centrifugation

Pilot scale centrifugation was carried out using a CARR Powerfuge™ (Section 2.3.3.1) using flocculated or unflocculated cells at a flow rate of 1 $L.min^{-1}$ using a bowl speed of 255 s^{-1} (corresponding to Q/Σ $1.61x10^{-08}$). Water was initially pumped through the unit until supernatant discharge was evident at which point the actual feed solution was quickly introduced into the feed line.

2.4.3.2 USD centrifugation

USD centrifugation was carried out using pre-sheared flocculated or unflocculated cells. 2.2 mL Eppendorf tubes were used in a bench top centrifuge Eppendorf 5424R (Eppendorf, Stevenage, UK) fitted with a FA-45-24-11 rotor and a working volume of 2 mL. Different rotational speeds were explored at a constant time and a temperature of 4˚C was set for the study of the effect of flocculation. USD studies to predict pilot scale centrifugation performance were carried out at 16˚C because this was the temperature that was measured during the scale-up studies.

2.4.3.3 Percentage clarification attained

The performance of each centrifuge was evaluated in terms of clarification of the supernatant using Equation 2.7. Clarification measurement was carried out by careful pipetting of the resultant supernatant from each Eppendorf tube (Section 2.4.3.2) or the supernatant collected from the CARR (Section 2.4.3.1).

Optical density (OD) of the supernatant was measured at 750 nm. OD_{ws} refers to well clarified supernatant after extended centrifugation of algal broth at 14000 rpm for 15 min. Subscripts f, s and ws stands for feed, supernatant and well spun respectively.

$$\text{Clarification} = \frac{\text{OD}_\text{f} - \text{OD}_\text{S}}{\text{OD}_\text{f} - \text{OD}_\text{WS}} \times 100 \quad (2\text{-}7)$$

2.5 Experimental set-up for linked USD- flocculation and centrifugation studies

Figure 2.7 shows the experimental set up for USD flocculation and centrifugation studies. Flocculant is loaded into a 20 mL syringe and flow is achieved using an Aladdin AL-1000 syringe pump (WPI, Hertfordshire, UK) at a set flowrate. The reactor was filled to approximately 71% capacity and flocculation was achieved as described in Section 2.4.1.2 after which sampling is carried out at regions closer to the cylinder wall in between the top and bottom impellers.

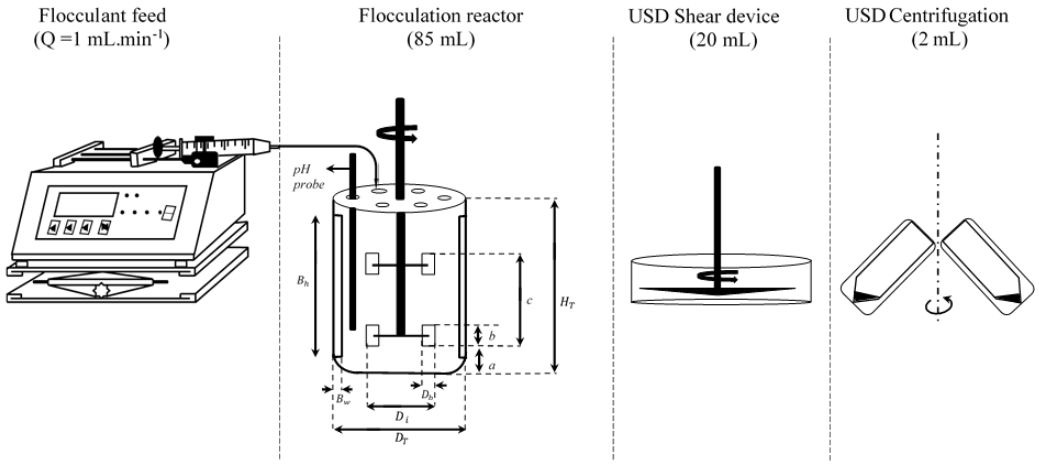

Figure 2-7-: Schematic diagram of experimental set up showing how USD- flocculation and centrifugation was achieved. Geometric ratios and dimensions are as described for scale down flocculation reactors in Section 2.3.1.2

2.6 Cell disruption methods

2.6.1 Homogenization

Cell disruption was performed using an APV Manton-Gaulin Lab 40 homogeniser (APV International, West Sussex, UK) with fresh algal broth from a mid-stationary phase growth. The homogenizer was operated at full capacity (40 mL) at three different pressures (200, 500 and 800 bar). At the pressures operated, different numbers of passes (1-3) were also explored in order to enhance release. Ethylene glycol was used to cool this equipment to 4ºC during homogenisation and samples were then used for lipid analysis (Section 2.7.3).

2.6.2 Sonication

An MSE soniprep-150 apparatus (Sanyo Electric, Osaka, Japan) was used for cell disruption by sonication. Several variables were used for sonication studies in order to determine the best conditions for lipid release and sensitivity analysis for the method. This included sonicating different volumes (1 - 2 mL) of algal broth at different intensities (10 and 15 ma), cycles (1 - 10) and also various cell densities (2 - 5 $g.L^{-1}$) using 10 s on and off. For small volumes and low cell densities (1 mL and 2 gL^{-1} respectively), samples were pooled to make up sufficient amount for particle size analysis (Section 2.10.7) of cell debris. The sonicator was operated with samples placed in ice water during each run.

2.7 Lipid analyses

All lipid amounts except when gravimetrically quantified (Section 2.7.1), were estimated using triolene as a standard. This was achieved by correlating the OD at 540 nm to the concentration (w/v) of the triolene (Appendix 1).

2.7.1 Total Lipid analysis

Total lipid analysis was performed gravimetrically. Algae cells were grown to the mid stationary phase when all the nitrogen in the media was totally depleted and then cells were

harvested. After centrifugation, salts were washed away with DI water twice and then the cells were lyophilized as described in Section 2.8. The cells were then weighed and lipid extracted using the Bligh & Dyer (1959) method. The total lipid extracted is washed out with small volume of chloroform and then evaporated with nitrogen before being weighed. All measurements were performed in triplicate.

2.7.2 Wet analyses of lipids (sonicated sample)

Using 15 mL centrifuge tube with a working volume of 10 mL, flocculated and unflocculated algae broth were centrifuged at different centrifugal forces. The supernatant is then decanted into another centrifuge tube and both tubes i.e. those containing supernatant and those with initial sediments are further centrifuged at 4000 rpm using an Eppendorf 5810R centrifuge with A-4-62 rotor to further dewater the cells. Media was decanted and replaced with an equivalent volume of chloroform-methanol (2:1) solution, vortexed and sonicated to release lipids (Section 2.10.6). 100 µL of these samples was pipetted into a glass microwell plate and evaporated in a 'thermo mixer comfort' (Eppendorf UK). Wet analyses of total lipids released was then carried out using sulfo-phospho-vanillin (SPV) method as described by Cheng *et al.* (2011) and OD of assay recorded using Tecan Safire^2 UV-VIS-IR fluorescence plate reader (Männedorf, Switzerland).

2.7.3 Wet analyses of lipids (Homogenized sample)

10 mL of well mixed homogenate was diluted with 10 mL of chloroform:methanol (2:1 v/v) solution and vortexed. This was decanted into a 50 mL Falcon tube and the mixture centrifuged at 4000 rpm using an 'Eppendorf centrifuge 5810R' with A-4-62 rotor to create a three phase liquid layer. The top two layers were carefully pipetted out and 100 µL of the bottom layer (chloroform + lipid) was pipetted into a glass microwell plate and evaporated in a 'thermo mixer comfort' (Eppendorf UK). Wet analyses of total lipids extracted was

then carried out using the sulfo-phospho-vanillin (SPV) method as described by Cheng et al. (2011).

2.8 Lyophilisation

Harvested algal broth was centrifuged at 4 °C for 10 min at 10,000 rpm using a Heraeus Fresco17 centrifuge (Thermo Scientific). The resultant supernatant was decanted and the pellets washed twice with DI water. The cells were then stored in a -80°C freezer for 24hr before being transferred to a vacuum freeze dryer (Edwards K4 Modulyo, Edwards UK) for 16-18 hr. The lyophilized cells were weighed using an Ohaus AP250D analytical balance for transesterification (Section 2.9) or used for FTIR analysis (Section 2.10.5).

2.9 Trans-esterification of algal lipids and GC-MS analysis

Algal lipids were first extracted using the Bligh & Dyer method (1959). Using a one-step transmethylation of lipid extracts with trimethyl sulfonium hydroxide (TMSH), these lipids were transesterified and the resultant FAMEs analysed using GC-MS. This analysis was carried out on Trace1310 gas chromatograph connected to ISQ single quadrupole MS (Thermo scientific) equipped with an Omegawax 250 capillary column (30m x 0.25mm x 0.25µm) (Sigma, UK). Using an injection volume of 1 µL in a split less mode, flow rate of 1.2 $mL.min^{-1}$ and helium as carrier gas, initial column temperature was set at 100°C for 2 min and analysis subsequently run at 230°C (with a rate increment of 4°C min^{-1} and hold time of 20 min). Peaks of methyl esters were identified by MS library and CAS number of corresponding commercially prepared FAME mix (Sigma, UK). FAMEs were quantified using a calibration curve drawn for each methyl ester (Appendix 11).

Equation 2.8 is a regression equation where Cetane number (CN) was calculated using a relationship that utilizes FAME compositions as described by Bamgboye & Hansen, (2008).

$$CN = 61.1 + 0.088x_1 + 0.133x_2 + 0.152x_3 - 0.101x_4 - 0.039x_5 - 0.243x_6 - 0.395x_7 \quad (2\text{-}8)$$

where x_1 to x_7 represents the weight percentages of methyl myristate (C14:0), palmitate (C16:0), palmitoleate (C16:1), stearate (C18:0), oleate (C18:1), linoleate (C18:2) and linolenate (C18:3) in transesterified lipids respectively.

2.10 Analytical methods

2.10.1 Quantification of biomass concentration

Algal growth was periodically quantified by OD measurement at 750 nm using an Ultrospec 500 pro spectrophotometer (Amersham Biosciences, UK). The broth was diluted with DI water wherever the OD approaches 1.0 OD units. The dry weight was determined by correlating the OD of exponentially growing cells to the corresponding weight of these cells on a predried and preweighed filter paper (Whatman, UK). This was dried to a constant weight and the readings used to draw a calibration curve (Appendix 3 and 4). Maximum specific growth rate (μ_{max}) and doubling time (t_d) were calculated using the equations:

$$\mu_{max} = \frac{\mathrm{Ln}\left({}^{OD_2}/_{OD_1}\right)}{t_2 - t_1} \quad (2\text{-}9)$$

$$t_d = \frac{\mathrm{Ln}\,2}{\mu_{max}} \quad (2\text{-}10)$$

where OD_1 and OD_2 denote the optical density at logarithmic phase at time t_1 and t_2 respectively.

2.10.2 pH measurements

Daily pH readings of algal culture pH and for pH adjustment before flocculation were carried out using a S20-K SevenEasy™ pH meter (Mettler Toledo, UK). The probe was calibrated using standard buffers 4.01, 7.00 and 9.21 prior to each use.

2.10.3 Viscosity measurement

Viscosity measurements were carried out using a Kinexus lab^{+} rheometer (Malvern, UK) with the appropriate geometry (either cone plate, PU-20 or PU-50) depending on the range of viscosity expected. 0.5 mL of sample was loaded on the lower plate and with a fixed gap size of 150 µm (for cone plate) or range between (200 – 1 mm) for parallel plates depending on the average particle size within the sample measured. Using the rSpace software at a set temperature of 25ºC, a shear stress – shear rate table was generated which displays the viscosity of the sample (example in Appendix 6). Torque mapping was carried out each time the geometry of the machine was changed.

2.10.4 Light intensity measurement

The light intensity of the Kuhner incubator shaker and the plate slabs in which cells were cultured was measured using a light meter LI-250A (LI-COR Biosciences, Nebraska USA). This instrument has a millivolt adapter for connection with a data logger and was connected to a LI-COR LI-190SA PAR Sensor which measures photosynthetically active radiation (PAR). When placed at the desired position, the sensor output (15s averages) was instantly shown on the display. Light intensities were routinely checked during cultures and storage.

2.10.5 Fourier Transform and Infrared Spectra (FTIR) Analysis

FTIR was carried out using a Spectrum Two Infrared Spectrometer (Pelkin Elmer, USA). A background scan was carried out on the equipment and the lyophilised- phototrophic, heterotrophic cells or their flocculated forms were placed on the stage. The samples were scanned using a wavelength frequency range of 400 – 5000 cm^{-1} and resolution of 4 cm^{-1}, each sample was scanned 20 times to produce the average spectrum.

2.10.6 Lipid release

Using optimal conditions from Section 2.6.2, centrifuged algae pellets were dissolved in chloroform-methanol solution and sonicated. This was then centrifuged and the chloroform portion containing lipids re-diluted with chloroform for samples whose concentration is above the assays detection level. Samples are then analysed for lipid (Section 2.7.2 and 2.7.3).

2.10.7 Particle size distribution

The size distribution of cell debris, whole cells or flocs generated were evaluated using a Malvern Mastersizer 2000E with a size detection range of 0.01-2000 µm. The size distribution in terms of percentage total particle volume was recorded using water as a dispersant medium and the refractive index was set to 1.03 (Aas, 1996). Flocculated samples to be analysed were collected directly from the flocculation reactor and all samples were added in a drop wise manner into the dispersant medium, which was being stirred at 1000 rpm until a laser obscuration of 12-13% was achieved. The results were measured in triplicate and average taken.

2.10.8 Microscopic images

Microscopic images were obtained using a Nikon Eclipse TE 2000-U inverted microscope (Nikon Instruments Europe B.V, Badhoevedorp, Netherlands) fitted with a charge-couple device camera. Using 20 x magnification, images showing size of flocs before and after being subjected to shear were obtained. Several flocculation studies were performed and for each run, triplicate images were captured and sizes confirmed with the Mastersizer 2000E as explained in Section 2.10.7 in order to avoid batch to batch sampling error. Image analysis was carried out with ‘ImageJ’ software (NIH, US).

2.10.9 Scanning Electron Microscopy (SEM)

High resolution images of filter membranes before and after filtration experiments were obtained using a Field Emission Scanning Electron Microscope (FESEM) (JSM-7401F, JEOL Limited, Japan). Wet samples were left to thoroughly dry and then firmly secured on a leit adhesive carbon tab before being placed on an aluminium stub. Using a high resolution ion beam coater (Model 681, Gatan Ltd, USA), these samples were sputter coated with Gold and Palladium which gives the specimen a high conductivity and reduced tendencies of damage during imaging. Images were then shot by placing the sample at a working distance of 8.5 - 10 mm while utilizing a low accelerating voltage of 2 kV.

2.10.10 Determination of floc density

A Brookhaven (DCP-100 particle sizer) device, a centrifugal disc photosedimentometer, was used to analyse the density of the microalgae cells and flocs. Using 1 mL of 50% v/v methanol to create a gradient in 20 mL deionized water, this was injected into the surface of the rotating annulus; serving as the spin fluid. The rotating drum was set to different rotational speeds in order to match the size distributions initially obtained using mastersizer 2000E (section 2.10.7). 500 rpm appeared to be the most ideal for the size ranges attained. 0.2 mL of the sample to be measured was injected onto the inner surface of the rotating annulus of spin fluid using 15 x 4" 90º blunt end pipetting needle. The temperature of the system was between 23 ± 2 ºC during all runs. All measurements were performed in triplicate.

2.10.11 Nutrient analysis

Nutrient analysis (glucose and ammonia) was conducted using Bioprofile® FLEX Analyser (Novabiomedical, U.S) for both shake flask and bioreactor.

3. Microalgae growth and flocculation

3.1 Introduction and aims

As described in Section 1.3 there exists a diverse range of microalgae due to their different origins. This is evidenced by their physiological differences (filamentous or single-celled), multiple growth modes and diverse metabolism. Due to the diversity of algae, a wide range of species could be studied under a range of culture conditions enabling them to produce a variety of complex biochemical compounds (Radmer, 1996). Microalgal cultures are generally characterized by the low biomass densities that can be achieved as a consequence of their long doubling time (Hu *et al.*, 2008). In order to enhance biomass production, screening of the ideal candidates that possess fast growth rate and high content of the desired product (Del Campo *et al.*, 2007) becomes necessary.

The low biomass productivity places a large burden on the downstream processes utilized (Section 1.4) because of the large amount of water used for culture which needs to be removed. Early volume reduction by methods such as centrifugation (Section 1.4.2.1) or filtration (Section 1.4.2.2) is necessary to minimise the scale of subsequent operations. Here pre-treatment steps prior to recovering the algal cells can be explored. The various pre-treatment options utilized in microalgal processing have been discussed in Section 1.4.1.

Given the above considerations, the aims of this first results chapter are to evaluate the growth kinetics of four different microalgae species with potential for biofuel production and to characterise flocculation as a potential pre-treatment step to aid cell recovery. The specific objectives of this chapter are as follows:

- To study the growth kinetics of the selected microalgae species under different cultivation conditions (phototrophic and heterotrophic).
- To study the impact of media composition on lipid production by the different algal strains as a basis for choosing one for further study.
- To design and characterise a series of scale-down flocculation reactors to be able to reproducibly produce flocs of the selected microalgae cells at small scale.
- To evaluate the influence of flocculation conditions on the particle size distribution and mechanical stability of the flocs generated.
- To scale-up the flocculation process in a larger scale stirred tank reactor (STR) using the optimised conditions from the scale-down flocculation reactors.

3.2 Growth kinetics of microalgae strains

3.2.1 Effect of medium formulation on biomass and lipid production

The initial experiments examined the influence of cultivation conditions on growth and lipid accumulation in a selection of microalgae species. Media composition is a key factor to consider since it consists of the various components these species will feed on thereby influencing cell growth and metabolism. The major elements required for algal growth were highlighted in Section 1.3.3. Apart from carbon, nitrogen is the next most important element contributing to the dry matter of microalgal cells since nitrogen deficiency is associated with enhanced lipid accumulation (Gouveia & Oliveira, 2009). For the medias chosen (**Table 2.1**), the nitrogen sources include yeast extract (EG), NH_4Cl (TBP) and $NaNO_3$ (BBM) since these are the nitrogen sources that algae are most able to readily assimilate (Ganuza *et al.*, 2008). Four microalgal species known for their biofuel potential were chosen. This include *C.vulgaris* (Spolaore et al. 2006; Illman *et al.*, 2000), *C.sorokiniana* (Illman *et al.*, 2000; Mata *et al.*, 2010), *C.reinhardtii* (Schenk *et al.*, 2008) and *S.obliquus* (Francisco *et al.*, 2010; Mata *et al.*, 2010).

Figures 3.1 and **3.2** show the measured growth kinetics for each of these species grown in the three different media either phototrophically or heterotrophically. Variations were observed in all cases of growth kinetics amongst all the species. The maximum biomass productivity was seen when cells are grown heterotrophically because glucose encourages biomass and lipid synthesis more than the production of pigments (Miao & Wu, 2006).

The low biomass concentration of phototrophic cultivation can be attributed to the low light intensities utilized (54 $\mu mols^{-1}m^{-2}$) (Section 2.2). Nonetheless *S.obliquus* obtained a maximum biomass concentration of 2.2 $g.L^{-1}$ in BBM which is higher than those in literature and this suggests a good combination of media and growth condition. *C.sorokiniana* exhibited the longest doubling time during phototrophic cultivation but in comparison to *C.vulgaris* and *C.reinhardtii,* cells was still actively growing throughout the time window studied suggesting that the maximum specific growth rate (μ_{max}) would have been better if the strain was allowed to grow for longer. In comparison to *S.obliquus,* a higher biomass was obtained by *C.sorokiniana* except for growth in BBM media.

For heterothrophic cultivation, the results are markedly different. In this case the shortest doubling times were recorded for *C.sorokiniana* and this organism's growth cycle was completed within the time of study. The highest biomass concentration of 5.7 ± 0.3 $g.L^{-1}$ was obtained for heterotrophic cultivation of *C.sorokiniana* in TBP medium. A detailed summary of growth kinetic parameters showing μ_{max}, t_d and total lipid accumulated is shown in **Table 3.1.**

As mentioned in Section 1.3.2.1, lipid content is an important parameter with regards to the suitability of an algal strain for biodiesel production. Hence, the total lipid content reported as percentage of total dry weight of the different algal strains cultured in the different media is shown in **Figure 3.3**. Lipid accumulation is known to be associated with nitrogen depletion in the culture medium (Converti *et al.,* 2009; Illman *et al.,* 2000; Stephenson *et al.,* 2010) hence cultures were harvested for analysis in the stationary phase. Some studies adopt a nitrogen replete medium for cultivation but deficiency of such an

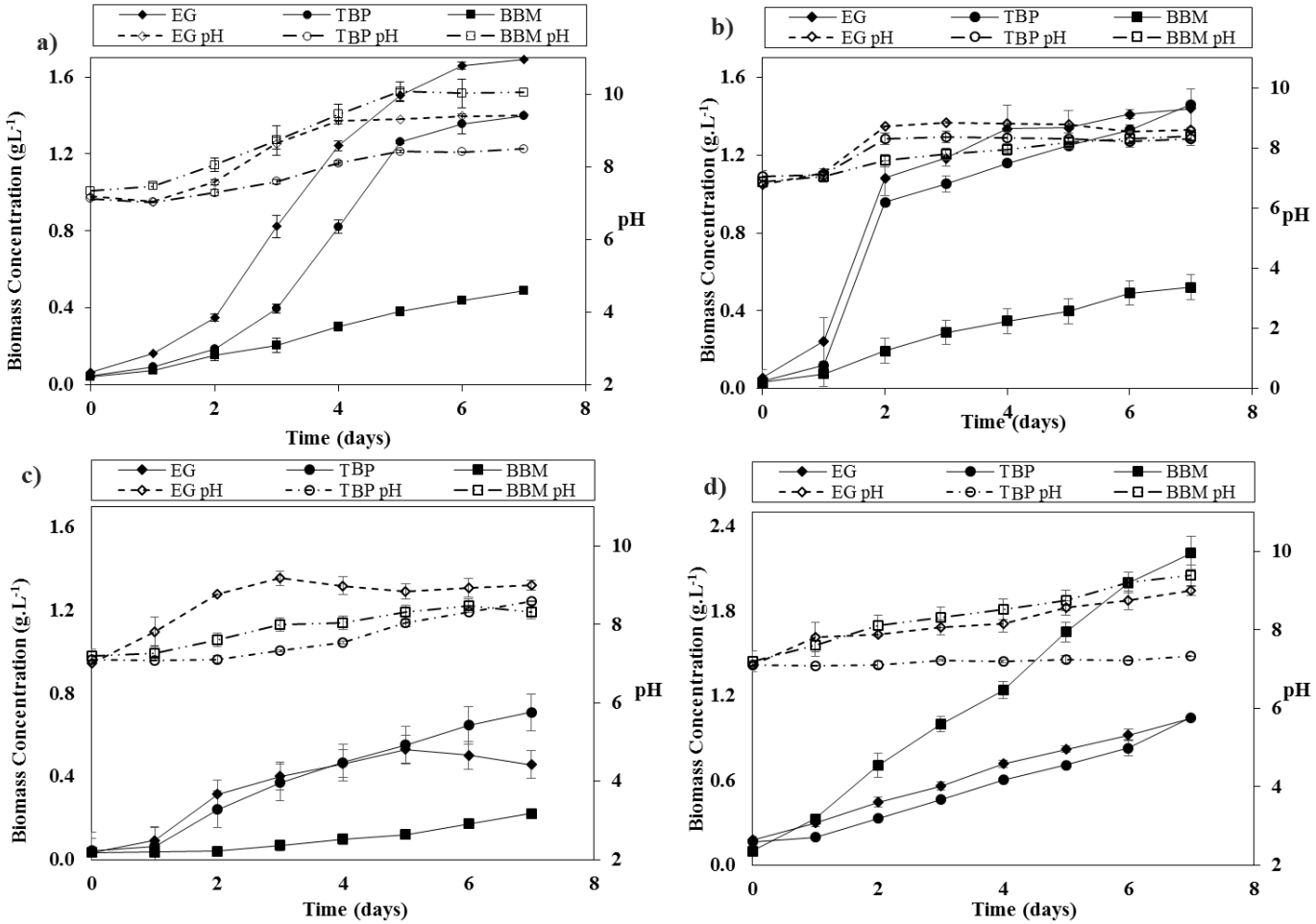

Figure 3-1: Growth kinetics of phototrophically grown microalgae species in different culture media (see section 2.2 for acronyms in legend): (a) *C.vulgaris,* (b) *C.sorokiniana,* (c) *C.reinhardtii* and (d) *S.obliquus*. Experiments performed as described in Section 2.2 and media compositions as described in **Table 2.1**. Error bars represent one standard deviation about the mean (n≥3).

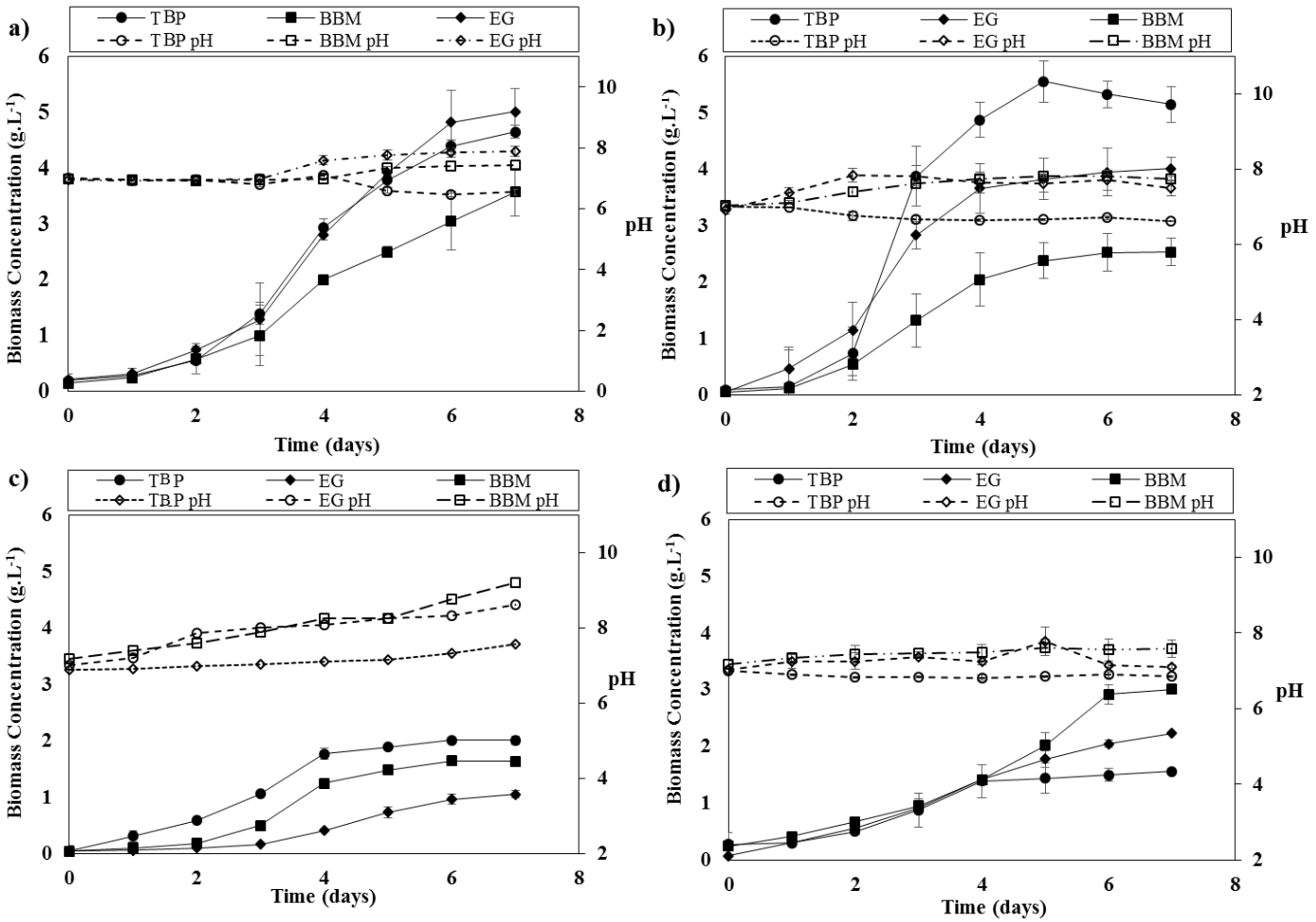

Figure 3-2: Growth kinetics of heterotrophically grown microalgae species in different culture media (see section 2.2 for acronyms in legend): (a) *C.vulgaris*, (b) *C.sorokiniana*, (c) *C.reinhardtii* and (d*) S.obliquus*. Experiments performed as described in Section 2.2 and media compositions as described in **Table 2.1**. Error bars represent one standard deviation about the mean (n≥3).

essential nutrient also serves as a signalling metabolite at the onset of cultivation that can alter primary and secondary metabolism (Bölling & Fiehn, 2005; Moseley *et al.*, 2009). Therefore, nitrogen rich media is recommended for algal cultivation. *C.vulgaris* demonstrated the highest lipid accumulation in the biomass for all three media with < 2% w/w variation with differing culture conditions. Lipid content ranged between 15-32% w/w which is in agreement with literature values of between 5-58% w/w for both phototrophic and heterotrophic cultures depending on cultivation condition (Chen *et al.*, 2010; Huerlimann *et al.*, 2010). The lipid content of *C.sorokiniana* grown in TBP did not vary significantly due to cultivation conditions (phototrophic or heterotrophic) although it varied in the other medias. In *C.rienhardtii* and *S.obliquus*, lipid fractions (% w/w) were found to be within lower limits of their ranges reported in literature. 4 - 13% w/w was obtained for *C.rienhardtii* while *S.obliquus* contained 5-14% w/w. It should be noted that even though *C.reinhardtii* was one of the earlier species investigated for biofuel production, this is the most suitable for genetic engineering since its complete genome sequence is already available (Huerlimann *et al.*, 2010).

The variation in lipid content seen across the different media types is possibly associated with the different sources and concentration of nitrogen (Leesing *et al.*, 2014). Utilizing ammonium as a nitrogen source either phototrophically or heterotrophically was seen to support lipid accumulation. This is because ammonium is the most preferred nitrogen source due to requirement of less energy for its uptake in comparison to other sources (Perez-Garcia *et al.*, 2011; Wilhelm *et al.*, 2006). Based on the data shown in **Figures 3.2** and **3.3** and the growth kinetic parameters shown in **Table 3.1** *C.sorokiniana* cultured heterotrophically on TBP media was chosen for further study. Furthermore, the lipid content of *C.sorokiniana* is high, the strain has been intensively studied and featured in many research works thus enabling quantitative comparison (Illman *et al.*, 2000; Rosenberg *et al.*, 2014).

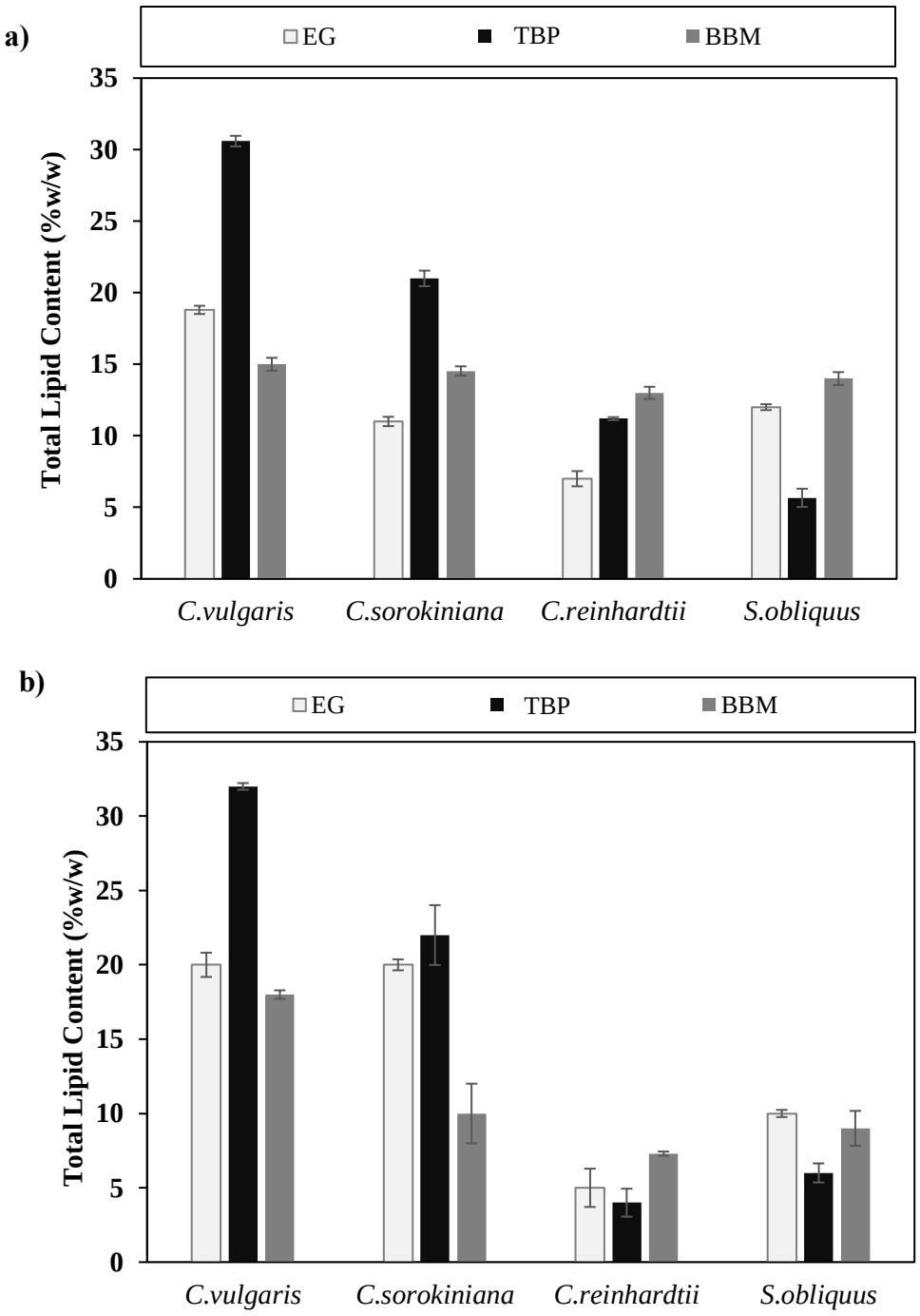

Figure 3-3: Total lipid accumulated by various microalgae strains cultured in different media: (a) phototrophically and (b) heterotrophically. Cells cultured as in Figures 3.1- 3.2 and harvested at the stationary phase when all nitrogen of the media is expected to have been used up. For low cell density cultures, several flasks were pooled in order to get sufficient biomass for analysis. Error bars represent one standard deviation about the mean (n=3).

Table 3-1: Summary of the growth kinetics and total lipid accumulated for phototrophically and heterotrophically grown microalgal cells. Data calculated from **Figures 3.1 – 3.3**.

Microalgal specie	Growth parameter and total lipid	Phototrophic			Heterotrophic		
		EG	**TBP**	**BBM**	**EG**	**TBP**	**BBM**
C.vulgaris	Biomass Conc. ($g.L^{-1}$)	1.69	1.36	0.48	5.01	4.65	3.57
	μ_{max} (hr^{-1})	0.027	0.021	0.013	0.018	0.016	0.023
	t_d (hr)	26	33	53	39	43	30
	Total Lipid (%w/w)	18.8	30.6	15	20	32	18
C.sorokiniana	Biomass Conc. ($g.L^{-1}$)	1.52	1.46	0.52	4.01	5.96	2.53
	μ_{max} (hr^{-1})	0.004	0.005	0.013	0.028	0.048	0.021
	t_d (hr)	173	139	53	25	14	33
	Total Lipid (%w/w)	11	21.1	14.53	20	22	10
C.reinhardtii	Biomass Conc. ($g.L^{-1}$)	0.53	0.71	0.22	1.06	2	1.65
	μ_{max} (hr^{-1})	0.007	0.025	0.012	0.012	0.017	0.0135
	t_d (hr)	99	28	58	58	41	51
	Total Lipid (%w/w)	7	11.2	13	5	4	7.3
S.obliquus	Biomass Conc. ($g.L^{-1}$)	1.04	1.05	2.21	2.23	1.56	3.01
	μ_{max} (hr^{-1})	0.007	0.009	0.01	0.012	0.009	0.013
	t_d (hr)	99	77	69	58	77	53
	Total Lipid (%w/w)	12	5.6	14	10	6	9

3.2.2 Scale-up of *C.sorokiniana* culture in TBP medium

In order to provide sufficient biomass of consistent quality for subsequent studies the scale-up of *C.sorokiniana* cultivation to a 7.5L stirred bioreactor scale was investigated. **Figure 3.4a** shows the successful scale-up of fermentation performance based on matched k_La between the shake flasks and the bioreactor as described by Ojo (2015). This entailed using a shaking / stirring rate of 180 rpm at both scales of operation. *C.sorokiniana* is a small 2 – 4.5 µm diameter organism that prefers being cultivated on nitrogen in the form of ammonia and glucose as an organic carbon source (Wan *et al.*, 2012). It has been reported that higher growth rates and respiration is obtained with glucose than with any other carbon source (Griffiths *et al.*, 1960). Due to possession of a mechanism that transports protons and sugars (hexose/H^+ symport system), *Chlorella spp* are able to readily uptake glucose from the media (Komor *et al.*, 1973; Komor & Tanner, 1974) supporting the efficient growth on glucose seen here.

Figure 3.4a also shows the decline in pH which is a characteristic of ammonia consumption from the TBP medium and which can lead to reduction in biomass yields if the pH is not controlled (Lee and Lee, 2002; Shi *et al.*, 2000; Yongmanitchai & Ward, 1991). Based on this data, the media was reformulated to increase buffering capacity and the growth period was seen to be longer than when initially grown in unmodified medium (results not shown).

Since carbon and nitrogen play an important role in biomass accumulation and product formation, their fate in the media and corresponding effect on lipid accumulation was studied (**Figure 3.4b**). This figure shows that the carbon source utilisation and metabolite production profiles at the different scales are identical. Lipid content was seen to increase in the late exponential and stationary phase of growth. Several hypotheses to explain the mechanism of lipid accumulation have been suggested. Some studies suggest media containing an excess of carbon coupled with nitrogen exhaustion can lead to lipid

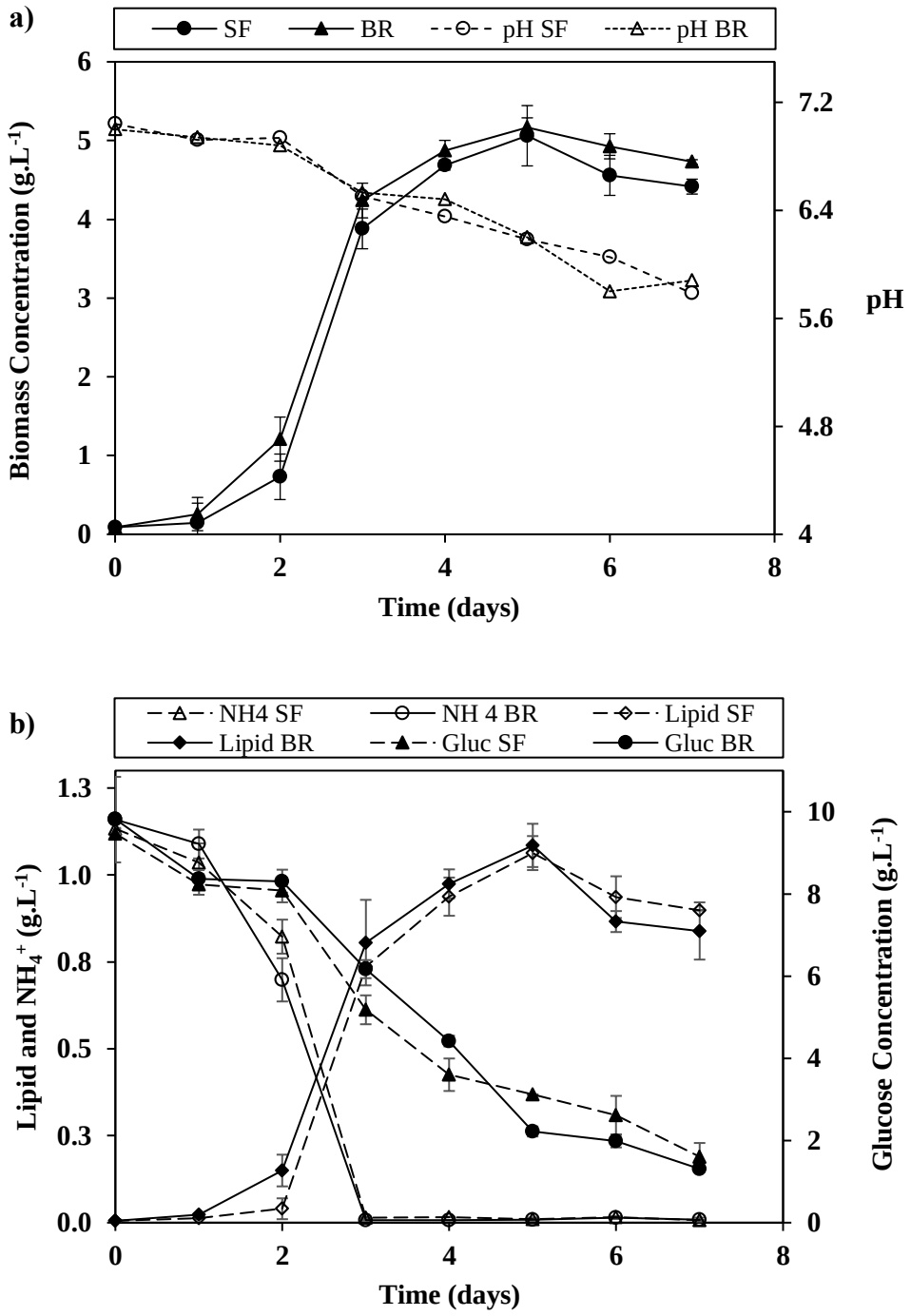

Figure 3-4: Comparison of growth kinetics of *C.sorokiniana* grown heterotrophically in shaken flasks (SF, 250mL) and a stirred bioreactor (BR, 7.5 L): (a) cell growth and medium pH and (b) corresponding nutrient uptake and total lipid levels. Experiments performed as described in Section 2.2 using scale-up criterion as described in Section 2.2.2. Error bars represent one standard deviation about the mean (n=3).

accumulation (Perez-Garcia *et al.*, 2011). Also, in heterotrophic cultures, conversion of sugars into lipid occurs when a higher rate of sugar consumption than that of cell generation is observed (Chen & Johns, 1991; Ratledge & Wynn, 2002). The yield of biomass on glucose, $Y_{X/S}$, recorded was 1.16 $g.g^{-1}$.

3.3 Flocculation as a harvesting pre-treatment step

It is known that the harvesting step has a significant influence on biodiesel production economics (Section 1.4). Microalgae are harvested in large volumes due to the generally low biomass concentrations. This large volume increases operational cost during dewatering (Uduman *et al.*, 2010); specifically, about 20-30% of the total cost of producing the biomass itself (Dragone *et al.*, 2010). An additional problem for dewatering is the small size of microalgal cells (Grima *et al.*, 2003). Considering this challenge, microalgae are usually harvested in two stages as described in Section 1.4. In this work, flocculation is proposed as a pre-treatment step (**Figure 1.6**) in order to reduce the volume of material processed further downstream. Also, the efficiency of DSP operations can be improved by flocculant conditioning (Ramsden & Hughes, 1990).

Flocculation is a process where solute particles collide and adhere to form 'flocs'. Different chemicals have been used for microalgal flocculation and these can be categorized into three main types as described in Section 1.4.1. Cationic polymers have been proven to be most effective for microalgal flocculation (Tenney *et al.*, 1969) with Chitosan specifically gaining wide interest due to various advantages (Section 1.4.1.1); the most important being its biodegradability and non-toxicity (Bustos-Ramírez *et al.*, 2013; Ravi Kumar, 2000). Due to the negative charge possessed by most algal cells, which prevents them from naturally flocculating in suspension (Brennan & Owende, 2010), addition of cationic polymers can link the cells to neutralize the charge.

Even though microalgal flocculation is established in wastewater treatment and the harvesting procedures involved are similar, the purpose of algal flocculation for biofuel

production differs. This is because biomass is needed for further processing, therefore, careful consideration for flocculant choice in order to recycle media or dispose of it safely has to be made.

3.4 Design of scale-down flocculation reactors

Flocculation is a difficult process to operate reproducibly. Therefore, standardization becomes vital in order to quantify and characterize the process. A series of scale-down flocculation reactors were designed (**Figure 3.5**) so that the operation could be performed reproducibly over a wide range of conditions using minimum quantities of materials. In this study, the 'large-scale' flocculation process will be carried out *in situ* the fermentation reactors hence, scale-down flocculation reactors are a geometric mimic of a standard STR

The internal arrangements of a design should depend on the objective of the operation intended (Walas, 1990). The major aims here are homogeneity and keeping flocs suspended during flocculation so that small flocs that are shortly bridged can continue to grow.

As shown in Section 2.3.1, the internal geometry of the flocculation reactors at both scales is the same. Agitation is accomplished by means of two Rushton impellers mounted on the shaft as in the case of the large scale flocculation reactors. Moreover, when an aspect ratio of $1 \leq H_T/D_T \leq 1.8$ as is used in this study then two or more impellers should be employed for mixing (Walas, 1990).

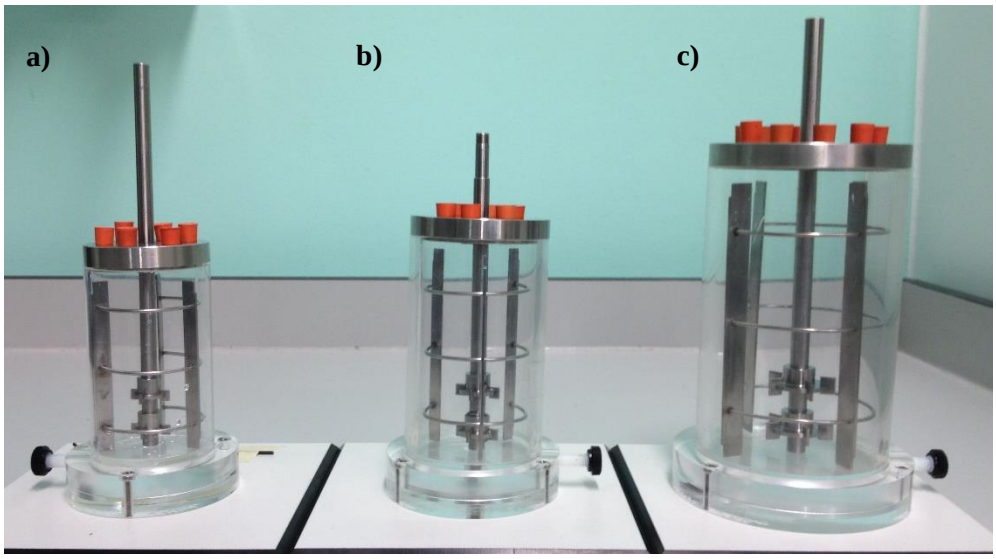

Figure 3-5: Photographs of the different scale-down flocculation reactors used in this work: (a) 120 mL (b) 250 mL and (c) 500 mL, with each having an adjustable 6-bladed Rushton turbine impeller. Dimensions and geometric ratios are given in Figure 2-1.

3.5 Standardization of flocculation conditions

Standardizing flocculation is vital in order to quantify and characterize the process. As mentioned in Section 3.4, reproducing a particular flocculation procedure is difficult, which is the reason for the wide variation in the flocculation efficiencies reported to date. In an attempt to overcome this challenge and to ensure reproducibility, factors affecting flocculation and flocculation conditions will be explored, optimized and fixed ahead of subsequent filtration (Chapter 4) and centrifugation (Chapter 5) studies.

3.5.1 Mixing time (t_m) characterisation

In order to ensure flocculation occurred under well-mixed and hence homogeneous conditions, mixing times in each reactor was studied as a function of impeller rotational speed. As mentioned in Section 2.3.1.2, study of the mixing time was achieved using pH indicator dyes. An approach that utilizes two pH indicators to estimate the mixing at the point when a uniform colour is obtained at a preselected pH value. This colorimetric method have been previously demonstrated in stirred reactors by Tissot *et al.* (2010). **Figures 3.6** and **3.7** show the progression of the acid-base reaction with time and the

associated change in colour at low and high rotational speeds in different sized scale-down reactors. Initially, a red coloured solution at t = 0 is stirred at the desired rotational speed and gradually turns yellowish-green upon addition of base. The examples shown here clearly indicate a relatively slow mixing time at a low impeller speed of 80 rpm in both scales of reactor. In contrast at a higher rotational speed of 350rpm the mixing time is seen to be around 8 seconds i.e. when the developing yellow colour appears homogeneous.

Figure 3.8 shows the measured mixing time as a function of impeller rotational speed where mixing time is seen to reduce with an increase in the speed of rotation. For example t_m values of 62 ± 0.2s and 11 ± 1.7s where obtained when rotational speed was increased from 60 rpm to 300 rpm respectively. Due to their common geometry, mixing time was the same for all three reactors. Homogeneity of the pH dyes used was achieved in a shortest mixing time of 7.9 ± 0.5s at a rotational speed of 350 rpm.

It was observed that slower rotational speeds took longer to mix which could delay flocculant time to reach other cells for effective agglomeration. While mixing time and homogeneity are important, several studies have shown shear induced by the impeller during flocculant addition greatly influences the sizes of flocs produced (Ahmad *et al.*, 2011; Byrne *et al.*, 2002; Pan *et al.*, 1999). Here, it is assumed that floc breakage should only occur if they are subjected to shear rates higher than those from their initial formation process. Nevertheless, Ahmad *et al.* (2011) further stated that particle toughness is influenced by shear rate during addition as impeller shear rates during ageing are insignificant. Based on these literature reports and the mixing time results obtained here, 350 rpm was employed during flocculant addition (to ensure rapid mixing and homogeneity) while 80 rpm was used for ageing of algae flocs (to minimise potential shear damage).

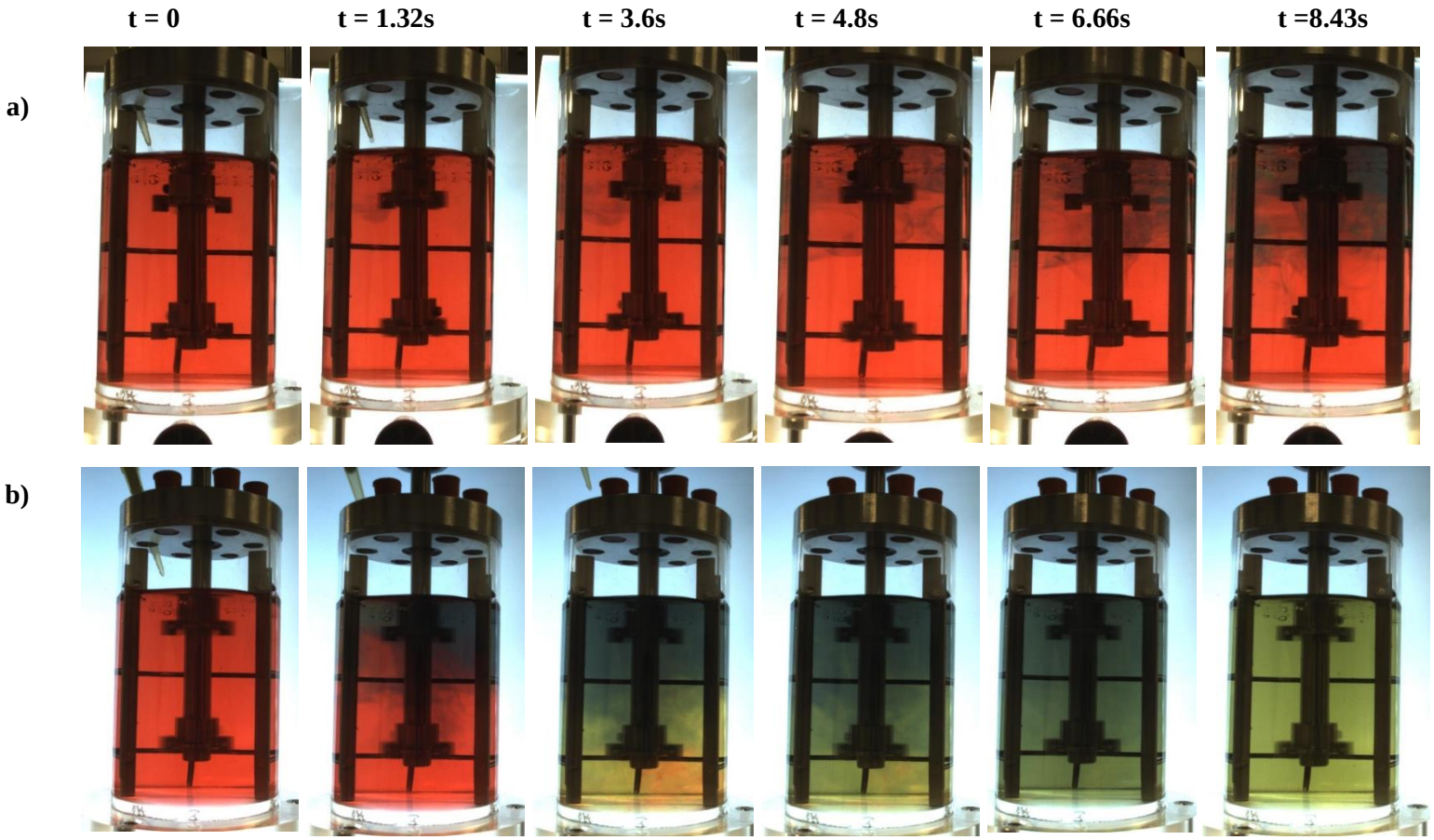

Figure 3-6: Time evolution of the mixing dynamics inside the 120 mL scale-down flocculation reactor: a) at 80 rpm and b) at 350 rpm. Reactor as shown in Figure 3.5(a). Mixing quantified using dual pH indicator dye method as described in Section 2.3.1.2.

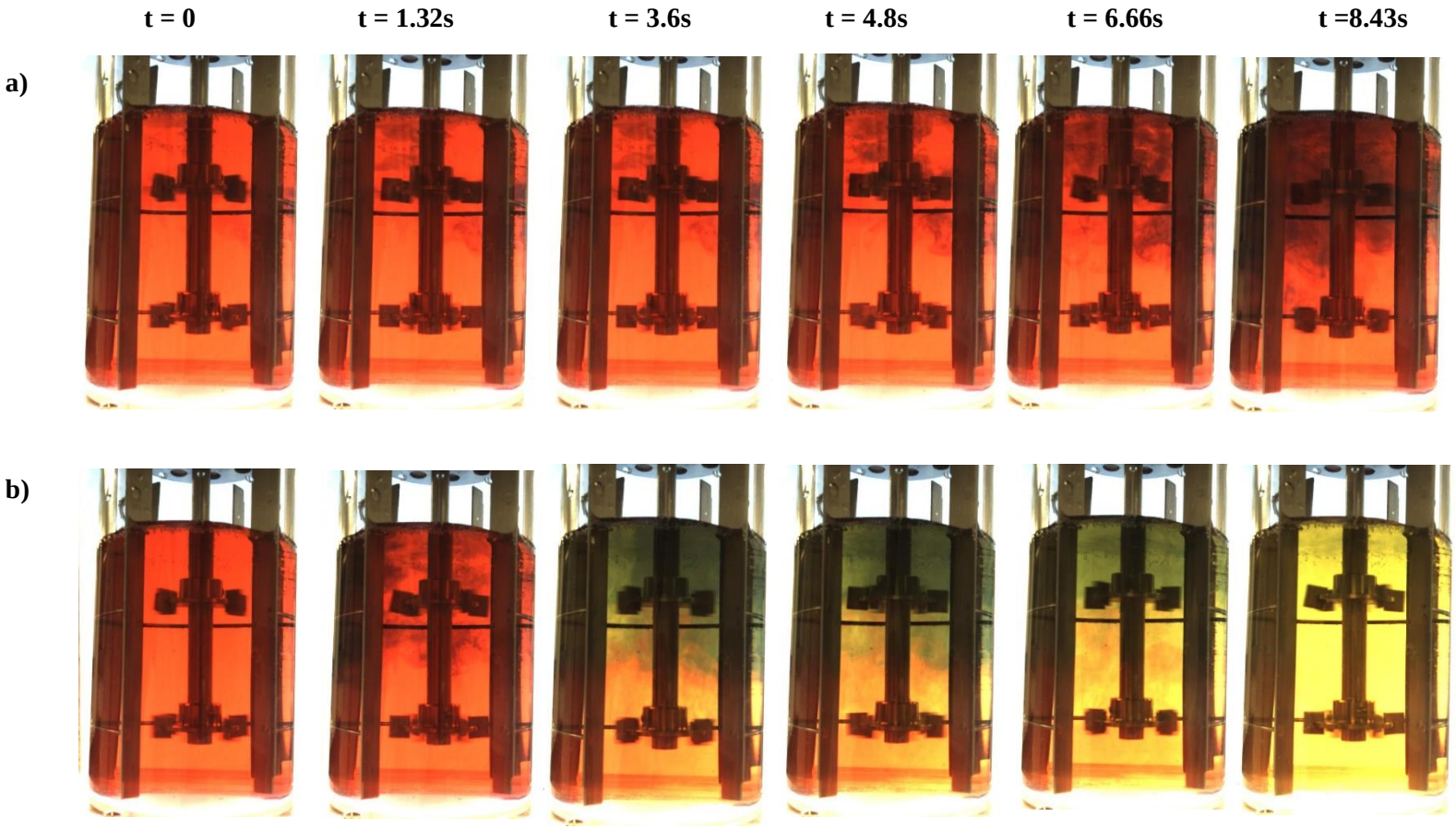

Figure 3-7: Time evolution of the mixing dynamics inside the 500 mL scale-down flocculation reactor: a) at 80 rpm and b) at 350 rpm. Reactor as shown in Figure 3.5(c). Mixing quantified using dual pH indicator dye method as described in Section 2.3.1.2.

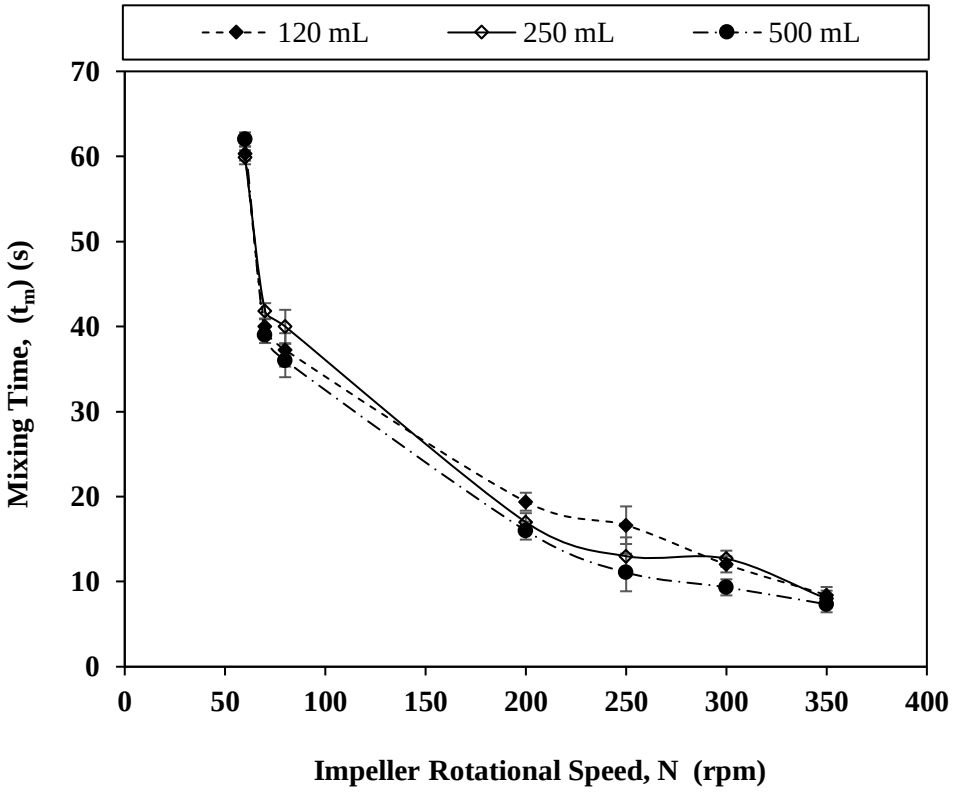

Figure 3-8: Measured liquid phase mixing time as a function of impeller rotational speed in each of the scale-down flocculation reactors. Reactors as shown in **Figure 3.5**. Mixing time measured as described in Section 2.3.1.2 while **Figure 3.6** and **3.7** shows the pictures of the colorimetric method obtained during the experiment. Error bars represents one standard deviation about the mean (n = 2).

3.6 Factors influencing flocculation

Several factors have been highlighted to affect flocculation efficiency as described in Section 1.4.1.1 including pH and flocculant addition rate.

3.6.1 Influence of pH

pH is an important variable in flocculation because it influences the charge of ionisable groups in the system and their interaction or repulsion. Several studies have reported flocculation using different flocculants at different pH ranges. For example, Harith *et al.* (2009) and Cheng *et al.* (2011) showed total charge neutralization at pH 8 and 8.5 using Chitosan to flocculate *C. calcitrans* and *C.sorokiniana* cells respectively. The behaviour of Chitosan is known to be influenced by pH, whereby in a weak acid environment, this biopolymer is known to be dominated by positive charges which tend to reduce in an alkaline medium due to coiling of the molecule (Gualtieri *et al.*, 1988). **Figure 3.9a**, shows the experimentally determined pH threshold for effective flocculation of *C.sorokiniana* using Chitosan. Recovery efficiency is the percentage amount of cells obtained after flocculation relative to the initial amount that could be obtained. In this case, recovery efficiency was measured as described in Section 2.4.1.2. The Chitosan concentration refers to the overall amount of Chitosan added to the flocculation reactor. The pH above which the recovery efficiency is greater than 85% is seen to be between pH 6 ± 1 at a Chitosan concentration of 5 $mg.mL^{-1}$. The order of increase in recovery efficiency and size of flocs for all the Chitosan concentrations tested increased from pH 9, 8, 7, 5 and 6 respectively. The highest recovery efficiency obtained was at pH 6 which is in line with the pKa value of the amino group for Chitosan which is approximately 6.5 (Filion *et al.*, 2007; Tourrette *et al.*, 2009). Therefore, subsequent experiments will utilize this pH for flocculation which is hereafter termed as the optimum pH.

Figure 3.9b shows the corresponding sizes of flocs formed at a concentration of 5 $mg.mL^{-1}$ which is where highest recovery was seen except for pH 9. The particle size d_{50} increases

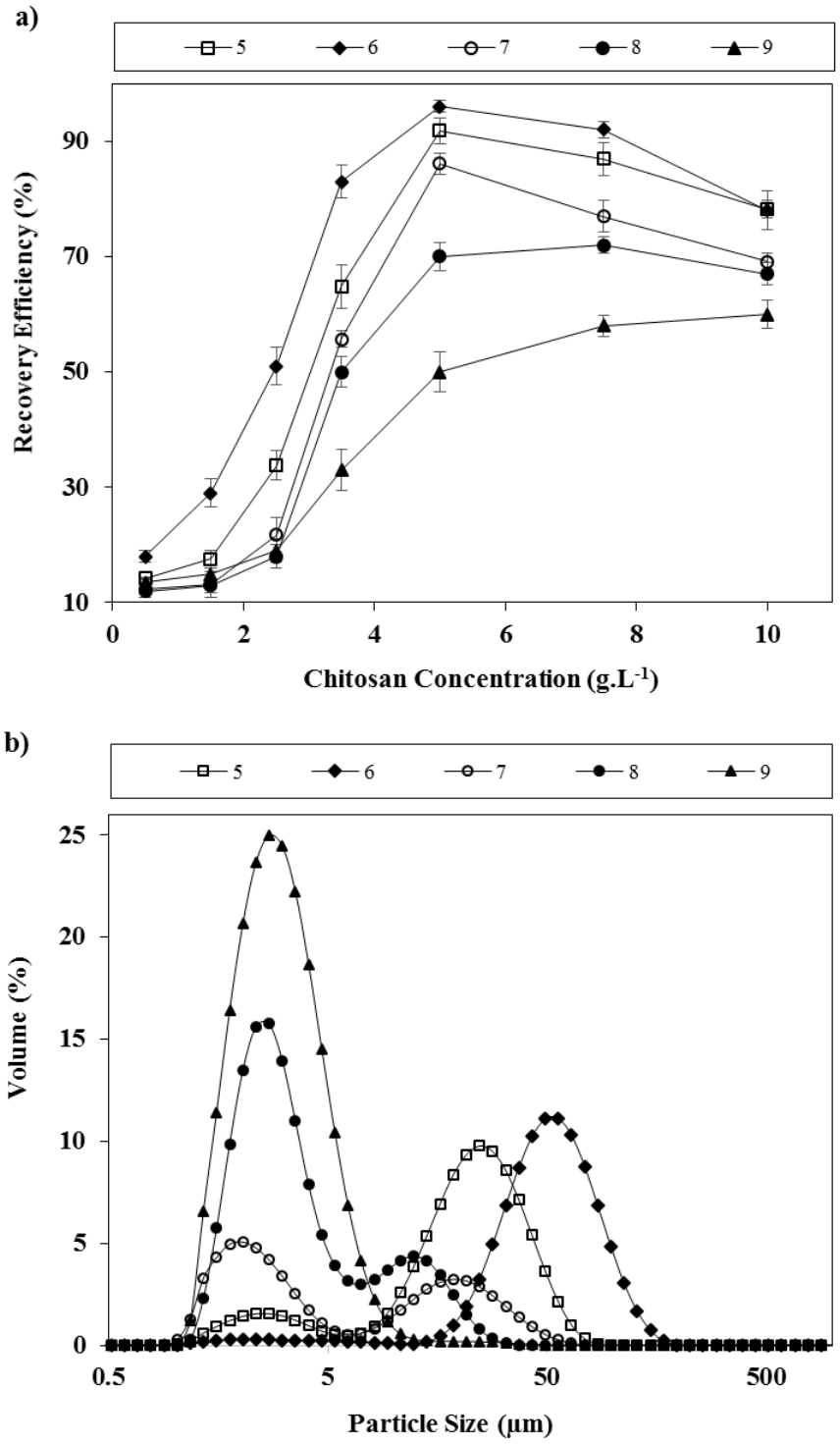

Figure 3-9: Effect of pH and Chitosan concentration on flocculation of *C.sorokiniana* cells: (a) recovery efficiency of flocculated cells at varying Chitosan concentration and b) particle size distribution of flocs produced at 5 $mg.mL^{-1}$ Chitosan concentration at various pH values (5-9). Experiments performed as described in Section 2.4.1.2; adding only 1mL of Chitosan solution to 85mL of broth containing 5.2 ± 0.18 $g.L^{-1}$ algal cell cultured heterotrophically as described in Section 2.2. Error bars represent one standard deviation about the mean ($n \geq 3$).

to higher diameters as the pH approaches the pKa of Chitosan and hence cell aggregation occurred which is as a result of predominance of positive charges in the medium. A substantial level of aggregation occurred at all the various pH ranges (especially at high Chitosan concentrations) which impacted on recovery. This verifies the electrostatic interaction between the amine functional groups of Chitosan to the anions predominating algal cell walls (Uduman *et al.*, 2010; Xu *et al.*, 2013).

3.6.2 Influence of flocculant addition rate

Another important variable that influences the flocculation process and the size of the generated flocs is the flocculant addition time referred to as t_{add}. t_{add} is the total time it takes to add the required amount of flocculant. **Figure 3.10** shows the impact of three different addition rates on the sizes of the flocs formed; size is seen to increase with a decrease in total addition time. Shorter t_{add} showed a size profile with bimodal distributions characterized by a higher proportion of bigger flocs to smaller ones while longer t_{add} (i.e. 1 $mL.min^{-1}$) exhibited a wider floc distribution. The Segregation Index (X_S) is a parameter used to characterize the degree of particle separation in fluid particle systems. It is known that with longer t_{add} there is a higher X_S and therefore improved mixing (Espuny *et al.*, 2014). This improvement in mixing could be the reason that flocs are broken because of exposure to hydrodynamic shear. A detailed study on how mixing time scales affect the sizes of flocs has been discussed elsewhere (Espuny *et al.*, 2014).

The mechanical stability of flocs is important to characterise since they are to be further processed using techniques known to induce hydrodynamic shear. Moreover, it has been highlighted in Section 3.5.1 that floc stability is influenced by shear rate during flocculant addition. Since floc rigidity is of importance, the shear stability of these flocs generated as a function of flocculant addition time was explored. **Figure 3.10b** shows microscopic images obtained after the flocs have been subjected to shear in the rotating disc shear device described in Section 2.3.3.2 at an energy dissipation rate of 2×10^5 $W.kg^{-1}$. It is evident

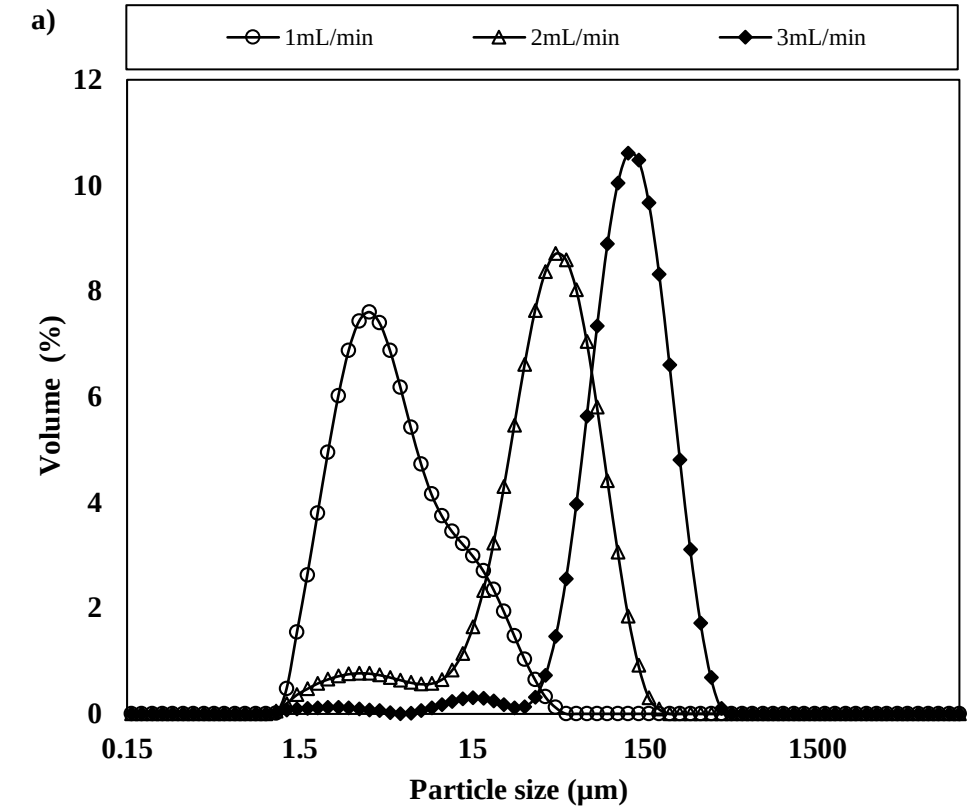

b)

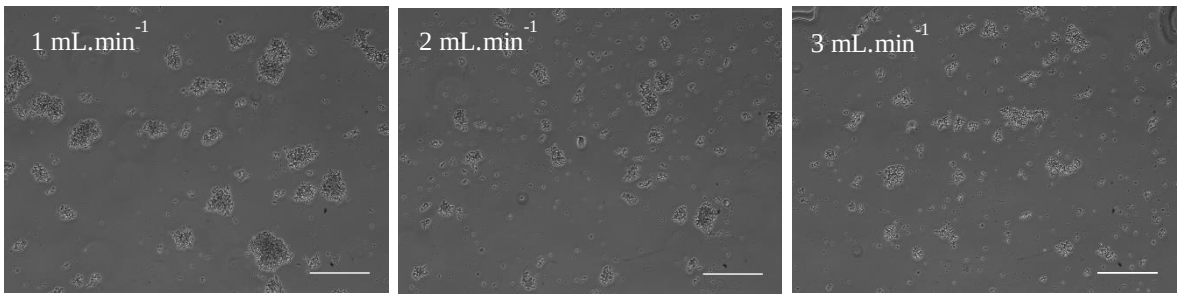

Figure 3-10: Influence of Chitosan addition rate on size of flocs: (a) effect of time of addition on particle size distribution of flocs and (b) effect of energy dissipation rate (2 x 10^5 $W.kg^{-1}$) on the flocs generated from **Figure 3.10a**. The choice of energy dissipation rate is based on those experienced in industrially relevant centrifuges (CARR Powerfuge™ and disc stack centrifuge). Flocculation was carried out using broth containing 3.5 $g.L^{-1}$ cells using experiment conditions as described in Section 2.4.1.2. Bar size is 50 µm.

that flocs produced with longer Chitosan addition times were more resistant to shear as bigger flocs are still seen post shear exposure. These results are similar to studies carried out by Berrill *et al.* (2008) which reported reduced stability of *E.coli* debris flocs obtained using short addition time in comparison to those produced using longer addition times. More so, heterogeneity in the floc size characteristics was seen with shorter addition times and this can be seen with the profile of 3 $mLmin^{-1}$ in **Figure 3.10a** (bimodal to trimodal distribution profile). Thus, the longer addition times of 1 $mL.min^{-1}$ are used in subsequent experiments.

3.6.3 Influence of broth ageing on flocculation efficiency

The state of the culture broth can influence flocculation process performance. In 1969, McGregor & Finn, highlighted the factors that affect the flocculation of homogeneous cultures; amongst them is physiological age. In this work the effect of cell age on flocculation efficiency showed that at room temperature, a 24 hr broth holding time does not affect the flocculation performance. **Figure 3.11** verifies this statement where it can be seen that the particle sizes of different concentration of flocculant added to freshly harvest algal culture and a 24 hr aged culture showed almost identical profile. These distribution profiles are within a ± 2.14% error when low flocculant is used whereas at high concentration, identical floc profile is formed. A twenty four hour holding time was deemed appropriate to mimic production delays or shift patterns in large manufacturing facilities. It is also important to study ageing since lysis of cells upon ageing may lead to release of intracellular components such as nucleic acids, proteins and polysaccharides thereby affecting the amount of flocculant required.

It is expected that cells will be stressed and some form of lysis evident when they are left stagnant or gently agitated after culture as normally seen with other microorganisms such as *E.coli*. This is not evident here which indicates the robustness of *C.sorokiniana*. It should

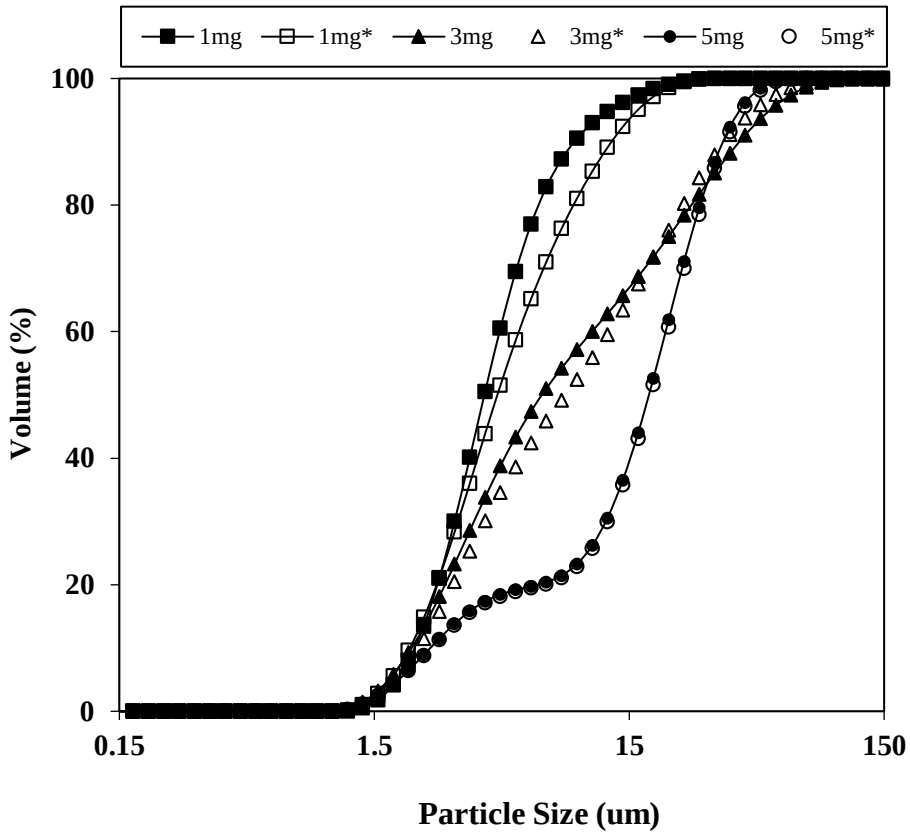

Figure 3-11: Effect of broth ageing on particle size distribution of *C.sorokiniana* flocs. (*) represent data from samples held for 24 hr while other data is for freshly harvested cells. Flocculation performed as described in Section 2.4.1.2 with 5.0 $g.L^{-1}$ algal cells cultured heterotrophically as described in Section 2.2.

be noted, however, that there was still un-utilised carbon source in the medium (see **Figure 3.4b**) at harvest and this may have contributed to the prolonged stability of the cells.

3.7 Optimization of flocculation conditions

In the preceding section, factors influencing flocculation (pH and flowrate for flocculant addition) were identified and fixed. However, the outcome of flocculation is still dependent on other operating parameters and therefore these will be explored further here in order to further optimise the process.

3.7.1 Effect of flocculant concentration on floc size

Flocculant concentration is a key variable for efficient flocculation as this influences floc sizes attained and as a result, it aids sedimentation (Mata *et al.*, 2010). **Figure 3.12** shows floc size to be strongly dependant on the concentration of Chitosan. Floc distributions obtained using varying amounts of Chitosan, 0.5 - 5 $mg.mL^{-1}$ corresponding to 1.09 - 10.89 mg Chitosan per gram of $algal_{dcw}$ was explored (using 5.4 $g.L^{-1}$ algal broth)(see Appendix 12 for sample calculation). The results indicate a shift in the distribution from mono-modal to bimodal distributions as Chitosan concentration increases. A low Chitosan dosage of 0.5-1.5 $mg.mL^{-1}$ exhibited only a slight change from single *C.sorokiniana* cells as indicated by characteristic particle size descriptors d_{50}, and d_{90} (**Table 3.2**). A significant increase in size and consistency in the distribution pattern of flocs was observed at higher Chitosan concentrations (**Figure 3.12**).

A continuous increase in Chitosan concentration will proportionally increase the size of the flocs but from a processing (see chapter 4 and 5) and economic point of view, an optimal dosage needs to be defined. A floc size big enough to aid fast settling was used as a bench mark. Unlike low concentrations of 0.5 - 3 $mg.mL^{-1}$, considerable sedimentation below the impellers was seen during ageing (visual observation) for higher Chitosan concentrations.

Additionally, Pan *et al.* (1999) reported that no significant change in the size of flocs and the settling velocity is seen after reaching optimal dosage. This is evident across all size

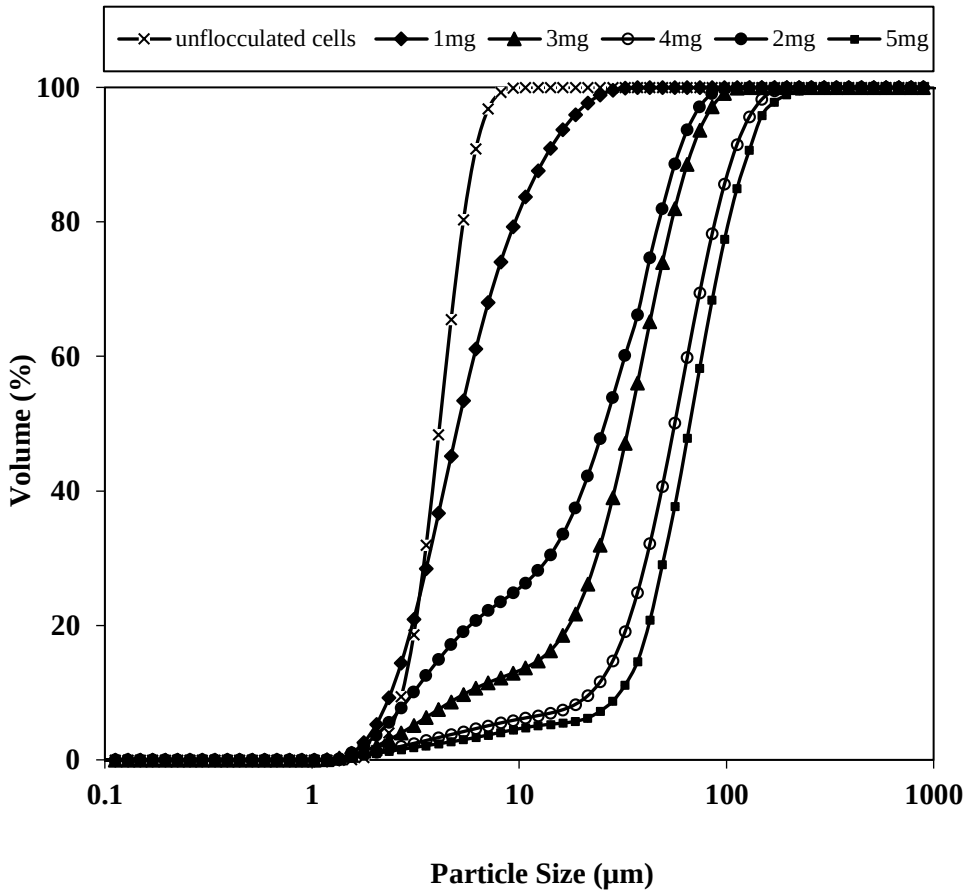

Figure 3-12: Cumulative particle size distribution of *C.sorokiniana* flocs with increasing flocculant amount. Broth containing 5.4 $g_{dcw}.L^{-1}$ cells (∗) was flocculated with Chitosan added to 85 mL of *C.sorokiniana* broth grown heterotrophically as described in Section 2.2. Flocculation experiments were performed as described in Section 2.4.1.

Chitosan Concentration ($mg.mL^{-1}$)	Mean Particle Size (µm)		
	d_{10}	d_{50}	d_{90}
Chlorella cells	2.4 ± 0.2	3.6 ± 0.2	5.1 ± 0.2
0.5	2.4 ± 0.1	5.2 ± 1.8	10.0 ± 4. 8
1.0	2.4 ± 0.0	6.4 ± 1.7	16.2 ± 3.5
1.5	3.3 ± 0.6	15.6 ± 2.4	34.8 ± 1.6
2.0	5.8 ± 0.6	17.9 ± 10.9	41.8 ± 20.5
2.5	20.7 ± 4.7	26.2 ± 5.4	50.1 ± 26.3
3.0	21.7 ± 4.2	49.2 ± 1.8	91.6 ± 0.9
3.5	23.4 ± 3.2	52.0 ± 0.2	92.1 ± 0.7
4.0	25.2 ± 0.3	52.4 ± 0.2	100.6 ± 2.8
4.5	25.6 ± 0.2	57.6 ± 1.9	106.7 ± 3.3
5.0	27.6 ± 1.2	60.4 ± 2.5	112.0 ± 0.9

Table 3-2: Ranges of floc diameters produced for flocculation of heterotrophically grown *C.sorokiniana* cells with increasing flocculant concentration. $d_{10,}$ d_{50} and d_{90} are particle diameter (µm) above which 90%, 50 % and 10% of the sample volume exists. Experiments performed as in Figure 3.12 and data represents one standard deviation about the mean (n>3).

descriptors for concentrations ≥ 4mg.mg^{-1} (**Table 3.2**). Moreover, other studies reported the use of higher concentrations of Chitosan and other flocculants even though the concentration of biomass from this study is a lot higher. Furthermore, reduced time to achieve fast aggregation in comparison to literature reports was observed. For example, Divakaran & Pillai, (2002) and (Xu *et al.*, 2013) continuously stirred the mixture for 30 and 15 mins respectively after which the mixture is allowed to sediment for another 30 mins. The better results seen here might be due to the controlled flocculation methodology used.

3.8 Scale-up of flocculation at constant tip speed

Having optimized and fixed flocculation conditions in the scale-down reactors it is necessary to ensure that similar flocculation performance is seen in the larger scale reactor. Several parameters are used to represent the hydrodynamic stresses in stirred vessels. Typical examples include the local turbulent energy per unit mass (ε), average turbulent energy dissipation (ε_{avr}) and impeller tip speed (V_{tip}). These have also been used as scale-up criteria for flocculation processes (Chester & Oldshue, 1987; Uhl & Von Essen, 1986).

Scaling down of processes also requires a mimic of conditions that can be replicated at both scale. As reported by Shamlou *et al.* (1996), particle growth and breakage is a function of hydrodynamic conditions inside the reactor. Scaling up on the basis of constant tip speed as used in this study is a typical example. Also, this correlation can be used if there is a partial geometric similarity between systems and also because impeller tip speed is an established parameter for impeller based mixing systems (Espuny *et al.*, 2014).

Figure 3.13 shows the particle size distribution of flocs produced using the 7.5L scale STR at optimal Chitosan dosage (9.86 ± 0.35 mg.g^{-1} of algal$_{dcw}$) and at a lower Chitosan dosage (2.18 mg.g^{-1} of algal$_{dcw}$). In both cases the size distributions showed a close match to those obtained in the scale down reactors which were operated at an equal impeller

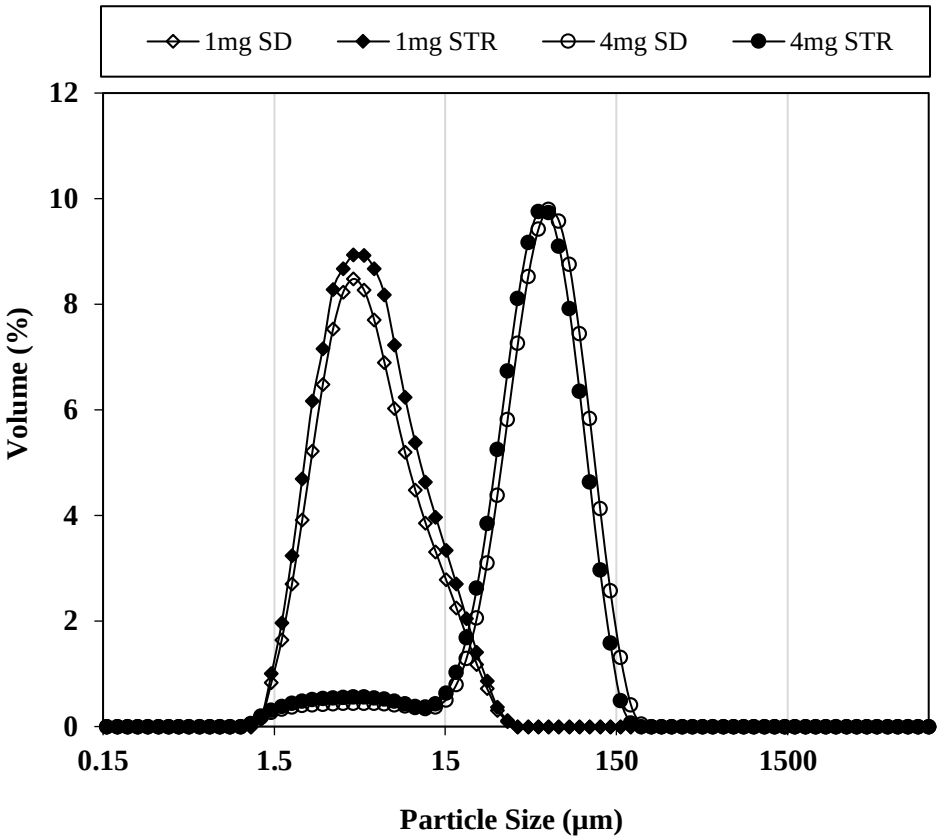

Figure 3-13: Scale-up of *C.sorokiniana* flocculation with Chitosan from 120 mL scale-down (SD) reactor to 7.5L STR. Flocculation was carried out at a fixed impeller tip speed (0.29 ms^{-1} during flocculant addition and 0.07 ms^{-1} during ageing) with varying flocculant concentration (1 and 4 $mg.mL^{-1}$ Chitosan) and flowrate of 0.06$L.hr^{-1}$. Data shown is from replicate experiments at each scale. Flocculation experiments performed as described in Section 2.4.1.

tip speed of 0.29 and 0.07 ms^{-1} (flocculant addition and ageing respectively). This is due to exposure to same shear rates. This results are comparable to studies carried out on post-centrifuge flocculation of *S.cerevisiae* by Espuny *et al*. (2014).

Additionally, in order to obtain agreement between the different scales, a constant flowrate of flocculant addition was used but the concentration of the flocculant solution was necessarily increased in order to avoid longer addition times at the large scale.

3.9 Summary

As stated in Section 3.1, the aims of this chapter were to establish reproducible and scalable conditions for the culture and flocculation of microalgal cells. As shown in **Figure 3.4** (scale-up of *C.sorokiniana* culture) and **Figure 3.13** (scale-up of flocculation with Chitosan), these initial aims have been achieved.

In terms of cell growth kinetics, four different microalgae strains were selected and cultured on three different media either phototrophically or heterotrophically. Heterotrophically cultured strains attained the highest biomass productivity (**Figure 3.2**) with *C.sorokiniana* considered as the best. This achieved a final biomass concentration of 5.96 $g.L^{-1}$ with the shortest doubling time of 14 hrs and a high lipid content of 22% (w/w) (**Table 3.1**). Media formulation was also seen to be important with regard to cell growth and in particular culture pH. Here the media was reformulated to increase the buffering capacity and better control pH. As shown in **Figure 3.4a**, this modification led to improved growth of *C.sorokiniana*. Ultimately, successful scale-up of *C.sorokiniana* growth on TBP medium from shake flask (250 mL) to bioreactor (7.5 L) scale was achieved using matched k_La as the scale-up basis (**Figure 3.4a**). Cultures performed under matched k_La conditions showed comparable growth rates and yields as well as comparable carbon source utilization and metabolite production profiles; suggesting the cells produced at the two scales were in a similar physiological state (**Figure 3.4b**).

Regarding the flocculation studies, three scale-down stirred flocculation reactors were initially designed and characterized based on mixing time (**Figure 3.6 - 3.8**). It was found that the main factors influencing flocculation were pH (**Figure 3.9**), t_{add} (**Figure 3.10**) and concentration of flocculant (**Figure 3.12**). Consequently these were fixed at pH 6, t_{add} of 0.06L.hr^{-1} and an optimal Chitosan concentration of 9.9 ± 0.4 mg.g^{-1} of algal dry cell weight was chosen. Standardizing and fixing these parameters enabled consistency and reproducibility in the particle size distributions of the flocs produced (**Figure 3.12** and **Table 3.2**). Scale-up of the flocculation process from the scale-down reactor (120 mL) to a 7.5L STR was achieved at a fixed impeller tip speed during flocculant addition and ageing (0.29 and 0.07 ms^{-1} respectively) (**Figure 3.13**).

In the following chapter, ultra scale-down methods for studying microalgal filtration and the impact of flocculation as a pre-treatment step will be investigated. The effect of growth conditions on filtration performance and membrane fouling will also be explored.

4. USD Microfiltration

4.1 Introduction

Harvesting and dewatering operations have been highlighted as a key challenge for economic processing of algae-derived biofuels (Pienkos & Darzins, 2009). Microfiltration is explored in this chapter as a solid-liquid separation choice for algal harvest as it is a major technique for dewatering and concentration used in other industry sectors (Section 1.4.2). Filtration processes can be achieved in two ways: (i) the classical mode of operation termed normal flow filtration (NFF) or dead-end filtration and (ii) cross flow (CFF) or tangential flow filtration (**Figure 4.1**). In both cases it is a pressure-driven process that consists of a permeable membrane to separate solids from liquid; the retained solids are termed the retentate while the material that passes through the membrane is called permeate.

Only a limited number of studies on algal separation using micro- and ultra- filtration have been reported in literature (Hung & Liu, 2006). Some studies have suggested mechanical dewatering operations such as filtration (Grima *et al.*, 2003) need to be followed by additional operations like thermal drying in order to obtain sufficiently concentrated biomass streams.

In this study, crossflow filtration is investigated as it is preferred due to the high permeate fluxes attained with minimal damage on cell integrity (Hung & Liu, 2006). Numerous parameters can influence filtration performance such as TMP, cross flow velocity (Song, 1998) membrane pore size and so on. Therefore, it is important to investigate effects of these operating parameters on the microfiltration of algal suspensions.

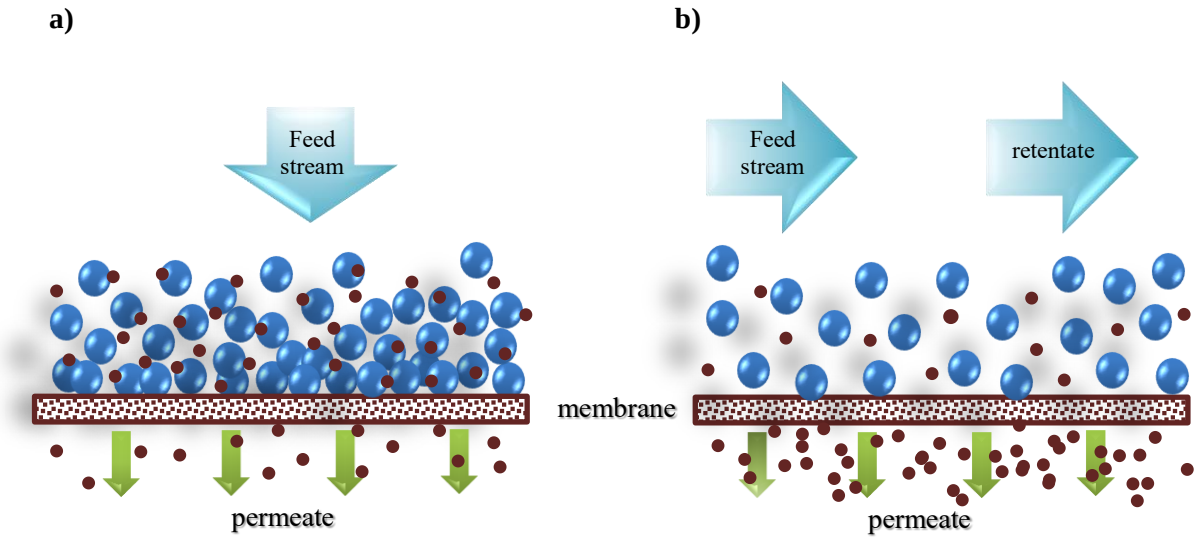

Figure 4-1: Schematic illustration of the operation of membrane filtration processes: (a) NFF or dead-end filtration and (b) CFF or tangential flow filtration. Large circles represent whole cells or solids larger than the membrane pore size (i.e. present in the feed solution) and small circles represent media components smaller than the membrane pore size

Also, exploring an appropriate pre-treatment step, such as flocculation (Chapter 3), can enhance the performance of membrane filtration (Babel & Takizawa, 2011). Consequently, the aim of this chapter will be to evaluate the processing parameters for microfiltration of algae using hollow fibre cartridges and to explore an ultra scale-down (USD) approach to mimic the lab scale hollow fibre results. The key objectives of this chapter are:

- To define factors influencing performance of algal broth filtration using hollow fibre cartridges.
- To study the effect of cell concentration on membrane performance.
- To explore the fouling characteristics (caused by extracellular organic matter (EOM)) as a result of culture conditions (photo- and hetero- trophic) and the consequences on membrane cleaning.
- To study the effect of a flocculation pre-treatment step on filtration efficiency.
- To mimic the lab scale findings using a scale-down filtration device for both flocculated and unflocculated cells.

4.2 Experimental setup and approach

Figure 4.2 is the experimental setup used for filtration process optimization and concentration experiments. As mentioned in Section 2.3.2.1, this was achieved on the AKTA crossflow rig using either the rotating disc filter (RDF) or the hollow fibre cartridge for USD and laboratory scale experiments respectively. The hollow fibre membrane configuration was selected based on knowledge of membrane formats being pursued by a number of algae-based companies (private communications). The pump control and pressure adjustments was done automatically by Unicorn software on the AKTA using the PID control system **(Figure 2.2b)**. This operates based on the instructions written and run in the method wizard. During process optimization for example, operating in total recycle mode utilized a TMP stepping protocol for three different crossflow velocities. **Figure 4.3**

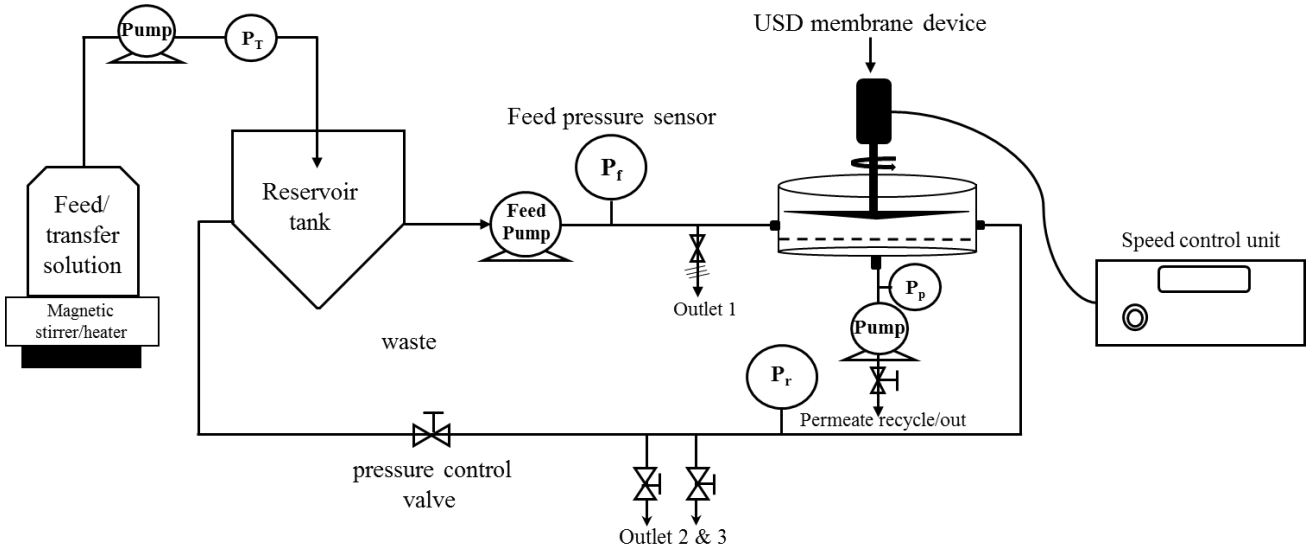

Figure 4-2: Schematic diagram of experimental setup for USD membrane and lab-scale hollow fibre experiments operated in either total recycle or dead-end mode. When used for lab-scale experiments, the USD membrane device is substituted with the appropriate cartridge. Experimental operation as described in Section 2.4.2.

illustrates this; where the process starts off with the highest flowrate (**Figure 4.3a**) as indicated by the flux values and corresponding time of occurrence down to the lowest flowrate employed (**Figure 4.3c**). When an experiment at a particular TMP is performed, the flux is monitored until a steady state flow is attained; this is then fixed and the control switches to the next TMP value. The feed was placed on a magnetic stirrer and constantly stirred during the entire filtration process in order to pump homogeneous broth into the system; this is of particular importance for concentration experiments especially when using a pre-flocculated feed. The feed was placed on a magnetic stirrer and constantly stirred during the entire filtration process in order to pump homogeneous broth into the system; this is of particular importance for concentration experiments especially when using a pre-flocculated feed. For lab experiments, the USD membrane device in **Figure 4.2** is substituted with the hollow fibre cartridge (Section 2.4.2.1). Prior to each run, the membrane is flushed with water followed by a water flux test. Then equilibration was performed using the culture media as a conditioning buffer. When in operation, the permeate port further away from the feed port was used in order for the feed to flow through the entire membrane area. At the end of an experiment, a cleaning cycle followed by a water flux test was carried out in order to assess the effectiveness of the cleaning step and cleanliness/quality status of the membrane respectively. The cleaning procedure includes recirculating tergazyme (an enzyme detergent) for 30min, followed by a rinse with warm water; 0.5M NaOH solution was then recirculated and both cleaning formulations are heated to 60°C such that their final temperature in the reservoir tank is around 50°C. The cleaning cycle was repeated when a low water flux was recorded. The hollow fibre cartridge were stored in 30% v/v ethanol solution between experiments.

Operating the USD membrane device in a crossflow fashion was achieved by rotating the disc inside the retentate chamber which mimics the hydrodynamic shear in the crossflow device due to the cross-flow velocity. The shear experienced on the surface of the membrane for the USD device is expressed in terms of average surface shear rate. Equation

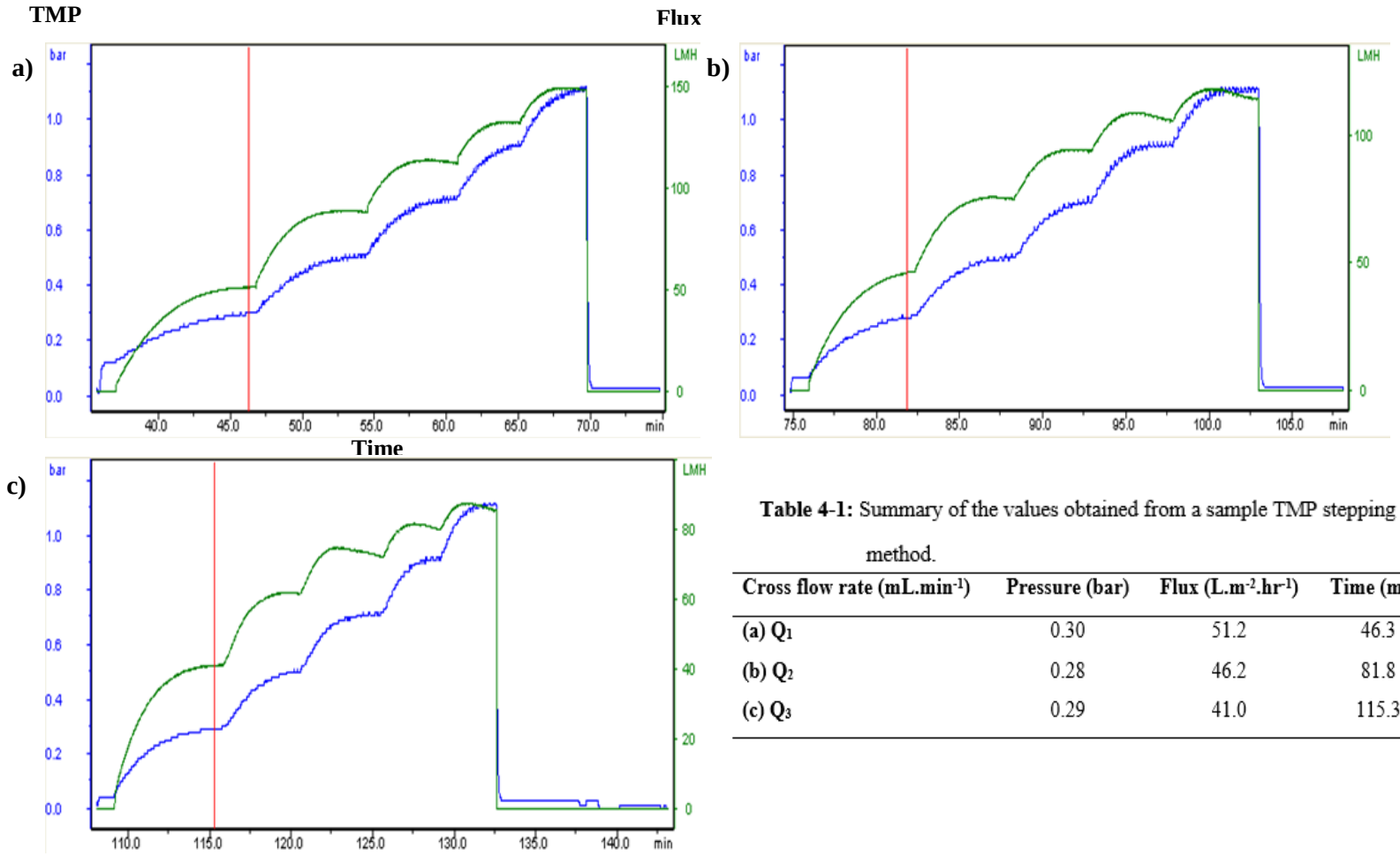

Table 4-1: Summary of the values obtained from a sample TMP stepping method.

Cross flow rate (mL.min^{-1})	Pressure (bar)	Flux (L.m^{-2}.hr^{-1})	Time (min)
(a) Q_1	0.30	51.2	46.3
(b) Q_2	0.28	46.2	81.8
(c) Q_3	0.29	41.0	115.3

Figure 4-3: Example of data from Unicorn showing an AKTA-generated stepping method to identify steady state profiles for flux at constant TMP. The graphs represent the different flowrates (Q) employed using a total recycle mode (a) high flow rate Q_1 which is run at 300 mL.min^{-1}; (b) Q_2-150 mL.min^{-1}; and (c) 75 mL.min^{-1}. It is evident that the flux (secondary axis) decreases as the flowrate is decreased. The graphs also show the stepping experiments for TMP over a range of 0-1.1 bar (primary y-axis) whose average steady point for flux was used to plot **Figure 4.4**. Experiments performed as described in Section 2.4.2.1

2.5 was used to calculate the disc rotational speed for mimicking the shear rate of the lab-scale cartridge. During USD critical flux determination, flux versus TMP profile had to be mimicked in the dead-end mode i.e. by varying the inlet flowrate as a result of unstable TMP values when operated in total recycle mode. This was so that fluctuations caused by unstable operating conditions which can lead to prediction problems at larger scale are avoided.

4.3 Effect of TMP and cross flow velocity on hollow fibre membrane flux

Initial filtration experiments were performed in the lab scale hollow fibre module. TMP and crossflow velocity are considered as the major parameters affecting fouling in crossflow microfiltration (Song, 1998) making it important to operate below critical values. To obtain these basic operating values, the effect of cross flow rate on flux at varying TMP was investigated. **Figure 4.4** shows that flux is directly proportional to both cross flow rate and TMP. Cake formation may be minimised by increasing cross flow velocity which directly relates to the hydrodynamic shear generated at the membrane surface. Since high velocities makes it difficult for algae to settle on the membrane, this induces higher flux. Measured permeate fluxes will typically increase as a function of TMP (Bacchin *et al.*, 2006) until a critical flux is reached; where flux is insensitive to further increase in TMP.

At low TMP's the flux increased almost linearly with increasing cross flow rate. The shear rate equivalent of each flowrate was calculated using Equation 2.3. High flow rates (150 and 300 $mL.min^{-1}$) which corresponded to shear rates of 4000 and 8000 s^{-1} showed increases in flux rates at increased TMP's for both photo- and hetero- trophic feeds (**Table 4.2**). For 75 $mL.min^{-1}$ (2000 s^{-1}), algal cell deposition or fouling begins to occur at higher TMP's especially for heterotrophic broth in comparison to phototrophic broth. With respect to culture age, no significant difference was seen when fresh or 24 hr old feed was filtered. This was observed for both hetero- and photo- tropically cultured broths.

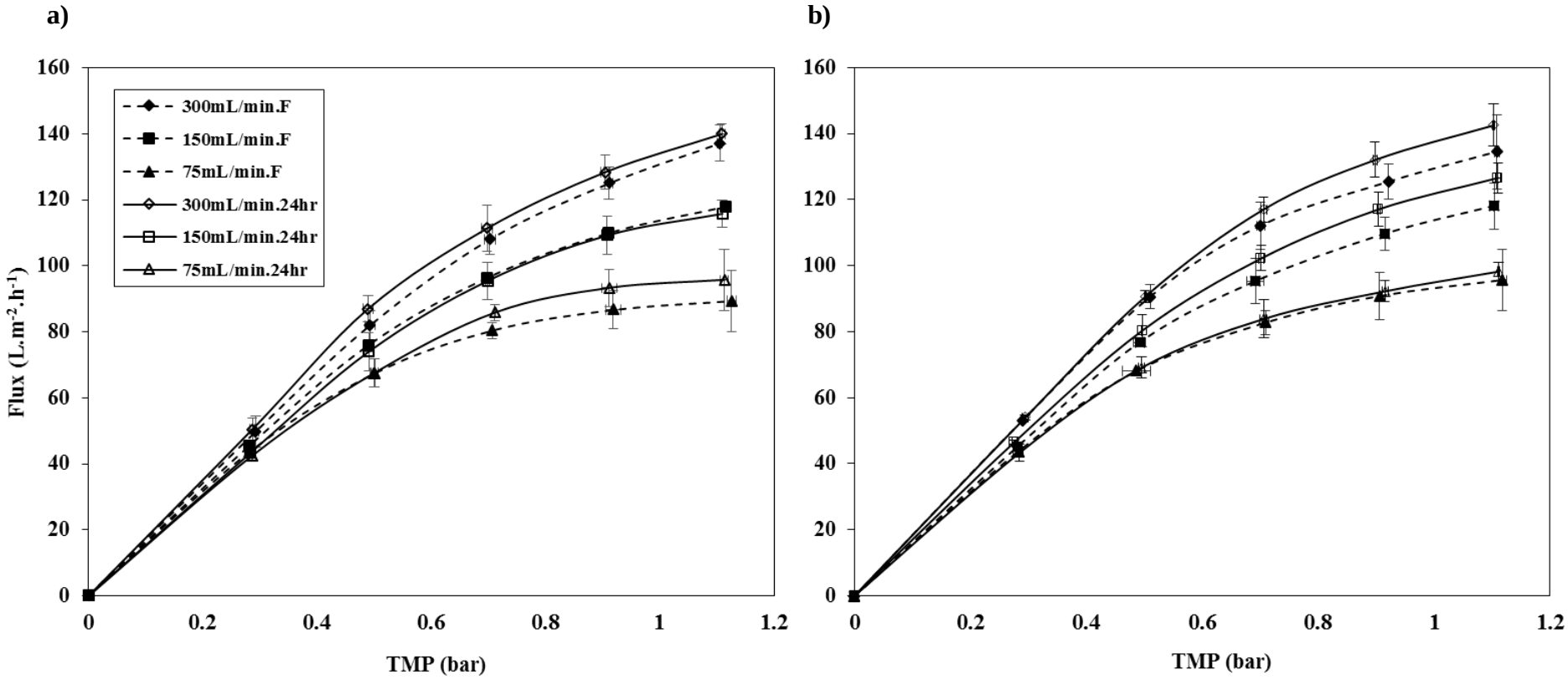

Figure 4-4: Graph of permeate flux ($L.m^{-2}.h^{-1}$) versus TMP (bar) for 5 $g.L^{-1}$ algal broth operated in total recycle mode for: (a) heterotrophic, and (b) phototrophic grown cultures. Solid and dotted lines or F and 24hr (on legend) stand for fresh and 24 hr old broth respectively. Detailed experimental conditions as described in Section 2.4.2.1. Data points were obtained by operating at crossflow rates recommended by the manufacturer. Error bars represent one standard deviation about the mean ($n \geq 3$).

Table 4-2: Summary of the recorded steady flux points obtained for (a) heterotrophic and (b) phototrophic algae culture at different flowrates (crossflow velocities). Experiments performed as described in **Figure 4.4**.

a) Flux ($L.m^{-2}.h^{-1}$)	**300 $mL.min^{-1}$**		**150 $mL.min^{-1}$**		**75 $mL.min^{-1}$**	
TMP	Fresh	24hrs	Fresh	24hrs	Fresh	24hrs
0.30	52.9	50.5	45.4	45.4	42.5	43.3
0.50	**87.0**	**82.0**	**74.0**	**76.0**	**67.5**	**67.5**
0.70	111.1	108.1	93.9	95.5	85.9	80.4
0.90	128.4	125.1	108.2	109.2	93.3	86.7
1.10	140.0	137.2	115.8	117.9	95.8	89.4

b) Flux ($L.m^{-2}.h^{-1}$)	**300 $mL.min^{-1}$**		**150 $mL.min^{-1}$**		**75 $mL.min^{-1}$**	
TMP	Fresh	24hrs	Fresh	24hrs	Fresh	24hrs
0.30	52.0	53.2	46.5	46.5	43.4	43.0
0.50	**90.6**	**88.8**	**80.3**	**76.8**	**69.1**	**68.9**
0.70	117.0	112.1	102.2	95.3	83.9	80.9
0.90	132.0	125.4	117.1	109.6	92.2	92.2
1.10	142.5	134.4	126.6	118.1	98.2	94.2

In order to preserve the membrane integrity, it is advisable to operate at low TMP's so that the mechanical strength of the membrane is sustained over time. Considering this, a TMP of 0.5 bar was chosen and a cross flow rate of 300 $mL.min^{-1}$ (8000 s^{-1}) for further investigation

4.4 Influence of initial biomass concentration on hollow fibre performance

The influence of initial biomass concentration on the time of filtration was studied. A point to note here is that less concentrated suspensions were prepared by appropriate dilution of the concentrated feed with spent media to avoid any changes in the physio-chemical properties of the suspension medium. **Figure 4.5** shows that the lower the biomass concentration, the shorter the processing time. Hence, filtration time is dependent on the initial biomass concentration of the feed as this also relates to the extent of permeate flow that can be achieved (flux). A study by Gerardo *et al.* (2014) reported that membrane performance is highly dependent upon cell concentration. Algal concentration can also affect membrane fouling since the amount of AOM (algogenic organic matter), a major fouling component secreted by algae (Zhang *et al.*, 2010), will be proportional to the amount of cells present. In evaluating the factors that influence the cost of a process such as membrane filtration, the initial biomass concentration and other operating parameters play a significant role. Nevertheless, different quantities of biomass would be recovered as product at the end of the harvesting cycle. However, the cost of harvesting microalgae has always been reported on a mass basis although process operating parameters such as temperature and membrane surface area can affect this.

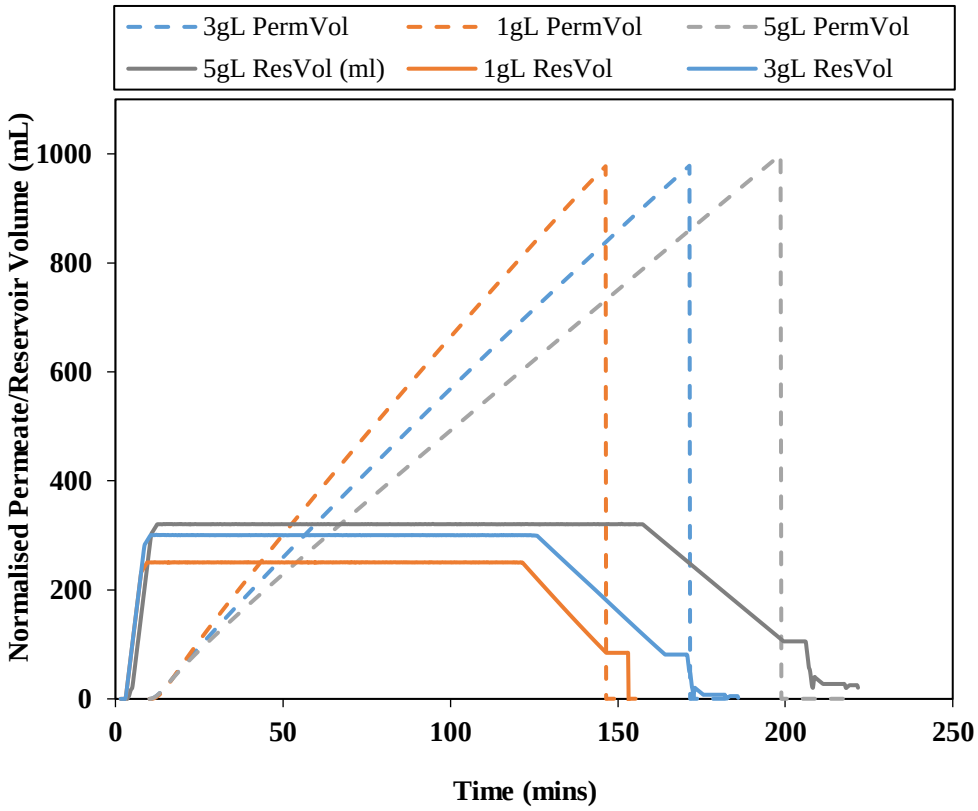

Figure 4-5: Influence of initial biomass concentration on the processing time based on 1L starting volume and 10x concentration factor. Solid lines represent reservoir volume while dotted lines are the corresponding permeate volume. Experimental conditions are as described in Section 2.4.2 with operating conditions in a concentration mode using a shear rate of 8000s^{-1}, temperature of 25°C and effective filtration area of 50 cm^2.

4.5 Influence of physiological state of culture on hollow fibre membrane fouling

Initial studies on filtration parameters showed no significant difference in the flux-TMP profile for fresh broth and broth kept overnight prior to use (Section 4.3). This section explores how the physical state of the membrane was affected due to variation in metabolism and /or age. It has been reported that the physiological state of the algal culture and EOM determines the rate of fouling (Babel & Takizawa, 2011; Wicaksana *et al.*, 2012).

4.5.1 Cleaning efficiency

Extracellular polymeric substances (EPS) of algae and cyanobacteria can act as a coating that can change the physio-chemical surface properties of the membrane. The performance of these membrane will then be affected by the fouling caused due to these extracellular compounds. Babel &Takizawa, (2010) showed that fouling of membrane caused by dewatering *Chlorella* was highly dependent on the amount of EOM present in the medium. Several studies have shown that these AOM are comprised mainly of polysaccharides, polysaccharide-like substances or proteins (Chiou *et al.*, 2010; Hung & Liu, 2006; Wicaksana *et al.*, 2012; Zhang *et al.*, 2010).

Figure 4.6 below shows how the physiological state of the microalgal culture affects the cleaning efficiency. Different effects were observed for the different culture types (photo- and hetero- trophic) and also how the culture age affects the extent of cleaning. In general, phototrophic broth fouls less than a heterotrophic one. Phototrophic broth attained the initial flux (water flux test) in short cleaning cycles; three cycles for 24 hr old broth and 4 cleaning cycles for freshly filtered broth. Heterotrophic broth on the other hand required more cleaning cycles. This characteristics can be linked to the extent of fouling caused by the different culture types which is attributed to the amount of EOM (released by the algae cells while metabolizing (Babel & Takizawa, 2011)) and algal cake deposit on the membrane. This was supported by FTIR analysis (**Figure 4.7**) which shows phototrophic

cells secretes less EPS components than heterotrophic cells. Membranes used for harvesting 24hr old broth (which is the broth kept at room temperature overnight after harvest) cleans faster than those used for freshly harvested broth.

In a study by Wicaksana *et al.* (2012), it was reported that the shear forces generated as a result of high cross flow velocity enhanced the transmission of EPS. One of the fouling control strategies for algal concentration process involved optimizing the cleaning method. Continuous washing of the filters (alternating an enzyme detergent with chemical solution) was found to improve the cleaning efficiency in comparison to cleaning with chemical only Also, the choice and use of enzyme detergent was because Tergazyme is assumed to facilitate the breakdown of adsorbed fouling compounds from membrane surfaces. This was however only able to sustain the membrane for 3-4 uses until irreversible fouling occurred and cleaning took longer than will realistically be accepted. Fouling is a major constraint as it shortens the lifespan of the membrane (Chiou *et al.*, 2010) because the organic composition of the foulant can remain even after chemical cleaning.

Having to look at the overall cost of membrane filtration, maintenance-associated cost such as cleaning will definitely play a role. The membrane type, use of detergent and temperature of the cleaning fluid have an effect on the cleaning efficiency.

4.5.2 FTIR and SEM to define EOM

FTIR analysis of the algal cells grown using different culture medium was carried out in order to find a correlation between the characteristic EPS and fouling. Spectra of the different cells studied showed similar functional groups on algal surface; these functional groups are identical to those reported for algae in literature (Chiou *et al.*, 2010; Her *et al.*, 2004; Hung & Liu, 2006). Strong absorption bands were seen at 3300 cm^{-1} which represents the presence of proteins due to stretching of N-H bonds, 2930 cm^{-1} due to asymmetric stretching of aliphatic -CH_2, 1640 cm^{-1} due to stretching of C=O bonds (amide I band),

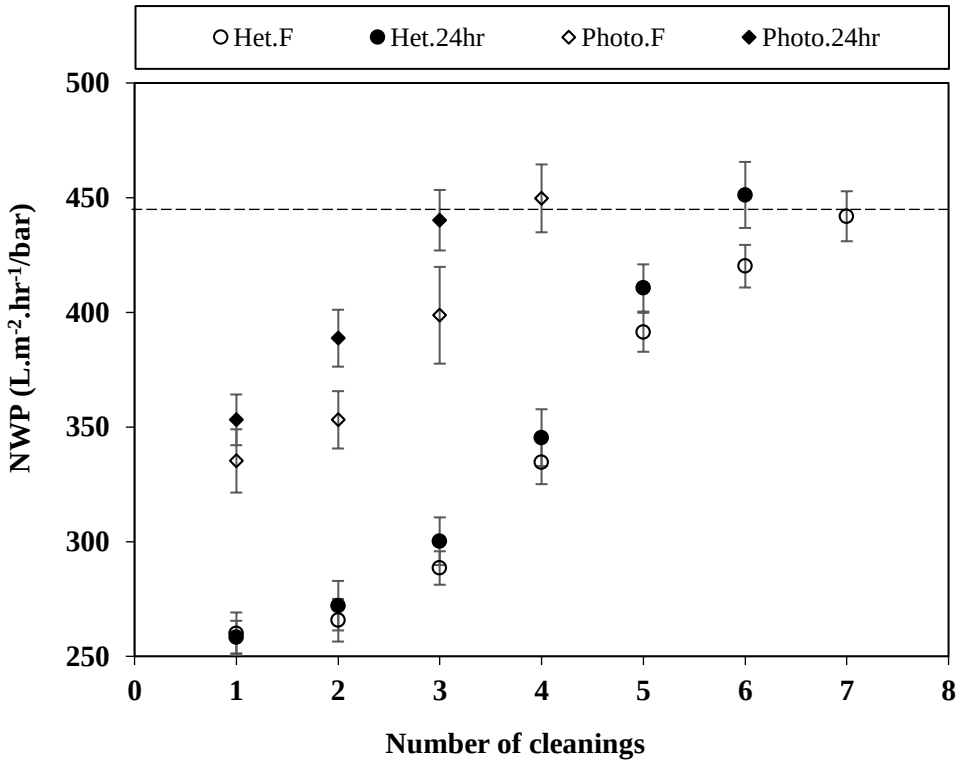

Figure 4-6: Influence of culture type on membrane fouling. Cells were grown as described in Section 2.2 and filtered using hollow fibre cartridges. Cleaning was achieved as described in Section 4.2 using Tergazyme and 0.5M NaOH at 50°C. Dotted line signifies the membrane permeability (NWP) where the membrane is considered clean. Error bars represent one standard deviation about the mean ($n \geq 3$).

1550 cm^{-1} due to deformation of N-H bonds (amide II band) as well as 1024 cm^{-1} due to C-O bonds which has been associated with polysaccharides (Her et al., 2004; Hung & Liu, 2006; Zhang *et al.*, 2010). Based on these spectra, protein and polysaccharide-like substances were revealed as major constituents of algal EPS. A point to note here is that FTIR analysis was run with the same quantity of cells for each experiment using a force gauge of 50. Heterotrophic cells contained more EPS (**Figure 4.7**) which is closely linked to the polysaccharides present in the media formulation. This is as a result of the intensity of the absorption peaks shown in comparison to phototrophic cells because the intensity of a spectra can be related to the amount of soluble EPS present (Chiou *et al.*, 2010). As algal cells in this study were harvested for their lipid, peaks at 1400 cm^{-1} denote membrane foulants contained lipids (Ramesh *et al.*, 2007). However, this was not recorded here because cell lysis was not experienced; pH of the media and permeate absorbance remain unchanged for the duration of the process except for flocculated feed where absorbance was seen to increase but this was attributed to the presence of Chitosan in the solution (Section 4.6).

Observation of the fresh and fouled USD filters for both heterotrophic and phototrophic broth using SEM is shown in **Figure 4.8**. The surface of the unused filter was seen to be clean and smooth whilst for the used membranes with heterotrophic broth the membrane was observed to possess foulants which was mostly deposited algal cake. The phototrophic broth showed randomly deposited algae but the filter pores was blocked with other AOM.

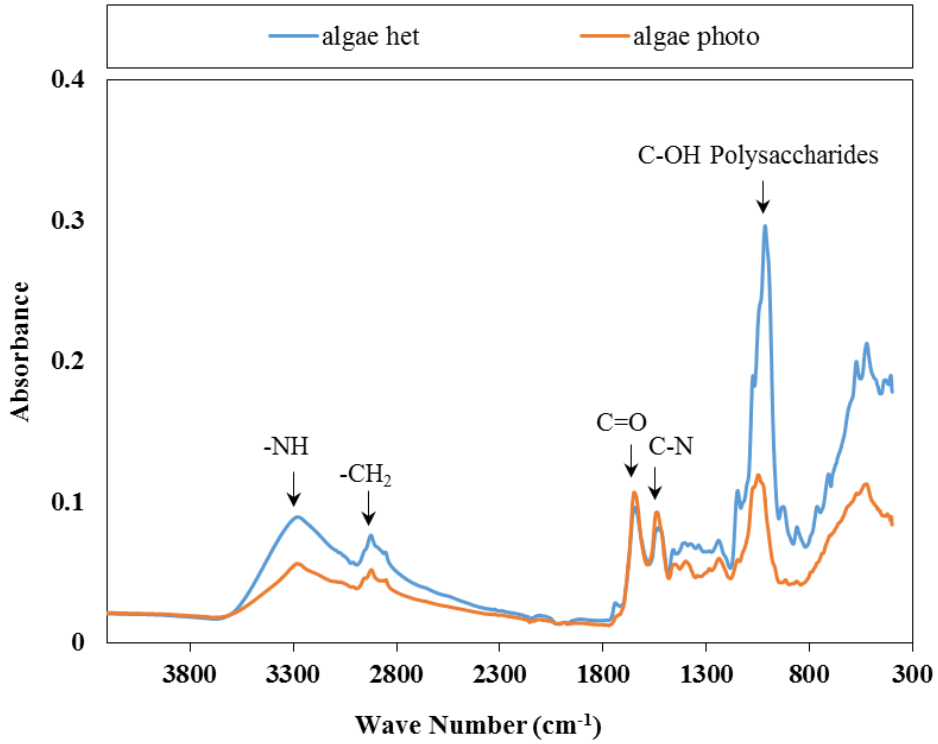

Figure 4-7: Use of FTIR to define EPS components on algal cell surfaces for heterotrophic (het) and phototrophically (photo) grown algae cells. Experiment was carried out as detailed in Section 2.10.5 with cells grown as described in Section 2.2.

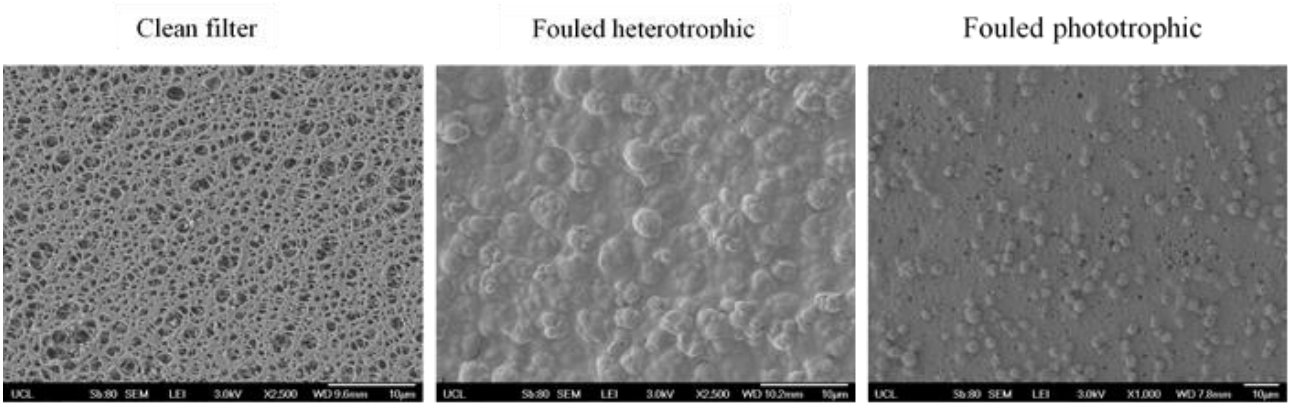

Figure 4-8: SEM images of a USD fresh filter and filter fouled with heterotrophic and phototrophic broth. Experiment was carried out using 5 $g.L^{-1}$ algal broth at TMP above the critical value.

4.6 Effect of broth pre-treatment (flocculation) on filtration performance and cleaning

Appropriate pre-treatment can enhance membrane performance due to the larger particle size of the suspensions being processed. Having established a reliable and reproducible method for the production of Chitosan flocculated *C.sorokiniana* cells (Chapter 3), the next step was to evaluate the impact of this pre-treatment on microfiltration performance. In this study, flocculation which leads to the formation of large flocs (Chapter 3) was explored prior to the membrane filtration since membrane-type dewatering of algal broth has been reported for different algae species but cell size influence is yet to be established (Gerardo *et al.*, 2014).

At the start of a concentration method, the permeate flux was seen to rise for a few minutes and then drastically drop until it attains a steady state in all conditions studied (**Figure 4.9a**). Flocculation was seen to impact on the initial flux which in turn influences the average permeation of the process. The greater the amount of flocculant, the higher the initial flux until steady flux is attained which was seen to be similar for the different flocculant concentrations tested. Increasing the Chitosan concentration from 1 to 2 $mg.mL^{-1}$ had only a slight effect on microfiltration; even though floc sizes (d_{50}) increased form 6.40 ± 1.71 to 17.90 ± 10.95 (Chapter 3). This did not make significantly impact on the microfiltration performance (with respect to time) as time-flux profile for both is seen to have minimal variation (**Figure 4.9**). Increasing the Chitosan concentration to 5 $mg.mL^{-1}$ made an impact by saving 20% of the processing time in comparison to the unflocculated feed.

Effect of pH, preconditioning and absorbance of the feed before filtration processes have also been reported to influence performance (Ohmori & Glatz, 1999). These parameters are therefore important during crossflow filtration. Changes in absorbance (on the permeate side) may denote cell lysis which is not desirable as loss of cellular components might be

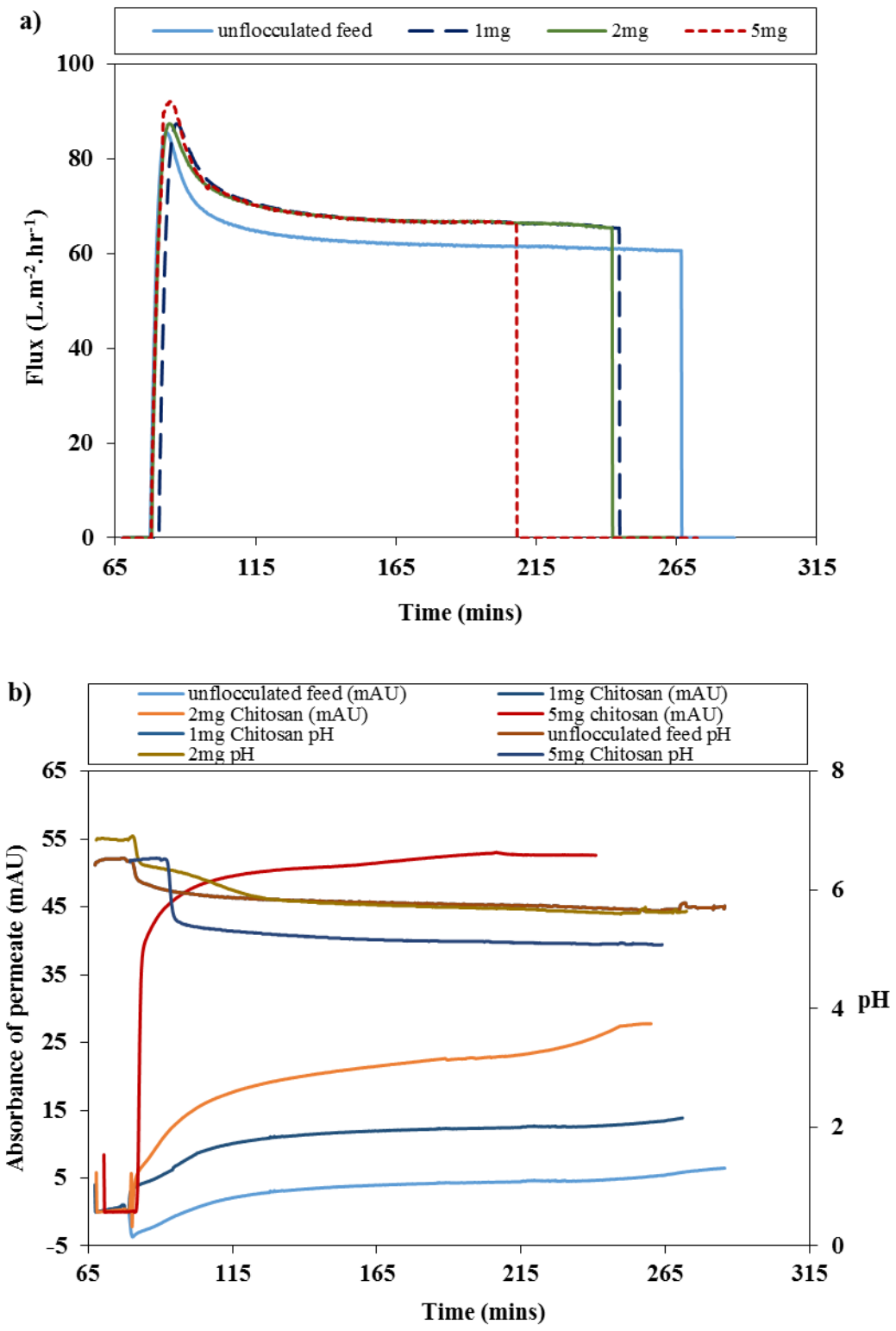

Figure 4-9: Effect of flocculation on microfiltration performance over time. Algal broth containing 5g.L^{-1} cells was: (a) flocculated as described in Section 2.4.1 and used for microfiltration studies (Section 2.4.2) and (b) the recorded pH and permeate absorbance were carried out automatically by the unicorn software of the AKTA crossflow system. An unflocculated feed was also processed as the control.

experienced. **Figure 4.9b** shows the change in absorbance and pH over time for the entire filtration process. It can be seen that the pH of the system did not change significantly especially at low Chitosan concentrations. The results were seen to overlap with pH of the unflocculated feed. Higher Chitosan concentration resulted in a lower pH but this still remained within range (≤ 0.5 of the initial pH). With respect to absorbance of permeate, this was seen to change/increase with an increase in the concentration of Chitosan. Further investigation into this revealed that it was the presence of Chitosan that changed the permeate turbidity rather than cell damage. Besides, the shear experienced by the cells/flocs was minimal in comparison to those *Chlorella* cells were exposed to during shear studies (Chapter 5) and this did not cause cell breakage.

4.6.1 Influence of flocculation on cleaning

Chitosan used for algal flocculation is a derivative of the natural polysaccharide Chitin which is obtained by its partial deacetylation (in its solid state) in the presence of an enzyme chitin deacetylase. The influence of Chitosan-flocculation on the media can be associated to the fouling properties and this depends on the type of Chitosan used (i.e. the degree of acetylation and distribution of the acetyl groups along the main chain in addition to the molecular weight). Also, Chitosan type/properties depends on the origin of the polymer

(Rinaudo, 2006). The degree of deacetylation of Chitin to form Chitosan also influences its solubility in aqueous acidic media (preparation of Chitosan solution used for flocculation; Section 2.4.1). Chitosan has a heterogeneous distribution of acetyl groups along its chains as a result of semi-crystalline morphology of Chitin when it is obtained by a solid-state reaction. The influence of the heterogeneous distribution of acetyl groups has been shown to be an important factor controlling solution properties (Aiba, 1991). The solubilisation on the other hand occurs by protonation of the $–NH_2$ function on the C-2 position (**Figure 4-10**) of the D-glucosamine repeat unit, through which the polysaccharide is converted to a polyelectrolyte in acidic media. Polysaccharides being a major foulant during filtration

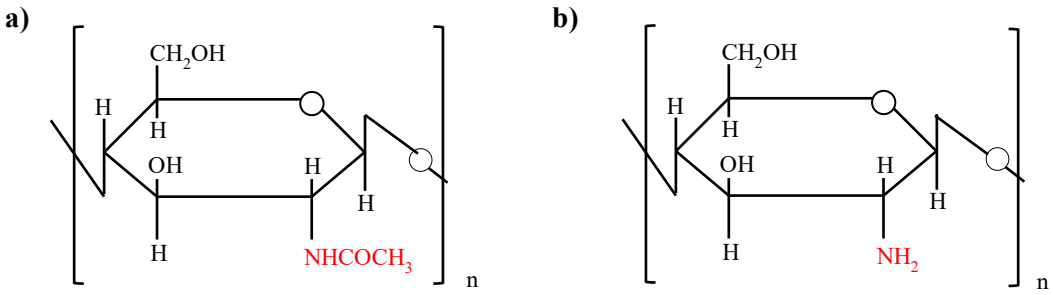

Figure 4-10: Chemical structure of (a) Chitin poly(N-acetyl-β-D glucosamine) and (b) Chitosan poly(D-glucosamine) repeat units. Data taken from Rinki *et al.* (2009)

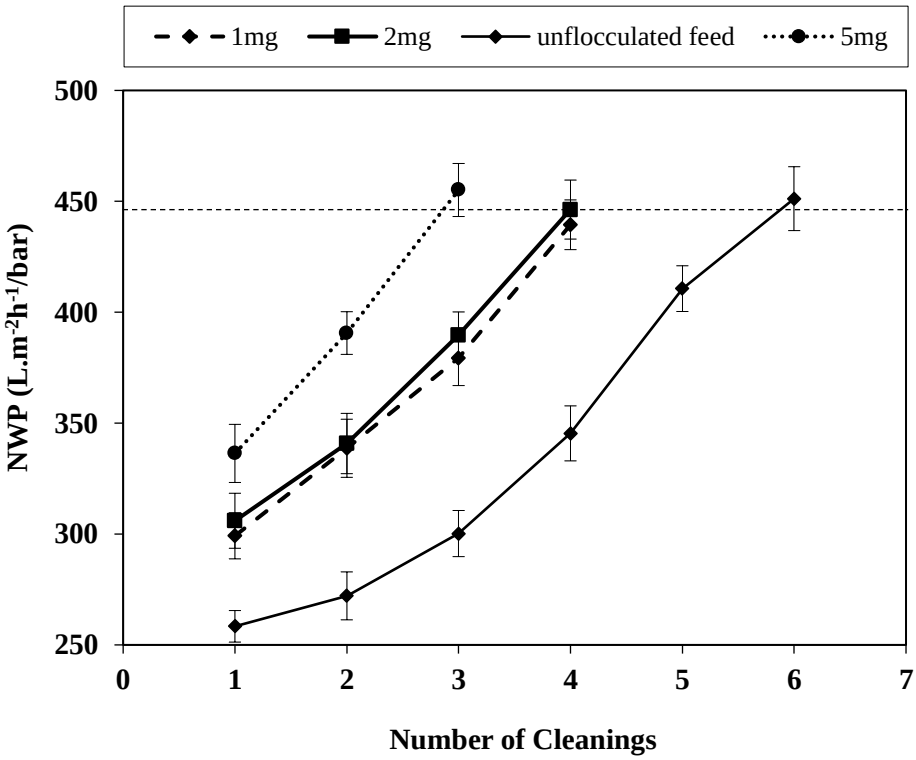

Figure 4-11: Comparison of the cleaning cycles required for membranes used for filtering unflocculated and flocculated broth. Algal broth was flocculated as described in Section 2.4.1 and cleaning was achieved as described in Section 4.5. Error bars represent one standard deviation about the mean (n = 3).

(Section 4.5.1) now finds application as a polyelectrolyte flocculant for algal cells possessing negatively charged cell walls and sometimes for other flocculation applications like protein recovery etc. Even though AOM (which consist of polysaccharides and polysaccharide-like substances) are the main components considered to cause membrane fouling, probably the fouling effect is due to those polysaccharides produced by metabolizing algae or reaction within the media during growth; this however needs to be carefully delineated. Nonetheless, the cleaning cycles required for a membrane used to dewater unflocculated heterotrophic broth is halved by flocculating these cells (using ≥ optimal Chitosan concentration) (**Figure 4.11**). Also, other pre-treatment types have been shown to produce valuable effects on coagulation of algae suspension by changing the characteristics and amount of EOM (Hung & Liu, 2006).

To further support the findings of flocculation effect on fouling, a close look at the FTIR spectrum of algae flocculated with low and high dosage of Chitosan (**Figure 4.12a**) shows that intensity of the functional groups decreased when flocculated with high dosage of Chitosan. This point supports **Figure 4.9** and **Figure 4.11** where high Chitosan dosage made more impact on filtration performance and cleaning respectively than low dosages. Additionally, **Figure 4.12b** illustrates that the spectra for high Chitosan flocculated cells (heterotrophically grown) has similar intensity of the major functional groups as to those phototrophically grown (and /or flocculated with low Chitosan dose). This explains why the cleanings are similar **Figure 4.6** and **Figure 4.11**. Phototrophic cells have previously been shown to possess less EPS components than their heterotrophic counterparts (**Figure 4.7**) and hence required lesser cleaning (**Figure 4.6)**.

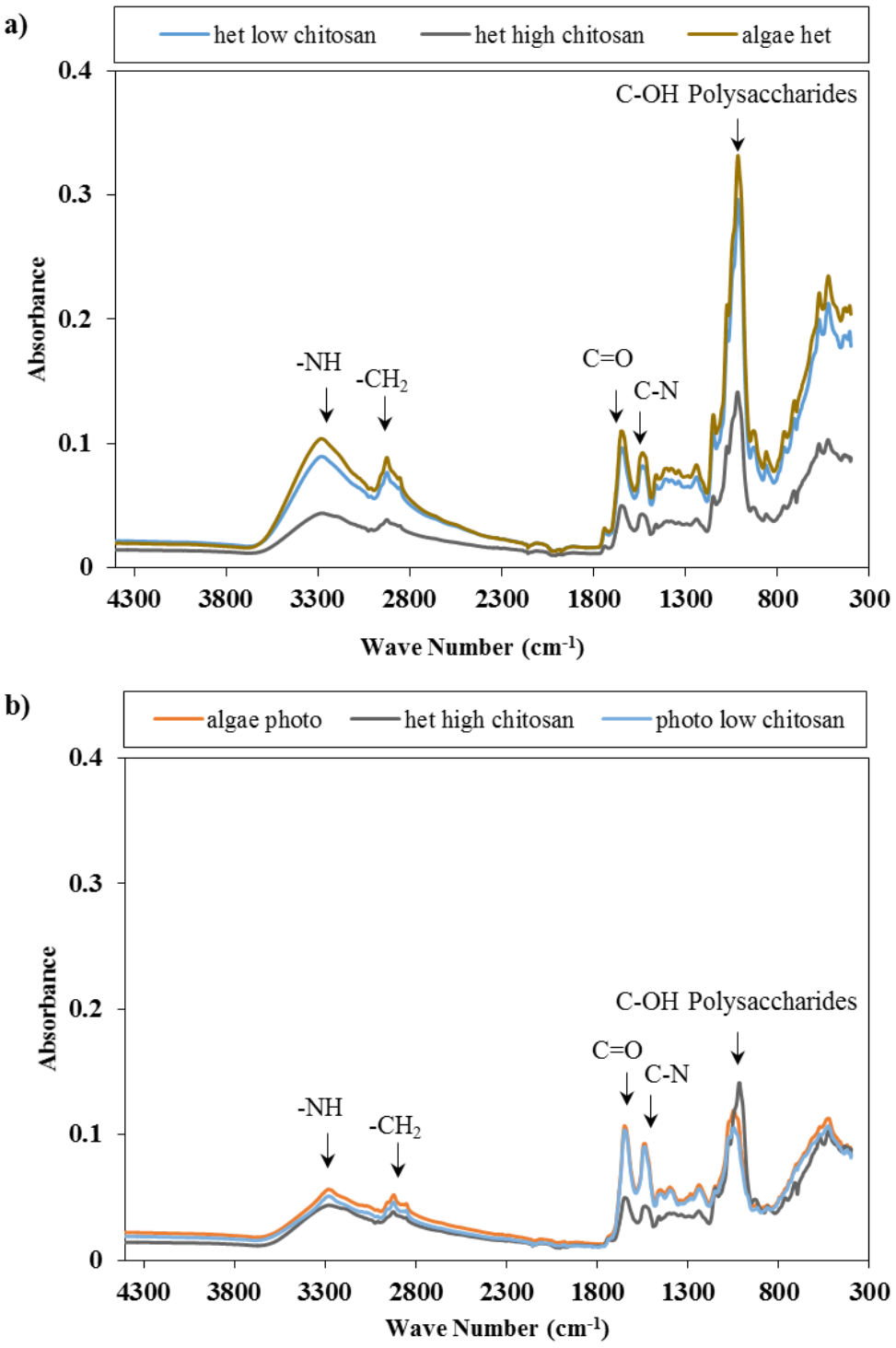

Figure 4-12: FTIR spectra comparing the EPS components of (a) flocculated and unflocculated heterotrophic cells and (b) flocculated phototrophic, unflocculated phototrophic and flocculated heterotrophic cells. Experiment was carried out as described in Section 2.10.5 with cells grown or flocculated as described in Sections 2.2.2 and 2.4.1.2 respectively.

4.7 USD verification of lab experiments

As described in Section 1.9, the development of a USD platform for early stage microalgae processing is the overall aim of this thesis. Scale down of unit operations is important as the smaller scale devices can be used for optimisation process, trouble shooting and validation studies (Van Reis *et al.*, 1997). It is however important to achieve consistent results across these scales of operation (scale- up or down). Since characterization of filtration performance was done in Section 4.3, the next step is to use USD methods to mimic the lab-scale systems on the basis of matched operating conditions.

4.7.1 Mimicking permeate flux and TMP profiles

As mentioned in Section 4.7, obtaining consistent results was of optimal importance, therefore, before using the USD device to evaluate filtration performance, a comparable crossflow filtration methodology had to be determined. In an effort to obtain steady state fluxes for each of the lab-scale and USD systems, crossflow microfiltration experiments was carried out at varying TMP conditions and matched shear rate. TMP and cross flow velocity are defining operating variables for membrane filtration at production scale acting as the physical driving force through the filter medium and influences fouling (section 4.3). Moreover, process flux is dependent on TMP (especially when operating at low feed concentration, low pressures and high crossflow rates) until the critical flux is reached. Steady flux in membrane filtration is a key criterion in measuring performance as it provides information needed for scaling-up filtration processes (Bacchin *et al.*, 2006).

Considering the above, the USD device was operated at constant TMP (between 0 and 1.1 bar) using a similar average surface shear rate as that of the lab-scale module (8000 s^{-1}). As shown in **Figure 4.13a** and **4.14a**, at the matched shear rate (calculated using equation 2.5) the flux measured in the USD membrane device was consistently lower than in the hollow fibre module. The reason for the difference is thought to be for one or a combination of these reasons:

(1) different membrane materials, as disc membranes are polyethersulfone (PES) while lab-scale cartridge is made of Polysulfone (PS) (**Figure 4.15**). Although the difference between PES and PS is minimal, it is expected that dissimilar clean membrane resistances would exist;

(2) variation in membrane porosity. It has been reported that slight difference may exist between the lab-scale and cut discs in the bubble point pressure (Rayat, 2010). Bubble point test is normally used to measures the maximum pore size in a given membrane (Mulder, 1996). Bubble point is indirectly proportional to pore diameter hence, a higher bubble point means a smaller pore diameter; and

(3) design limitation. The hollow fibres consist of turbulence promoters and screens which are considered to aid filtration. Therefore, consideration was given to the practical design limitation of the USD device to compensate for absence of these turbulence promoters, screens etc.

As a result of the higher flux profiles attained in the lab-scale and also the fouling experienced on the USD membrane at matched shear rate; and since the wall shear rate calculations for screened channels are normally assumed to be approximate or relative values (Millipore, 1998), the shear rate and feed flow rate of the USD device was increased. The shear rate was increased up to a value of 13100 s^{-1} where there was closer agreement between the USD and hollow fibre devices. This increase improved the performance of the USD device and similar flux profile to that of the lab scale was seen (profiles within ≤10 $L.m^{-2}.h^{-1}$) **Figure 4.13**.

In addition, the flat sheet disks used in the USD membrane device would have been made of the same material and have the same pore size as the hollow fibre membrane cartridge. Unfortunately this was not possible. The hollow fibre cartridge comprised of a polysulfone membrane with 500 kD molecular weight cut off. Based on the manufacturers recommendation of the closest available flat sheet membrane, a polyethersulfone (**Figure**

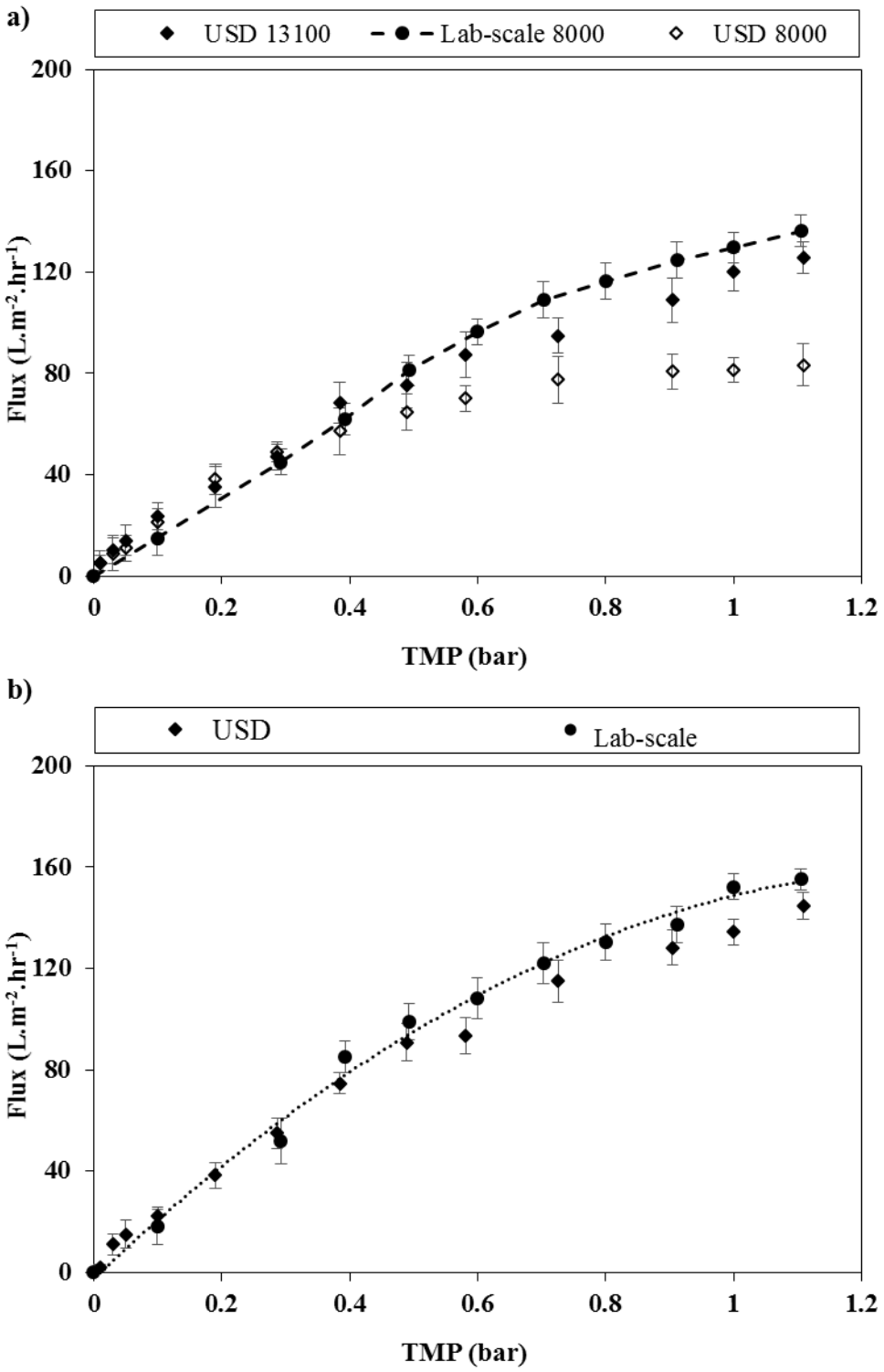

Figure 4-13: Comparison of flux and TMP relationship determined with laboratory hollow fibre (500kD) and USD membrane device (0.03µm discs) in a dead-end mode: (a) unflocculated feed at matched shear rates and at increased shear rate (13100 s^{-1}) and flow rate for USD and (b) flocculated feed with lab scale at 8000 s^{-1} and shear rate of USD device at 13100 s^{-1}. Experiments performed as described in Section 2.4.2. Error bars represent one standard deviation about the mean (n = 3).

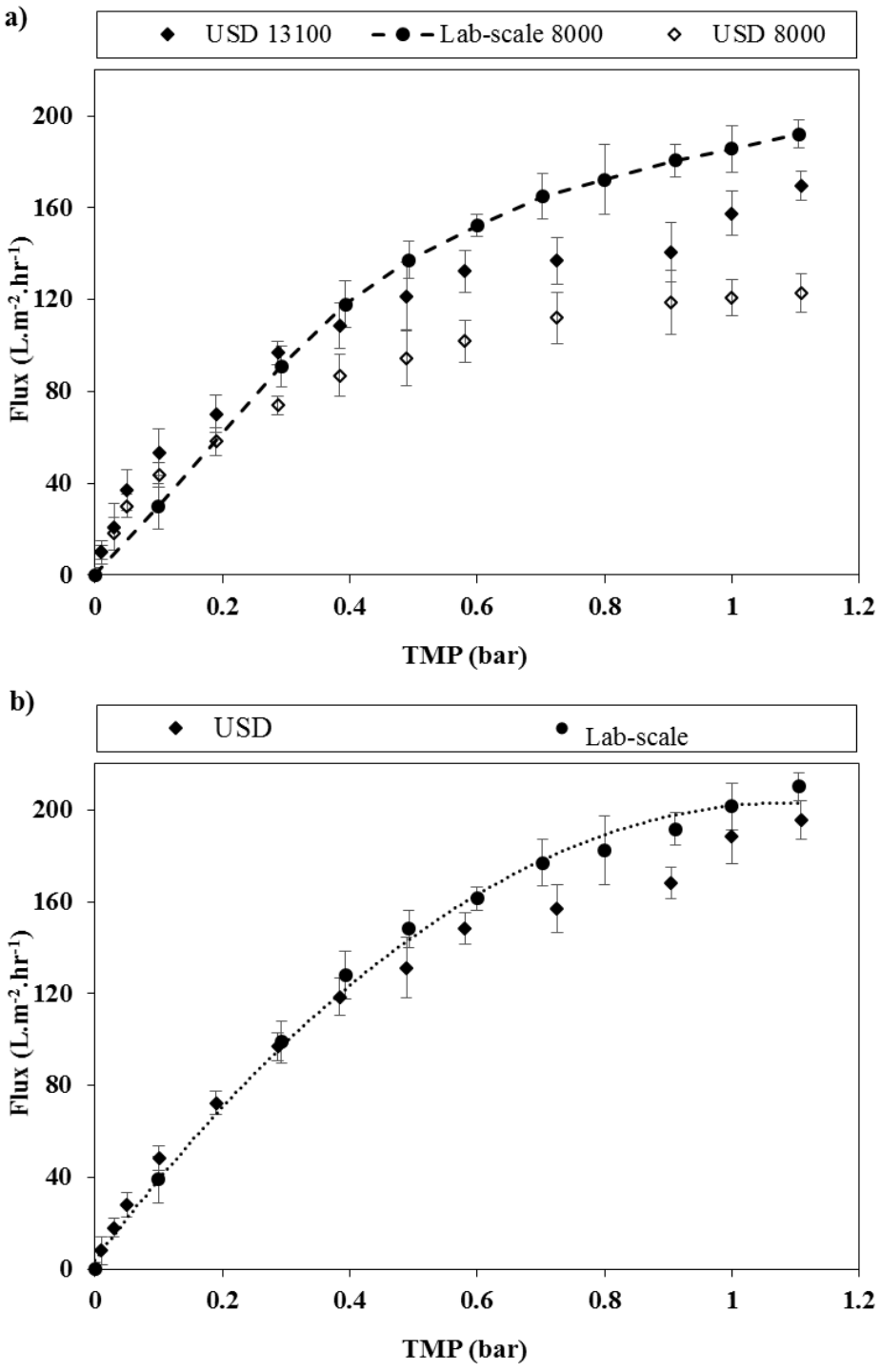

Figure 4-14: Flux and TMP relationship determined with laboratory hollow fibre (0.2 µm) and USD membrane (0.2µm discs) in a dead-end mode. (a) unflocculated feed at matched shear rates and at increased shear rate for USD (13100 s^{-1}) and (b) flocculated feed with lab scale at 8000s^{-1} and shear rate of USD device at 13100 s^{-1}. Experiments performed as described in Section 2.4.2. Error bars represent one standard deviation about the mean ($n \geq 2$).

4.15) membrane was used with a 0.03µm pore size. In order to overcome bubble point variation, a confirmation experiment using a 0.2 µm hollow fibre and disc membranes where used to re-run same experiment as **Figure 4.13**. Given the overlapping error bars the differences in the profiles are not statistically significant (**Figure 4.13** and **4.14**).

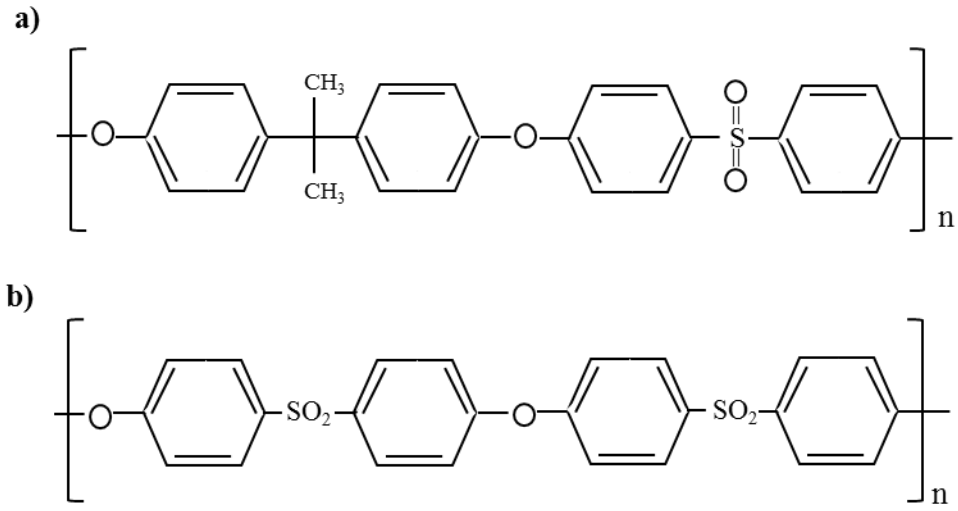

Figure 4-15: Chemical structure of: (a) polysulfone and (b) polyethersulfone repeat units.

4.7.2 Comparison of the filtration outcome parameters for USD and lab experiments

Before the USD device was used to evaluate filtration performance of algal suspensions, a comparable crossflow filtration methodology was first established to determine steady state flux. From the graphs presented in **Figure 4.13** and **4.14**, it can be seen that matching points (linear relationship) were obtained at TMP values ≤ 0.5 bar. On this basis, the USD device was suggested to be operated using a TMP of 0.5 bar, increased flowrate and shear rate of 13100 s^{-1} since this conditions fall within the range where there is similar trend with the lab-scale system and no significant changes in the permeate flux was seen.

Scaling down of membrane area requires a consequent reduction in the feed volume in order to keep the operation time as those of the large scale. Hence, using constant volume to surface area ratio, a concentration experiment was conducted in order to obtain and compare filtration outcomes with lab scale data **Figure 4.16**. Very similar flux values for USD and lab-scale experiments were recorded for both flocculated and unflocculated feeds. Also, pH and absorbance has been reported to be important parameters (Section 4.6) with regards to product condition. This was investigated during the USD studies and comparable results to those obtained during lab studies were obtained. Overall, the results obtained are comparable for both flocculated and unfloculated feeds.

To further explore the applicability of the USD device as a tool for fast and early data accusation, the characteristic nature of fouling was explored. SEM images of fouled membranes due to different biomass concentration is shown (**Figure 4.17** and **Figure 4.18**). Filtration is mostly applied at lab-scale because of membrane-clogging, formation of compressible filter cakes and principally high maintenance cost when operated at large-scale (Schenk *et al.*, 2008). Therefore, USD to predict and optimize process parameters will be beneficial at early stages of process development. For example, in **Figure 4.17** heterotrophically grown algal cells were observed to constitute foulants (in the form of algal cell deposit) and heavy coverage of membrane pores by other foulants (this reduced with decrease in biomass concentration). Other foulants included adsorbed or bonded biological and organic compounds (section 4.5.2) which is evident covering the filter pores.

The USD findings were verified at lab-scale and similar characteristics was seen. **Figure 4.18** is the phototrophic version that can support the data's for FTIR which suggests less EPS than heterotrophic (Section 4.5.2). This rapid data accusation and flexibility of the USD are rather expensive to be performed at larger scales (for example, destroying lab-scale cartridges for SEM imaging).

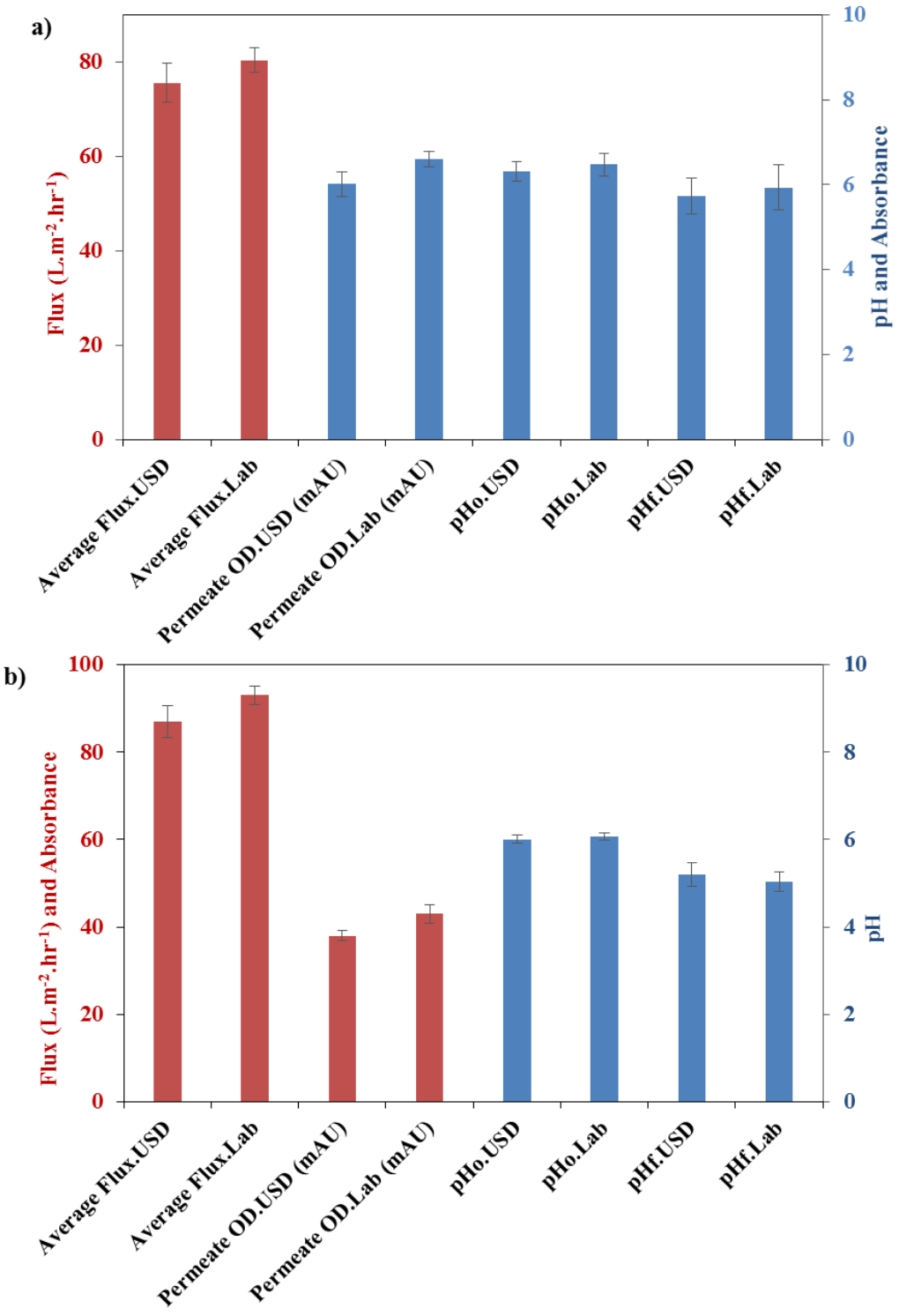

Figure 4-16: Comparison of laboratory and USD filtration performance in concentration mode. Experiment was performed using 5g.L^{-1} algal broth and operating conditions: TMP 0.5 bar, shear rate of 8000 s^{-1} and 13100 s^{-1} for lab and USD device respectively: (a) unflocculated, (b) flocculated with 9.5 mg of Chitosan per gram of algal dry cell weight. Both scales had similar final broth load per filter area (20 mL.cm^{-2}). Experiments performed as described in Section 2.4.2. Error bars represent one standard deviation about the mean (n = 3).

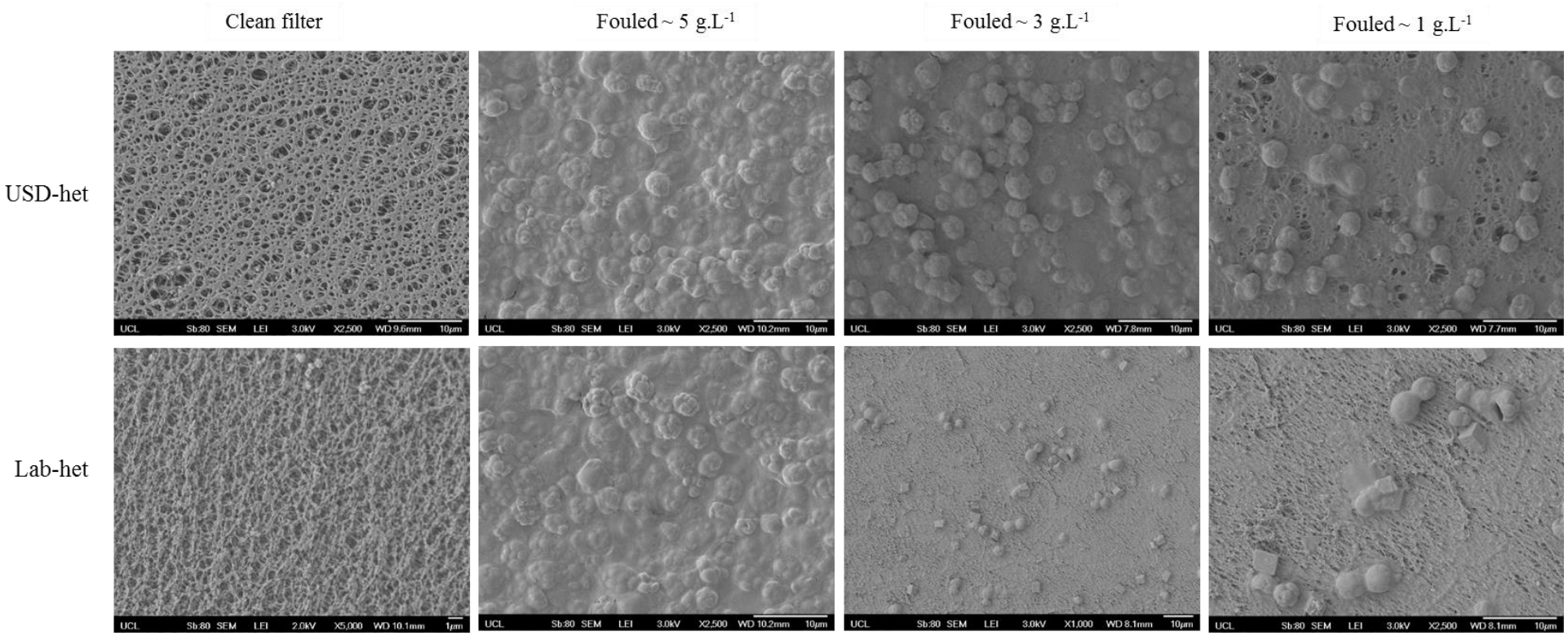

Figure 4-17: SEM images of clean and fouled USD membrane and hollow fibre filters after filtering heterotrophic broth at different cell concentrations. Experiment was carried out using operating conditions above critical TMP (0.7 bar). Filters were prepared and images taken as described in Section 2.10.9.

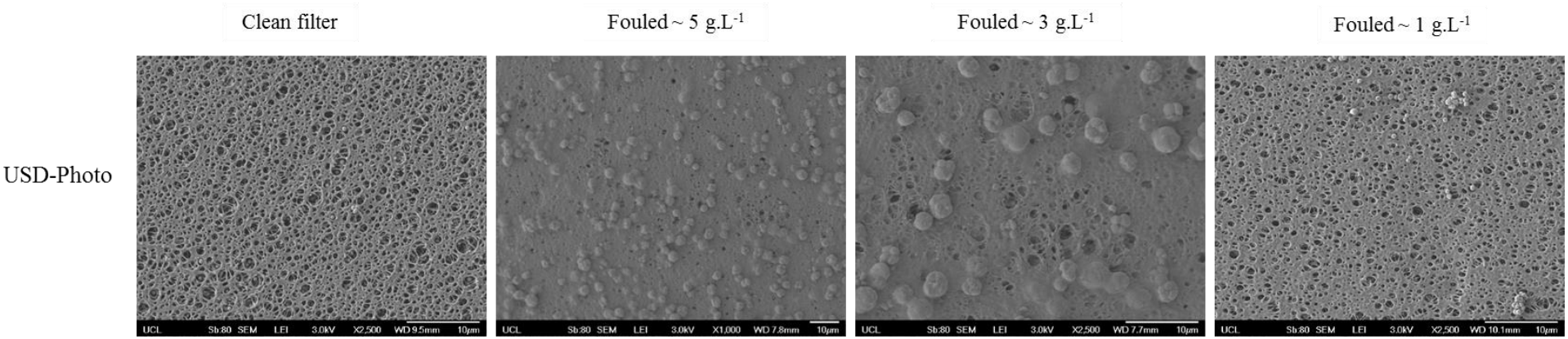

Figure 4-18: SEM images of clean and fouled USD membrane filters after filtering phototrophic broth at different cell concentrations. Experiment was carried out using operating conditions above critical TMP (0.7 bar). Filters were prepared and images taken as described in section 2.10.9.

4.8 Summary

As described in Section 4.1, the overall aim of this chapter was to explore and characterize algal harvest using microfiltration and to establish a USD method to mimic the findings. Key process parameters influencing filtration performance were explored including the effect of the physiological state of the algal culture on fouling (**Figure 4.7** and **4.8**) and consequently cleaning (**Figure 4.6**), the effect of broth pre-treatment (flocculation) on filtration performance (**Figure 4.9a**) and its influence on cleaning (**Figure 4.11**).

It was observed that the type and extent of fouling was dependent on the physiological state of the culture due the amount of EOM present. Further characterization of the different culture types using FTIR revealed that heterotrophically cultured cells possessed more EPS than their phototrophic counterparts (**Figure 4.7**). This was also evident during cleaning of the membranes after use, as longer cycles where required for heterotrophic compared to phototrophic.

With regards to broth pre-treatment, this was seen to influence cleaning positively (**Figure 4.11**) and aids filtration. FTIR spectra of the pre-treated broth showed lower intensities of the major EPS components in comparison to untreated cells (**Figure 4.12a**). This had an important benefit of reducing the number of cleaning cycles required.

Ultimately, a USD approach to cross-flow membrane filtration was successfully established that could accurately reproduce flux-TMP profiles at a defined shear rate. This was achieved at elevated shear rates in the USD device due to absence of spacers (turbulence promoter) which is a key element in a crossflow filter (**Figure 4.13** and **4.14**). Other filtration outcomes, such as flux, initial and final pH of the feed and absorbance of permeate were also in good agreement between the two scales for both unflocculated and flocculated feed (**Figure 4.16**). The advantage of the USD approach was that it required a 14-fold decrease in the volume of broth to undertake studies at match volume:surface area.

Finally, a further advantage of the USD method was that it enabled direct investigation and visualisation of the fouling characteristics of the heterotrophic and phototrophic broth on the membrane surface using SEM (**Figure 4.17** and **Figure 4.18**). Confirmation of the USD findings using lab-scale cartridges showed similar fouling characteristics between the two scales (**Figure 4.17**).

While a USD approach to study the filtration performance of microalgae suspensions has been established, the maximum concentration factor achieved was only 10-fold. Higher concentration cell suspensions are often required for subsequent operations such as lipid extraction from the biomass. Consequently the next chapter will investigate USD method for algal biomass recovery by centrifugation as this should enable grater dewatering of the algal cell suspensions. The impact of flocculation as a pre-treatment step on overall centrifugation efficiency will again be investigated.

5. USD Centrifugation

5.1 Introduction

Centrifugation has been highlighted as one of the key steps utilized in algal processing for biomass recovery and concentration (Section 1.4.2); it is a reliable and effective technique (Uduman *et al.*, 2010). Although the flocculation (Chapter 3) and filtration (Chapter 4) studies described in previous chapters have proven successful for concentrating algal biomass, these methods alone may not be sufficient for producing the required dewatering level as shown in **Figure 5.1.** This can be problematic further downstream (Mohn, 1978) and also microfiltration operations generally require longer processing times (Grima *et al.*, 2003). However, using centrifugation in algal processing has been reported to be energy intensive and requires high capital investment (Sim *et al.*, 1988). These disadvantages need to be considered alongside the fact that an increase in biomass concentration can decrease the cost of extraction and purification (Uduman *et al.*, 2010).

At present, commercial production and processing equipment for microalgae remain at a nascent stage, and methods for predicting behaviour during scale-up are generally not available (González-López *et al.*, 2012). USD technologies have some unique characteristics, as highlighted in Section 1.8, including the ability to rapidly investigate a range of operating conditions and the accurate prediction of large scale process performance (Titchener-Hooker *et al.*, 2008) using only small quantities of material. In other industry sectors the application of USD helps ensure rapid process evaluation and enables fast development of successful operations at industrial scale (Tustian *et al.*, 2007).

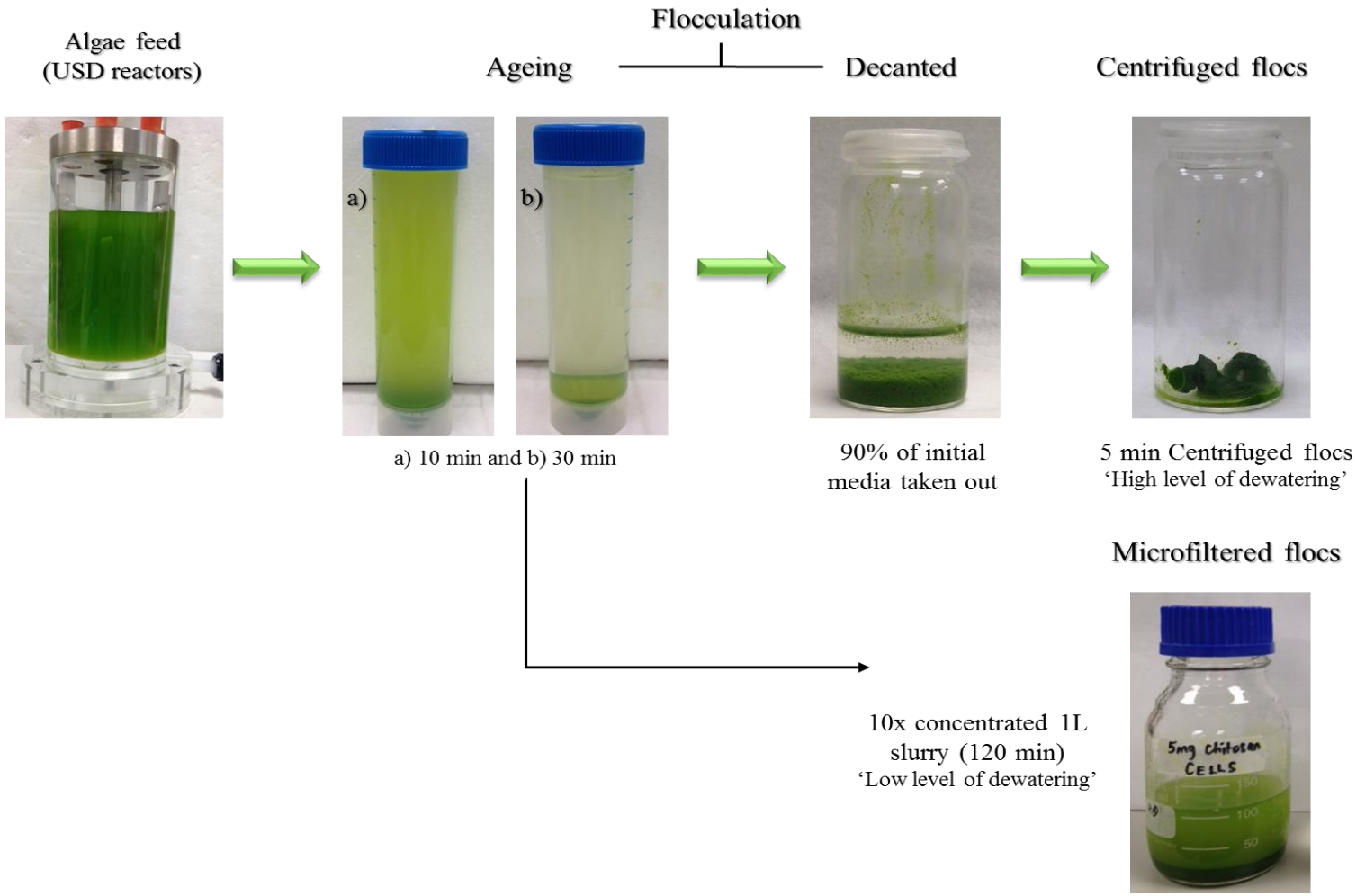

Figure 5-1: Photographs of the various dewatering steps used in this project. Showing the time it takes to settle and the level of dewatering achieved.

The aim of this chapter, therefore, is to establish a USD method for the study of centrifugation for microalgae recovery and concentration. This will also be used to investigate the impact of flocculation as a pre-treatment step on centrifugation performance. The specific objectives of this chapter are as follows:

- To characterize algal broth base on parameters that influence centrifugation efficiency.
- To study the mechanical stability of algal flocs by exposing them to shear equivalent to those experienced in industrial centrifuges.
- To explore the influence of flocculated and unflocculated cells on USD centrifugation.
- To validate the USD centrifugation predictions against the performance of a pilot scale centrifuge (CARR Powerfuge^{TM} centrifuge).
- To evaluate the impact of processing conditions (flocculation plus centrifugation) on lipid recovery.

5.2 Factors affecting centrifugation

The fundamental parameters involved in centrifugation for effective clarification or dewatering are expressed by Stokes Law (Equation 1.1). For a centrifugation operation clarification is also a function of the applied flow rate, temperature and applied centrifugal force, as well as the Sigma coefficient (Section 1.8.1). The broth characteristic with the largest effect on separation efficiency will be the quantity and behaviour of the smallest particles in the system (Shelef & Sukenik, 1984).

5.2.1 Particle diameter and culture viscosity

The algal broth to be processed was characterised in terms of the particle size of the cells produced (**Figure 5.2**) and the viscosity of the broth (**Figure 5.3**). An example of the mono

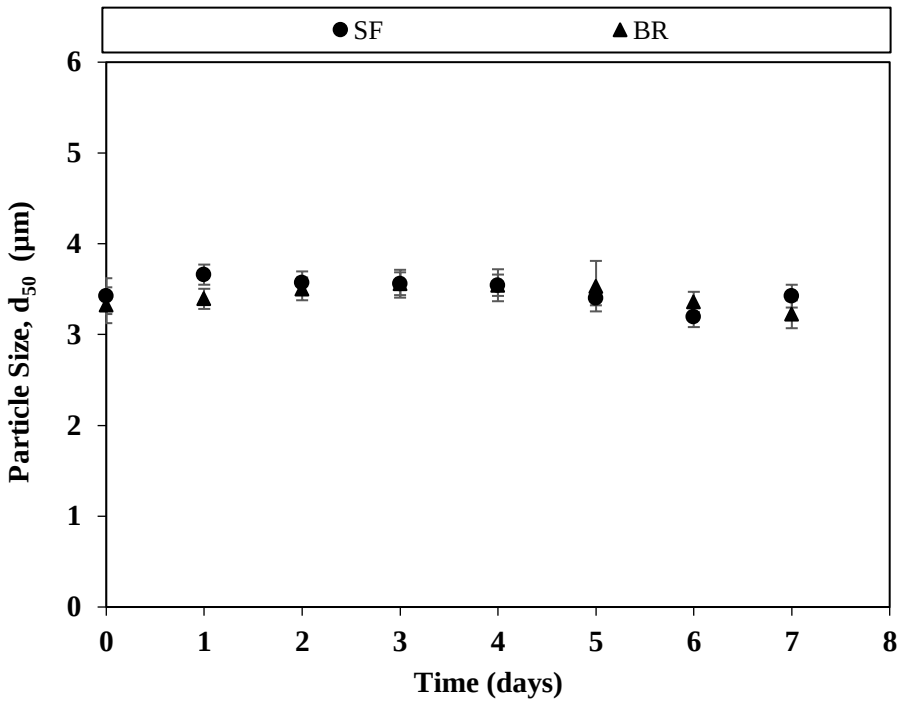

Figure 5-2: Particle size of *C.sorokiniana* cells grown heterotrophically in shake flasks (SF, 250mL) and a stirred bioreactor (BR, 7.5 L). Cells were grown as described in Section 2.2 and particle size d_{50} measured using a Mastersizer 2000E as described in Section 2.10.7. Error bars represent one standard deviation about the mean ($n \geq 3$).

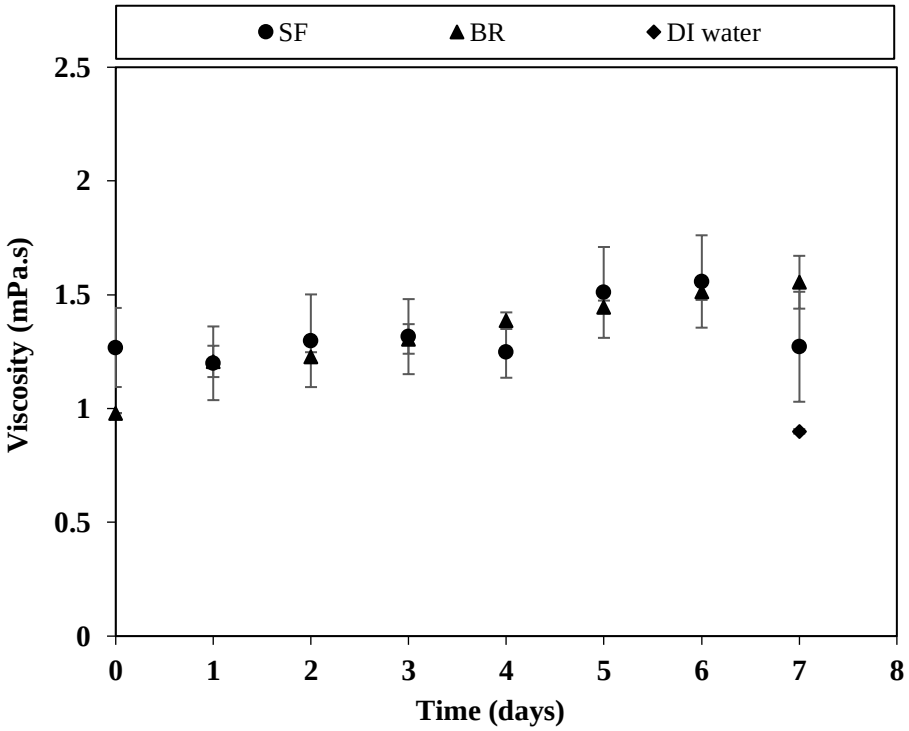

Figure 5-3: Viscosity of *C.sorokiniana* broth and DI water at 25ºC. Cells were grown heterotrophically as described in Section 2.2.1 and 2.2.2 in shake flasks (SF, 250mL) and a stirred bioreactor (BR, 7.5 L) respectively. Viscosity was measured as described in Section 2.10.3. Error bars represent one standard deviation about the mean ($n = 3$).

modal size distribution of cells obtained from both shaken and stirred cultures is shown in **Appendix 5**.

The mean particle size (d_{50}) was seen not to change significantly throughout the time window studied for both shake flasks and bioreactor cultures. An average diameter of 3.6 ± 0.2 µm was recorded suggesting the need to operate the centrifugation process at low flow throughputs (Sim *et al.*, 1988) which will increase processing times.

The measured size is within the range reported in literature and it has been reported that such sizes - 3 to 30 mm diameter (Grima *et al.*, 2003) or the microscopic size of microalgal cells (2 - 200µm) (Rawat *et al.*, 2013) as being problematic to the recovery of biomass.

Likewise, the viscosity of the broth did not change markedly during either shaken or stirred cultures and remained close to that of water (**Figure 5.3**). This suggests that no cell damage, intracellular leakage or excretion of viscous metabolites was experienced. The measured viscosities are within the range of those reported for green or blue green algae (Petkov & Bratkova, 1996).

5.2.2 Influence of flocculant on broth viscosity

Viscosity is a hydrodynamic drag force opposing settling of solid particles suspended in a fluid (Themelis, 1995). The greater the viscosity of a solution, the slower the settling velocity of the suspended particles. Chitosan is non polar, does not dissolve in organic solvents and aqueous bases (Kubota *et al.*, 2000) and hence it is initially dissolved in HCl during preparation (Section 2.4.1.1) forming a viscous solution. The viscosity of the flocculation solution was observed to increase with an increase in the amount of Chitosan **(Figure 5.4)**. However, this did not significantly change the viscosity of the algal broth because of the small percentage (1.2%v/v) added in comparison to the bulk volume flocculated. Low concentrations of Chitosan solution has viscosities close to that of water whereas the highest viscosity used in this work was 14-fold more viscous than water.

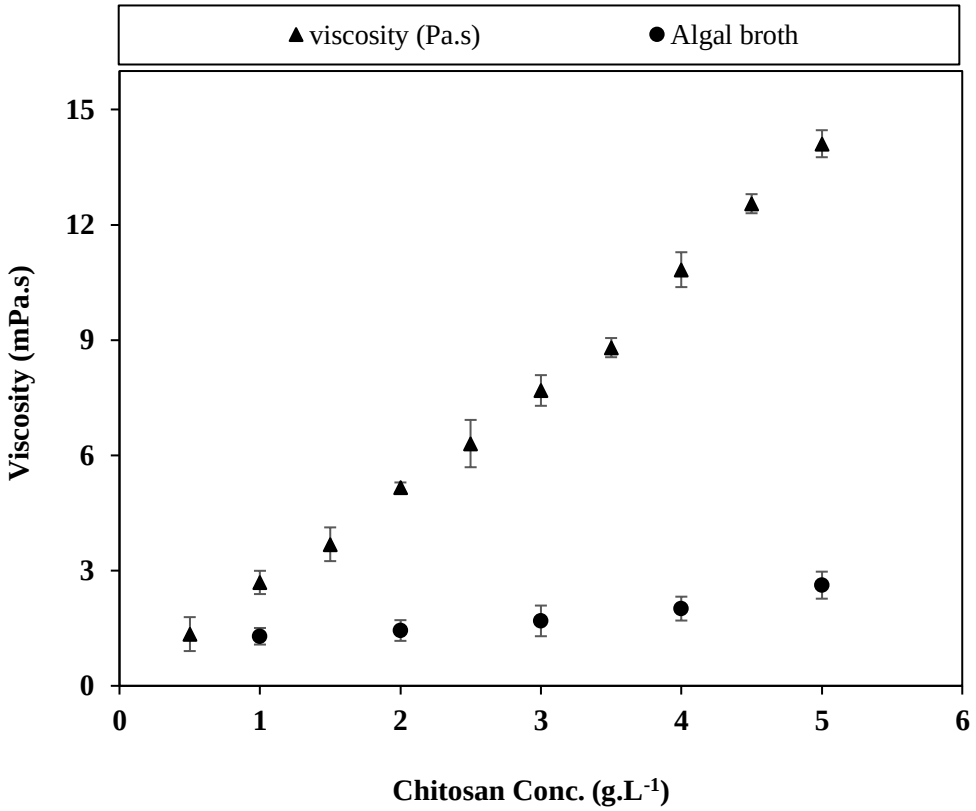

Figure 5-4: Viscosity of different concentrations of Chitosan solutions and the corresponding flocculated solutions. Solutions were prepared as described in Section 2.4.1.1 and 1 mL of each solution was used to flocculate 85 mL of *C.sorokiniana* broth containing 5 $g.L^{-1}$ cells in the flocculation reactor (Section 3.5).

Nonetheless, flocculating 85 mL of algal broth with a 1 mL of 5 $mg.mL^{-1}$ dose of Chitosan solution only increased the viscosity of the broth from 1.09 mPas to 2.6 mPas.

5.2.3 Density of *C.sorokiniana* cells and flocs

Another parameter that influences centrifugation performance is the particle density. Centrifugation involves sedimentation based on density difference of the medium components and particle size. Therefore, the density of the *Chlorella* cells and those of the flocs derived from flocculating heterotrophic *Chlorella* broth was measured using a combination of electrical sensing zone and centrifugal sedimentation technique (Taylor *et al.*, 1986). This technique utilized spinning a fluid (methanol and water) in the centrifugal disc photosedimentometer (Section 2.10.10) and then the cells or flocs were added while the annulus was spun at 500 rpm. **Figure 5.5** shows that the density of the flocs increases with an increase in flocculant concentration. This is due to bridging of the cells by Chitosan and/or an increase in floc size (**Figure 3.12**).

According to Equation 1.1, the density difference of the fluid and the suspended particles is directly proportional to the settling velocity. The density of the broth (medium plus cells) was seen to be close to that of water and spin fluid (**Figure 5.5**). Flocculation can lead to the formation of flocs with low densities especially when the concentration of the flocculant is low (Uduman *et al.*, 2010). Considerable difference between the spin fluid (ρ_s) and the suspended particles (ρ_c) was seen after increasing the amount of flocculant. Chitosan is a polymer with medium to high molecular weight (Roussy *et al.*, 2005) and this aids the bridging mechanism thereby increasing weight. Also, precision in density measurement is influenced by the choice of carrier solutions (Godin *et al.*, 2007) since density of particles tends to increase or vary with the density of the suspending solvent or spin fluid (Taylor *et al.*, 1986). Therefore, careful consideration has to be made in selecting the spin fluid that will give accurate density measurement.

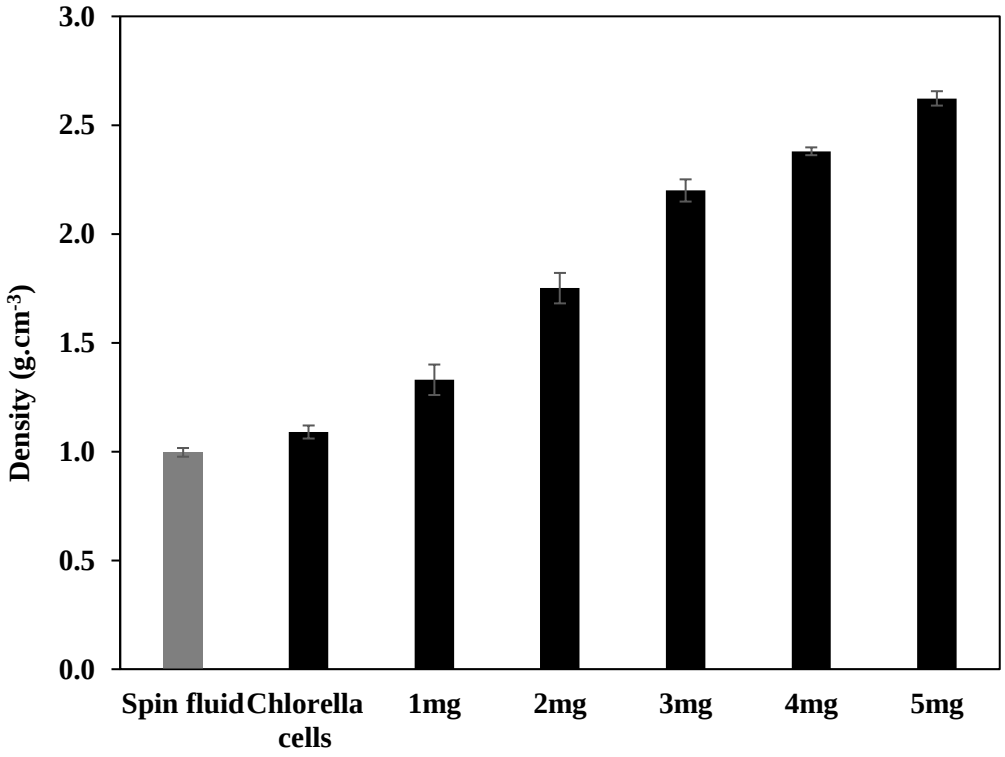

Figure 5-5: Estimated density of *C.sorokiniana* cells and flocs. Density was predicted as described in Section 2.10.10 and by matching the median diameter (d_{50}) from the Mastersizer distribution (**Table 3.2**) with the particle settling characteristics. Error bars represent one standard deviation about the mean (n = 3).

Table 5-1: Operating details for the centrifugal disc photodensitometer with a summary of the sedimentation data. (ρ_c - ρ_s) is the density difference of the cells/flocs and the spin fluid.

Composition	**Temp. (ºC)**	**viscosity (mPa.s)**	**ρ ($g.cm^{-3}$)**	**ρ_c - ρ_s ($g.cm^{-3}$)**
Deionized water	23 ± 2	1.00	0.9982	-
Spin fluid (5% methanol in water)	23 ± 1	-	0.9965	-
Chlorella broth	25 ± 0	1.09	1.09	0.09
1 mg floc	23 ± 2	1.29	1.33	0.34
2 mg floc	24 ± 1	1.44	1.75	0.75
3 mg floc	23 ± 2	1.69	2.20	1.20
4 mg floc	23 ± 2	2.01	2.38	1.38
5 mg floc	23 ± 1	2.62	2.62	1.62

The biggest floc was seen to be 2.6 fold denser than the spin fluid (**Table 5.1**) while single *Chlorella* cells had a density of 1.09 $g.cm^{-3}$ which is in agreement with literature where average density of algae was reported to be 1.04 -1.23 $g.cm^{-3}$ (Edzwald, 1993).

The viscosity of the feed sample was seen to slightly increase due to flocculant viscosity (**Figure 5.4**). This was assumed not to affect the density measurement since the sample volume is only a small percentage (~ 5%) of the overall spin fluid used.

5.3 Mechanical stability of flocs

5.3.1 Flocs obtained with different concentration of Chitosan

The mechanical stability of *C.sorokiniana* – Chitosan flocs was evaluated. This plays an important role in determining whether breakage occurs in the feed zone of industrial centrifuges as feed damage has been reported to occur at this locations (Boychyn *et al.*, 2004) since it is where highest energy dissipation rates are experienced. The shear studies were performed in the rotating disc device (Section 2.3.3.2) which has previously been used for studies on the shear sensitivity of different biological materials (Boychyn *et al.*, 2000; Lee *et al.*, 2002) and USD studies for centrifugation (Boychyn *et al.*, 2001; Hutchinson *et al.*, 2006). The flocs were subjected to varying levels of shear, classified into low, medium and high shear rates (**Table 5.2**). The choices being the energy dissipation rates of centrifuges utilized in biotechnological industries; mainly disc stack and CARR Powerfuge™. Computational fluid dynamics (CFD) analysis of the feed zones of these centrifuges revealed that the minimum and maximum shear experienced in a CSA disc stack centrifuge are 2.86×10^4 $W.kg^{-1}$and 2×10^5 $W.kg^{-1}$ respectively while for CARR, it was recorded as 2×10^5 $W.kg^{-1}$ and 1.4×10^6 $W.kg^{-1}$ respectively; all in flooded condition (Boychyn et al., 2004).

Visual examination of *C.sorokiniana* flocs before and after exposure to shear indicate that the flocs are broken down when exposed to levels of shear above 2.86×10^4 $W.kg^{-1}$ (**Figure**

5.6). For Chitosan concentrations below 3 mg.mL^{-1}, the flocs break down to single cells even under low shear conditions (2.0 x 10^5 W.kg^{-1}) whilst for doses ≥ 4 mg (**Table 5.2**) it is reasonable to assume the excess of this biopolymer in the medium stabilizes the smaller flocs as they are produced. The CARR powerfuge™ used here for scale-up studies (Section 5.7) is considered a high shear centrifuge as the minimum shear experienced in this machine is the maximum for disc stack centrifuges (2.0 x 10^5 W.kg^{-1}) (Boychyn *et al.*, 2004). Nonetheless, the dewatering capacity of this equipment is superior to that achieved by disc stack designs and this parameter is important in subsequent microalgal processing where moisture in the harvested biomass can significantly influence the economics of product recovery further downstream (Mohn, 1978).

Unflocculated algae cells with a size range of 3.6 ± 0.2 µm were found to be stable when exposed to the highest shear rate (**Table 5.2**) and suffered no measurable mechanical or hydrodynamic damage which would have resulted in the formation of smaller-sized cell debris. This can be attributed to the possession of rigid cell walls with sporopollenin-like properties (Faegri, K., Iversen, 1964). It is known that the morphology and composition of *Chlorella* cell walls vary between species and from strain to strain (Atkinson *et al.*, 1972). In addition, these properties are also dependant on growth conditions.

Possessing a resilient cell wall also protects *Chlorella* cells from impact of harsh processing steps that might lead to yield losses due to cell wall damage and intracellular product leakage. Low shear stresses may not induce breakage but can affect growth and cell division (Vandanjon *et al.*, 1999), however, centrifugation has successfully been used as a concentration step for developing extended shelf-life concentrates of some microalgal species (Heasman *et al.*, 2000) and reduced shipment volumes. It has also been suggested that shear is independent of concentration of microalgal cells within a range.

It was observed that 1 – 3 mg.mL^{-1} Chitosan concentration induced flocculation but the mechanical stability of these flocs was seen to be weak. This was confirmed by microscopic and particle size measurements which showed sheared cell sizes to be closely.

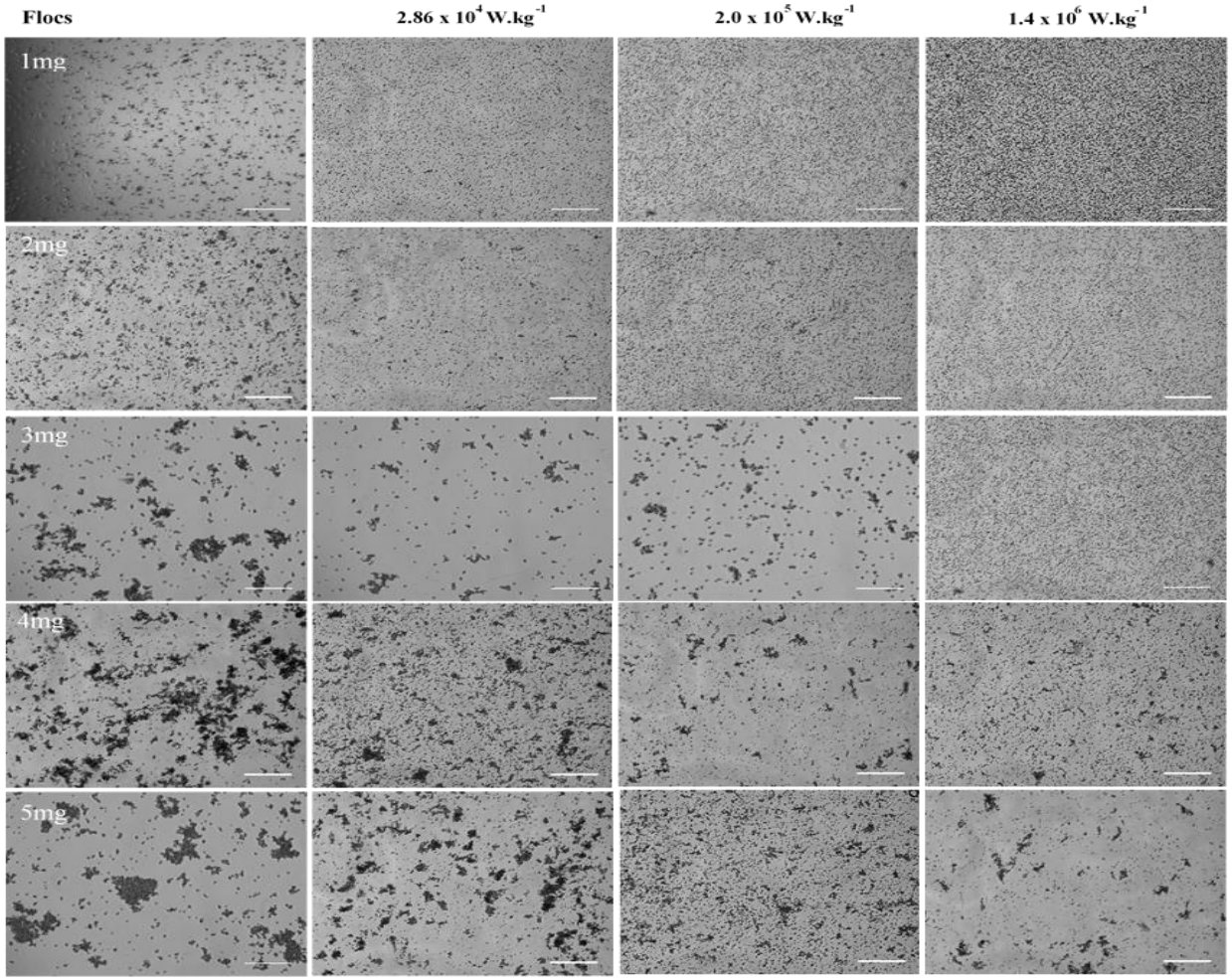

Figure 5-6: Illustration of the effect of shear on Chitosan-flocculated *C.sorokiniana* cells at different flocculant concentration. From left to right - No shear, 2.86 x 10^4 W.kg^{-1}, 2.0 x 10^5 W.kg^{-1} and 1.4 x 10^6 W.kg^{-1} energy dissipation rates. Flocculation was performed as described in Section 2.4.1.2 using 5.4 gL^{-1} DCW cells. Bar size represents 100µm

Table 5-2: Measured *C.sorokiniana* floc diameters (µm) (d_{50}) with increasing Chitosan concentration and shear rate. Flocs prepared in either the 120 mL scale-down flocculation reactor or the 7.5L STR as described in Section 2.4.1.2. Flocs exposed to shear in the USD shear device as described in Section 2.3.3.2. Errors shown represent one standard deviation about the mean ($n \geq 3$).

Chitosan Concentration ($mg.mL^{-1}$)	**Energy Dissipition Rate (Wkg^{-1})**			
	No shear	**2.86×10^4**	**2.0×10^5**	**1.4×10^6**
No flocculant	3.6 ± 0.2	3.6 ± 0.3	3.5 ± 0.1	3.5 ± 0.3
1.0	6.4 ± 1.7	3.8 ± 1.3	3.8 ± 0.9	3.8 ± 0.9
2.0	17.9 ± 10.9	4.4 ± 1.0	3.9 ± 1.3	3.9 ± 1.3
3.0	49.2 ± 1.8	4.8 ± 1.8	4.5 ± 1.6	4.3 ±1.7
4.0	52.4 ± 0.2	28.3 ± 0.9	16.3 ± 0.3	15.4 ± 0.3
5.0	60.4 ± 2.5	31.6 ± 2.0	21.1 ± 0.5	18.3 ± 0.5
7.5 L STR	51.7 ± 0.5	28.3 ± 1.0	14.9 ± 0.4	15.4 ± 0.8

compared to single *C.sorokiniana* cells with a mean size range of 3.8 ± 1.3 µm to 4.8 ± 1.8 µm after shear. Whereas using ≥ 4 $mg.mL^{-1}$ Chitosan dosage, a significant resistance to shear was observed; with mean size increasing with increment in flocculant dosage across all shear rates. For instance, 15.4 ± 0.3 and 18.3 ± 0.5 µm were obtained for 4 and 5 $mg.mL^{-1}$ respectively at a high shear rate. This suggests the use of optimal flocculant dosage for varied centrifuge types as flocs derived have shown significant resistance to shear.

5.3.2 Flocs obtained during flocculant addition

Flocs obtained when exploring the effect of flocculant flowrate on the sizes of flocs produced were exposed to shear (2.0×10^5 $W.kg^{-1}$) to ascertain whether the flocculant flowrate influenced the hydrodynamic and mechanical stability of the flocs produced. In the previous chapter, three different flow rates were employed (**Figure 3.10**) and subsequent floc images post exposure to high shear were obtained. The flocs produced with slow flowrates were more resistant to shear as bigger flocs were seen after shearing (**Figure 3.10b**)

5.4 USD evaluation of influence of flocculation on centrifugation efficiency

Having established a reliable scale-down method for the production of Chitosan flocculated *C. sorokiniana* cells (Chapter 3), the next step was to use USD methods to evaluate the impact of flocculation on centrifugation performance. Microalgal cells have a density which is close to that of water (**Figure 5.5**); this causing an extremely slow sedimentation rate under gravity due to the insignificant density difference (Millero & Lepple,1973). The size and stability of the flocs (Section 5.3.1) were found to greatly impact on clarification performance. As shown in **Figure 5.7**, clarification increased with increasing Chitosan concentration for unsheared flocs. The highest clarification was measured at concentrations ≥ 4 $mg.mL^{-1}$ as indicated by the dashed line in **Figure 5.7** and

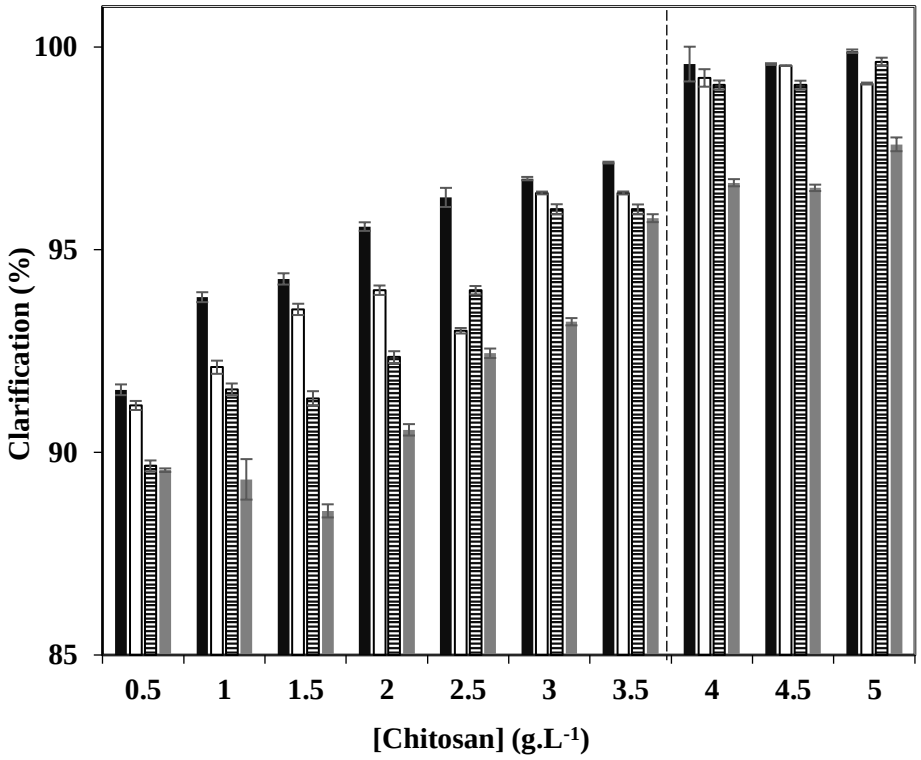

Figure 5-7: USD centrifugation clarification efficiency of flocculated *C.sorokiniana* broth. Dashed line indicates Chitosan concentration above which the effect of shear on clarification becomes insignificant: no shear (solid black); 2.86 x 10^4 W.kg^{-1} (solid white); 2.0 x 10^5 W.kg^{-1} (horizontal black); 1.4 x 10^6 W.kg^{-1} (solid grey). Error bars represent one standard deviation about the mean ($n \geq 3$).

hence this was considered the optimal dosage. At this concentration, little effect of shear on clarification was observed even though the flocs were broken. The average floc diameters obtained after exposure to shear were sufficiently large enough to sediment rapidly under the conditions applied. However at low Chitosan dosage, the interaction between the algal cells and Chitosan polymers does not produce large or stable-enough flocs to withstand the level of shear found in disc stack and CARR Powerfuge^{TM} centrifuge designs. Consequently, this was shown to break the flocs back to single cells (**Figure 5.6**) and hence the reason for the low clarification as compared to those obtained using ≥ 4 mg concentration (**Figure 5.7**).

The low clarification efficiencies measured for small Chitosan dosage may be as a result of the actual flocculation mechanism with this polymer (Section 1.4.1.1) which is assumed to be a combination of incomplete charge neutralization and static patch effects (Xu *et al.*, 2013). Less than 8.71 mg of Chitosan per g_{dcw} of algae was not sufficient to neutralize the charges of cells at the biomass concentrations density studied.

5.5 Overall influence of flocculation on centrifugation performance

The performance of pilot scale centrifugation processes is influenced by the choice of operating conditions. Settling velocity is dependent on flow rate, density, temperature as well as feed condition (Section 5.2). Flocculating algal cells by means of a flocculating agent to form flocs which aids separation not only reduces the time for processing but also the force required to achieve this. Also, using USD centrifugation, a wide range of process conditions (such as settling velocities, flowrates, shear rates etc.) can be explored with minimal quantity of material.

Figure 5.8 shows a comparison of the USD clarification efficiencies achieved by flocculated and unflocculated algal cells at 2 different rotational speeds using three different working volumes. The variation in volume was selected to represent flow rate in continuous flow centrifuges where an increase in flow rate is indirectly proportional to

clarification of supernatant because the residence time of this feed in the settling compartment is reduced. This can further be explained by the sigma correlation (Section 1.8.1) which captures all operating and equipment variables. The Sigma Factor (Σ) is then used in correlation to flow rate to produce equivalent settling area (Q/Σ); which is used to compare the performance of different types of centrifuges. Therefore, the varying rotational speed and volume used for here led to differences in the term plotted on the X-axis of **Figure 5.8**.

Both treated and untreated samples exhibited a decrease in clarification with an increase in volume and decrease in rotational speed. Flocculated cells achieved a high supernatant clarity of > 99% at low centrifugal forces ($V_{lab}/ct\Sigma \leq 1.7e^{-7}$). Microscopy (**Figure 5.6**) shows that not all the flocs were broken down at this optimal Chitosan dosage and hence centrifugation performance is enhanced by the size increment due to flocculant addition. When flocculation is used as a pre-treatment step, cells settle rapidly and 90% of the culture volume can be decanted (**Figure 5.1**); this further reduces the volume of material transferred for centrifugation thereby saving more time and consequently energy.

In general, flocculation enabled high clarification efficiencies to be achieved at lower rotational speeds.

5.6 Influence of process conditions on lipid recovery

The choice of biomass recovery strategy can have impacts further downstream. **Figure 5.9** shows a large variation between the mass balance of lipid (% total) that can be recovered from flocculated and unflocculated cells after centrifugation under different conditions. Cultures in stationary phase of growth were centrifuged at different centrifugal forces. First, the total lipids contained in these cells (serving as control) was used as a base line assuming all cells were captured and this was used to determine the percentage of product loss due to downstream processing. Total lipids are comprised of neutral, glycol- and

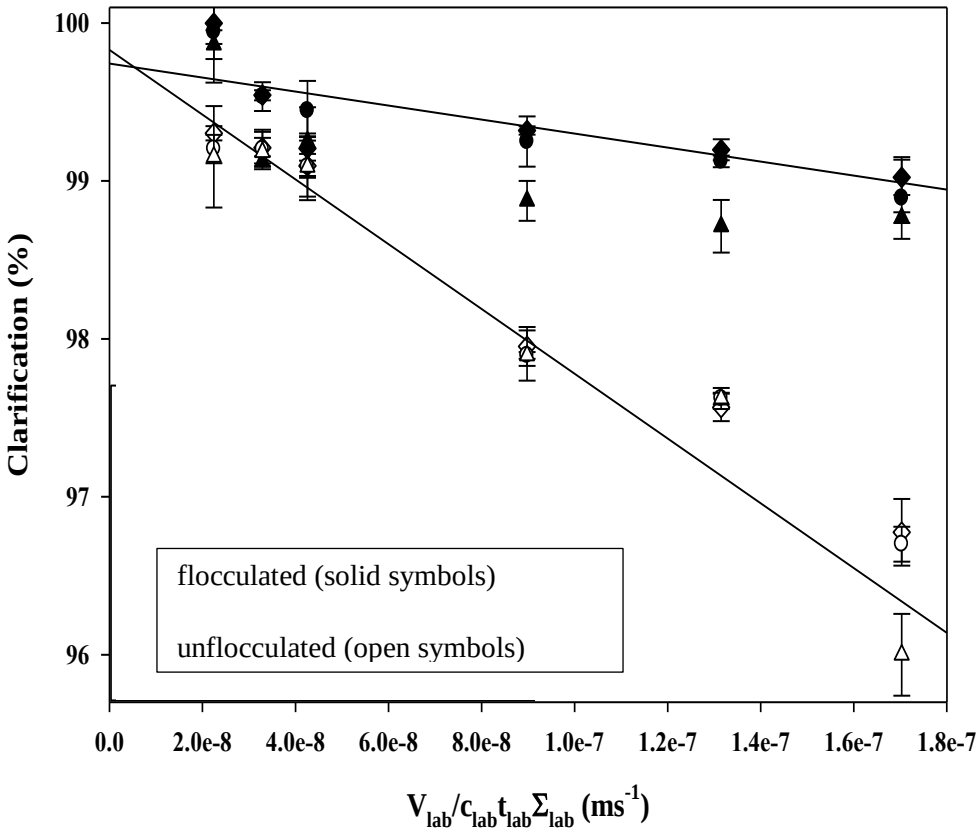

Figure 5-8: Effect of flocculation on USD centrifugal recovery of microalgae. Clarification plotted against equivalent flow rate or settling area for *C.sorokiniana* cells centrifuged in a laboratory bench top centrifuge at two different speeds and three different volumes; flocculated, no shear (♦), flocculated, low shear (●), flocculated, high shear (▲), unflocculated, no shear (◊), unflocculated, low shear (○) and unflocculated, high shear (Δ). The biomass concentration of feed used was 5.4 $g.L^{-1}$ and temperature was 4°C. Error bars represent one standard deviation about the mean (n=3). Solid lines fitted by linear regression to average vales of flocculated ($R^2 = 0.994$) and unflocculated ($R^2 = 0.987$) data sets.

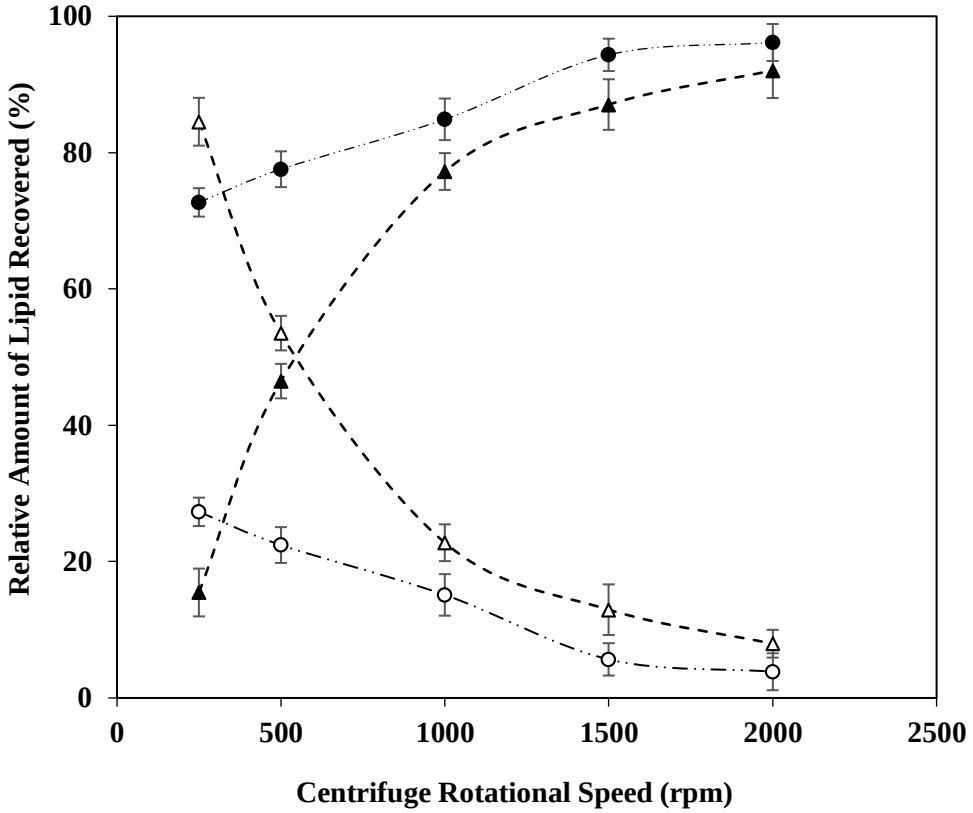

Figure 5-9: Effect of flocculation on lipid recovery. Three sets of conditions of broth containing 5.9 ± 0.2 $g.L^{-1}$ *C.sorokiniana* cells were used: 10 mL of broth spun for half an hour which served as reference sample, flocculated (●) and unflocculated (▲) cells centrifuged at different rotational speeds. The subsequent supernatant: flocculated (○) and unflocculated (Δ) were further respun together with the pellets as described in Section 2.7.2. Amount of lipid recovered is plotted against centrifugal speed (rpm).

phospho- lipids (NL, GL and PL) which can vary considerably depending on the species and cultivation conditions. Heterotrophic cultivation of algae is known to support the biosynthesis of storage lipids which can represent approximately 81% of total lipids (Liu *et al.*, 2011). A trend of increased recovery with increase centrifugal force and decline in losses with supernatant was seen for both conditions. As shown in **Figure 5.9**, flocculation of cells at the optimal Chitosan dosage has a significant impact on lipid recovery. Addition of Chitosan aids coagulation and bond formation between Chitosan and algal cells is compatible with further processing. Under the same disruption conditions, lipid recovered for flocculated and unflocculated cells at the lowest centrifugal forces was 72.7 and 15.5% respectively. Even at an increased centrifugal force (500 rpm), only 46.5% of product was recovered with unflocculated cultures in comparison to 77.6% for the flocculated counterparts.

5.7 Scale-up verification of USD predictions

5.7.1 USD to explore specific operating ranges of the CARR powerfuge™

To be useful, USD must satisfactorily predict larger scale unit operation performance. In this case, a comparison of morphological properties, dewatering and yield productivities between the two scales used for centrifugation has been examined. Scale-up based on achieving a high level of dewatering was explored and this verifies the choice of CARR powerfuge™ despite its relative high shear level and also because of the influence of high moisture content (>85%) of algal biomass on subsequent processing steps and cost (Grima et al., 2003).

Previous publications (Boychyn *et al.*, 2001; Boychyn *et al.*, 2004; Hutchinson *et al.*, 2006) have described how protein precipitates and whole cells such as mammalian cells are prone to hydrodynamic shear damage in a continuous flow centrifuge. This poses a challenge on subsequent processing steps, as yield losses increase proportionally to cell damage. Scale-up of USD to large scale centrifuges was achieved by pre shearing the feed prior to bench

centrifugation (Section 1.8.1). This pre shearing concept was adapted in the scale-up verification presented in **Figure 5.10** which shows a sigma plot with data points of USD and pilot centrifugation studies in a ± 0.5% agreement. The shear rates utilized are as explained in Section 5.3.1 whereas the parameters used for operating the pilot centrifuge where predicted using the sigma concept developed by Ambler (1959) (Equation 5.1) before being validated.

$$\frac{Q_P}{C_P \Sigma_P} = \frac{V_{USD}}{C_{USD} t_{USD} \Sigma_{USD}} \tag{5-1}$$

C.sorokiniana single cells exhibited high shear resistance as cell sizes remained unchanged after exposure to high shear forces (**Table 5.2**); however, flocs showed minimal breakage due to this shear effect (**Figure 5.10**). The operating windows surrounding the two scales (CARR powerfuge™ and USD centrifugation) in reaching a desired specific settling velocity was unexplorable. At those ranges $2.0e^{-8} \leq V/ct\Sigma \leq 1.7e^{-7}$ (**Figure 5.8**), it was observed that USD centrifugation obtained significant difference between flocculated and unflocculated cells. It should be noted that all centrifuges have a minimum residence time which is a limitation attributed to bowl capacity and cooling requirements (Boychyn *et al.*, 2004). Also, bench top centrifugation of flocculated algal broth reached a plateau ($V/ct\Sigma \leq 1.6e^{-8}$) below which clarity was 100%. Nonetheless, a wide window of operation is possible with USD applications using minimal material and large data generation.

Ultimately, USD predictions of the clarification performance in the CARR powerfuge™ was accurately verified as shown in **Figure 5.10;** flocculation also had a beneficial effect on clarification under the operating conditions found in the CARR centrifuge.

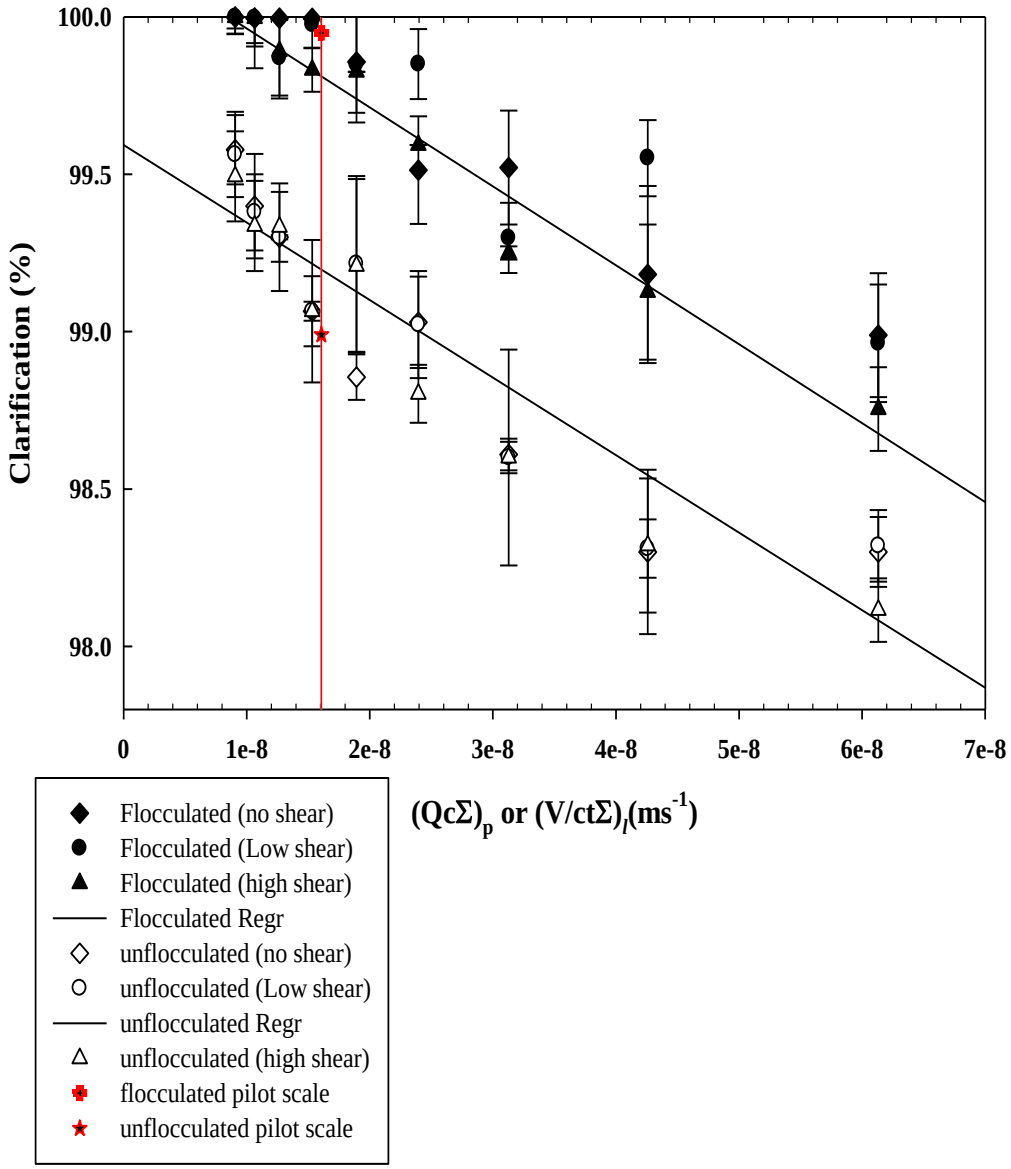

Figure 5-10: Comparison of USD clarification and scale-up verification of the benefits of flocculation on biomass recovery. Clarification plotted against equivalent flow rate or settling area for *C.sorokiniana* cells centrifuged in a CARR Powerfuge™ at a constant Sigma factor as described in Equation 5-1. The biomass concentration of feed used was 5.4 $g_{dcw}.L^{-1}$ and error bars represents one standard deviation about the mean ($n \geq 2$). USD centrifugation was performed under the same conditions as CARR, using a temperature of 16˚C.

5.7.2 FAME composition of flocculated and unflocculated cells

Biodiesel quality depends on the fatty acid (FA) profile and structural features of various FAMEs. In Europe, this needs to comply with EN 14214 standard (Brennan & Owende, 2010). These FA's however vary between species and with less variation due to changing conditions such as growth phases and media types (Huerlimann *et al.*, 2010). There is a limit to the content of FA's with four or more double bonds due to susceptibility of oxidation during storage (Chisti, 2007), minimum CN (Lu *et al.*, 2012) and the iodine value. For this reasons, both flocculated and unflocculataed broth were analysed for their FAME composition in order to clarify any changes the pre-treatment step might have on the biodiesel quality. **Table 5.3** shows the FA composition of the oil extracts which illustrates similar FAME profile with no significant difference between the two conditions. This was the reason for choosing GC-MS for its enhanced selectivity, sensitivity and ability to separate co-eluting peaks. A representative chromatogram of the flocculated feeds FAMEs is shown in **Figure 5.11**.

Twenty five FAs were detected and the dominant FAMEs recorded include palmitic, linoleic, oleic, stearic, and ɣ-linolenic acid which accounted for approximately 70% of the total FAMEs. C16 and C18 lipids are major components of *C.sorokiniana* (Lu *et al.*, 2012) and also common in biodiesel production (Huerlimann *et al.*, 2010; Ojo *et al.*, 2014). The values obtained for the %wt of *C.sorokiniana* FA's showed predominance in saturated fatty acids (relating to iodine number) compared to mono- and poly- unsaturated FA's (**Table 5.3**). Biodiesel properties that influences the fuel properties include CN, cold flow properties, oxidative stability, viscosity, heat of combustion, lubricity, iodine value as well as exhaust emissions (Francisco *et al.*, 2010). Furthermore, reports have shown CN to be a prime indicator of biodiesel quality through its ignition quality (Bamgboye & Hansen, 2008; Francisco *et al.*, 2010) with an EN ISO 5165 standard minimum range of 51 . Nevertheless, different microalgal species have exhibited ranges between 52.2 and 56.7 which is in accordance with various country standards (Francisco *et al.*, 2010). The CN

Table 5-3: Comparison of fatty acid methyl ester profile (dry wt. %) of lipid recovered from unflocculated and flocculated *C.sorokiniana* cells. FAME compositions quantified using a standard as described in Section 2.9.

Methyl esters	**FAME Formula**	**Unflocculated sample**	**Flocculated sample (USD)**	**Flocculated sample (Pilot)**
Caproic	C6	0.67 ± 0.7	0.74 ± 0.5	0.72 ± 0.3
Capric	C10	0.37 ± 0.0	0.33 ± 0.1	0.35 ± 0.0
Lauric	C12:0	0.16 ± 0.0	0.16 ± 0.0	0.16 ± 0.0
Tridecanoic	C13:0	1.13 ± 0.4	1.35 ± 0.4	0.37 ± 0.0
Myristic	C14:0	1.57 ± 0.6	1.88 ± 0.7	1.85 ± 0.7
Myristoleic	C14:1	0.15 ± 0.0	0.19 ± 0.0	0.19 ± 0.0
Pentadecanoic	C15:0	6.96 ± 2.1	5.97 ± 1.0	5.97 ± 1.1
cis-10-Pentadecenoic	C15:1	0.64 ± 0.2	0.52 ± 0.1	0.59 ± 0.2
2,4 -Pentadienoic	C15:2	3.16 ± 0.1	3.12 ± 0.1	3.00 ± 0.0
Pentatrienoic	C15:3	0.96 ± 0.0	0.92 ± 0.0	0.92 ± 0.0
Palmitic	C16:0	28.78 ± 2.6	27.09 ± 1.9	28.55 ± 1.1
Palmitoleic	C16:1	4.74 ± 0.2	5.06 ± 0.4	4.97 ± 0.2
Heptadecanoic	C17:0	0.89 ± 0.0	0.93 ± 0.0	0.93 ± 0.0
cis-10-Heptadecenoic	C17:1	2.03 ± 0.0	2.18 ± 0.0	2.18 ± 0.0
Stearic	C18:0	5.70 ± 0.9	5.74 ± 0.3	5.73 ± 0.8
Octadecenoic	C18:1	0.94 ± 0.0	0.93 ± 0.0	0.94 ± 0.0
Elaidic	C18:ln9t	2.43 ± 0.9	2.01 ± 0.3	2.44 ± 0.6
Oleic	C18:ln9c	12.62 ± 1.2	10.54 ± 0.8	12.3 ± 0.9
Linolelaidic	C18:2n6t	0.04 ± 0.0	0.6 ± 0.1	0.44 ± 0.0
Linoleic	C18:2n6c	22.09 ± 0.1	24.98 ± 0.0	22.1 ± 0.1
Arachidic	C20:0	0.06 ± 0.0	0.12 ± 0.1	0.11 ± 0.0
γ - Linolenic	C18:3n6	0.17 ± 0.0	0.22 ± 0.1	0.13 ± 0.0
α-Linoleic acid	C18:3n3	0.79 ± 0.0	0.7 ± 0.0	0.71 ± 0.0
cis-5,8,11,14,17-Eicosapentaenoic	C20:5n3	0.94 ± 0.1	0.05 ± 0.0	0.17 ± 0.1
Nervonic	C24:1	0.98 ± 0.3	3.35 ± 0.3	3.22 ± 0.2
SFA (%)		46.3	44.3	44.7
MUFA (%)		23.6	24.8	26.8
PUFA (%)		29.1	30.6	27.5
TOTAL (%)		99	99.7	99.0

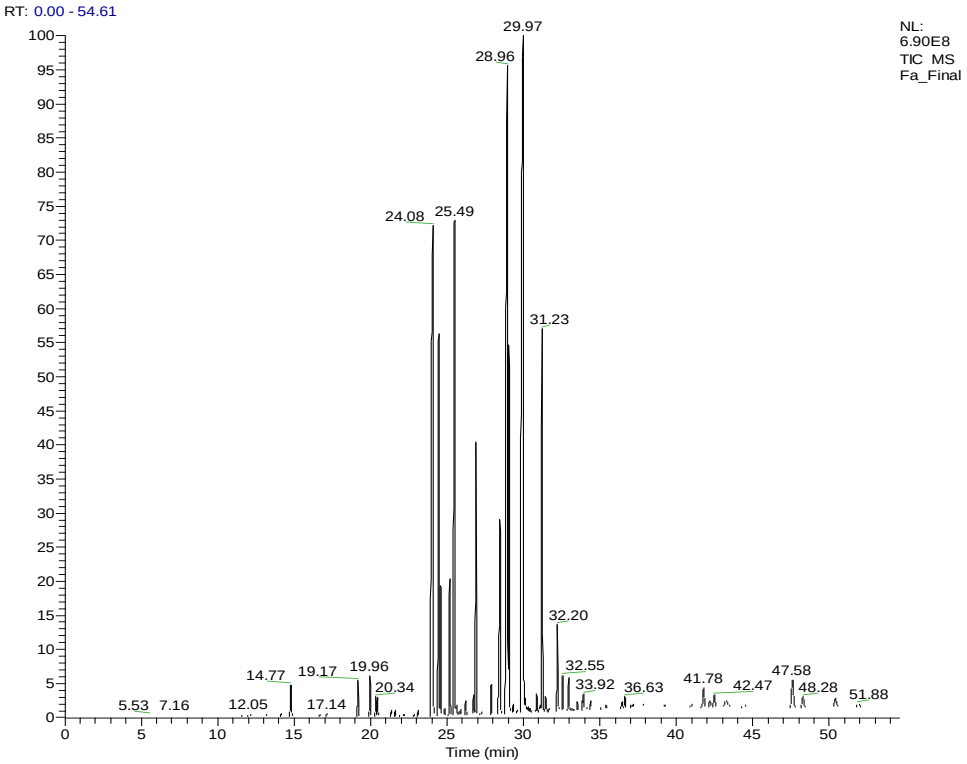

Figure 5-11: GC-MS chromatogram of FAME analysis produced from lipid recovered from flocculated *C.sorokiniana* cells using 9.9 mg Chitosan per gram of algal$_{dcw}$. GC-MS performed as described in Section 2.9.

was calculated using Equation 2.8 and was recorded as 65.17 and 65.02 for flocculated and unflocculated cells respectively. The higher the value the better the ignition quality. The non-interference of Chitosan with final products is not only seen here but also in a study by (Riske *et al.*, 2007) for mammalian cell culture.

5.8 Summary

As described in Section 5.1, the overall aim of this chapter was to establish a USD method for algal biomass recovery by centrifugation in order to investigate the impact of flocculation as a pre-treatment step and to verify this at scale. **Figure 5.10** shows the successful implementation of the USD prediction from Equation 5.1 and verification using a CARR powerfuge™ for both flocculated and unflocculated cells.

The initial objectives of characterizing broth based on parameters that affect centrifugation revealed that *C.sorokinina* cells grown in shake flasks and bioreactor remained unaffected by the hydrodynamics (i.e. orbital shaking and agitation respectively) throughout the growth period. An average size of 3.6 ± 0.2 was measured (**Figure 5.2)** while viscosity and density of algal broth was seen to be close to that of water (**Figure 5.3** and **Figure 5.5** respectively). The density of flocs also increased with increase in their sizes. The viscosity and density was measured because behaviour of a fluid in flow is related to the intrinsic properties of the fluid.

With respect to flocculant used, the solution viscosity was observed to increase with an increase in the amount of Chitosan. This did not significantly increase the viscosity of the broth because of the small percentage added (1.2%v/v) in comparison to the bulk volume flocculated **(Figure 5.4)**. Study of the mechanical stability of the flocs showed that at an optimal Chitosan concentration of ≥ 4 mg.mL^{-1}, flocs were observed to be shear stable with mean size increasing with an increase in flocculant dose across the shear rates studied **(Figure 5.6)**.

More so, evaluation of the influence of flocculation on centrifugation efficiency showed that low Chitosan dosage (where total breakage of flocs was seen with shear), recorded low clarification efficiencies in comparison to those obtained at optimal dosage of ≥ 4 $mg.mL^{-1}$ **(Figure 5.7)**. Based on this, the optimal dosage was calculated as 9.9 ± 0.4 mg of Chitosan per gram of $algal_{dcw}$ which verifies the optimal value obtained in Chapter 3. Using this optimal concentration, a study on the influence of flocculation on centrifugation performance showed the benefits of increased particle size on settling; where USD centrifugation of flocculated and unflocculated cells revealed high clarity of the supernatant ($\geq 99\%$) at low centrifugal forces ($V_{lab}/ct\Sigma \leq 1.7e^{-7}$) (**Figure 5.8**).

Finally, using USD to explore the influence of process condition on lipid recovery showed significant impact of flocculation combined with centrifugation. A difference of 57.2% lipid recovery at low centrifugal forces was seen **(Figure 5.9)**. Comparison of the trans-esterified lipids from flocculated centrifuged -USD and -7.5L STR cells showed similar FAME profile **(Table 5.3)**.

The following chapter will explore various cell disruption processes and compare how the dewatering step affects the lipid productivity through transesterification.

6. Cell disruption and Transesterification

6.1 Introduction

In biodiesel production lipid productivity is an important factor (Section 1.3.2.3). The extraction of intracellular lipid first requires cell disruption in which the cellular structure is broken apart and product is released (Middelberg, 1995). The choice of cell disruption method (Section 1.5) is usually based on optimisation of the amount of product recovered from the cell. A larger number of factors may affect disruption of microbial cells, however, no comprehensive theory of this process is available in literature (Doucha & Lívanský, 2008).

Also, little attention is generally given to characterisation of the process stream properties following disruption, e.g. particle size distribution, yet such properties have been shown to have a strong impact on subsequent unit operations (van Hee *et al.*, 2004). While some information on the diruption of other microbes can be found in literature, there are very few reports on algal disruption (Doucha & Lívanský, 2008). Several methods are utilized in microalgal biodiesel production and this includes mechanical and non-mechanical action (Mata *et al*., 2010). Although considerable attention is given to mechanical methods these continue to be preferred for large-scale processes (Balasundaram *et al.*, 2009; Middelberg, 1995).

After cell disruption, biodiesel is produced by transesterifying the lipids released (Section 1.5) with an appropriate alcohol (**Figure 1.4**). Extracted oil is preferably highly dewatered in order to avoid yield losses through reactions like saponification (Fukuda *et al.*, 2001).

The aim of this chapter is to establish and compare the use of sonication and homogenization as small-scale cell disruption operations for lipid release from harvested microalgae. In order to do that, we need to establish each cell disruption method. Furthermore, the impact of different biomass recovery methods on transesterification will be explored. Specific objectives are:

- To optimize sonication variables based on extent of micronization of cell debris
- To carry out sensitivity analysis on the lipid assay.
- To explore homogenization parameters.
- To study transesterification of extracted oils from *C.sorokiniana* cells based on different biomass recovery conditions i.e. microfiltration (Chapter 4) or centrifugation (Chapter 5).

6.2 Establishment of sonication for cell disruption

This method of cell disruption is extensively used at laboratory scale. Although it has significant potential, further information is needed on feasibility for commercial-scale operation (Dragone *et al.*, 2010) and hence more research is needed (Harun *et al.*, 2010). Sonication is a method that exposes algae cells to high intensity ultrasonic waves, which create tiny cavitation bubbles around a cell. When the bubbles collapse, they emit shockwaves that rupture the cell wall thereby releasing intracellular products into solution. Cell disruption can influence the extent of product recovery, the nature of suspension to be processed (Balasundaram *et al.*, 2009) and can also ease subsequent purification steps (Harrison, 1991). The form and quality of the final product can also be affected because most of the energy that is absorbed by a cell suspension is transformed into heat hence the reason the sample must be cooled during processing (Section 2.6.2). The operating variables for sonication that will facilitate product release without affecting product quantity include: sonication frequency, number of cycles used, cell density etc. These are studied in the following sections.

6.2.1 Effect of volume on particle size

To study the effect of sample volume on cell disruption, the sample to be sonicated was split into two aliquots; 1 and 1.5 mL. This was observed not to have an effect on the cell debris particle profile (**Figure 6.1** and **6.2**). When using fewer cycles (**Figure 6.1**) and varied sonication intensity (**Figure (a)** and **(b)**), this did not influence the effect of volume on cell micronization (particle size attained after prolonged disruption) as particle profiles were seen to still overlap. Further increment of the number of cycles (**Figure 6.2**) and keeping other variables the same as in **Figure 6.1** did not provide any additional difference.

6.2.2 Effect of sonication intensity on particle size

The influence of sonication intensity on particle disintegration was also studied. Since numerous variables can be studied during sonication, a combination of cell concentration and number of cycles were investigated at sonication frequencies of 10 and 15. **Figure 6.3** and **6.4** shows that an increase in the wave frequency increases the rate of particle disruption. This is evident by a clear shift to smaller particle sizes when the 15 ma intensity is used in comparison to whole algal cells and those sonicated using 10 ma.

When the number of cycles was varied between 4 and 8 cycles, the distance between the two frequencies (10 and 15) did not vary significantly as shown in (**Figure 6.3 (a) and 6.4 (a)**) and (**Figure 6.3 (b) and 6.4 (b)**) respectively. The same was observed for varied cell concentrations of 3.0 and 4.2 $g.L^{-1}$ where only the intensity impacted on micronization of cell debris.

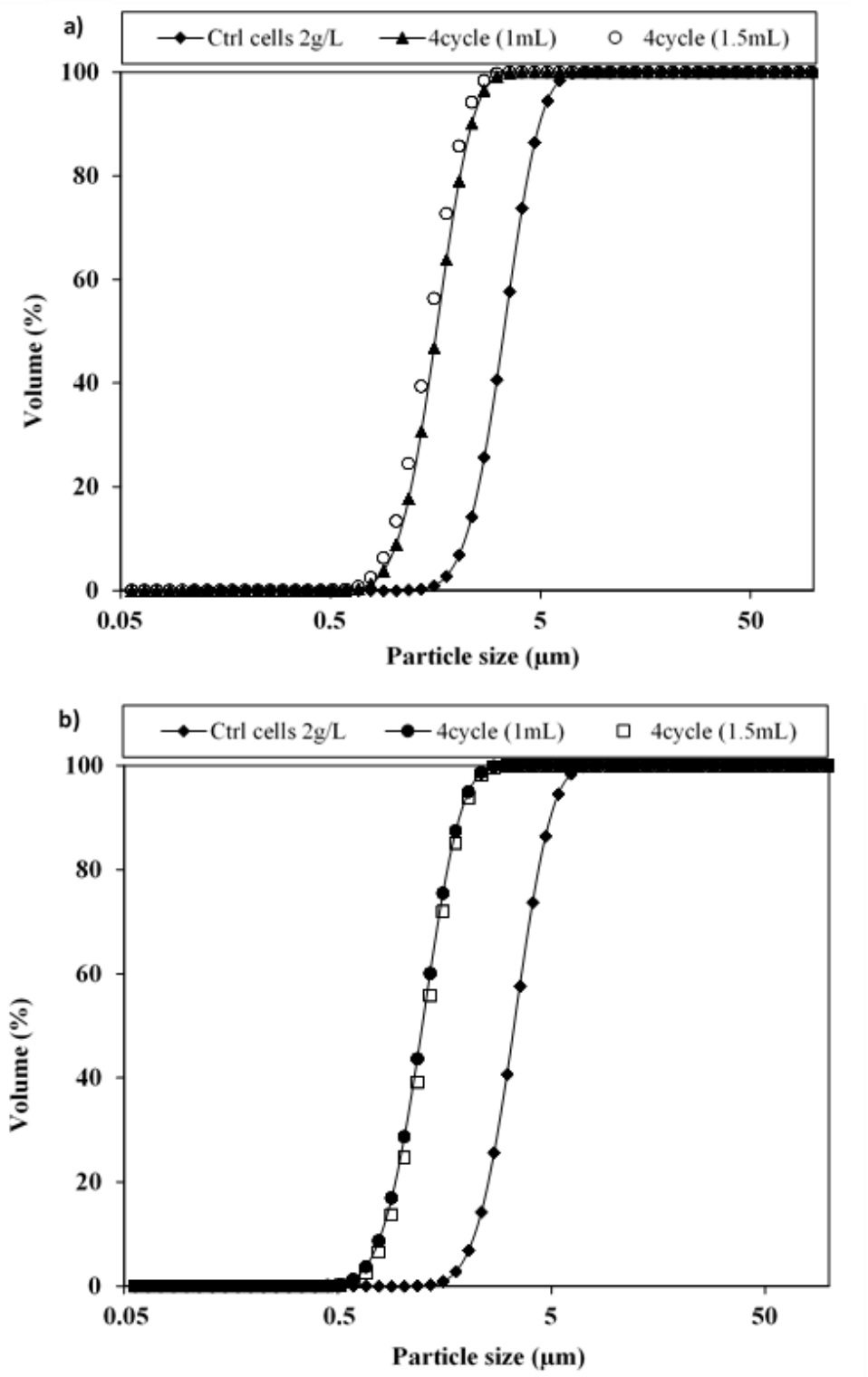

Figure 6-1: Effect of sample volume on cell disruption frequency for (a) 10 and (b) 15 (Ctrl = control cell suspension). Cells were disrupted using 4 cycles and contained 2 $g.L^{-1}$ cells grown heterotrophically as described in Section 2.2.1. Sonication performed as described in Section 2.6.2.

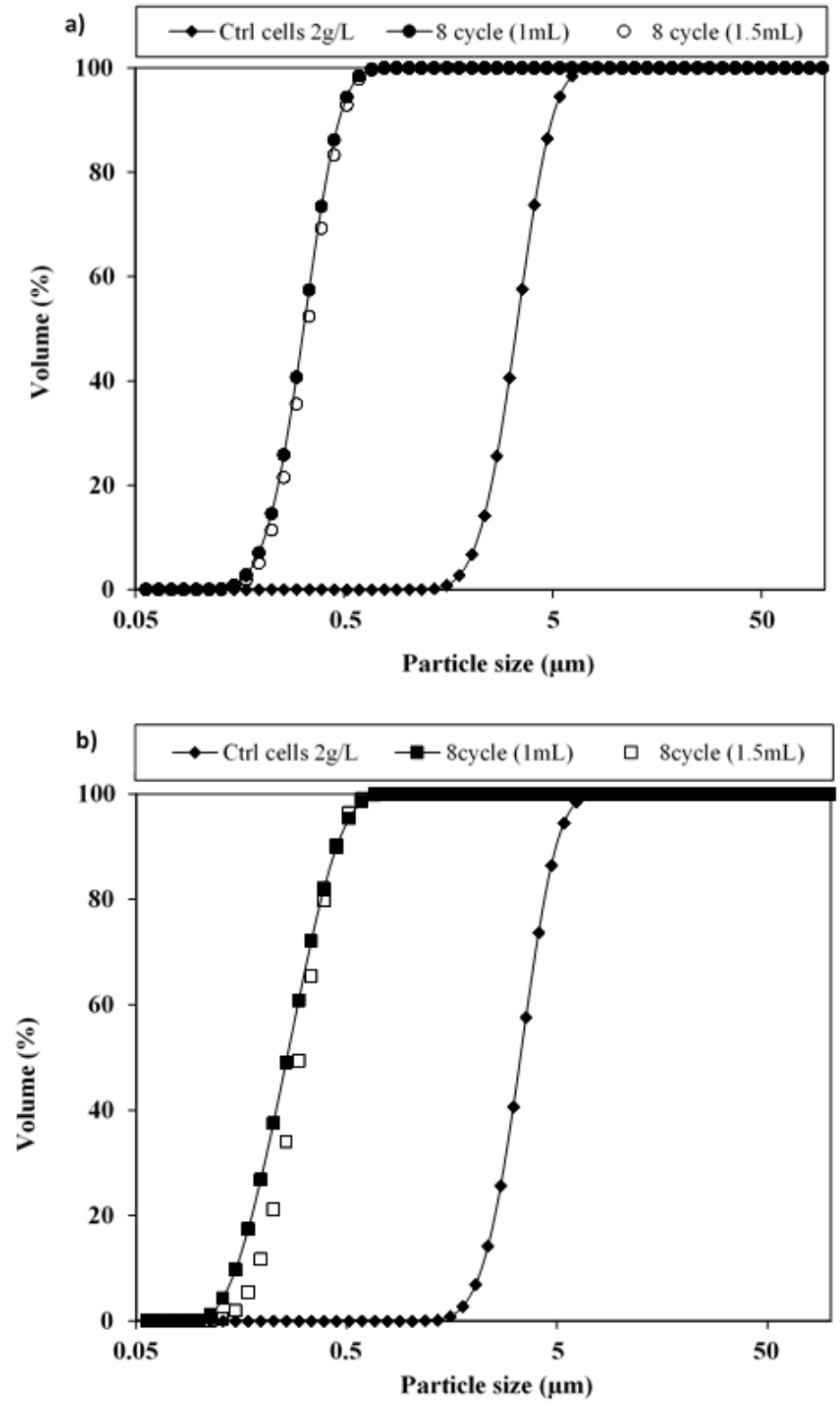

Figure 6-2: Effect of volume on cell disruption (a) intensity of 10 and (b) intensity of 15. Cells were disrupted using 8 cycles and contained 2 $g.L^{-1}$ cells grown heterotrophically as described in Section 2.2.1. Sonication performed as described in Section 2.6.2.

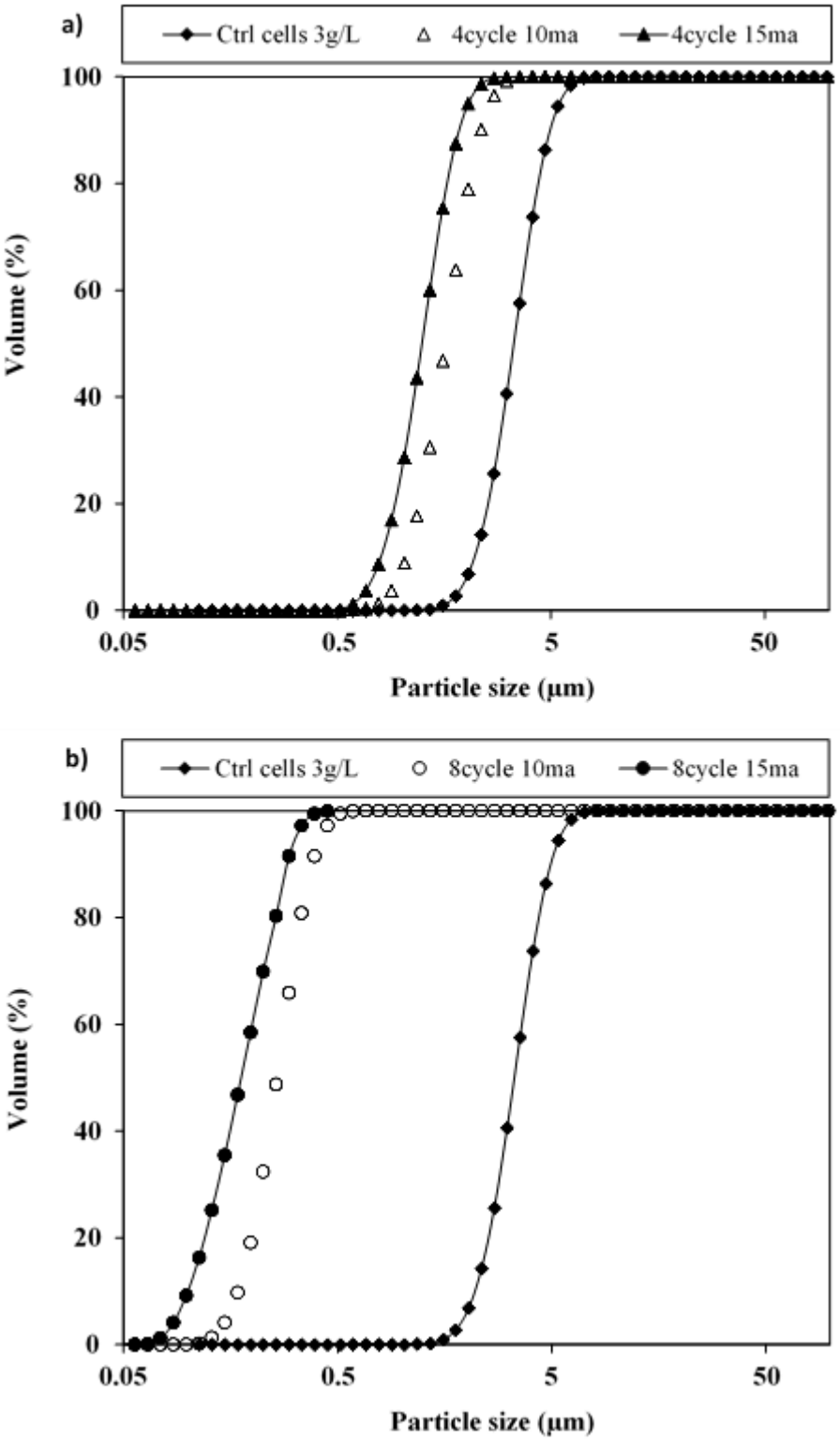

Figure 6-3: Effect of sonication intensity on the particle size of disrupted cells. Cells were sonicated using (a) 4 cycles and (b) 8 cycles and each vial contained 3 $g.L^{-1}$ cells grown heterotrophically as described in Section 2.2.1. Particle size distribution measured as described in Section 2.10.7.

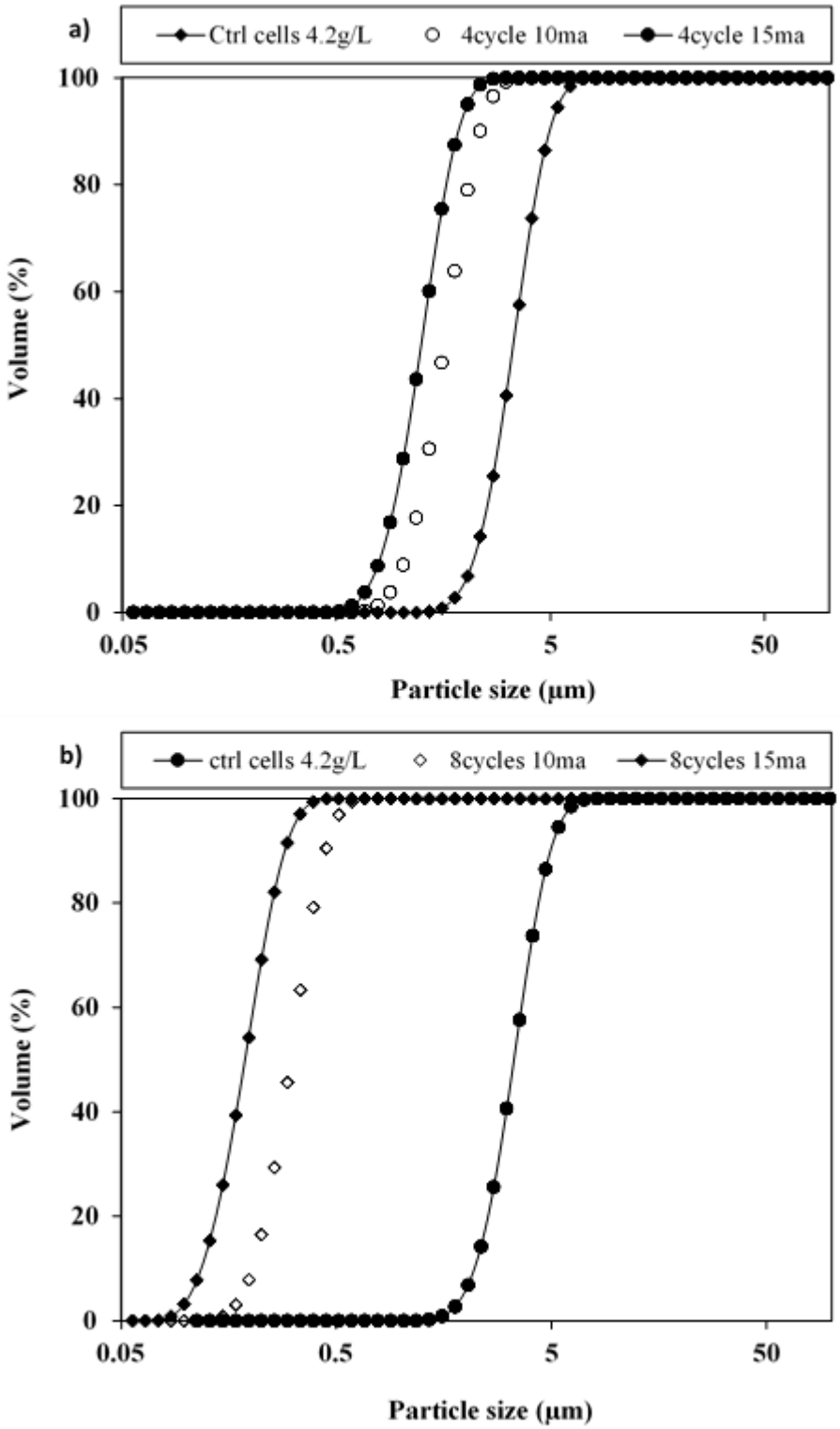

Figure 6-4: Effect of sonication intensity on particle size of disrupted cells. Cells were sonicated using (a) 4 cycles and (b) 8 cycles and each vial contained 4.2 $g.L^{-1}$ cells grown heterotrophically as described in Section 2.2.1. Particle size distribution measured as described in Section 2.10.7.

6.2.3 Effect of number of cycles and sonication intensity on lipid release

The number of cycles and sonication intensity are clearly two important variables in sonication. Increasing the number of rounds of sonication disrupts cells that were omitted in the previous cycle but also further disrupts existing cell debris. **Figure 6.5** shows a clear shift to smaller particle sizes as the number of cycle's increases from 1 to 10. This is as a result of continuous degradation of the disrupted cells by several cycles of ultrasonic wave exposure. A good example of the benefit of combining sonication intensity and number of cycles is shown between **Figure 6.5 (a)** and **(b)**; here the particle profile of 1 cycle which initially overlapped whole cells (**Figure 6.5a**) was seen to shift further away in **Figure 6.5b** (this is indicated by the red oval in the figure). Also, in the red arrows pointing down showing the small particles attained using 10 and 8 cycles having a shift further away from 0.1 µm point. This is also in agreement with Section 6.2.2 where sonication intensity was observed to produce smaller particles.

In order to study the effect of these parameters (number of cycles and sonication intensity) on lipid release, those cycles (4, 8 and 10) which were responsible for increasing cell disruption were studied further. 2 $g.L^{-1}$ cells of algae broth was sonicated at these three different numbers whilst being subjected to waves of increasing intensity. Although smaller particles were acquired using 15ma (**Figure 6.5b**), less lipid was released **(Figure 6.6)**. As expected, the amount of lipid extracted was proportional to the increase in the number of cycles, even though, the difference in the quantity recorded using 8 and 10 cycles is very small and within experimental error. In contrast, using high ultrasonic waves did not benefit product extraction as the quantities obtained are approximately 71% less than those achieved at the lower intensity.

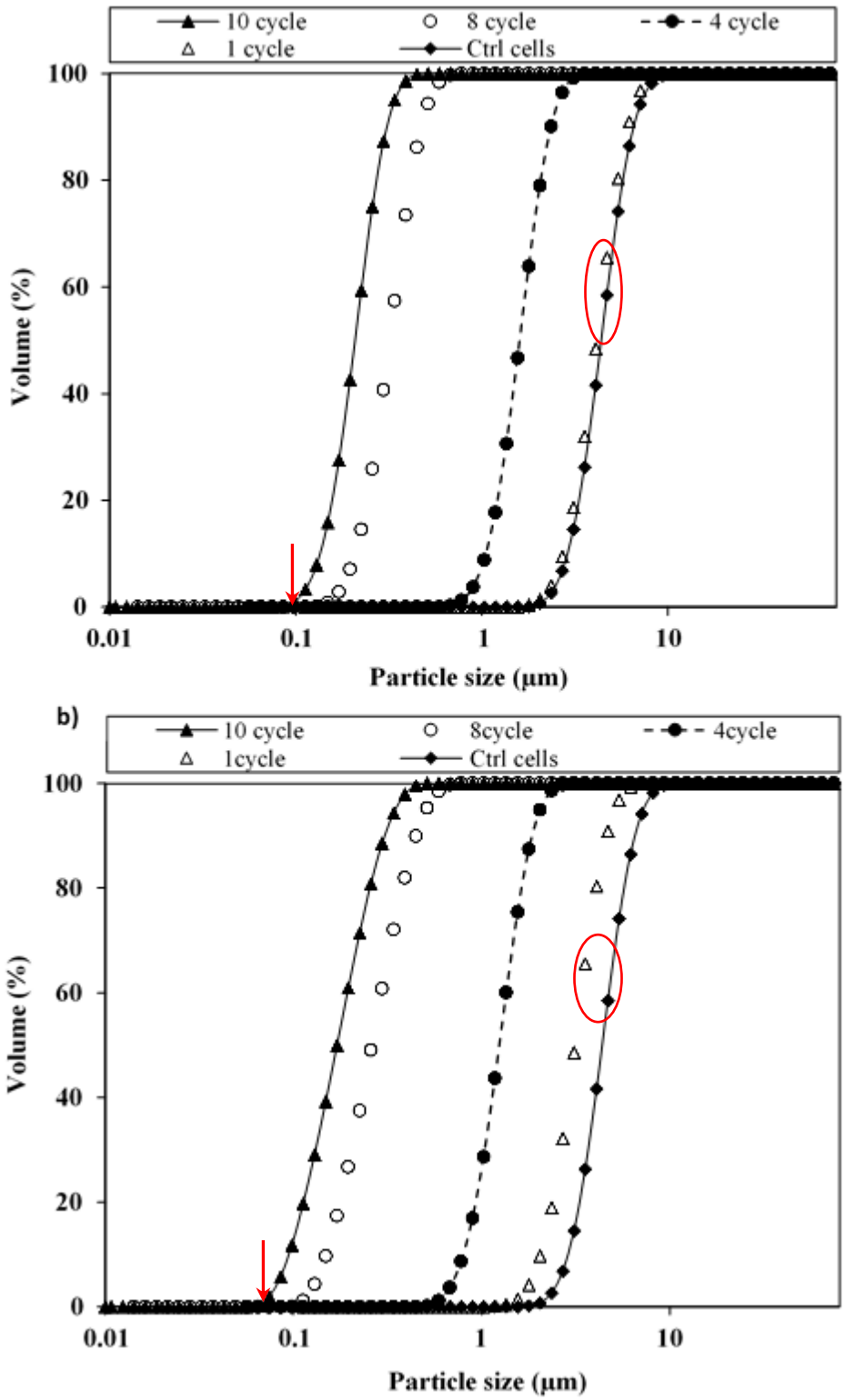

Figure 6-5: Effect of number of sonication cycles on cell disruption. Cells were sonicated using an intensity of (a) 10 and (b) 15. Each vial contained 2 $g.L^{-1}$ cells grown heterotrophically as described in Section 2.2.1.

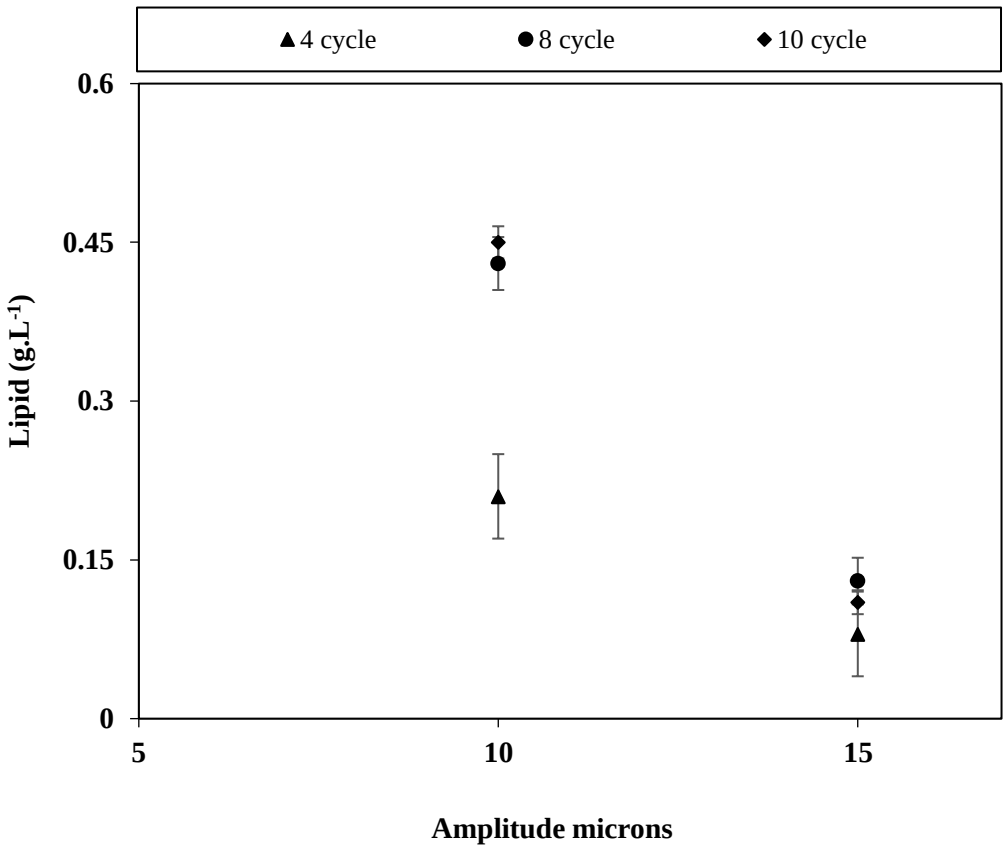

Figure 6-6: The effect of number of sonication cycles and intensity on lipid release. Experiment was carried out using 2.10 ± 0.08 gL-1 cells as described in Section 2.6.2. Lipid released was quantified as described in Section 2.10.6. Error bars represent one standard deviation about the mean (n=3).

6.2.4 Effect of biomass concentration on lipid assay (sensitivity analysis)

Sulphur phosphor vanillin (SPV) assays produce a charged coloured complex (distinct pink colour) due to the reaction of the carbonium ion (produced by a reaction between unsaturated compounds and sulphuric acid) and activated carbonyl group of phospho-vanillin. Quantification of the lipid was achieved by creating a calibration curve using a standard lipid (Appendix 1). Known concentration of this lipid standard (triolene) were used and a linear relationship between absorbance and concentration was found with a strong correlation coefficient ($R^2 > 99$).

Figure 6.7a shows brownish to black coloured solution with increasing number of cycles instead of pink due to high amount of lipid contained in the sample. As explained earlier in Section 6.2.3, increasing the intensity to 15 ma does not increase lipid yield. This is seen from the colour intensity of the images (either undiluted **Figure 6.7a** or diluted **Figure 6**.7**b**). The increasing intensity of this pink coloration is an indication of more lipids present in the sample (Mishra 2013). This is similar to studies by Cheng *et al.*, (2011) which showed an increase in colour development with an increase in sample loading volumes.

Figure 6.8 shows the effect of cell density on the absorbance readings measured using Tecan Safire^2 UV-VIS-IR fluorescence plate reader. This equipment has a capacity of reading optical densities up to 4 AU. Increasing the cell concentration is seen to increase proportionally with the optical densities with higher concentrations exceeding the capacity of the machine (>3 $g.L^{-1}$). Therefore, samples approaching this biomass concentration (3$g.L^{-1}$) were therefore diluted in order to obtain the pink coloration expected (for example **Figure 6.7b**).

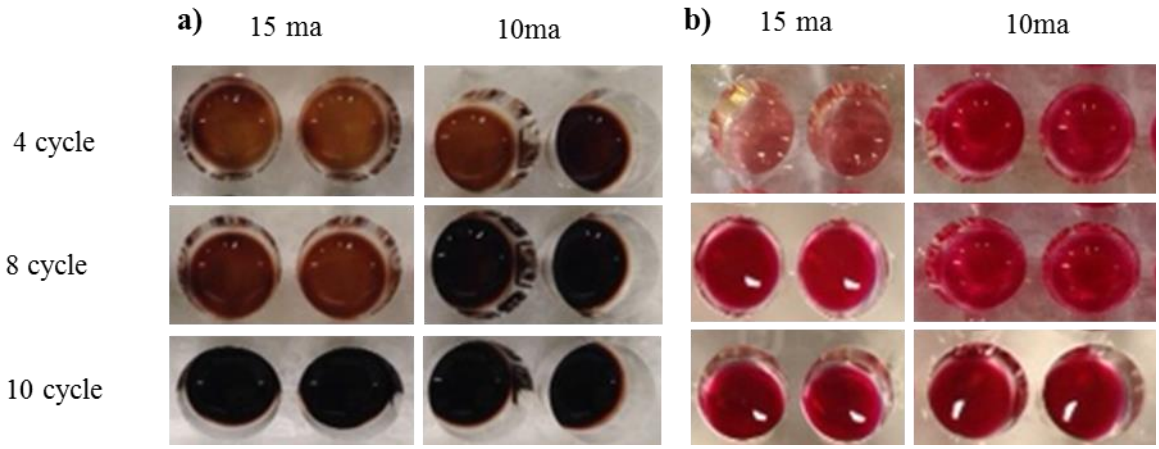

Figure 6-7: Representative photographs of lipid assay at different sonication intensity and cycles (a) without dilution (b) after diluting with chloroform methanol. Experiment was carried out using 5.5 ± 0.4 gL^{-1} cells and performed as described in Section 2.6.2 and Section 2.7.2.

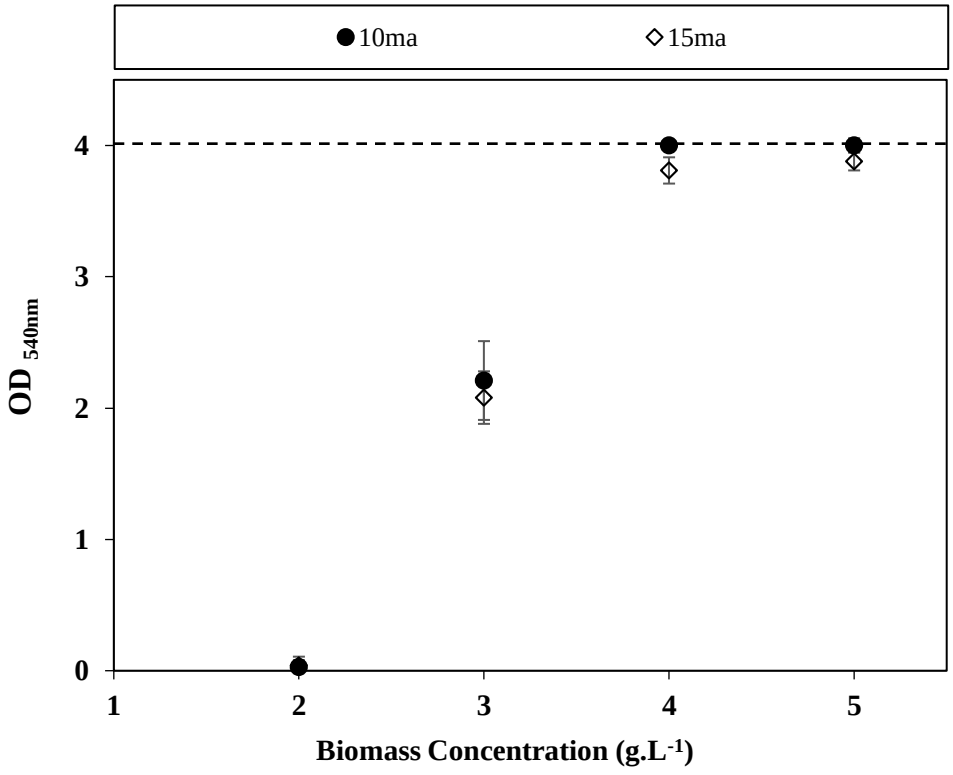

Figure 6-8: Effect of cell concentration on absorbance of the lipid assay used in this work. Cells were grown heterotrophically in TBP media as described in Section 2.2 and lipid quantification performed using the SPV method as described in Section 2.7.2.

6.3 Establishment of homogenization for cell disruption

Homogenization has been successfully used as a cell disruption method for microalgae (Brennan & Owende, 2010) and has been adapted from applications with intracellular bioproduct release from other microorganisms (Middelberg, 1994). Homogenization is studied here in order to benchmark lipid release by sonication with an industry standard method of cell disruption.

6.3.1 Effect of number of passes

The effect of the number of passes through the homogeniser on the disruption of *C.sorokiniana* cells is shown in **Figure 6.9**. This shows that lipid release is proportional to the number of passes and that there is a strong influence of the operating pressure on the disruption process in the homogenizer. Comparison of the number of passes, in particular 3 pass shows that a 4 fold increase was seen when the pressure was increased from 200 to 800 bars. By operating the homogenizer at higher pressures, it is possible to decrease the number of passes of the cell slurry through the homogenizer for a given degree of disruption (Chisti & Moo-Young, 1986; Bury *et al.*, 2001). More so, a reduced number of passes would allow increased throughput and minimize downstream clarification issues which are caused by the formation of very fine debris with increasing passages. However, the deactivation of heat sensitive products may limit the operating pressure, which in turn may increase the number of passages required (Kula & Schiitte, 1987).

6.3.2 Effect of cell concentration

The influence of cell concentration on the degree of cell disruption is disputed in the literature. While some studies show an influence due to cell concentration (Doulah *et al.*, 1975) others (Englert & Robinson, 1981; Hetherington *et al.*, 1971) found cell concentration to have little or no effect on disruption. Studies by Chisti & Moo-Young, (1986) reported a range of concentration (10 - 80%w/v) to have no significant effect on

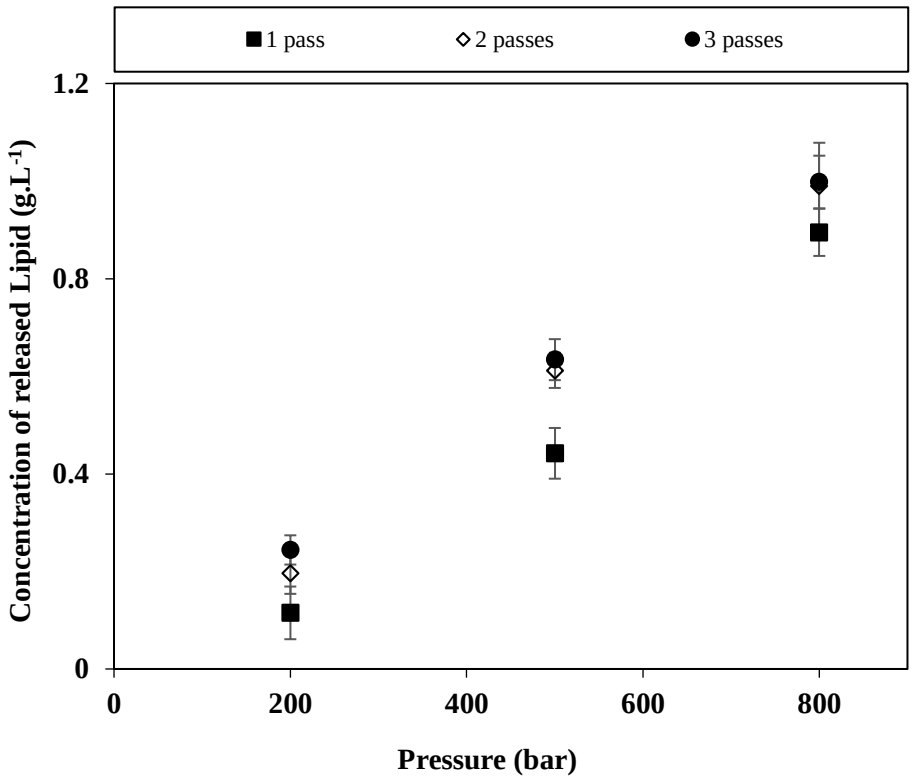

Figure 6-9: Effect of homogenization parameters on concentration of lipid released from *C. sorokiniana* cells. Cells were grown heterotrophically as described in Section 2.2 and homogenisation performed as described in Section 2.6.1. Lipid analysis was carried out as described in Section 2.7.3. Error bars represent one standard deviation about the mean (n=3).

disruption rate. Other studies have also suggested that the cell concentration in the feed should be as high as possible in order to minimize the power consumption per unit of disrupted cells mass (Mogren *et al.*, 1974; Schütte & Kula, 1990). In this study, varying the cell concentration did not show a significant influence on micronization of cell debris (**Figure 6.10**). Experiments using *C.sorokiniana* concentrations of 1 and 3 $g.L^{-1}$ had similar particle size profiles. 5 $g.L^{-1}$ however showed a different particle pattern between 0.5 and 21.4 µm.

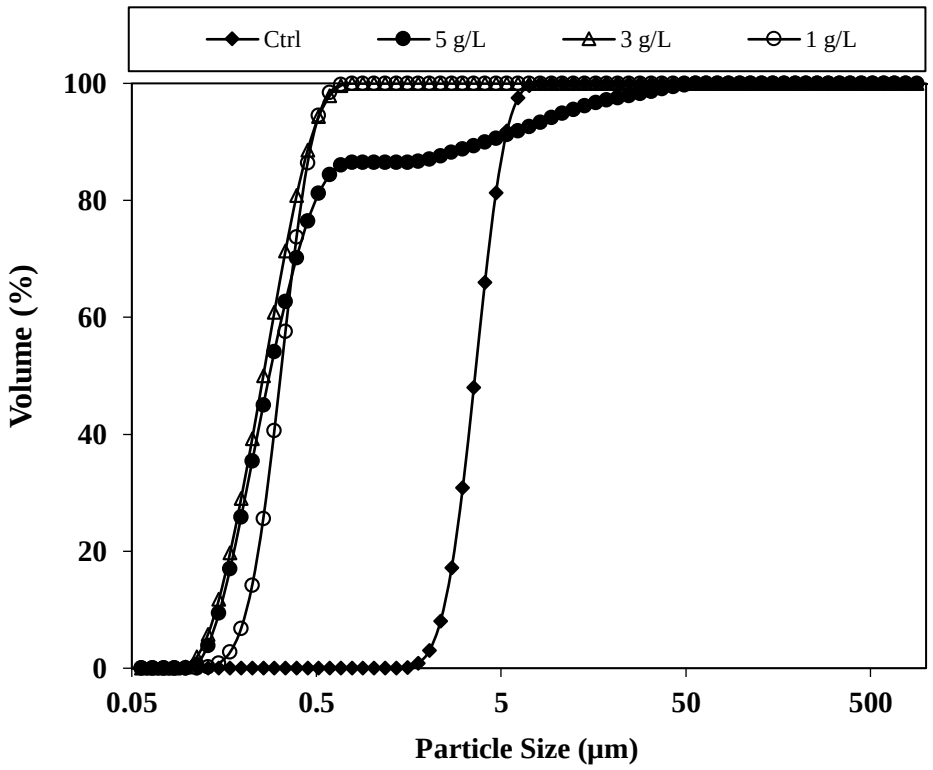

Figure 6-10: Particle profile produced by homogenising different biomass concentration of *C.sorokiniana* broth. Experiments were performed using fresh algal broth from a mid-stationary phase culture. Readjustment of cell concentration was achieved by diluting with spent media in order to keep chemical composition of the media the same. Broth was homogenized as described in Section 2.6.1 using 800 bar and 3 passes.

In this thesis USD methods for both membrane filtration (Chapter 4) and centrifugation (Chapter 5) have been established. As shown in **Figure 1.6** the USD methods enable evaluation of different solid-liquid separation steps on subsequent cell disruption and the pre-treatment of the cells by flocculation. Flocculation benefits on yield was minimal, hence in this chapter, only untreated feed was used to show the benefit of the USD methods in microalgae downstream processing. Moreover, **Table 5.3** compared the FA composition of the oil extracts from flocculated- and unflocculated- centrifuged cells and this was found to possess similar FAME profile.

Samples of broth from a single heterotrophic culture of *C.sorokiniana* were taken through different processing sequences. These comprised of cell culturing (in shake flasks), solid-liquid separation (USD- centrifugation and microfiltration), extraction of the lipids and transesterification.

6.4 Transesterification

In microalgal cells, polar and neutral lipids are the major classes of lipids synthesized (Vigeolas *et al.*, 2012). Neutral lipids are composed of monoacylglycerols, diacylglycerols, triacylglycerols, sterols and sterol esters (Guschina & Harwood, 2006) while polar lipids which are mainly glycosyl- and phosphosyl- glycerides are found on membrane surfaces. In transesterification (Section 1.5) of algal lipids, triglycerols are mostly esterified to produce biodiesel of the required quality (Section 5.7.2).

From **Table 6.1**, it can be seen that there is difference in the yield of the FAMEs following transesterification depending on the harvesting method adapted. USD centrifugation was observed to possess higher yield (dry wt. %) of major components (C16 and C18) of biodiesel as highlighted in **Table 6.1**. A specific example can be seen in the values obtained for Palmitic- and Stearic- methyl esters, C16 and C18 respectively; where 28.8 and 5.7% was recorded for centrifugation while 12.3 and 1.7% for microfiltration recovered cells.

Table 6-1: Comparison of transesterified lipid (dry wt. %) recovered from centrifuged or filtered *C.sorokiniana* broth. Samples were transesterified following extraction of the lipids using Bligh and dyer method (1959) after which GC-MS was used to characterize the FAMEs (Section 2.9). This was then quantified using a calibration curve drawn for each methyl ester (example of curve in Appendix).

Methyl esters	**FAME Formula**	**USD Centrifugation**	**USD Filtration**
Caproic	C6	0.67 ± 0.7	0.33 ± 0.2
Capric	C10	0.37 ± 0.0	0.93 ± 0.4
Lauric	C12:0	0.16 ± 0.0	7.20 ± 0.1
Tridecanoic	C13:0	1.13 ± 0.4	5.15 ± 0.4
Myristic	C14:0	1.57 ± 0.6	1.88 ± 0.7
Myristoleic	C14:1	0.15 ± 0.0	0.11 ± 0.0
Pentadecanoic	C15:0	6.96 ± 2.1	3.33 ± 0.9
cis-10-Pentadecenoic	C15:1	0.64 ± 0.2	0.52 ± 0.1
2,4 -Pentadienoic	C15:2	3.16 ± 0.1	3.12 ± 0.1
Pentatrienoic	C15:3	0.96 ± 0.0	0.92 ± 0.0
Palmitic	C16:0	28.78 ± 2.6	12.33 ± 1.9
Palmitoleic	C16:1	4.74 ± 0.2	1.08 ± 0.2
Heptadecanoic	C17:0	0.89 ± 0.0	4.90 ± 0.3
cis-10-Heptadecenoic	C17:1	2.03 ± 0.0	2.18 ± 0.0
Stearic	C18:0	5.70 ± 0.9	1.77 ± 0.3
Octadecenoic	C18:1	0.94 ± 0.0	2.08 ± 0.4
Elaidic	C18:ln9t	2.43 ± 0.9	4.80 ± 0.5
Oleic	C18:ln9c	12.62 ± 1.2	<0.01
Linolelaidic	C18:2n6t	0.04 ± 0.0	3.51 ± 0.2
Linoleic	C18:2n6c	22.09 ± 0.1	27.48 ± 0.4
Arachidic	C20:0	0.06 ± 0.0	<0.01
γ - Linolenic	C18:3n6	0.17 ± 0.0	5.02 ± 0.2
α-Linoleic acid	C18:3n3	0.79 ± 0.0	1.40 ± 0.3
cis-5,8,11,14,17-Eicosapentaenoic	C20:5n3	0.94 ± 0.1	3.05 ± 0.1
Nervonic	C24:1	0.98 ± 0.3	5.85 ± 0.6
SFA (%)		46.3	37.82
MUFA (%)		23.6	16.62
PUFA (%)		29.1	44.5
TOTAL (%)		99	98.9

Another major difference is in the possession of Oleic and Arachidic acid methyl esters; it has been reported that biodiesel with good ignitability usually contains high C18 such as Oleic acid methyl ester (methyl oleate) content, this in turn gives lower levels of NO, hydrocarbons etc. (Yamane *et al.*, 2001). Using microfiltration as a recovery option, oleic as well as Arachidic acid were obtained at statistically insignificant values.

During the transesterification reaction, the reacting components i.e. alcohol and glycerides have to be considerably dewatered because water causes a partial reaction change to saponification, which produces soap (Fukuda et al., 2001). **Figure 5.1** shows the moisture content of each recovery method and microfiltration (using CFF) can be seen to contain about 80-85% water which has to either be centrifuged to further dewater or freeze dried directly (as carried out in this study) which is not the most preferred option.

6.5 Summary

As described in Section 6.1 the overall aim of this chapter was to establish and compare the use of sonication and homogenization as small-scale cell disruption operations for lipid release from harvested cells. Also the impact of biomass recovery method on transesterification was studied.

Sonication was preferred choice for cell disruption because volumes compatible with USD studies; the volume of feed required for sonication can be as small as 1 - 1.5 mL whereas 40 mL was required for homogenization. For sonication, this was used for all experiments irrespective of the conditions employed (number of cycles, cell concentration or sonication intensity). Also, it is often the preferred cell disruption method at the laboratory scale (Wenger *et al.*, 2008). In conclusion, a comparison of the disruption efficiencies of sonication and homogenization, showed that cell disruption and lipid release in both cases are similar lipid on mass/mass basis (**Figure 6.6** and **Figure 6.9)**.

.

Initial objectives of exploring sonication parameters revealed that varying the volume of the sample did not have any effect on debris particle profile (**Figure 6.1 and Figure 6.2**). Increasing the wave frequency increased the rate of particle disintegration (**Figure 6.3**) while for the effect of number of cycles, it was observed that increasing the number of rounds sonication occurs micronizes the debris further (**Figure 6.5**).

Cell disruption methods are known to significantly differ due to variations in disruption properties (van Hee *et al.*, 2006). For homogenization, the effect of number of passes showed that lipid release is proportional to the number to passes and is also influenced by the operating pressure (**Figure 6.9**). In **Figure 6.10**, 5 $g.L^{-1}$ broth was homogenized using 800 bar, 3 passes where a percentage of large particles was seen. This could be particle aggregates.

Finally, this thesis has established USD methods for membrane filtration (Chapter 4), centrifugation (Chapter 5) and cell disruption (Section 6.2). Broth from a single heterotrophic culture of *C.sorokiniana* was taken through different processing sequences (**Figure 1.6**) and tranesterified (Section 6.4). Transesterification of centrifuged or filtered broth showed that centrifugation produces the slurry in the desired form suitable for biodiesel production as not all major biodiesel components that affects its quality were detected using filtered slurry (**Table 6.1**). The reason for this could be because of the dewatering abilities of each method since reports have shown that the reacting components for biodiesel production have to be considerably dewatered. Further, the pictorial moisture content of the recovery methods used in this thesis is shown in **Figure 5.1.** Water is known to cause a partial reaction change to saponification (Fukuda *et al.*, 2001).

7. Conclusions and Future Work

7.1 Summary and overall conclusions

The overall aim of this project is to establish an ultra scale-down platform for the rapid evaluation of pre-treatment and recovery operations for microalgae downstream process (**Figure 7.1**). This was successfully achieved for flocculation (Chapter 3), microfiltration (Chapter 4) and centrifugation (Chapter 5) operations. The establishment of a USD platform for algal downstream processing will benefit whole bioprocess development for microalgae since the process technology surrounding the economic production of microalgal products at manufacturing scale is still poorly defined (Section 1.9). In particular, microalgae dewatering technologies has hindered the prospects of its use as a feasible technology (Chapter 1). Based upon literature, research has indicated that it may be more beneficial to harvest biomass in two steps: bulk harvesting and thickening (Wang *et al.*, 2008) (Section 1.4). In this thesis, a scenario of using flocculation as a pre-treatment step prior to microfiltration and centrifugation was explored (**Figure 7.1**). For the initial flocculation step, Chitosan was used because of its biodegradability and non-toxicity (Bustos-Ramírez *et al.*, 2013; Ravi Kumar, 2000) (Section 3.3).

In Chapter 1, a series of objectives were outlined (Section 1.9) in order to achieve the overall thesis aim. These followed a sequential order as follows:

- Choose a suitable strain and scale-up the growth kinetics from shake flask to lab bioreactor scale;
- Design, fabricate and characterize scale-down flocculation reactors that can operate reproducibly and mimic conventional stirred flocculation reactors;

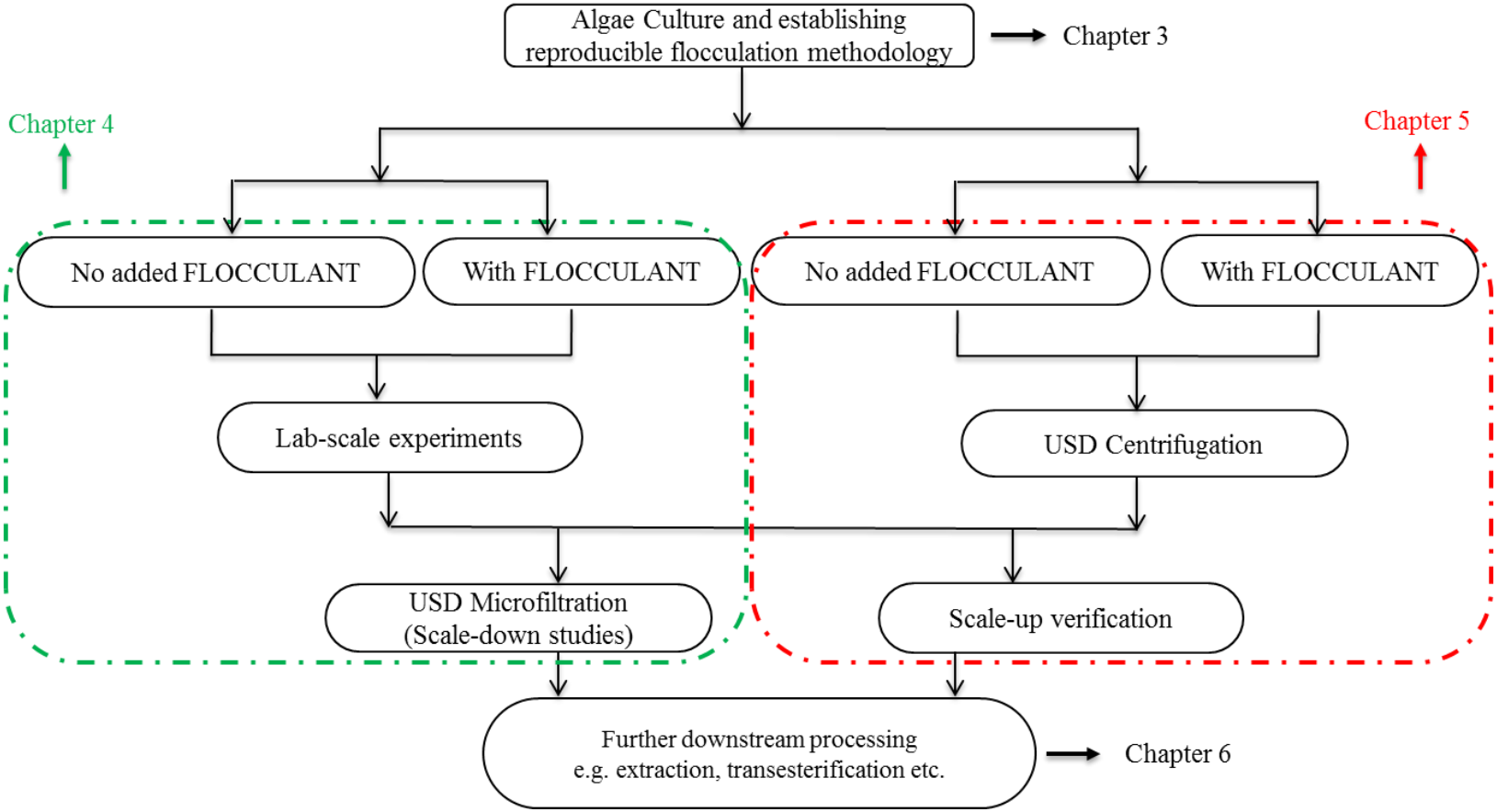

Figure 7-1: Overview of the USD platform established in this work. Figure indicates the primary unit operation that were addressed and the various process sequences that was evaluated.

- Establish a USD method for the study of microalgae microfiltration processes and the impact of flocculation as a pre-treatment step;
- Establish a USD method for the study of centrifugation for microalgae recovery and the impact of flocculation as a pre-treatment step;
- Establish and compare the use of sonication and homogenization as small scale cell disruption operations for lipid release from harvested cells;
- Use the USD platform to study the various downstream process options shown in **Figure 7.1** and their impact on overall lipid extraction and transesterification.

Identifying a suitable strain with high biomass productivity is still an important first step in microalgae process development. In this study, heterotrophically cultured strains were preferred because they attained the highest biomass productivity (**Figure 3.2**). *C. sorokiniana* was the organism selected for investigation as it exhibited a short doubling time and a high lipid content of 22% (w/w) (**Table 3.1**). Scale-up studies showed comparable growth rates, yields, as well as carbon source utilization and metabolite production profiles in the shake flask (250 mL) and bioreactor (7.5 L) suggesting the cells produced at the two scales were in a similar physiological state (**Figure 3.4**).

Establishment of a flocculation methodology involved the design (Section 3.4) and characterization (**Figure 3.6**-**3.8**) of scale-down stirred flocculation reactors. A scale-down approach was considered useful since it was highlighted in Chapter 3 that one of the major problems with flocculation is the difficulty of operating the process reproducibly. Therefore in Chapter 3, standardizing and fixing the parameters (pH (**Figure 3.9**), t_{add} (**Figure 3.10**) and concentration of flocculant (**Figure 3.12**)) that influence flocculation enables consistency and reproducibility in the particle size distributions of the flocs produced (**Figure 3.12** and **Table 3.2**). Scale-up of the flocculation process from the scale-down reactor (120 mL) to a 7.5L STR was achieved at a matched impeller tip speed during flocculant addition and ageing (**Figure 3.13**).

Initial microfiltration studies in Chapter 4 focussed on establishing conditions for a lab-scale, hollow fibre-based process for cell recovery and concentration. In this study, difference in the amount of EOM due to culture type and hence cleaning (Section 4.5) was observed. Flocculation was seen to benefit the overall filtration performance and subsequently cleaning (Section 4.6). Scaling-down of the process was successfully achieved using an RDF. Comparable steady state flux profiles with those of lab-scale within $\leq$10 $L.m^{-2}.h^{-1}$ difference was obtained. This was achieved with a 14-fold reduction in volume and approximately 14.5-fold reduction in membrane area. Other key operation variables considered during CFF such as flux and pH, were also in good agreement between the two scales for both unflocculated and flocculated feed (**Figure 4.16**).

In Chapter 5, a USD methodology for algal biomass recovery by centrifugation was established (**Figure 5.8**). This was used to explore flocculation as a pre-treatment step (**Figure 5.8**), a process that was shown to be scalable up to pilot scale (**Figure 5.10**). Study of the influence of flocculation on centrifugation efficiency showed that low Chitosan dosage (where total breakage of flocs was seen with shear), resulted in low clarification efficiencies compared to those obtained at an optimal dosage of $\geq$ 4 $mg.mL^{-1}$ **(Figure 5.7)**. Based on this, the optimal dosage was calculated as 9.9 ± 0.4 mg of chitosan per g_{DCW} of algae. Flocculation was also shown not to affect the composition of the final lipid produced at both USD and pilot scale **(Table 5.3)**. The USD approach only required 2-10 mL of material which is 400-2000 fold less than was required for the pilot scale study.

Scale translation is valuable as it aids research and development by reducing the uncertainties of developmental delays and thus accelerates product commercialization. Here, the approach is illustrated by examples using small-scale mimics for operations such as flocculation, centrifugation, filtration, linkage of some of these operations and their successful scale-up/down. A good example in this thesis was the ability to view the fouling characteristics (at USD level) of phototrophic broth using SEM micrographs in Chapter 4.

The application of USD to microalgal downstream processing is considered novel and will give a wider opportunity to the understanding and development of different processes and/or unit operations.

Chapter 6 of this thesis explored sonication and homogenization as small scale cell disruption options for lipid release of heterotrophically grown *C.sorokiniana*. Comparison of the optimal conditions of the two methods showed cell disruption and lipid release were similar in both cases on a $g.g^{-1}$ basis; **Figure 3.4** (sonication) and **Figure 6.9** (homogenization). This was important in order to have established a cell disruption method compatible with the scale of operation of the USD operations.

Finally, to demonstrate the potential of the whole USD platform, the whole primary process sequence options were investigated (**Figure 7.1**) Comparison of the transesterified -centrifuged and -microfiltered cells shows some major differences in terms of yield of FAME (**Table 6.1**). Primary recovery stages are therefore critical and optimum choices of operations, together with sequence of operations, needs to be explored on a case-by-case basis.

In terms of the wider implications of this work, the ability to rapidly select and optimize the numerous processes that exist for harvesting microalgae will not only reduce the process cost, but can render the whole scheme economically feasible. Existing literature is not conclusive enough to define a optimal DSP sequence (Shelef & Sukenik, 1984). This is because there are a wide range of choices for process design in each step of the algal production sequence. Given the constraints in resources at early stages of process development, USD will aid optimization up to validation studies at reduced risk, cost and time. Finally, centrifugation is known to be more energy intensive than tangential flow filtration, but the throughput in terms of product quality (**Table 6.1**) and consumables (i.e. membranes used for filtration and this being the most sensitive variable for overall cost)

has rendered centrifugation a better choice for dewatering and harvesting microalgae cells with a prior flocculation step to enhance the process.

7.2 Recommendations for future research

Section 7.1 highlighted the high level outcomes of the research performed in this thesis. This section will present suggestions for future work in order to further explore the ability of using predictive USD tools in microalgae bioprocessing.

- In Chapter 3, flocculation reactors were characterized and scaled-down using heterotrophically grown *C.sorokiniana* cells. Further studies should be performed in order to verify the applicability of these reactors with other microalgae strains and phototrophically grown cells.
- To better define the method of scale translation between the USD membrane device used in Chapter 4 and the hollow fibre cartridge further work could be undertaken using the same membrane material at the two scales. In relation to this, experiments accessing different membrane types and pore sizes could also be explored to further aid process optimisation studies.
- Successful scale translation between the USD RDF and the hollow fibre cartridge was not achieved at matched shear rates as expected (Section 4.7.1). This was due to turbulence promotors present in the larger lab-scale device. Therefore, Future work should focus on redesigning the device as follows: (1) in order to accurately mimic the larger scale modules, the prototype should be fitted with screens and turbulence promoters as to those present in the cartridges being mimicked. Studies on the effect of these turbulence promoters based on feed hydrodynamics and the overall influence on filtration outcomes should be evaluated; and (2) CFD modelling of the device is recommended in order to develop and confirm shear rate predictions.

- In Chapter 5, the generic nature of the USD methodology for centrifugation should be established by repeating the study for phototrophically grown cells. Furthermore, confirmation of the accurate scale-up predictions should be undertaken using different designs of large scale centrifuges.
- Cell disruption studies (Chapter 6) could be done more systematically with applications such as statistical Design of Experiments (DoE), since numerous variables are involved.
- It was mentioned in the initial aims that downstream processing options (**Figure 7.1**) will be compared on the overall impact on lipid extraction. This was however not accomplished because a common ground has to be provided for the two solid-liquid separation systems. Therefore, studies on the best operating conditions at which the highest moisture content that can be attained for microfiltration and centrifugation will be most ideal to allow the cost implication and efficiency of each process to be evaluated thereby give a rational basis for comparison of the two systems.
- Finally, considering the biofuel applications being considered, it would important to further characterization the FAMEs produced in terms of their physical properties and combustion properties in formulated fuels.

References

Aas E. 1996. Refractive index of phytoplankton derived from its metabolite composition. *J. Plankton Res.* **18**:2223–2249.

Ahmad a. L, Mat Yasin NH, Derek CJC, Lim JK. 2011. Optimization of microalgae coagulation process using chitosan. *Chem. Eng. J.* **173**:879–882.

Aiba S ichi. 1991. Studies on chitosan: 3. Evidence for the presence of random and block copolymer structures in partially N-acetylated chitosans. *Int. J. Biol. Macromol.* **13**:40.

Allard B, Rager MN, Templier J. 2002. Occurrence of high molecular weight lipids (C80 +) in the trilaminar outer cell walls of some freshwater microalgae. A reappraisal of algaenan structure. *Org. Geochem.* **33**:789–801.

Ambler C. 1959. The theory of scaling up laboratory data for the sedimentation type centrifuge. *J Biochem Microbiol Technol Eng* **1**:185–205.

Ambler CM. 1952. The evaluation of centrifuge performance. *Chem. Eng. Prog.* **48**:150–158.

Andrew JJN. 2007. Energy science principles, technology and impacts. New York: Oxford University Press.

Arbex M, Perobelli FS. 2010. Solow meets Leontief: Economic growth and energy consumption. *Energy Econ.* **32**:43–53.

Aslan S, Kapdan IK. 2006. Batch kinetics of nitrogen and phosphorus removal from synthetic wastewater by algae. *Ecol. Eng.* **28**:64–70.

Association for the study of peak oil and gas (ASPO). 2004. Energy Security. http://www.peakoil.net/Oil_tsunami.html.

Atkinson AW, Gunning BES, John PCL. 1972. Sporopollenin in the cell wall of Chlorella and other algae: Ultrastructure, chemistry, and incorporation of 14C-acetate, studied in synchronous cultures. *Planta* **107**:1–32.

Babel S, Takizawa S. 2010. Microfiltration membrane fouling and cake behavior during algal filtration. *Desalination* **261**:46–51.

Babel S, Takizawa S. 2011. Chemical pretreatment for reduction of membrane fouling caused by algae. *Desalination* **274**:171–176.

Bacchin P, Aimar P, Field RW. 2006. Critical and sustainable fluxes: Theory, experiments and applications. *J. Memb. Sci.*

Balasundaram B, Harrison S, Bracewell DG. 2009. Advances in product release strategies and impact on bioprocess design. *Trends Biotechnol.* **27**:477–485.

Bamgboye AI, Hansen AC. 2008. Prediction of cetane number of biodiesel fuel from the fatty acid methyl ester (FAME) composition. *Int. Agrophysics* **22**:21–29.

Barsanti L, Gualtieri P. 2005. Algae: anatomy, biochemistry, and biotechnology. *Vasa* 1-301 p.

Behrens P, Kyle D. 1996. Microalgae as a source of fatty acids. *J. Food Lipids* **3**:259–272.

Benemann JR, Oswald WJ. 1996. Systems and Economic Analysis of Microalgae Ponds for Conversion of CO2 to Biomass. *Final Rep. to Dep. Energy, Pittsburgh Energy Technol. Cent.*:DOE/PC/93204–T5.

Berrill A, Ho S V., Bracewell DG. 2008. Ultra scale-down to define and improve the relationship between flocculation and disc-stack centrifugation. *Biotechnol. Prog.* **24**:426–431.

Bilanovic D, Andargatchew A, Kroeger T, Shelef G. 2009. Freshwater and marine microalgae sequestering of CO2 at different C and N concentrations - Response surface methodology analysis. *Energy Convers. Manag.* **50**:262–267.

Bligh EG, Dyer WJ. 1959. A rapid method of total lipid extraction and purification. *Can. J. Biochem. Physiol.* **37**:911–917.

Bölling C, Fiehn O. 2005. Metabolite profiling of Chlamydomonas reinhardtii under nutrient deprivation. *Plant Physiol.* **139**:1995–2005.

Borowitzka MA. 1988. Algal Growth Media and Sources. In: . *Micro-algal Biotechnol.*, pp. 456–465.

Borowitzka MA. 1997. Microalgae for aquaculture: Opportunities and constraints. *J. Appl. Phycol.* **9**:393–401.

Boswell, K.D.B.; Gladue, R., Prima, B. and Kyle DJ. 1992. SCO Production by Fermentative Microalgae. In industrial Applications of Single Cell Oils. Ed. D.J. Kyle and C. Ratledge. Champaign, IL: American Oil Chemists' Society 274-286 p.

Boulding N, Yim SSS, Keshavarz-Moore E, Ayazi Shamlou P, Berry M. 2002. Ultra scaledown to predict filtering centrifugation of secreted antibody fragments from fungal broth. *Biotechnol. Bioeng.* **79**:381–388.

Bouzerar R, Jaffrin MY, Ding LH, Paullier P. 2000. Influence of geometry and angular velocity on performance of a rotating disk filter. *Aiche J.* **46**:257–265.

Boychyn M, Doyle W, Bulmer M, More J, Hoare M. 2000. Laboratory scaledown of protein purification processes involving fractional precipitation and centrifugal recovery. *Biotechnol. Bioeng.* **69**:1–10.

Boychyn M, Yim SSS, Bulmer M, More J, Bracewell DG, Hoare M. 2004. Performance prediction of industrial centrifuges using scale-down models. *Bioprocess Biosyst. Eng.* **26**:385–391.

Boychyn M, Yim SSS, Ayazi Shamlou P, Bulmer M, More J, Hoare M. 2001. Characterization of flow intensity in continuous centrifuges for the development of laboratory mimics. *Chem. Eng. Sci.* **56**:4759–4770.

BP. 2011. BP Statistical Review of World Energy. *Nucl. Energy*.

BP. 2015. BP Statistical Review of World Energy. *Oil Sect. - Stat. Rev. World Energy*.

Bratby J. 2006. Coagulation and Flocculation in Water and Wastewater Treatment. *Water*. Vol. 2nd 43-53 p.

Brennan L, Owende P. 2010. Biofuels from microalgae-A review of technologies for production, processing, and extractions of biofuels and co-products. *Renew. Sustain. Energy Rev.* **14**:557–577.

Brou A, Jaffrin MY, Ding LH, Courtois J. 2003. Microfiltration and ultrafiltration of polysaccharides produced by fermentation using a rotating disk dynamic filtration system. *Biotechnol. Bioeng.* **82**:429–437.

Brown LM. 1996. Uptake of carbon dioxide from flue gas by microalgae. *Energy Convers. Manag.* **37**:1363–1367.

Bruton T, Lyons H, Lerat Y, Stanley M, Rasmussen MB. 2009. A Review of the Potential of Marine Algae as a Source of Biofuel in Ireland. *Sustain. Energy Irel. Dublin*:88.

Bustos-Ramírez K, Martínez-Hernández AL, Martínez-Barrera G, de Icaza M, Castaño VM, Velasco-Santos C. 2013. Covalently bonded chitosan on graphene oxide via redox reaction. *Materials (Basel).* **6**:911–926.

Byrne EP, Fitzpatrick JJ, Pampel LW, Titchener-Hooker NJ. 2002. Influence of shear on particle size and fractal dimension of whey protein precipitates: Implications for scale-up and centrifugal clarification efficiency. *Chem. Eng. Sci.* **57**:3767–3779.

Del Campo JA, García-González M, Guerrero MG. 2007. Outdoor cultivation of microalgae for carotenoid production: Current state and perspectives. *Appl. Microbiol. Biotechnol.*

Çelekli A, Yavuzatmaca M, Bozkurt H. 2009. Modeling of biomass production by Spirulina platensis as function of phosphate concentrations and pH regimes. *Bioresour. Technol.* **100**:3625–3629.

Chen CY, Yeh KL, Su HM, Lo YC, Chen WM, Chang JS. 2010. Strategies to enhance cell growth and achieve high-level oil production of a Chlorella vulgaris isolate. *Biotechnol. Prog.* **26**:679–686.

Chen F, Johns MR. 1991. Effect of C/N ratio and aeration on the fatty acid composition of heterotrophic Chlorella sorokiniana. *J. Appl. Phycol.* **3**:203–209.

Chen P, Min M, Chen Y, Wang L, Li Y, Chen Q, Wang C, Wan Y, Wang X, Cheng Y, Deng S, Hennessy K, Lin X, Liu Y, Wang Y, Martinez B, Ruan R. 2009. Review of

the biological and engineering aspects of algae to fuels approach. *Int. J. Agric. Biol. Eng.*

Cheng YS, Zheng Y, Labavitch JM, Vandergheynst JS. 2011a. The impact of cell wall carbohydrate composition on the chitosan flocculation of Chlorella. *Process Biochem.* **46**:1927–1933.

Cheng YS, Zheng Y, VanderGheynst JS. 2011b. Rapid quantitative analysis of lipids using a colorimetric method in a microplate format. *Lipids* **46**:95–103.

Chester and Oldshue S. 1987. Biotechnology processes: scale-up and mixing. In: . *New York Am. Inst. Chem. Eng.*, p. p 155– 167.

Chiou YT, Hsieh ML, Yeh HH. 2010. Effect of algal extracellular polymer substances on UF membrane fouling. *Desalination* **250**:648–652.

Chisti Y. 2007. Biodiesel from microalgae. *Biotechnol. Adv.* **25**:294–306.

Chisti Y. 2008. Biodiesel from microalgae beats bioethanol. *Trends Biotechnol.* **26**:126–131.

Chisti Y, Moo-Young M. 1986. Disruption of microbial cells for intracellular products. *Enzyme Microb. Technol.* **8**:194–204.

Clasen, J., Mischke, U., Drikas, M. & Chow C. 2000. An improved method for detecting electrophoretic mobility of algae during the destabilisation process of flocculation: flocculant demand of different species and the impact of DOC. *J. Water Serv. Res. Technol.* **49**:89–101.

Colman B, Rotatore C. 1995. Photosynthetic inorganic carbon uptake and accumulation in two marine diatoms. *Plant Cell Env.* **18**:919–924.

Converti A, Casazza AA, Ortiz EY, Perego P, Del Borghi M. 2009. Effect of temperature and nitrogen concentration on the growth and lipid content of Nannochloropsis oculata and Chlorella vulgaris for biodiesel production. *Chem. Eng. Process. Process Intensif.* **48**:1146–1151.

Dai Z, Dukhin S, Fornasiero D, Ralston J. 1998. The Inertial Hydrodynamic Interaction of Particles and Rising Bubbles with Mobile Surfaces. *J. Colloid Interface Sci.* **197**:275–292.

Demirbaş A. 2001. Relationships between lignin contents and heating values of biomass. *Energy Convers. Manag.* **42**:183–188.

Deng X, Li Y, Fei X. 2009. Microalgae: A promising feedstock for biodiesel. *African J. Microbiol. Res.* **3**:1008–1014.

Dijkstra AJ. 2006. Revisiting the formation of trans isomers during partial hydrogenation of triacylglycerol oils. *Eur. J. Lipid Sci. Technol.*

Dismukes GC, Carrieri D, Bennette N, Ananyev GM, Posewitz MC. 2008. Aquatic phototrophs: efficient alternatives to land-based crops for biofuels. *Curr. Opin. Biotechnol.*

Divakaran R, Pillai VNS. 2002. Flocculation of algae using chitosan. *J. Appl. Phycol.* **14**:419–422.

Doucha J, Lívanský K. 2008. Influence of processing parameters on disintegration of Chlorella cells in various types of homogenizers. *Appl. Microbiol. Biotechnol.* **81**:431–440.

Doucha J, Straka F, Lívanský K. 2005. Utilization of flue gas for cultivation of microalgae (Chlorella sp.) in an outdoor open thin-layer photobioreactor. *J. Appl. Phycol.* **17**:403–412.

Doulah M.S; Hammond, T.H.; Brookman JS. et al. 1975. A hydrodynamic mechanism for the disintegration of Sacchammyces cerevisiae in an industrial homogenizer. *Biotechnol. Bioeng* **17**:845– 858.

Dragone G, Fernandes B, Vicente A, Teixeira J. 2010. Third generation biofuels from microalgae. *Curr. Res. Technol. Educ. Top. Appl. Microbiol. Microb. Biotechnol.*:1355–1366.

Edzwald JK. 1993. Coagulation in drinking water treatment: Particles, organics and coagulants. In: . *Water Sci. Technol.*, Vol. 27, pp. 21–35.

Edzwald JK. 2010. Dissolved air flotation and me. *Water Res.*

Englert CR, Robinson CW. 1981. Disruption of Candida utiZis Cells in High Pressure Flow Devices *. *Biotechnol. Bioeng.* **23**:765–780.

Eriksen NT. 2008. The technology of microalgal culturing. *Biotechnol. Lett.*

Espuny Garcia del Real G, Davies J, Bracewell DG. 2014. Scale-down characterization of post-centrifuge flocculation processes for high-throughput process development. *Biotechnol. Bioeng.* **111**:2486–2498.

Essen U and Von. 1986. Scale-up of equipment for agitating liquids. In: Mixing: theory and practice. In: Uhl VW, GJ, editor. *London Acad. Press* volume 3. Orlando, p. p 221–225.

Faegri, K., Iversen J. 1964. Textbook of pollen analysis. New York: Hafner Pub. Co.

Filion D, Lavertu M, Buschmann MD. 2007. Ionization and Solubility of Chitosan Solutions Related to Thermosensitive Chitosan / Glycerol-Phosphate Systems Ionization and Solubility of Chitosan Solutions Related to Thermosensitive Chitosan / Glycerol-Phosphate Systems:3224–3234.

Francis P, Martinez DM, Taghipour F, Bowen BD, Haynes CA. 2006. Optimizing the rotor design for controlled-shear affinity filtration using computational fluid dynamics. *Biotechnol. Bioeng.* **95**:1207–1217.

Francisco É C, Neves DB, Jacob-Lopes E, Franco TT. 2010. Microalgae as feedstock for biodiesel production: Carbon dioxide sequestration, lipid production and biofuel quality. *J. Chem. Technol. Biotechnol.* **85**:395–403.

Fukuda H, Kondo a, Noda H. 2001. Biodiesel fuel production by transesterification of oils. *J. Biosci. Bioeng.* **92**:405–16.

Ganuza E, Anderson a. J, Ratledge C. 2008. High-cell-density cultivation of Schizochytrium sp. in an ammonium/pH-auxostat fed-batch system. *Biotechnol. Lett.* **30**:1559–1564.

Gerardo ML, Oatley-Radcliffe DL, Lovitt RW. 2014. Minimizing the energy requirement of dewatering Scenedesmus sp. by microfiltration: Performance, costs, and feasibility. *Environ. Sci. Technol.* **48**:845–853.

Gillet S, Decottignies P, Chardonnet S, Le Maréchal P. 2006. Cadmium response and redoxin targets in Chlamydomonas reinhardtii: A proteomic approach. *Photosynth. Res.* **89**:201–211.

Gochin RJ, Solari J. 1983. The role of hydrophobicity in dissolved air flotation. *Water Res.* **17**:651–657.

Godin M, Bryan AK, Burg TP, Babcock K, Manalis SR. 2007. Measuring the mass, density, and size of particles and cells using a suspended microchannel resonator. *Appl. Phys. Lett.* **91**:1–4.

González-López C V., Acién Fernández FG, Fernández-Sevilla JM, Sánchez Fernández JF, Molina Grima E. 2012. Development of a process for efficient use of CO 2 from flue gases in the production of photosynthetic microorganisms. *Biotechnol. Bioeng.* **109**:1637–1650.

Gouveia L, Oliveira AC. 2009. Microalgae as a raw material for biofuels production. *J. Ind. Microbiol. Biotechnol.* **36**:269–274.

Greenwell HC, Laurens LML, Shields RJ, Lovitt RW, Flynn KJ. 2010. Placing microalgae on the biofuels priority list: a review of the technological challenges. *J. R. Soc. Interface* **7**:703–726.

Griffiths DJ, Thresher CL, Street HE. 1960. The Heterotrophic Nutrition of Chlorella vulgaris. *Ann Bot* **24**:1–11.

Griffiths MJ, Harrison STL. 2009. Lipid productivity as a key characteristic for choosing algal species for biodiesel production. *J. Appl. Phycol.* **21**:493–507.

Grima ME, Belarbi EH, Acién Fernández FG, Robles Medina A, Chisti Y. 2003. Recovery of microalgal biomass and metabolites: Process options and economics. *Biotechnol. Adv.* **20**:491–515.

Grobbelaar JU. 2007. Algal Nutrition – Mineral Nutrition. In: . *Handb. Microalgal Cult.* Oxford: Blackwell Publishing, Oxford, UK, pp. 95–115.

Gualtieri P, Barsanti L, Passarelli V. 1988. Harvesting Euglena fracilis cells with a nontoxic flocculant. *J. Microbiol. Methods*.

Gudin C TC. 1986. Bioconversion of solar energy into organic chemicals by microalgae. *Adv. Biotechnol. Processes* **6**:73–110.

Guedes AC, Amaro HM, Malcata FX. 2011. Microalgae as sources of high added-value compounds-a brief review of recent work. *Biotechnol. Prog.*

Gunstone FD, Hilditch TP. 1945. The Union of Gaseous Oxygen with Methyl Oleate, Linoleate, and Linolenate. *J. Chem. Soc.*:836–841.

Guschina I a., Harwood JL. 2006. Lipids and lipid metabolism in eukaryotic algae. *Prog. Lipid Res.* **45**:160–186.

Hankamer B, Lehr F, Rupprecht J, Mussgnug JH, Posten C, Kruse O. 2007. Photosynthetic biomass and H2 production by green algae: From bioengineering to bioreactor scale-up. In: . *Physiol. Plant.*, Vol. 131, pp. 10–21.

Hanotu J, Bandulasena HCH, Zimmerman WB. 2012. Microflotation performance for algal separation. *Biotechnol. Bioeng.* **109**:1663–1673.

Harith, Z. T, Ariff, A. B, Yusoff, F. M, Mohamed, M. S, Shariff M, Din M. 2009. Effect of different flocculants on the flocculation performance of microalgae, Chaetoceros calcitrans, cells. *African J. Biotechnol.* **8**:5971–5978.

Harrison STL. 1991. Bacterial cell disruption: A key unit operation in the recovery of intracellular products. *Biotechnol. Adv.*

Harun R, Singh M, Forde GM, Danquah MK. 2010. Bioprocess engineering of microalgae to produce a variety of consumer products. *Renew. Sustain. Energy Rev.* **14**:1037–1047.

Heasman M, Diemar J, O'Connor W, Sushames T, Foulkes L. 2000. Development of extended shelf-life microalgae concentrate diets harvested by centrifugation for bivalve molluscs - a summary. *Aquac. Res.* **31**:637–659.

Van Hee P, Elumbaring ACMR, van der Lans RGJM, Van der Wielen LAM. 2006. Selective recovery of polyhydroxyalkanoate inclusion bodies from fermentation broth by dissolved-air flotation. *J. Colloid Interface Sci.* **297**:595–606.

Van Hee P, Middelberg APJ, van der Lans RGJM, van der Wielen L a. M. 2004. Relation between cell disruption conditions, cell debris particle size, and inclusion body release. *Biotechnol. Bioeng.* **88**:100–110.

Hejazi MA, Wijffels RH. 2004. Milking of microalgae. *Trends Biotechnol.* **22**:189–194.

Her N, Amy G, Park HR, Song M. 2004. Characterizing algogenic organic matter (AOM) and evaluating associated NF membrane fouling. *Water Res.* **38**:1427–1438.

Hetherington P.J.; Follows M, Dunnill P LM. 1971. Release of protein from baker's yeast (Saccharomyces cerevisiae) by disruption in an industrial homogenizer. *Trans Inst Chem Eng* **49**:142–148.

Hosny AY. 1996. Separating oil from oil-water emulsions by electroflotation technique. *Sep. Technol.* **6**:9–17.

Hu Q, Sommerfeld M, Jarvis E, Ghirardi M, Posewitz M, Seibert M, Darzins A. 2008. Microalgal triacylglycerols as feedstocks for biofuel production: Perspectives and advances. *Plant J.*

Huerlimann R, de Nys R, Heimann K. 2010. Growth, lipid content, productivity, and fatty acid composition of tropical microalgae for scale-up production. *Biotechnol. Bioeng.* **107**:245–257.

Huertas IE, Colman B, Espie GS, Lubian LM. 2000. Active transport of CO2 by three species of marine microalgae. *J. Phycol.* **36**:314–320.

Hung MT, Liu JC. 2006. Microfiltration for separation of green algae from water. *Colloids Surfaces B Biointerfaces* **51**:157–164.

Huntley ME, Redalje DG. 2007. CO2 mitigation and renewable oil from photosynthetic microbes: A new appraisal. *Mitig. Adapt. Strateg. Glob. Chang.* Vol. 12 573-608 p.

Hutchinson N, Bingham N, Murrell N, Farid S, Hoare M. 2006. Shear stress analysis of mammalian cell suspensions for prediction of industrial centrifugation and its verification. *Biotechnol. Bioeng.* **95**:483–491.

Illman AM, Scragg AH, Shales SW. 2000. Increase in Chlorella strains calorific values when grown in low nitrogen medium. *Enzyme Microb. Technol.* **27**:631–635.

IPCC IPOCC. 2007. IPCC Fourth Assessment Report: Climate Change 2007. *Intergov. Panel Clim. Chang.* Vol. 4 213-252 p.

Jackson NB, Liddell JM, Lye GJ. 2006. An automated microscale technique for the quantitative and parallel analysis of microfiltration operations. *J. Memb. Sci.* **276**:31–41.

Jaffrin MY. 2008. Dynamic shear-enhanced membrane filtration: A review of rotating disks, rotating membranes and vibrating systems. *J. Memb. Sci.* **324**:7–25.

Kadam KL. 2002. Environmental implications of power generation via coal-microalgae cofiring. *Energy* **27**:905–922.

Kaplan, D.; Richmond, A.E.; Dubinsky, Z.; Aaronson S. 2008. Algal nutrition. In: . *Handb. Microalgal Cult. Biotechnol. Appl. Phycol.*, pp. 147–198.

Kempken R, Preissmann A, Berthold W. 1995. Clarification of animal cell cultures on a large scale by continuous centrifugation. *J. Ind. Microbiol.* **14**:52–57.

Knothe GG. JHV, Krahl J. 2005. The Biodiesel Handbook. *Appl. Sci.* Vol. 2 302 p.

Knuckey RM, Brown MR, Robert R, Frampton DMF. 2006. Production of microalgal concentrates by flocculation and their assessment as aquaculture feeds. *Aquac. Eng.* **35**:300–313.

Komor E, Tanner W. 1974. The hexose-proton symport system of Chlorella vulgaris. Specificity, stoichiometry and energetics of sugar-induced proton uptake. *Eur. J. Biochem.* **44**:219–223.

Komor E, Haass D, Komor B, Tanner W. 1973. The active hexose-uptake system of Chlorella vulgaris. *Eur. J. Biochem.* **39**:193–200.

Kong S, Aucamp J, Titchener-Hooker NJ. 2010. Studies on membrane sterile filtration of plasmid DNA using an automated multiwell technique. *J. Memb. Sci.* **353**:144–150.

Kubota N, Tatsumoto N, Sano T, Toya K. 2000. A simple preparation of half N-acetylated chitosan highly soluble in water and aqueous organic solvents. *Carbohydr. Res.* **324**:268–274.

Kula M, Schiitte H. 1987. Purification of Proteins and the Disruption of Microbial Cells. *Biotechnol. Prog.* **3**:31–42.

Lander R, Daniels C MF. 2005. Efficient, scalable clarification of diverse bioprocess streams using a novel pilot-scale tubular bowl centrifuge. *Bioprocess Int.* **4**:32–40.

Larson E. 2008. Biofuel production technologies: status, prospects and implications for trade and development. In: . *United Nations Conf. Trade Dev.*

Lavoie, A.; De La Noue, J.; Serodes JB. 1984. Recovery of Microalgae in Wastewater: A Comparative Study of Different Flocculating Agents. *Can. J. Civ. Eng.* **11**:266–272.

Lee JY, Yoo C, Jun SY, Ahn CY, Oh HM. 2010. Comparison of several methods for effective lipid extraction from microalgae. In: . *Bioresour. Technol.*, Vol. 101,.

Lee KALC. 2002. Nitrogen Removal from Wastewaters by Microalgae Without Consuming Organic Carbon Sources. *J. Microbiol. Biotechnol* **12**:979–985.

Lee R. 1980. Phycology. New York: Cambridge University Press.

Lee SS, Burt A, Russotti G, Buckland B. 1995. Microfiltration of recombinant yeast cells using a rotating disk dynamic filtration system. In: . *Biotechnol. Bioeng.*, Vol. 48, pp. 386–400.

Lee YK. 2001. Microalgal mass culture systems and methods: Their limitation and potential. In: . *J. Appl. Phycol.*, Vol. 13, pp. 307–315.

Leesing Ratanaporn, Papone Thidarat PM. 2014. Effect of Nitrogen and Carbon Sources on Growth and Lipid Production from Mixotrophic Growth of Chlorella sp. KKU-S2. *Int. J. Biol. Biomol. Agric. Food Biotechnol. Eng.* **8**:368–371.

Leung WWF. 1998. Industrial Centrifugation Technology. McGraw-Hill Education.

Levy MS, Ciccolini LAS, Yim SSS, Tsai JT, Titchener-Hooker N, Shamlou PA, Dunnill P. 1999. The effects of material properties and fluid flow intensity on plasmid DNA recovery during cell lysis. *Chem. Eng. Sci.* **54**:3171–3178.

Li X, Xu H, Wu Q. 2007. Large-scale biodiesel production from microalga Chlorella protothecoides through heterotrophic cultivation in bioreactors. *Biotechnol. Bioeng.* **98**:764–771.

Li Y, Horsman M, Wu N, Lan CQ, Dubois-calero N. 2008. Biofuels from microalgae. *Biotechnol. Prog* **24**:815–820.

Liu J, Huang J, Sun Z, Zhong Y, Jiang Y, Chen F. 2011. Differential lipid and fatty acid profiles of photoautotrophic and heterotrophic Chlorella zofingiensis: Assessment of algal oils for biodiesel production. *Bioresour. Technol.* **102**:106–110.

Lopes AG, Khan N, Liddell J, Keshavarz-Moore E. 2012. An ultra scale-down approach to assess the impact of the choice of recombinant P. pastoris strain on dewatering performance in centrifuges. *Biotechnol. Prog.* **28**:1029–1036.

Lu S, Wang J, Niu Y, Yang J, Zhou J, Yuan Y. 2012. Metabolic profiling reveals growth related FAME productivity and quality of Chlorella sorokiniana with different inoculum sizes. *Biotechnol. Bioeng.* **109**:1651–1662.

Lydersen, B. K., D'Elia, N., Nelson KL. 1994. Bioprocess engineering: systems, equipment and facilities. NY, USA: John Wiley & Sons, Inc.

Ma G. 2009. Development of Ultra Scale-down Shear Filtration System and Modelling of Large Scale Diafiltration System.

Ma G, Aucamp J, Gerontas S, Eardley-Patel R, Craig A, Hoare M, Zhou Y. 2010. Mimic of a large-scale diafiltration process by using ultra scale-down rotating disc filter. *Biotechnol. Prog.* **26**:466–476.

Mackay D ST. 1988. Choosing between centrifugation and crossflow microfiltration. *Chem. Eng. J.* **477**:45–50.

Mannweiler K, Hoare M. 1992. The scale-down of an industrial disc stack centrifuge. *Bioprocess Eng.* **8**:19–25.

Mata TM, Martins A a., Caetano NS. 2010. Microalgae for biodiesel production and other applications: A review. *Renew. Sustain. Energy Rev.* **14**:217–232.

Maybury JP, Hoare M, Dunnill P. 2000. The use of laboratory centrifugation studies to predict performance of industrial machines: Studies of shear-insensitive and shear-sensitive materials. *Biotechnol. Bioeng.* **67**:265–273.

McGregor WC, Finn RK. 1969. Factors affecting the flocculation of bacteria by chemical additives. *Biotechnol. Bioeng.* **11**:127–138.

Mendes-Pinto MM, Raposo MFJ, Bowen J, Young AJ, Morais R. 2001. Evaluation of different cell disruption processes on encysted cells of Haematococcus pluvialis: Effects on astaxanthin recovery and implications for bio-availability. *J. Appl. Phycol.* **13**:19–24.

Metting FB. 1996. Biodiversity and application of microalgae. *J. Ind. Microbiol. Biotechnol.* **17**:477–489.

Metzger P, Largeau C. 2005. Botryococcus braunii: A rich source for hydrocarbons and related ether lipids. *Appl. Microbiol. Biotechnol.*

Miao X, Wu Q. 2006. Biodiesel production from heterotrophic microalgal oil. *Bioresour. Technol.* **97**:841–846.

Middelberg APJ. 1995. Process-scale disruption of microorganisms. *Biotechnol. Adv.* **13**:491–551.

Middelberg AP. 1994. The release of intracellular bioproducts. In: Subramanian G, editor. *Biosep. Bioprocess. a Handb.*:131–64.

Miettinen T, Ralston J, Fornasiero D. 2010. The limits of fine particle flotation. *Miner. Eng.* **23**:420–437.

Millero FJ, Lepple FK. 1973. The density and expansibility of artificial seawater solutions from 0 to 40°C and 0 to 21‰ chlorinity. *Mar. Chem.*

Millipore. 1998. Calculation of wall shear rate in turbulence promoted TFF devices. Bedford, MA.

Miron AS, Gomez AC, Camacho FG, Grima EM, Chisti Y. 1999. Comparative evaluation of compact photobioreactors for large-scale monoculture of microalgae. *Prog. Ind. Microbiol.* **35**:249–270.

Mogren H, Lindblom M, Hedenskog G. 1974. Mechanical disintegration of microorganisms in an industrial homogenizer. *Biotechnol. Bioeng.* **16**:261–274.

Mohn FH. 1980. Experiences and strategies in the recovery of biomass from mass cultures of microalgae. In: . *Algal Biomass*, pp. 471–547.

Mohn F. 1978. Improved technologies for the harvesting and processing of microalgae and their impact on production costs. *Arch Hydrobiol, Beih Ergeb Limnol* **1**:228– 53.

Molina E, Fernández J, Acién FG, Chisti Y. 2001. Tubular photobioreactor design for algal cultures. In: . *J. Biotechnol.*, Vol. 92, pp. 113–131.

Moore A. 2008. Biofuels are dead: long live biofuels(?) - Part one. *New Biotechnol.* **25**:6–12.

Moreno J, Vargas MÁ, Rodríguez H, Rivas J, Guerrero MG. 2003. Outdoor cultivation of a nitrogen-fixing marine cyanobacterium, Anabaena sp. ATCC 33047. In: . *Biomol. Eng.*, Vol. 20, pp. 191–197.

Moseley JL, Gonzalez-Ballester D, Pootakham W, Bailey S, Grossman AR. 2009. Genetic interactions between regulators chlamydomonas phosphorus and sulfur deprivation responses. *Genetics* **181**:889–905.

Mulder M. 1996. Basic principles of membrane technology. *J. Memb. Sci.* **72**:564.

Muller-Feuga a., Le Guedes R, Herve a., Durand P. 1998. Comparison of artificial light photobioreactors and other production systems using Porphyridium cruentum. *J. Appl. Phycol.* **10**:83–90.

Muñoz R, Guieysse B. 2006. Algal-bacterial processes for the treatment of hazardous contaminants: A review. *Water Res.*

Murkes C. JC. 1988. Crossflow Filtration: Theory and Practice. New York Wiley.

Mussgnug JH, Thomas-Hall S, Rupprecht J, Foo A, Klassen V, McDowall A, Schenk PM, Kruse O, Hankamer B. 2007. Engineering photosynthetic light capture: Impacts on improved solar energy to biomass conversion. *Plant Biotechnol. J.* **5**:802–814.

Norsker N-H, Barbosa MJ, Vermuë MH, Wijffels RH. 2010. Microalgal production--a close look at the economics. *Biotechnol. Adv.* **29**:24–7.

Nurdogan Y, Oswald WJ. 1996. Tube settling of high-rate pond algae. *Water Sci. Technol.* **33**:229–241.

Ohmori K, Glatz CE. 1999. Effects of pH and ionic strength on microfiltration of C. glutamicum. *J. Memb. Sci.* **153**:23–32.

Ojo EO. 2015. Photobioreactor Technologies for High-Throughput MicroalgaeCultivation; University College London.

Ojo EO, Auta H, Baganz F, Lye GJ. 2014. Engineering characterisation of a shaken, single-use photobioreactor for early stage microalgae cultivation using Chlorella sorokiniana. *Bioresour. Technol.* **173**:367–375.

Ojo EO, Auta H, Baganz F, Lye GJ. 2015. Design and parallelisation of a miniature photobioreactor platform for microalgal culture evaluation and optimisation. *Biochem. Eng. J.* **103**:93–102.

Olaizola M. 2003. Commercial development of microalgal biotechnology: From the test tube to the marketplace. In: . *Biomol. Eng.*, Vol. 20, pp. 459–466.

Packer M. 2009. Algal capture of carbon dioxide; biomass generation as a tool for greenhouse gas mitigation with reference to New Zealand energy strategy and policy. *Energy Policy* **37**:3428–3437.

Pan JR, Huang C, Chuang YC, Wu CC. 1999. Dewatering characteristics of algae-containing alum sludge. *Colloids Surfaces A Physicochem. Eng. Asp.* **150**:185–190.

Pascal AA, Liu Z, Broess K, van Oort B, van Amerongen H, Wang C, Horton P, Robert B, Chang W, Ruban A. 2005. Molecular basis of photoprotection and control of photosynthetic light-harvesting. *Nature* **436**:134–137.

Perez-Garcia O, Escalante FME, de-Bashan LE, Bashan Y. 2011. Heterotrophic cultures of microalgae: Metabolism and potential products. *Water Res.* **45**:11–36.

Petkov, Georgi D.; Bratkova SG. 1996. Viscosity of algal cultures and estimation of turbulency in devices for the mass culture of microalgae. *Arch. Hydrobiol. Suppl. Algol. Stud.* **81**:99–104.

Petrusevski B, Bolier G, Van Breemen AN, Alaerts GJ. 1995. Tangential flow filtration: A method to concentrate freshwater algae. *Water Res.* **29**:1419–1424.

Pienkos PT, Darzins A. 2009. The promise and challenges of microalgal-derived biofuels. *Biofuels, Bioprod. Biorefining* **3**:431–440.

Posten CWC. 2012. Microalgal Biotechnology Integration and Economy. In: . Berlin, p. 320.

Posten C. 2009. Design principles of photo-bioreactors for cultivation of microalgae. *Eng. Life Sci.* **9**:165–177.

Pulz O, Scheibenbogen K. 1998. Photobioreactors : Design and Performance with Respect to Light Energy Input. *Adv. Biochem. Eng. Biotechnol.* **59**:123–152.

Radmer R. 1996. Algal diversity and commercial algal products. *Bioscience* **46**:263–270.

Ramesh A, Lee DJ, Lai JY. 2007. Membrane biofouling by extracellular polymeric substances or soluble microbial products from membrane bioreactor sludge. *Appl. Microbiol. Biotechnol.* **74**:699–707.

Ramsden DK, Hughes J. 1990. The Flocculation of Bacteria Using Cationic Flocculants and Chitosan. *Biotechnol. Tech.* **4**:55 – 60.

Rao AR, Dayananda C, Sarada R, Shamala TR, Ravishankar GA. 2007. Effect of salinity on growth of green alga Botryococcus braunii and its constituents. *Bioresour. Technol.* **98**:560–564.

Ratledge C, Cohen Z. 2008. Microbial and algal oils: Do they have a future for biodiesel or as commodity oils? *Lipid Technol.* **20**:155–160.

Ratledge C, Wynn JP. 2002. The biochemistry and molecular biology of lipid accumulation in oleaginous microorganisms. *Adv. Appl. Microbiol.* **51**:1–51.

Ravi Kumar MN. 2000. A review of chitin and chitosan applications. *React. Funct. Polym.*

Rawat I, Ranjith Kumar R, Mutanda T, Bux F. 2013. Biodiesel from microalgae: A critical evaluation from laboratory to large scale production. *Appl. Energy* **103**:444–467.

Rayat A. 2010. Microscale Bioprocessing Platform for the Evaluation of Membrane Filtration Processes for Primary Recovery; University college London.

Van Reis R, Goodrich EM, Yson CL, Frautschy LN, Dzengeleski S, Lutz H. 1997. Linear scale ultrafiltration. *Biotechnol. Bioeng.* **55**:737–746.

REN21. 2013. Renewable Energy Policy Network for the 21st Century.

Rinaudo M. 2006. Chitin and chitosan: Properties and applications. *Prog. Polym. Sci.* **31**:603–632.

Rinki K, Tripathi S, Dutta PK, Dutta J, Hunt AJ, Macquarrie DJ, Clark JH. 2009. Direct chitosan scaffold formation via chitin whiskers by a supercritical carbon dioxide method: a green approach. *J. Mater. Chem.* **19**:8651.

Riske F, Schroeder J, Belliveau J, Kang X, Kutzko J, Menon MK. 2007. The use of chitosan as a flocculant in mammalian cell culture dramatically improves clarification throughput without adversely impacting monoclonal antibody recovery. *J. Biotechnol.* **128**:813–823.

Rodriguez G, Weheliye W, Anderlei T, Micheletti M, Yianneskis M, Ducci a. 2013. Mixing time and kinetic energy measurements in a shaken cylindrical bioreactor. *Chem. Eng. Res. Des.* **91**:2084–2097.

Rosenberg JN, Kobayashi N, Barnes A, Noel EA, Betenbaugh MJ, Oyler GA. 2014. Comparative analyses of three Chlorella species in response to light and sugar reveal distinctive lipid accumulation patterns in the microalga C. sorokiniana. *PLoS One* **9**.

Roussy J, Van Vooren M, Dempsey B a., Guibal E. 2005. Influence of chitosan characteristics on the coagulation and the flocculation of bentonite suspensions. *Water Res.* **39**:3247–3258.

Ruhsing Pan J, Huang C, Chen S, Chung YC. 1999. Evaluation of a modified chitosan biopolymer for coagulation of colloidal particles. *Colloids Surfaces A Physicochem. Eng. Asp.* **147**:359–364.

Rumpus J. 1998. Scale down of recovery and dewatering in industrial centrifuges; University College London.

Salte H, King JMP, Baganz F, Hoare M, Titchener-Hooker NJ. 2006. A methodology for centrifuge selection for the separation of high solids density cell broths by visualisation of performance using windows of operation. *Biotechnol. Bioeng.* **95**:1218–1227.

Schenk PM, Thomas-Hall SR, Stephens E, Marx UC, Mussgnug JH, Posten C, Kruse O, Hankamer B. 2008. Second Generation Biofuels: High-Efficiency Microalgae for Biodiesel Production. *BioEnergy Res.*

Schütte H KM. 1990. Bead Mill disruption. In: Asenjo JA (ed) Separation Processes in Biotechnology. *Bioprocess Technol.*:107–141.

Shamlou P, Gierczycki A, Titchener-Hooker N. 1996. Breakage of flocs in liquid suspensions agitated by vibrating and rotating mixers.

Sharma YC, Singh B. 2009. Development of biodiesel: Current scenario. *Renew. Sustain. Energy Rev.*

Sheehan J. 1998. A Look Back at the U.S. Department of Energy's Aquatic Species Program—Biodiesel from Algae. *Program*.

Shelef G, Sukenik a. 1984. Microalgae Harvesting and Processing : A Literature Review:65.

Shi J, Podola B, Melkonian M. 2007. Removal of nitrogen and phosphorus from wastewater using microalgae immobilized on twin layers: An experimental study. *J. Appl. Phycol.* **19**:417–423.

Shi XM, Zhang XW, Chen F. 2000. Heterotrophic production of biomass and lutein by Chlorella protothecoides on various nitrogen sources. *Enzyme Microb. Technol.* **27**:312–318.

Sikkema J, de Bont JA, Poolman B. 1995. Mechanisms of membrane toxicity of hydrocarbons. *Microbiol. Rev.* **59**:201–22.

Sim T-S, Goh a., Becker EW. 1988. Comparison of centrifugation, dissolved air flotation and drum filtration techniques for harvesting sewage-grown algae. *Biomass* **16**:51–62.

Song L. 1998. Flux decline in crossflow microfiltration and ultrafiltration: Mechanisms and modeling of membrane fouling. *J. Memb. Sci.* **139**:183–200.

Spolaore P, Joannis-Cassan C, Duran E, Isambert A. 2006. Commercial applications of microalgae. *J. Biosci. Bioeng.* **101**:87–96.

Stephenson A, Dennis J, Howe C. 2010. Influence of nitrogen-limitation regime on the production by Chlorella vulgaris of lipids for biodiesel feedstocks. *Biofuels* **1**:47–58.

Sugiyama J, Vuong R, Chanzy H. 1991. Electron-Diffraction Study on the 2 Crystalline Phases Occurring in Native Cellulose From an Algal Cell-Wall. *Macromolecules* **24**:4168–4175.

Svarovsky L. 2001. Separation by centrifugal sedimentation. In: Butterworth-Heinemann, editor. *Solid Liq. Sep.* Fourth Edi.

Tabatabaei M, Tohidfar M, Jouzani GS, Safarnejad M, Pazouki M. 2011. Biodiesel production from genetically engineered microalgae: Future of bioenergy in Iran. *Renew. Sustain. Energy Rev.* **15**:1918–1927.

Taha T, Cui ZF. 2002. CFD modelling of gas-sparged ultrafiltration in tubular membranes. *J. Memb. Sci.* **210**:13–27.

Tait AS, Aucamp JP, Bugeon A, Hoare M. 2009. Ultra scale-down prediction using microwell technology of the industrial scale clarification characteristics by centrifugation of mammalian cell broths. *Biotechnol. Bioeng.* **104**:321–331.

Taylor, G.; Hoare, M.; Gray, D.R.; Marston FAO. Size and density of protein inclusion bodies. *Nature*:6–9.

Tenney MW, Echelberger WF, Schuessler RG, Pavoni JL. 1969. Algal flocculation with synthetic organic polyelectrolytes. *Appl. Microbiol.* **18**:965–971.

Terry KL, Raymond LP. 1985. System design for the autotrophic production of microalgae. *Enzyme Microb. Technol.*

Themelis NJ. 1995. Transport and Chemical Rate Phenomena illustrate. Gordon and Breach Publishers 22 p.

Tissot S, Farhat M, Hacker DL, Anderlei T, Kühner M, Comninellis C, Wurm F. 2010. Determination of a scale-up factor from mixing time studies in orbitally shaken bioreactors. *Biochem. Eng. J.* **52**:181–186.

Titchener-Hooker NJ, Dunnill P, Hoare M. 2008. Micro biochemical engineering to accelerate the design of industrial-scale downstream processes for biopharmaceutical proteins. *Biotechnol. Bioeng.* **100**:473–487.

Tourrette A, De Geyter N, Jocic D, Morent R, Warmoeskerken MMCG, Leys C. 2009. Incorporation of poly(N-isopropylacrylamide)/chitosan microgel onto plasma functionalized cotton fibre surface. *Colloids Surfaces A Physicochem. Eng. Asp.* **352**:126–135.

Tripathi BN, Gaur JP. 2004. Relationship between copper- and zinc-induced oxidative stress and proline accumulation in Scenedesmus sp. *Planta* **219**:397–404.

Tustian a. D, Salte H, Willoughby N a., Hassan I, Rose MH, Baganz F, Hoare M, Titchener-Hooker NJ. 2007. Adapted Ultra Scale-Down Approach for Predicting the Centrifugal Separation Behavior of High Cell Density Cultures. *Biotechnol. Prog.* **23**:1404–1410.

Uduman N, Qi Y, Danquah MK, Forde GM, Hoadley A. 2010. Dewatering of microalgal cultures: A major bottleneck to algae-based fuels. *J. Renew. Sustain. Energy* **2**.

Ugwu CU, Aoyagi H, Uchiyama H. 2008. Photobioreactors for mass cultivation of algae. *Bioresour. Technol.* **99**:4021–8.

Vandanjon L, Rossignol N, Jaouen P, Robert JM, Quéméneur F. 1999. Effects of shear on two microalgae species. Contribution of pumps and valves in tangential flow filtration systems. *Biotechnol. Bioeng.* **63**:1–9.

Vesilind PA. 1970. Estimation of sludge centrifuge performance. *J. Sanit. Eng. Div.* **96**:805–818.

Vigeolas H, Duby F, Kaymak E, Niessen G, Motte P, Franck F, Remacle C. 2012. Isolation and partial characterization of mutants with elevated lipid content in Chlorella sorokiniana and Scenedesmus obliquus. *J. Biotechnol.* **162**:3–12.

Wahlen BD, Willis RM, Seefeldt LC. 2011. Biodiesel production by simultaneous extraction and conversion of total lipids from microalgae, cyanobacteria, and wild mixed-cultures. *Bioresour. Technol.* **102**:2724–2730.

Walas S. 1990. Chemical Process Equipment - Selection and Design.

Wan MX, Wang RM, Xia JL, Rosenberg JN, Nie ZY, Kobayashi N, Oyler G a., Betenbaugh MJ. 2012. Physiological evaluation of a new Chlorella sorokiniana isolate for its biomass production and lipid accumulation in photoautotrophic and heterotrophic cultures. *Biotechnol. Bioeng.* **109**:1958–1964.

Wang B, Li Y, Wu N, Lan CQ. 2008. CO(2) bio-mitigation using microalgae. *Appl. Microbiol. Biotechnol.* **79**:707–18.

Watanabe, Y. & Saiki H. 1997. Development of a photobioreactor incorporating Chlorella sp. for removal of CO2 in stack gas. *Energy Convers. Manag.* **38**:S499–S503.

Welsh DT, Bartoli M, Nizzoli D, Castaldelli G, Riou SA, Viaroli P. 2000. Denitrification, nitrogen fixation, community primary productivity and inorganic-N and oxygen fluxes in an intertidal Zostera noltii meadow. *Mar. Ecol. Prog. Ser.* **208**:65–77.

Wenger MD, DePhillips P, Bracewell DG. 2008. A Microscale Yeast Cell Disruption Technique for Integrated Process Development Strategies. *Biotechnol. Prog.* **24**:606–614.

Wicaksana F, Fane AG, Pongpairoj P, Field R. 2012. Microfiltration of algae (Chlorella sorokiniana): Critical flux, fouling and transmission. *J. Memb. Sci.* **387-388**:83–92.

Wilhelm C, Büchel C, Fisahn J, Goss R, Jakob T, LaRoche J, Lavaud J, Lohr M, Riebesell U, Stehfest K, Valentin K, Kroth PG. 2006. The Regulation of Carbon and Nutrient Assimilation in Diatoms is Significantly Different from Green Algae. *Protist* **157**:91–124.

Xu H, Miao X, Wu Q. 2006. High quality biodiesel production from a microalga Chlorella protothecoides by heterotrophic growth in fermenters. *J. Biotechnol.* **126**:499–507.

Xu Y, Purton S, Baganz F. 2013. Chitosan flocculation to aid the harvesting of the microalga Chlorella sorokiniana. *Bioresour. Technol.* **129**:296–301.

Yamane K, Ueta a, Shimamoto Y. 2001. Influence of physical and chemical properties of biodiesel fuels on injection, combustin and exhaust emission characteristics in a direct injection compression ignition engine. *Int. J. Engine Res.* **2**:249–261.

Yang C, Hua Q, Shimizu K. 2000. Energetics and carbon metabolism during growth of microalgal cells under photoautotrophic, mixotrophic and cyclic light-autotrophic/dark-heterotrophic conditions. *Biochem. Eng. J.* **6**:87–102.

Yongmanitchai W, Ward OP. 1991. Growth of and omega-3 fatty acid production by Phaeodactylum tricornutum under different culture conditions. *Appl. Environ. Microbiol.* **57**:419–425.

Zhang X, Hu Q, Sommerfeld M, Puruhito E, Chen Y. 2010. Harvesting algal biomass for biofuels using ultrafiltration membranes. *Bioresour. Technol.* **101**:5297–5304.

Zimmerman WB, Zandi M, Hemaka Bandulasena HC, Tesa?? V, James Gilmour D, Ying K. 2011. Design of an airlift loop bioreactor and pilot scales studies with fluidic oscillator induced microbubbles for growth of a microalgae Dunaliella salina. *Appl. Energy* **88**:3357–3369.

Appendices

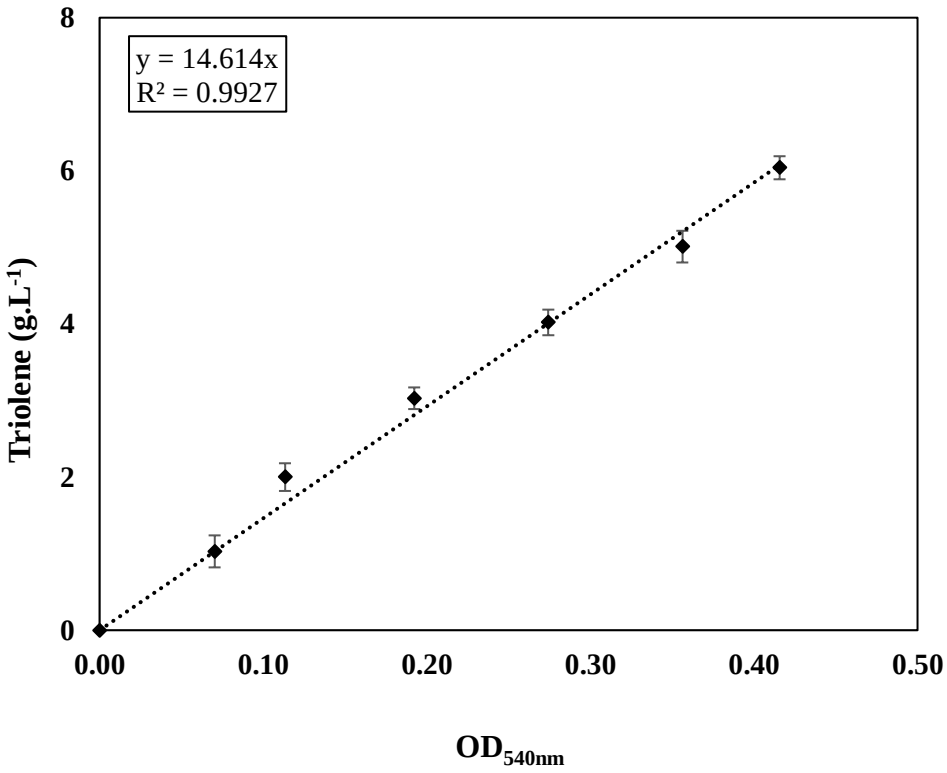

Appendix 1: Triolene calibration curve for quantification of algal lipids. Experiment was carried out using SPV method as described by Cheng *et al.* (2011) and this is described in Section 2.7. Error bars represents one standard deviation about the mean ($n \geq 5$).

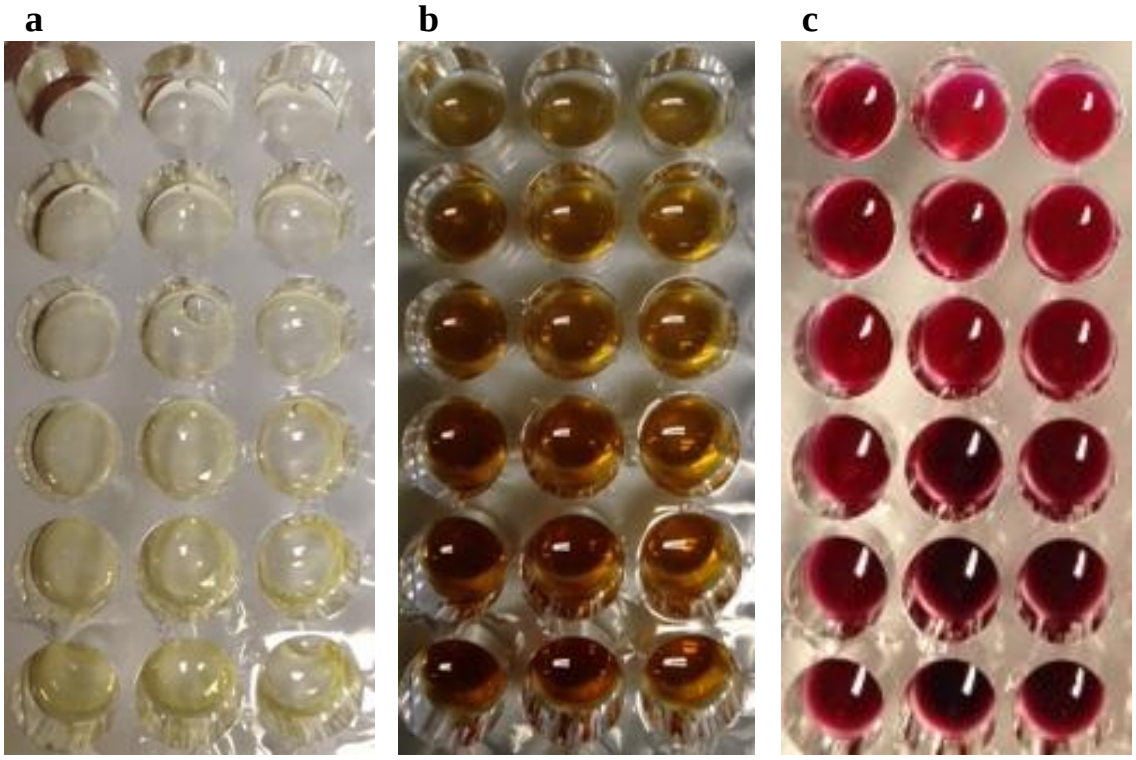

Appendix 2: Image showing the phases of sulphur phosphor-vanillin (SPV) analysis (a) lipid + H_2SO_4; (b) solution from (a) after heating for 20mints at 85 ± 5°C; and (c) reaction of lipid, H_2SO_4 and SPV after 10 min. Experiment was conducted using triolene at increasing concentrations and colour in (c) was obtained using 40 times dilution.

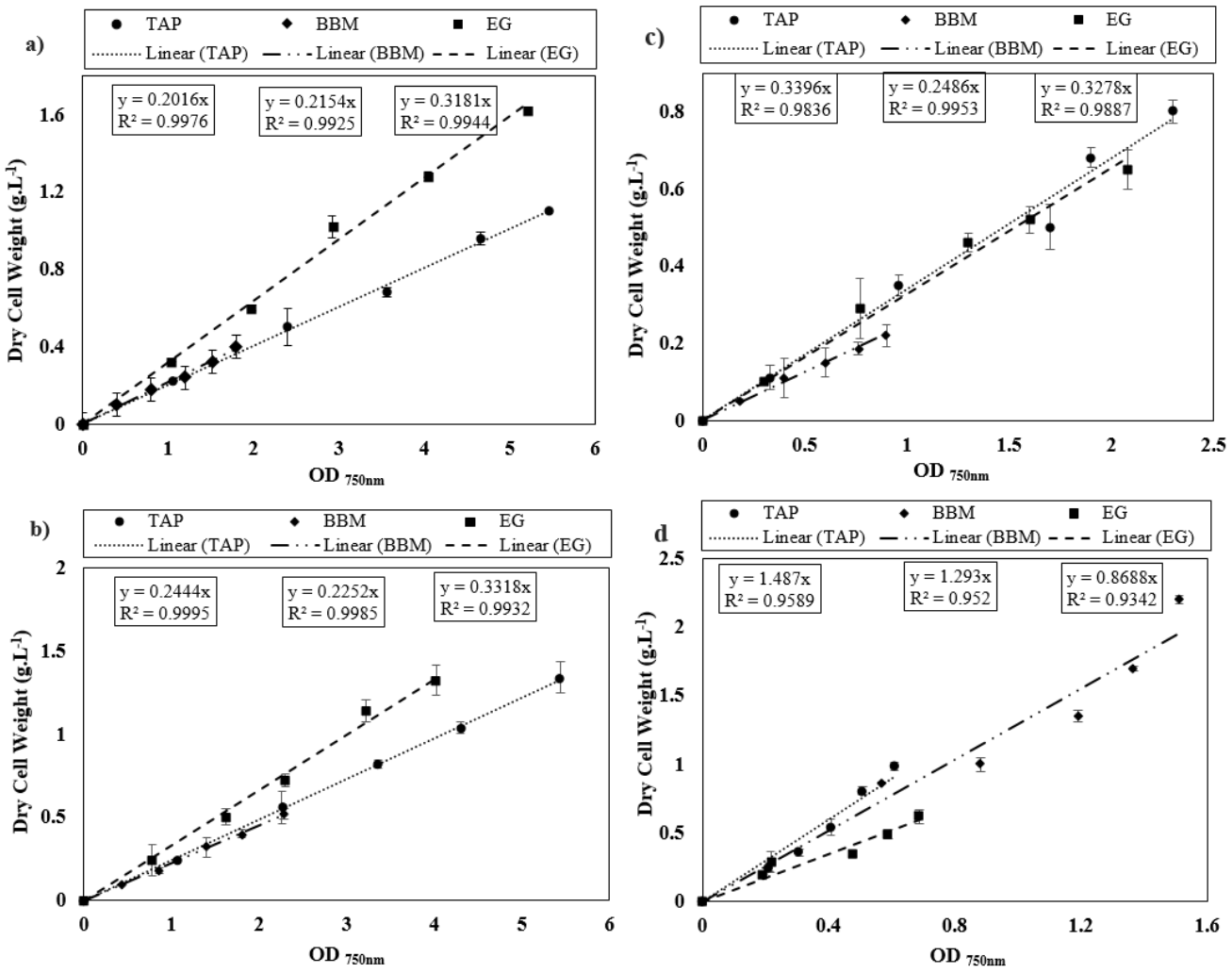

Appendix 3: Optical density versus corresponding dry cell weight measurements for a) *Chlorella Vulgaris* b) *Chlorella sorokiniana* c) *Chlamydomonas reinhardtii* and d) *Scenedesmus obliquus*. TAP in legend is equivalent to TBP as mentioned throughout the thesis. Cells were grown phototrophically as described in Section 2.2 after preparing the SF as described in Section 2.2.1.

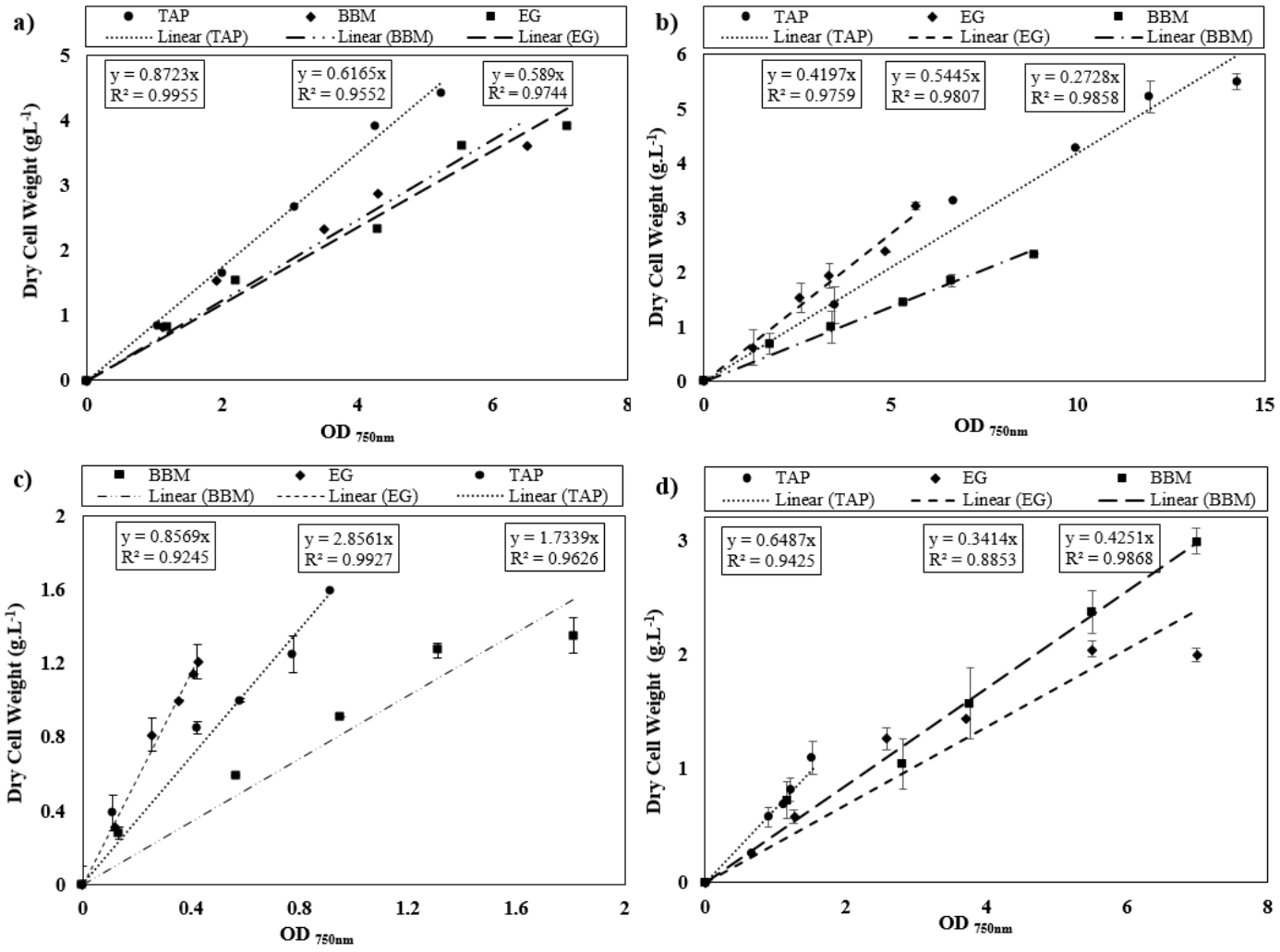

Appendix 4: Optical density versus corresponding dry cell weight measurements for a) *Chlorella Vulgaris* b) *Chlorella sorokiniana* c) *Chlamydomonas reinhardtii* and d) *Scenedesmus obliquus.* TAP in legend is equivalent to TBP as mentioned throughout the thesis. Cells were grown heterotrophically as described in Section 2.2 after preparing the SF as described in Section 2.2.1.

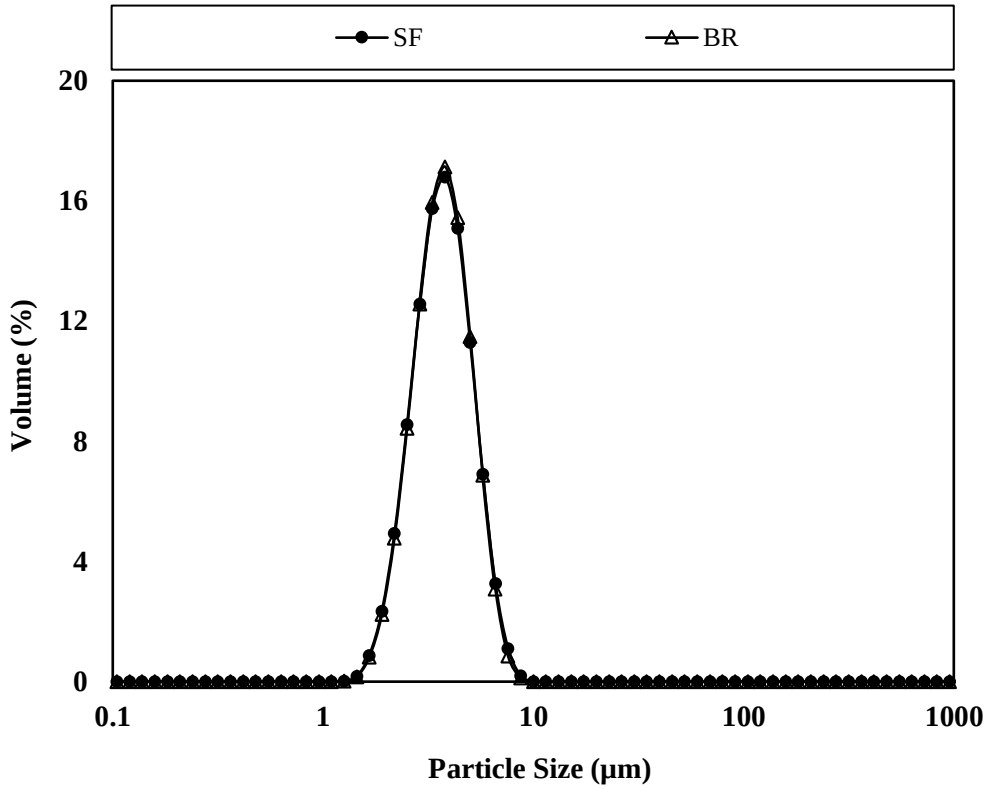

Appendix 5: Monomodal size distribution of cells obtained for shaken (SF) and stirred (Bioreactor; BR) cultures grown as described in section 2.2.1 and 2.2.2 respectively. Particle size distribution measured as described in Section 2.10.7.

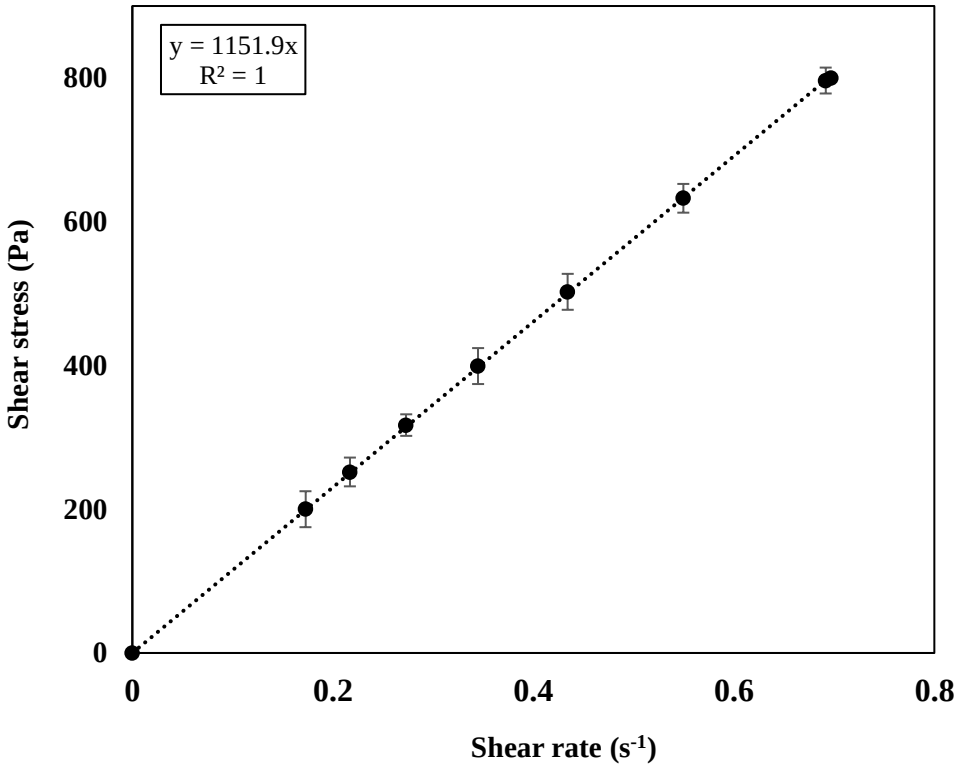

Appendix 6: Example of a stress stress-shear rate graph used for calculating viscosity of heterotrophically grown *C.sorokiniana*. Viscosity was measured as described in Section 2.10.3 using a Kinexus lab^{+} rheometer and results obtained presented in Section 5.2.1.

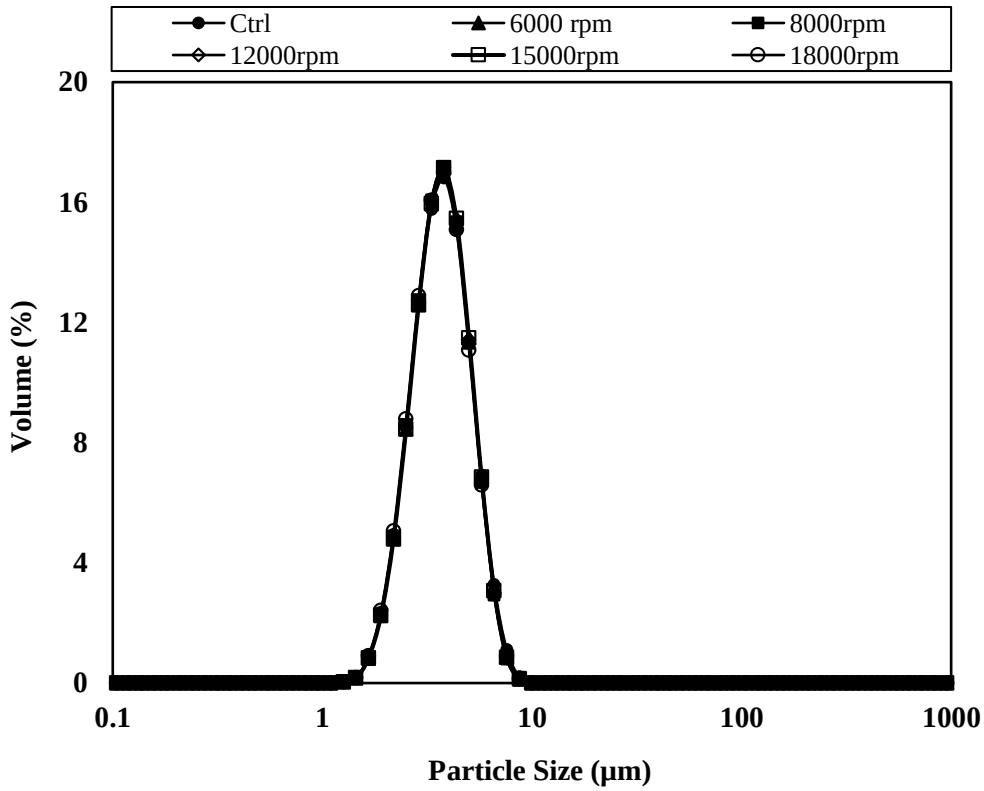

Appendix 7: Particle size distribution of single *C.sorokiniana* cells post exposure to different shear rates in the USD shear device (Section 2.3.3.2). Ctrl = control cell suspension.

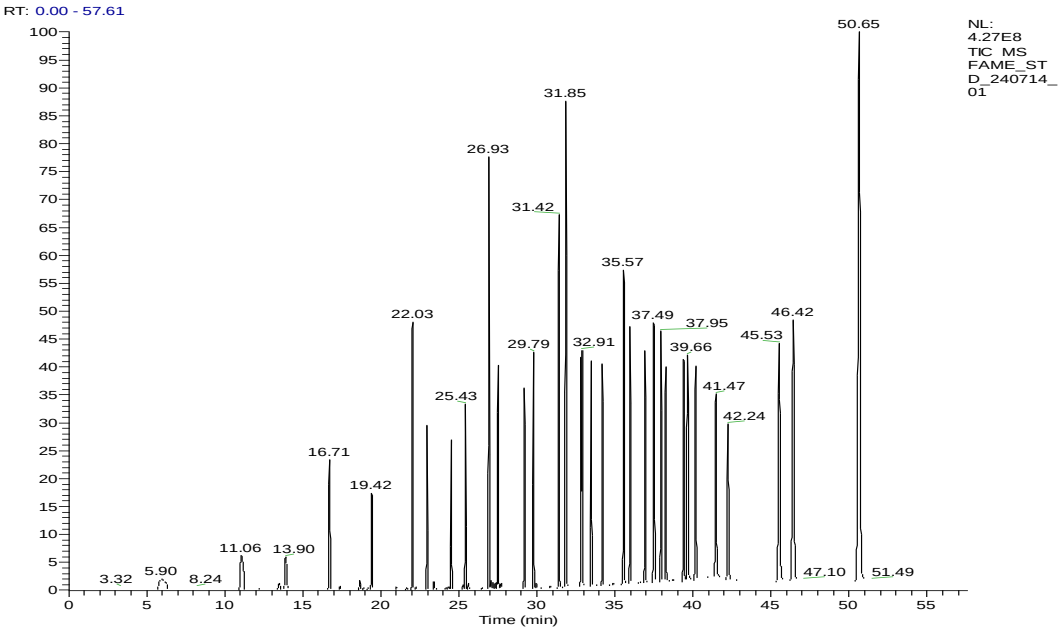

Appendix 8: Example of a GC-MS chromatogram obtained using a commercially prepared FAME mix standard solution. GC-MS was performed as described in Section 2.9.

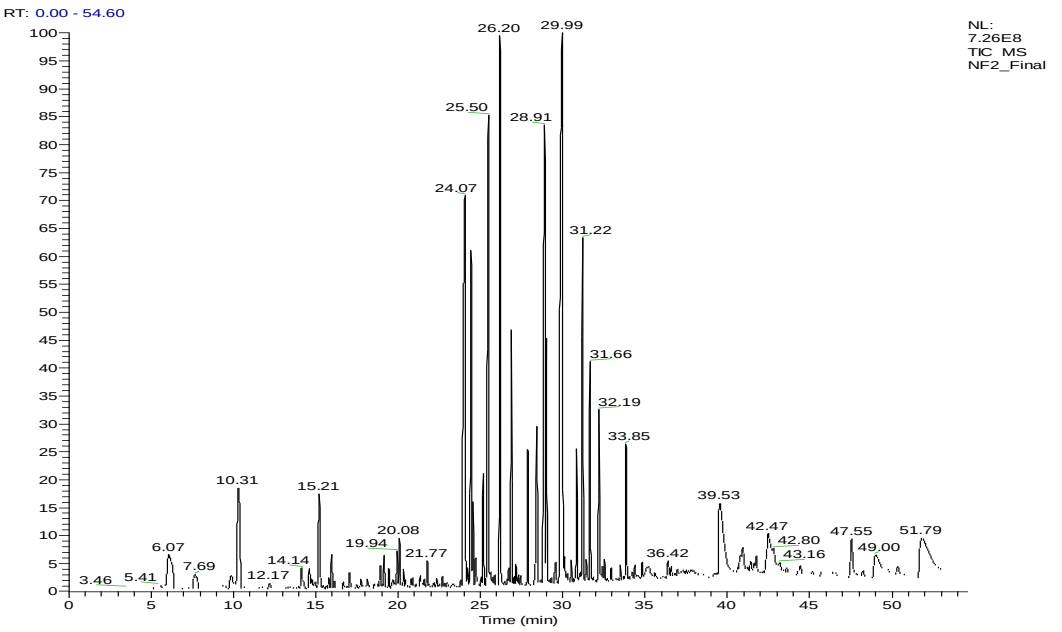

Appendix 9: Example of a GC-MS chromatogram obtained for unfloculated *C.sorokiniana* extracted lipids. Lipids were extracted and GC-MS performed as described in Section 2.9.

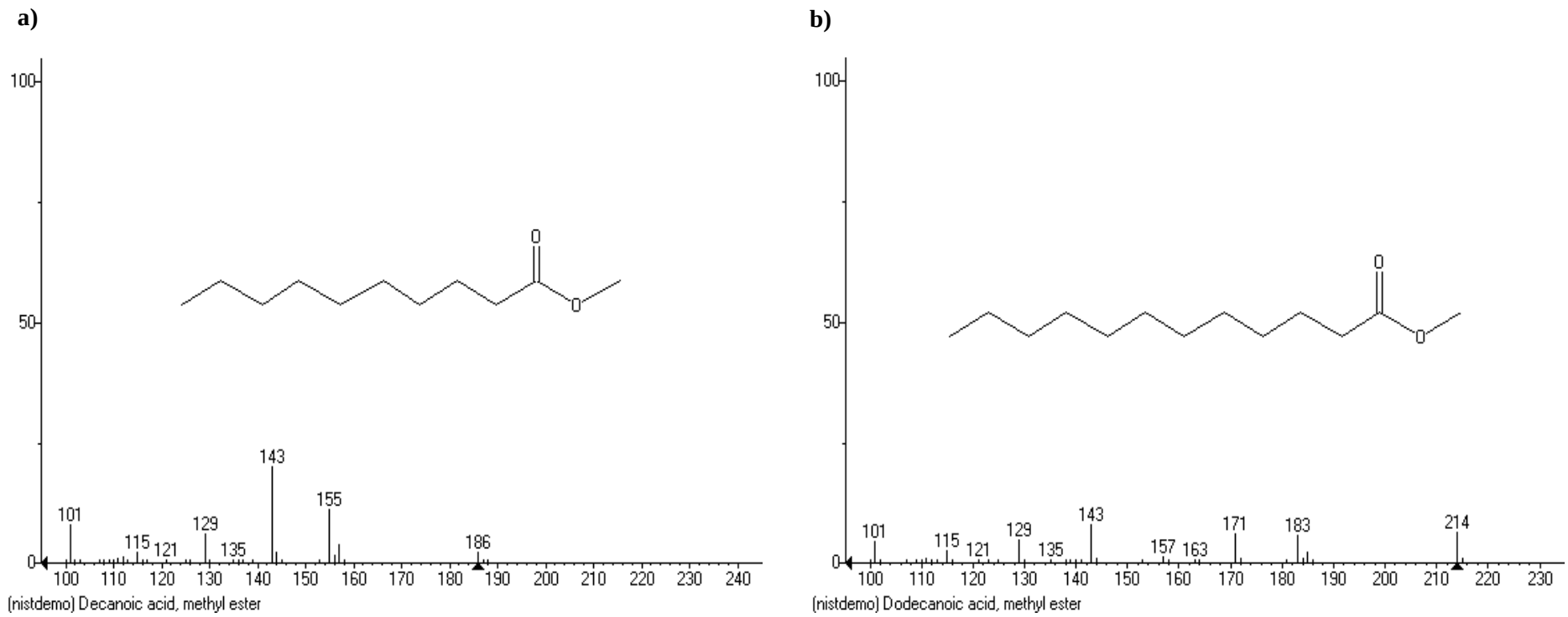

Appendix 10: Examples of matching compounds from the mass spectrometry (MS) library for peaks on the GC-MS chromatogram. a) Capric acid methyl ester also known as decanoic acid, methyl ester $C_{11}H_{22}O_2$, eluted at a retention time 11.06 min, molecular weight 186 g.mol and CAS number 110-42-9; and b) lauric acid methyl ester also known as dodecanoic acid, methyl ester $C_{13}H_{26}O_2$, eluted at a retention time 16.71 min, molecular weight 214 g.mol and CAS number 111-82-0. Experiment was carried out as described in Section 2.9.

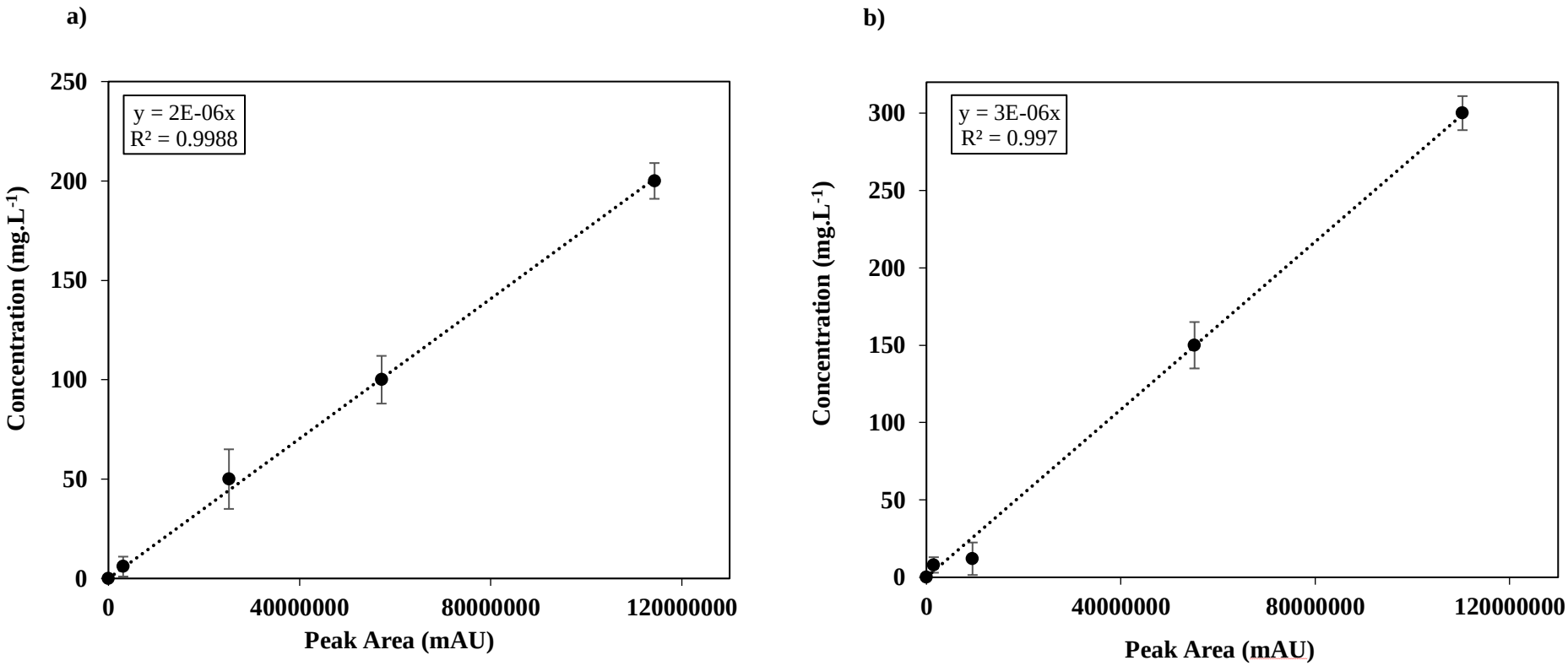

Appendix 11: Calibration curve for selected FAME's (a) capric acid (C10); and (b) palmitic acid (C16). Experiment was carried out as described in Section 2.9 with each point representing different concentrations of FAME standard prepared by diluting with dichloromethane. Error bars represents one standard deviation about the mean (n = 3).

Appendix 12: Sample calculation for amount of Chitosan used during flocculation

The final concentration of Chitosan in each solution prepared ranged from 0.5 – 5 $mg.mL^{-1}$ (Section 2.4.1.1). From section 3.7.1 (Pg. 107), Chitosan amounts 0.5, 4.5 and 5mg corresponds to of 1.09, 9.80 and 10.89 mg per gram $algal_{dcw}$ respectively. This was calculated as follows:

Total amount of algal broth in flocculation reactor	= 85 mL
Amount of Chitosan added	= 1 mL
Chitosan Concentration	= 0.5,4.5 or 5 $mg.mL^{-1}$
Broth Concentration	= 5.4 $g.L^{-1}$

Amount of algal cells in 85 mLs of broth: $$\frac{85\ \text{mL} \times 5.4\ \text{g}}{1000\ \text{mL}} = 0.459\ \text{g}$$

Example 1: using 1 mL of 0.5 $mg.mL^{-1}$ Chitosan Conc.

$$= \frac{0.5\ \text{mg Chitosan}}{0.459\ \text{g of algae}}$$

= 1.09 mg Chitosan g^{-1} of $algae_{dcw}$

Example 2: using 1 mL of 4.5 $mg.mL^{-1}$ Chitosan Conc.

$$= \frac{4.5\ \text{mg Chitosan}}{0.459\ \text{g of algae}}$$

= 9.80 mg Chitosan g^{-1} of $algae_{dcw}$

Example 3: using 1 mL of 5 $mg.mL^{-1}$ Chitosan Conc.

$$= \frac{5\ \text{mg Chitosan}}{0.459\ \text{g of algae}}$$

= 10.89 mg Chitosan g^{-1} of $algae_{dcw}$